STUDIES OF TNF-ALPHA IN ALPHA-ONE ANTITRYPSIN DEFICIENT AND HEALTHY SUBJECTS

by

JENNIE MARGARET GANE

A thesis submitted to

The University of Birmingham

For the degree of

Doctor of Philosophy

School of Clinical and Experimental Medicine

The University of Birmingham

June 2016

ABSTRACT

TNF-α, a pro-inflammatory cytokine, is implicated in the immune response in chronic obstructive pulmonary disease (COPD) secondary to Alpha-One Antitrypsin Deficiency (A1ATD). This thesis firstly describes studies in monocytes from A1ATD-related COPD subjects, examining the effect of the rs361525 TNF-A single nucleotide polymorphism, previously associated with 100-fold greater TNF-α concentration in the sputum of affected patients. Secondly, the autocrine effects of TNF-α on monocytes from healthy subjects are considered, in particular the differential roles of its two receptors, TNF-α receptor 1 (TNFR1) and 2 (TNFR2), an important topic given recent interest in selective TNFR1 blockade in TNF-α associated diseases.

Unexpectedly, *TNF-α* mRNA expression and secreted protein was not greater in A1ATD-related COPD subjects with the rs361525 polymorphism when compared to matched wild-type subjects. Reasons may include the cell type and stimulus used or inadequate power. In monocytes from healthy subjects, autocrine binding of TNF-α increased production of pro- and anti-inflammatory cytokines. Trends were observed for TNFR1 blockade to reduce both types of cytokine, for IL-10 to be reduced by TNFR2 blockade and for TNFR1 expression at the monocyte surface to be up-regulated by TNF-α-TNFR2 binding. Further studies are required to fully characterise the relative roles of TNFR1 and TNFR2 in monocytes.

DEDICATION

This thesis is dedicated to my grandparents, Margaret and Clifford Spooner.

ACKNOWLEDGEMENTS

Firstly I would like to thank my supervisors, Professor Robert Stockley and Dr Elizabeth Sapey for their support and advice throughout my PhD. Thanks also go to Dr Gillian McNab for teaching me the laboratory techniques required for the studies in this thesis and to Peter Nightingale for providing statistical advice where necessary.

I would also like to thank my parents, Elaine and Chris, and my husband Richard for their support throughout this process.

Finally, I wish to thank the West Midlands Chest Fund for funding this research.

Table of contents

List of figures

List of tables

Abbreviations

AA	Homozygous for the rs361525 polymorphism
A1ATD	Alpha-1 antitrypsin deficiency
AG	Heterozygous for rs361525 polymorphism
AM	Alveolar macrophage
APC	Antigen presenting cell
AP-1	Activator protein-1
AREs	Adenosyl-uridyl-rich elements
ASK	Apoptosis signal-regulating kinase 1
ATF-2	Activating transcription factor 2
ATP	Adenosine triphosphate
AUC	Area-under-the-curve
BAL	Bronchoalveolar lavage
BMI	Body mass index
BP	Base pair
BSA	Bovine serum albumin
CAT	Chloramphenicol acetyltransferase
CB	Chronic bronchitis
CCL5	Chemokine C-C motif ligand 5
CCR2	C-C chemokine receptor type 2
CD	Cluster of differentiation
cDNA	Complementary deoxyribonucleic acid
ChIP	Chromatin immunoprecipitation
CI	Confidence interval
cIAP	Cellular inhibitor of apoptosis
CM	Culture medium
COPD	Chronic obstructive pulmonary disease
CRD	Cysteine rich domain

CRE	Cis-regulatory element
CREB	Cyclic AMP response element-binding protein
CSE	Cigarette smoke extract
CT	Cycle threshold
CV%	Coefficient of variation percentage
DLCO	Diffusing capacity of the lung for carbon monoxide
(ds)DNA	(Double stranded) deoxyribonucleic acid
dNTP	(deoxyribose containing) Nucleotide triphosphates
EC	Effective concentration
EDTA	Ethylenediaminetetraacetic acid
Egr-1	Early growth response protein 1
ELISA	Enzyme linked immunosorbent assay
Elk	ETS domain-containing protein
ERK	Extracellular-signal-regulated kinase
Ets	E26 transformation-specific transcription factor
FADD	FAS-associated death domain
FBS	Fetal bovine serum
FEV1	Forced expiratory volume in one second
FLIP	FLICE-like inhibitory protein
FRET	Fluorescent resonant energy transfer
GAPDH	Glyceraldehyde 3-phosphate dehydrogenase
GG	Wild type genotype at position -237 of TNF-A gene
GM-CSF	Granulocyte macrophage colony stimulating factor
GOLD	Global initiative for chronic obstructive lung disease
GWAS	Genome wide association studies
HLA	Human leucocyte antigen
HRCT	High resolution computed tomography
HRP	Horse radish peroxidase

IBD	Inflammatory bowel disease
ICAM	Intercellular adhesion molecule
IFN-γ	Interferon gamma
Ig	Immunoglobulin (A, M, G or E)
IL	Interleukin
IM	Interstitial macrophages
IQR	Interquartile range
JNK	c-Jun N-terminal kinase
KCO	Transfer coefficient of carbon monoxide
kDa	Kilodalton
kPa	Kilopascal
KO	Knock out
lncRNAs	Long-non coding RNAs
LPS	Lipopolysaccharide
LTA/LTB	Lymphotoxin alpha/beta genes
LTB4	Leukotriene B4
Ly6C	Lymphocyte antigen 6C
(m)Ab	(Monoclonal) antibody
MAPK(K)	Mitogen activated protein kinase (kinase)
MAP3K	MAP kinase kinase kinase
MCP-1	Monocyte chemotactic protein 1
M-CSF	Macrophage colony stimulating factor
MDM	Monocyte derived macrophage
MEKK-3	Mitogen activated protein kinase kinase kinase
MFI	Median fluorescence intensity
MGB	Minor groove binder
MHC	Major histocompatibility complex
MI	Myocardial infarction

MK-2	MAPK-activated protein kinase-2
Ml	Millilitre
MMPs	Matrix metalloproteases
Mnk1	MAP kinase-interacting serine/threonine-protein kinase 1
MPO	Myeloperoxidase
mRNA	Messenger ribonucleic acid
mTNF-α	Membrane TNF-α
N	Number of subjects
NKC	Natural killer cells
NFAT	Nuclear factor of activated T-cells
NFκB	Nuclear factor kappa-light-chain-enhancer of B cells
ng	Nanogram
nm	Nanometre
nM	Nanomolar
NIK	NFκB inducing kinase
NKC	Natural killer cell
NO	Nitric oxide
NRF	NFκB repressing factor
NrF2	Nuclear factor (erythroid-derived 2)-like 2
$PaO_2/PaCO_2$	Partial pressures of oxygen/carbon dioxide
PBEC	Primary bronchial epithelial cell
PBS	Phosphate buffered saline
PE	Phycoerythrin
pg	Picogram
PerCP	Peridinin chlorophyll protein complex
PHA	Phytohaemagglutinin
PI3K	Phosphatidylinositide 3-kinase
pM	Picomolar

PMA	Phorbol 12-myristate 13-acetate
PMBCs	Peripheral blood mononuclear cells
polyA	Polyadenine
RANTES	Regulated on activation, normal T cell expressed and secreted
RCT	Randomised controlled trial (double-blind and placebo controlled unless otherwise specified)
RIP-1	Receptor activating protein 1
RNA	Ribonucleic acid
RNAase	Ribonuclease
ROS	Reactive oxygen species
RPMI	Roswell Park Memorial Institute medium
RT-qPCR	Real-time quantitative polymerase chain reaction
SD	Standard deviation
SE	Standard error
SNP	Single nucleotide polymorphism
SODD	Silencer of death domain molecule
Sp1	Specificity protein 1
sTNF-α	Soluble TNF-α
sTNFR	Soluble TNF-α receptor
TACE	Tumour necrosis factor-α-converting enzyme
TAK-1	Transforming growth factor-beta-activated kinase
TGF-β	Transforming growth factor beta
TH	T-helper
TIMP	Tissue inhibitors of metalloproteinases
TMB	Tetramethylbenzidine
TNF-α	Tumour necrosis factor alpha
TNFR	Tumour necrosis factor alpha receptor
TLR	Toll-like receptor
T-reg	T-regulatory cells

TRAF	TNF receptor-associated factor
TRADD	Tumour necrosis factor receptor type 1-associated death domain
T. cruzi	Trypanosoma cruzi
UTR	Un-translated region
VA	Alveolar volume
(F)VC	(Forced) vital capacity
VCAM	Vascular adhesion molecule 1
WT	Wild type
µg/µM/µL	Microgram/micromolar/microlitre
7-AAD	7-Amino-Actinomycin

CHAPTER 1

INTRODUCTION

1 Introduction

1.1 TNF-α overview

Tumour necrosis factor alpha (TNF-α) is the most important member of the extensive TNF superfamily of inflammatory cytokines (1). The protein was initially identified in the 1970's after studies revealed that a serum factor induced by the bacterial endotoxin, lipopolysaccharide (LPS), could induce tumour regression in mice (2). Since then numerous laboratories have investigated the many roles of this pleiotropic protein, in both physiological circumstances and pathological disease states. The major source in humans is monocytes and macrophages (3), although other immune cells can also secrete TNF-α, including natural killer cells (NKCs) and B-lymphocytes (4) and non-immune cells including endothelial cells, neurones and fibroblasts (5). TNF-α is initially produced as a 26 kilodalton (kDa) protein (233 amino acids) which is expressed across the cell membrane in trimerised form before being cleaved by the metalloproteinase enzyme, tumour necrosis factor-α-converting enzyme (TACE). The resultant soluble cytokine has a molecular weight of 17kDa (157 amino acids) and again forms a trimer in order to bind to either either of its two receptors (6). Although membrane expressed TNF-α is commonly referred to as pro-TNF-α this form is able to activate intracellular signalling pathways in its own right (7). The two TNF-α receptors are known as tumour necrosis factor alpha receptor 1 (TNFR1) and TNFR2. TNFR1 is found on most cell types in humans whilst TNFR2 is restricted to leukocytes and vascular endothelial cells (4). The widespread presence of TNFR1 explains the broad and diverse range of effects that TNF-α can induce as the cytokine can essentially trigger intra-cellular signalling events in almost any cell type.

Historically TNF-α was believed to be an entirely pro-inflammatory cytokine, however it has become clearer over recent decades that the role of TNF-α is more complex, encompassing

pro-inflammatory and pro-fibrotic effects and also functions that limit and resolve inflammation. These effects are dependent on a variety of incompletely understood factors such as differential receptor activation and the specific organ involved in each disease process (5, 8).

As an early phase cytokine TNF-α is rapidly up-regulated upon exposure to infectious agents or cell injury (3). Subsequent TNF-α receptor ligation is able to induce the relocation of transcription factors such as nuclear factor kappa B (NFκB) and activator protein-1 (AP-1) to the nucleus in effector cells leading to transcription of pro-inflammatory cytokines/chemokines such as interleukin 6 (IL-6), IL-1β and IL-8 (hereafter referred to by its alternative name, CXCL8, an alpha chemokine and a key neutrophil chemo-attractant) (9, 10). Thus TNF-α plays a vital role in coordinating the necessary cytokine milieu and the movement of inflammatory effector cells to sites of both bacterial (11, 12) and viral infection (13). The cytokine directly encourages inflammatory cell influx by up-regulating adhesion molecules on vascular endothelial cells and leukocytes (14). TNF-α is involved in priming neutrophils to release toxic products such as reactive oxygen species (ROS) and can increase the random movement of neutrophils (15-17). TNF-α signalling is important in promoting the formation of fully functioning granuloma to control intracellular infection such as that caused by mycobacteria (18). In addition TNF-α is able to induce cellular apoptosis in some scenarios and hence acts as one control mechanism for the eventual termination of inflammation in the normal individual (19, 20).

TNF-α is also an important cytokine in many chronic inflammatory diseases, including rheumatoid arthritis, inflammatory bowel disease (IBD), ankylosing spondylitis and psoriasis, as evidenced by the clinical effectiveness of monoclonal antibodies (mAbs) targeting the TNF-α protein in-vivo in these conditions (21-27). Rarely however, anti-TNF-α therapy can

worsen or induce autoimmune disease such as multiple sclerosis (28), vasculitis and lupus-like syndromes (29). Thus whilst generalised blockade of the TNF-α protein itself has undoubtedly revolutionised the treatment of a number of chronic inflammatory diseases, not all patients with those diseases respond and the reasons for this are not yet certain but may relate to the differential roles of the two TNF-α receptors in particular pathologies.

In murine and human studies TNF-α is also believed to play a role in the inflammatory response of chronic obstructive pulmonary disease (COPD) and is discussed further in 1.4.

1.2 **Chronic obstructive pulmonary disease**

1.2.1 Definition and burden of disease

COPD is a common chronic inflammatory lung disease, in general associated with a personal history of smoking. The disease affects an estimated 3 million people in the UK (30) and was recently ranked as the seventh leading cause of death in developed countries in the Global Burden of Disease Study (31) making it a significant public health problem. Pulmonary symptoms of COPD include the gradual onset of worsening exertional dyspnoea, wheeze and productive or non-productive cough. Patients predominantly have irreversible airflow obstruction on lung function testing and the degree of obstruction expressed as percentage of predicted (referenced against healthy age and sex matched populations) is used in classifying subjects into categories of disease severity (30). Many patients experience exacerbations, characterised by periodic deterioration of their symptoms. Exacerbations may be driven by infection, either bacterial or viral, or by non-infectious causes such as exposure to air pollution (32-34).

COPD is in fact an umbrella term encompassing a number of pulmonary pathologies, which often coexist in individual patients but do not all have to be present. Emphysema is the

permanent breakdown of extracellular matrix in the parenchyma of the lung leading to destruction and enlargement of the alveolar airspaces which lie distal to the terminal bronchioles (35). Emphysema is strictly a pathological diagnosis but in reality can now be routinely diagnosed using high resolution computed tomography (HRCT) scanning of the chest. Chronic bronchitis (CB) is a clinical diagnosis defined by cough productive of sputum for at least three months in each of two consecutive years (36). Obstructive bronchiolitis, more commonly referred to as small airways disease, is characterised by inflammation and remodelling of airways approximately 2mm in diameter (divisions 12-23 of the 28 divisions of the human bronchial tree) increasing the resistance to airflow on expiration (37). Increasingly it is recognised that many patients with COPD also have coexistent bronchiectasis, a condition in which bronchi are permanently dilated and thickened, in a localised or more diffuse pattern. Classically this is associated with the expectoration of moderate to large volumes of sputum on a daily basis and predisposes potentially to recurrent lower respiratory tract infections, although in some patients the condition may be silent (38).

Patients with COPD also carry a greater risk of developing a number of other diseases such as ischaemic heart disease, skeletal muscle wasting, osteoporosis and the metabolic syndrome, even after controlling for other risk factors such as smoking (30). Circulating TNF-α which may or may not have "spilled over" from the lungs of COPD patients has been implicated in the pathogenesis of some of these comorbidities and is discussed further in 1.4 (39).

The major environmental risk factor for developing COPD is cigarette smoking (40), although biomass exposure is also recognised (41) and outdoor air pollution plays a role in exacerbations (34). Whilst much work has gone into identifying genetic risks factors the main inherited cause of COPD remains Alpha-One Antitrypsin Deficiency (A1ATD) (42),

responsible for 1 to 2 % of cases of COPD (43). Unfortunately as yet there exists no truly disease modifying pharmacological treatment for COPD.

1.2.2 Mechanisms of COPD at a cellular level

Much work has been conducted to investigate the pathological processes that lead to the development of COPD. This topic has been extensively reviewed and whilst there still remains unanswered questions we now have a broad understanding of the cell types involved as summarised below (35).

Neutrophils release a number of serine proteases, most notably elastase, which when released in high enough concentration can overcome buffering anti-protease proteins and cause extracellular matrix degradation (44, 45). When this occurs at the acinus, individual alveoli are broken down and coalesce to form larger airspaces with a subsequent reduction in surface area for gas exchange (emphysema) (46). Another consequence of this extracellular matrix breakdown is loss of elasticity of the lung parenchyma which manifests itself as functional airway obstruction due to small airway collapse early during expiration (30).

Neutrophils produce other proteases such as proteinase 3 as well as ROS and inflammatory cytokines which contribute to the development of COPD (47-49). Macrophages (and monocytes) also produce proteases, in the form of matrix metalloproteases (MMPs), ROS and inflammatory cytokines and chemokines such as TNF-α and CXCL8 (50-52). In addition, macrophages have a prominent role in surveillance and in the phagocytosis and clearance of unwanted or harmful material, such as bacteria, inhaled particles and apoptotic epithelial cells (efferocytosis) (53, 54). Efferocytosis is important as reduced clearance of apoptotic cells may lead to their unwanted necrosis with amplified inflammation as a result (55). There is

evidence to suggest that macrophage and neutrophil function may be altered in COPD and as yet it is unclear whether this is a cause or effect phenomenon (54, 56).

Other immune cells are also likely to play a role, although this has been less well defined than for neutrophils and macrophages. Dendritic cells act as antigen presenting cells (APCs) and may be responsible for inducing an adaptive immune response in COPD through presentation of bacterial peptides or autoantigens (57). Adaptive immune cells, which in some studies have been shown to be up-regulated in COPD patients, include cluster of differentiation (CD) 8 T-cells, which release cytotoxic mediators such as perforin and granzyme (58), CD4 T-helper (TH)-1 cells and lastly plasma B-cells, which might produce autoantibodies (35, 57). In a subset of patients eosinophils are increased in the airway secretions and can predict systemic corticosteroid responsive disease (59).

Structural cells within the lung also participate actively in COPD pathogenesis. Epithelial cells undergo squamous metaplasia and release pro-inflammatory cytokines (60). Goblet cells undergo hyperplasia, contributing to mucus hypersecretion, and hypertrophy (61). The smooth muscle of small airways increases in mass, leading to reduced airway radius (62), and also releases pro-inflammatory cytokines and growth factors (63). Fibroblasts in moderate to severe COPD subjects show a pro-inflammatory phenotype and may be less able to repair damaged elastin fibres, thereby contributing to the development of emphysema (64).

In the circulation, monocytes from COPD subjects who are losing weight secrete more TNF-α than monocytes from non weight-losing COPD subjects or healthy controls (65), suggesting this cell type might play a role in the systemic effects of the disease. In addition, circulating monocytes from COPD subjects appear primed to become pro-inflammatory type macrophages irrespective of external stimuli, at least in-vitro (66).

1.3 **A1ATD-related COPD**

A1ATD is an inherited condition that presents with early onset COPD, of both emphysema and CB phenotypes and often goes undiagnosed (42). Spirometric and gas transfer values begin to decline in the third decade in those subjects who present with symptoms and disease progression is accelerated by smoking (67). Liver disease may also develop depending on the specific genotype involved. Other presentations of the disease include neonatal liver failure, panniculitis and vasculitis (42). The multiple functions of the A1AT protein are being increasingly characterised, and the most important of these is the buffering effect of the protein against neutrophil serine proteases such as neutrophil elastase and proteinase 3 (68-70). A markedly reduced serum concentration of A1AT thus leads to excessive proteinase mediated lung damage, as the local pericellular concentration of proteinases vastly exceeds that of the A1AT buffer (71). Treatment of A1ATD-related COPD follows that of usual COPD and in some countries human intravenous A1AT is given periodically to increase systemic and local A1AT concentrations (42).

The A1AT protein is coded for on chromosome 14 at position 14q32.1 by a gene named serpinA1 ("serine proteinase inhibitor A1"), and is manufactured as a 52kDa glycoprotein by liver hepatocytes and secreted into the circulation (42). Relative deficiency of the A1AT protein occurs as a result of a variety of single nucleotide polymorphisms (SNPs) in the gene. The normal allele is termed M and can be expressed in a co-dominant fashion with abnormal alleles, most commonly Z or S. Other less common alleles include F, I, P and null alleles. The most common genotypes to result in decreased serum concentration of A1AT below the recognised protective level of 11 micromolar (μM) include ZZ and SZ. MZ and MS genotypes generally produce enough A1AT to protect against the development of lung damage and affected subjects are regarded as carriers. Whilst null alleles lead to absence of

any production of A1AT the more common Z and S alleles do lead to protein manufacture (42). For example, the only difference in the Z variety of A1AT compared to the normal M protein is a glutamate to lysine substitution at position 342. However, this change leads to profound consequences, specifically the acquired ability of adjacent A1AT protein molecules to slot one into the other, with the subsequent formation of polymers which are largely unable to be secreted in to the circulation. It is because of this accumulation of polymerised A1ATD that liver cirhhosis can develop in later years (72). What A1AT is secreted into the circulation will easily form polymers in the blood and lung (42). It should be noted that the penetrance of A1ATD is variable and may depend on other genetic susceptibility factors and/or environmental exposures.

Whilst many of the described cellular mechanisms for the development of usual COPD also apply to A1ATD-related COPD there are some features that are especially relevant or unique to A1ATD. These are summarised in figure 1.1.

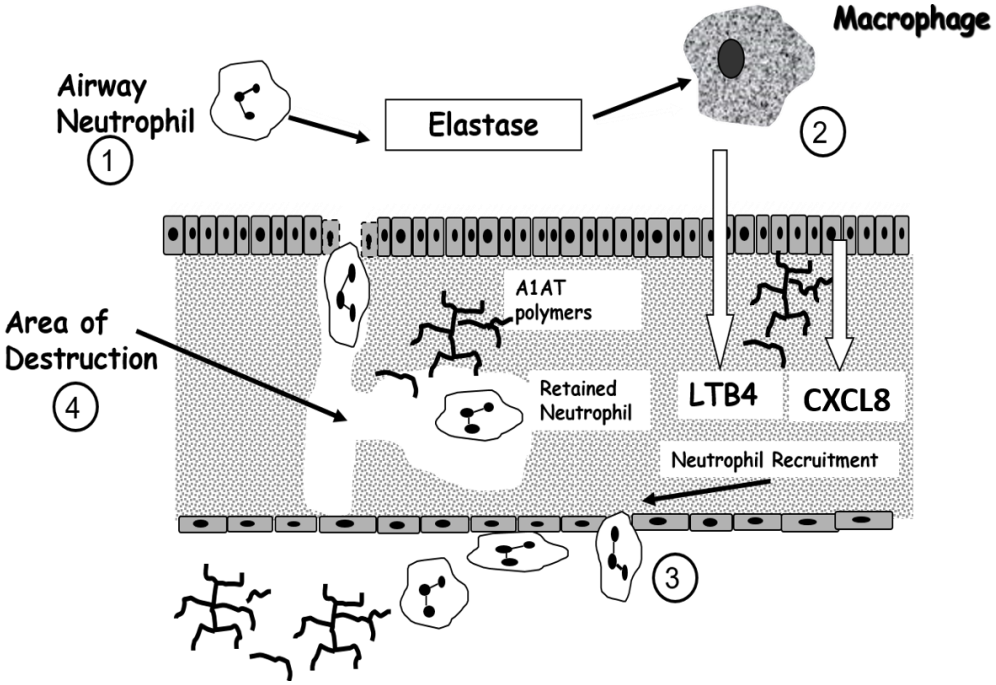

Figure 1-1 Mechanisms of pulmonary damage in A1ATD

1) Neutrophils present in the airway secrete elastase in response to toxic stimuli such as cigarette smoke. 2) Elastase stimulates the release of the neutrophil chemoattractant leukotriene B4 (LTB4) by macrophages. 3) LTB4 secretion and CXCL8 secretion by epithelial cells (73) lead to the recruitment of neutrophils from the circulation. 4) Neutrophils pass through the lung interstitium on the way to the airway lumen and elastase and other proteases are released to facililate this passage through the connective tissue. The relative lack of A1AT in the immediate vicinity of each neutrophil means the pericellular concentration of proteases overwhelms the available functioning A1AT and is able to break down elastin fibres for a longer time period and in a greater surrounding area (before diffusing outwards until a low enough concentration is reached that the available A1AT can meet the buffering needs) than neutrophils in non-A1ATD lungs can (71). In addition, any A1AT polymers present are themselves pro-inflammatory as they act as a further neutrophil chemoattractant (74). Reproduced with the permission of Professor Robert Stockley (42).

1.3.1 The relationship between A1AT and TNF-α

In recent years work has emerged supporting the concept that A1AT plays an important role in modulating TNF-α pathways. Bergin *et al* showed that neutrophils from patients with ZZ A1ATD (but no airway obstruction yet) had more mTNF-α on their surface, secreted more sTNF-α and released more secondary and tertiary neutrophil degranulation products than

neutrophils from MM control subjects. Exogenous sTNF-α induced more neutrophil degranulation in ZZ subjects and importantly this was abrogated by pre-treatment with A1AT. The mechanism for this was determined to be due to interruption of TNF-α binding to either of its receptors by A1AT binding to them in its place. As a result TNF-α autocrine loops in neutrophils were interrupted, down-regulating further production of *TNF-α* messenger ribonucleic acid (mRNA) (75). Thus, increased secretion of TNF-α by neutrophils from ZZ subjects can be explained by the relative lack of negative feedback control due to decreased circulating A1AT. In addition the same group showed that A1AT inhibits the action of TACE (76) and therefore in A1ATD patients enhanced TACE activity may occur leading to greater TNF-α and TNFR1 secretion (75). In LPS-stimulated human monocytes the addition of A1AT led to an initial increase in TNF-α output but over time caused a marked reduction (77). Lastly, Lockett *et al* also demonstrated in pulmonary microvascular endothelial cells that A1AT reduced TNF-α secretion by inhibiting the action of TACE (78). Taken together these studies suggest that TNF-α may play a more important role in A1ATD-related COPD than in usual COPD.

1.4 **TNF-α in COPD**

Whilst the cytokine network in COPD is undoubtedly complex (79), numerous studies have suggested a role for TNF-α in COPD pathogenesis. The principal studies are summarised in table 1.1 and can be broadly divided into three categories: animal studies, human cross-sectional studies and human prospective studies. A general critique of these studies is provided below.

The human studies are subject to a number of significant limitations, the most important being that even in well-designed studies any association found between TNF-α and a particular outcome or disease process cannot prove causality. Cross sectional studies are limited to

investigating patients at one point in time and hence are unable to investigate the role of mediators in disease pathogenesis at varying disease stages in the same cohort. Prospective studies are less limited for this reason as they allow individual subjects to be followed over time hence acting as their own controls, for example when investigating the potential role of TNF-α in exacerbations (80, 81). However, no prospective studies have been conducted for more than three years, presumably because COPD is a slowly progressive disease, making sampling of patients over long periods of time a costly challenge. There remain a number of other limitations which make drawing definitive conclusions difficult from the human studies outlined in the table. The populations investigated were of varying size, with heterogeneity in the COPD groups across studies and only limited matching of COPD and control groups within studies.

Overall, the available evidence varies as to whether TNF-α is increased in the airways (sputum), the alveoli (bronchoalveolar lavage (BAL)) and the circulation of patients with *stable* COPD. There is stronger evidence from the larger prospective studies to suggest it is increased in the serum and airways during bacterial and non-bacterial exacerbations. It is unsurprising that this is the case given the vital role of TNF-α in coordinating the innate immune response to viruses and bacteria. The available studies cannot answer the question of whether this TNF-α response is excessive, perhaps contributing to the acceleration of disease progression observed in patients who are frequent exacerbators (82), or physiological. The cross sectional and prospective studies showed that TNF-α correlated (in some cases) with clinical indices of severity of disease and co-morbidities such as osteoporosis and skeletal muscle inflammation and wasting, suggesting a possible systemic role for TNF-α in COPD.

The strongest evidence for a role for TNF-α in COPD pathogenesis comes from animal studies, whereby mouse models with knockout of both TNF-α receptors are highly protected

to impressive extents from developing emphysema in response to cigarette smoke extract (CSE). Investigators also in one case confirmed a reduction in the development of small airways disease as result of receptor knockout (83). Animal models are undoubtedly useful but like human studies have some limitations, namely, questions over their pathological resemblance to human disease, particularly to later stages, a lack of exacerbations and the automatic cessation of disease progression on removal of CSE (84).

Taken in the context of the animal model work it is unlikely that all the positive findings in human studies are purely related to associations between TNF-α and clinical indices/events, suggesting instead that the presence of TNF-α induces a pro-inflammatory cascade that contributes to tissue damage. Whilst not *causing* COPD never-the-less TNF-α is an important cytokine in the disease, perhaps especially in A1ATD-related COPD, given the unique role the A1AT protein plays in TNF-α regulation as discussed in 1.3.1.

Table 1-1 Summary of studies investigating the possible role of TNF-α in the pathogenesis of COPD

Study design	Findings	Author/ reference
Animal models	Guinea pigs exposed to long term CSE developed emphysema with raised plasma TNF-α. Mice exposed to acute CSE developed increase in mRNA and plasma TNF-α.	Wright *et al* (46)
	TNF-α receptor KO mice (in contrast to WT mice) do not express mRNA for neutrophil and monocyte chemokines, do not have an inflammatory cell influx or any connective tissue breakdown in the lungs in response to acute CSE.	Churg *et al* (85)
	TNF-α receptor KO mice exposed to CSE for 6 months had less pulmonary inflammatory cells and proteases present on lavage and were 70% protected from the development of airspace enlargement (emphysema), compared to WT mice.	Churg *et al* (86)
	TNF-α receptor KO mice exposed to CSE for 6 months were protected from developing small airways remodelling.	Churg *et al* (83)
	TNF-α receptor KO mice exposed to CSE for 6 months did not produce *MMP* mRNA in the walls of small intrapulmonary arteries. MMPs are thought to contribute to long term pulmonary vascular changes in COPD.	Wright *et al* (87)

Study design	Findings	Author/ reference
Human models (cross sectional): Pulmonary	Induced sputum from stable COPD patients (most GOLD stages II and III) contained more TNF-α than the induced sputum from healthy smokers and healthy controls (n=20 in each group). Higher TNF-α was also noted in the sputum from healthy smokers compared to healthy controls.	Hacievliyagil *et al* (88)
	Induced sputum from stable COPD subjects (n=14) contained more TNF-α than that of non-smokers or healthy smoking controls.	Keatings *et al* (89)
	Induced sputum from stable COPD patients (n=18) showed no difference in TNF-α compared to healthy smoking controls, but did have more sTNFR1.	Vernooy *et al* (90)
	BAL fluid from stable COPD subjects classed as frequent exacerbators contained more TNF-α than healthy smoking and non-smoking controls and from COPD subjects who weren't frequent exacerbators.	Tumkaya *et al* (91)
	Lung tissue stimulated with LPS ex-vivo produced greater TNF-α in subjects with stable GOLD stage I (n=11) or II COPD (n=13) compared to healthy controls.	Hackett *et al* (92)
	Bronchial intraepithelial T-cells from moderate to severe stable COPD subjects (n=10) produced more TNF-α than T-cells from healthy controls, healthy smokers and subjects with mild COPD. TNF-α production by these T-cells in the lower airways correlated negatively with FEV1.	Hodge *et al* (93)
	Induced sputum from exacerbating severe COPD subjects (n=19) did not contain more TNF-α than induced sputum from COPD subjects with mild-moderate disease (n=20).	Hacievliyagil *et al* (94)
	Spontaneous sputum samples from exacerbating CB subjects (n=45) contained varying concentrations of TNF-α depending on the bacteria isolated.	Sethi *et al* (33)

Study design	Findings	Author/ reference
Human models (cross sectional): Systemic	Serum TNF-α higher in stable COPD subjects (n=83) compared to healthy controls. Serum TNF-α higher in COPD subjects with an exacerbation (n=20) compared to stable COPD subjects.	Karadag *et al* (95)
	Serum TNF-α higher in COPD subjects (n=27) than healthy age matched controls. sTNFR1/2 also higher. All 3 parameters correlated negatively with the partial pressure of arterial oxygen. All 3 parameters higher in COPD subgroup with severe hypoxia vs non-severe hypoxia. All 3 parameters highest in malnourished subgroup with concomitant hypoxia.	Takabatake *et al* (96)
	No differences in plasma TNF-α or sTNFR1/2 (which far exceeded TNF-α in concentration) in CB subjects (n=15) compared to non-smoking age matched healthy controls.	Sapey *et al* (97)
	Serum TNF-α was associated negatively with fat free mass index in stable COPD subjects (n=222), but not in healthy smokers or healthy controls.	Gaki *et al* (98)
	Serum TNF-α was found to be an independent predictor of low bone mineral density (i.e. osteoporosis) in 672 COPD subjects with mostly moderately severe disease.	Liang *et al* (99)
	TNF-α induced by LPS stimulation of whole blood was greater in severe COPD subjects compared to moderately affected patients. The concentration of TNF-α induced by LPS stimulation of whole blood correlated negatively with FEV1.	von Haehling *et al* (100)
	A higher proportion of circulating CD8 T-cells from stable GOLD II-IV COPD subjects (n=30) produced TNF-α compared to healthy controls. However, GOLD IV subjects had a lower proportion positive for TNF-α compared to less severe stages of COPD and the proportion positive had a moderate positive correlation with gas transfer factor.	Paats *et al* (101)
	Subjects with mild COPD (n=27) had higher plasma, and induced sputum concentration of TNF-α compared to age matched healthy controls.	Foschino *et al* (102)

Study design	Findings	Author/ reference
Human models (cross sectional): Other	Quadriceps muscle biopsies from COPD subjects (n=11) had higher *TNF-α* mRNA expression at rest than those from healthy controls. Not all COPD subjects were hypoxic.	Rabinovich *et al* (103)
	External intercostal muscle biopsies from COPD subjects (n=25) had higher *TNF-α* mRNA and protein expression than those from healthy age matched controls. *TNF-α* mRNA correlated negatively with maximum inspiratory sustainable pressure in COPD subjects.	Casadevall *et al* (104)
	No differences in serum TNF-α between 4 groups of COPD subjects based upon BMI (n=44 in total). *TNF-α* mRNA in adipose tissue (probably secreted by macrophages) was positively correlated with BMI and predicted insulin resistance. There was no up-regulation of adipose tissue *TNF-α* mRNA in the cachectic group compared to other groups. No healthy control comparison.	Skyba *et al* (105)
	Quadriceps muscle biopsies from patients with severe COPD and with high *TNF-α* mRNA expression (n=17), had reduced mRNA expression of enzymes involved in oxidative metabolism compared to biopsies from mild COPD patients (n=17) and healthy controls (n=10) with *low* muscle *TNF-α* mRNA expression.	Remels *et al* (106)

Study design	Findings	Author/ reference
Human models (prospective): Pulmonary and Systemic	TNF-α concentration was higher in the sputum of COPD patients with a bacterial exacerbation than those with a non-bacterial exacerbation. Change in TNF-α concentration in sputum from baseline to exacerbation was only significant in the subjects with a bacterial exacerbation.	Bathoorn *et al* (81)
	Subjects with moderate to severe COPD (n=14) were followed up before and after an exacerbation. TNF-α concentration in the sputum increased at the time of the exacerbation and had decreased back to baseline levels by one month.	Aaron *et al* (80)
	Serum TNF-α higher in COPD subjects (n=1755) than in healthy controls but lower than in healthy smokers/ex-smokers. Having a persistently raised inflammatory phenotype (2 or more serum biomarkers, which could include TNF-α) raised at baseline and one year was predictive of increased risk of exacerbation and all-cause mortality at 3 years.	Agusti *et al* (107)
	COPD subjects (n=408) with "high" plasma TNF-α (>2.2 pg/ml) at years 0 and 1 had a greater decline in fat free mass over time *if* cachectic at baseline.	Eagan *et al* (108)
	Serum TNF-α higher in GOLD III and IV disease (n=253) than other stages. A model combining IL-6, CXCL8, IL-16 and TNF-α results predicted worse lung function, symptoms and mortality if in the highest quartile for those pro-inflammatory biomarkers. No difference in BMI between highest and lowest quartiles for TNF-α levels.	Pinto-Plata *et al* (109)
	Serum TNF-α raised in COPD subjects (n=63) at the time of an exacerbation compared to resolution and in the stable state.	Krommidas *et al* (110)
	Serum TNF-α raised in COPD subjects (n=93) at the time of an exacerbation compared to resolution and in the stable state.	Markoulaki *et al* (111)

The table summarises the evidence suggesting a role for TNF-α in COPD pathogenesis from human and animal studies. A general critique of these studies is provided in the text.

BAL- bronchoalveolar lavage; BMI- body mass index; CB- chronic bronchitis; CSE- cigarette smoke extract; COPD- chronic obstructive pulmonary disease; FEV1- Forced expiratory volume in one second ; GOLD- Global initiative for chronic obstructive lung disease; KO- knock out ; LPS- lipopolysaccharide; MMP- matrix metalloprotease; mRNA- messenger ribonucleic acid; sTNFR- soluble TNF-α receptor; WT- wild type.

1.4.1 TNF-α blockade in COPD

In view of the animal and human studies which suggested a role for TNF-α in COPD, clinical studies were designed to test the effects of TNF-α blockade in the disease. Two types of anti-TNF-α molecules are available. Monoclonal antibodies which bind to TNF-α can be chimeric, containing mouse and human deoxyribonucleic acid (DNA) (infliximab), humanised (certolizumab) or fully human in source (adalimumab, golimumab) (112). Etanercept is a receptor fusion protein whereby the DNA coding for TNFR2 and the constant end of human immunoglobulin 1 (IgG1) were sequenced and combined to produce a molecule which is capable of binding trimerised TNF-α. All five agents can bind both soluble TNF-α (sTNF-α) and membrane TNF-α (mTNF-α) (112). Anti-TNF-α mAbs had initially been developed to treat sepsis, without success, but following promising early trials by Feldmann *et al's* group of a chimeric mAb in rheumatoid arthritis interest in these mAbs exploded and they are now routinely used in rheumatoid arthritis, psoriasis, ankylosing spondylitis and IBD (23).

The first study in COPD was a small phase 2 randomised controlled trial (RCT) in which 14 mild/moderate COPD patients were randomised to receive three doses of infliximab over a six week period and eight to receive placebo. TNF-α blockade in this short term study had no effect on the primary outcome of sputum neutrophilia, nor on lung function or quality of life (113). A larger RCT conducted by Rennard *et al* randomised patients with moderate to severe

COPD to one of two doses of infliximab (n=79) or to placebo (n=77) for a total of six doses over 24 weeks, following patients up for 44 weeks from the start of the trial (114). The primary end-point for this study was a clinical outcome, the Chronic Respiratory Questionnaire, along with multiple secondary clinical outcomes, such as exacerbation frequency, and physiological outcomes. All outcomes were negative, although post-hoc analysis revealed significant improvements in the 6 minute walk distance of young or cachectic subjects. Of note a greater number of patients in the active treatment group developed cancer or pneumonia and although this was not statistically significant, raised serious issues about this therapeutic approach.

Whilst it is disappointing that these studies have not shown positive results it must be considered that blockade of TNF-α in moderate to severe COPD may be too late in the disease trajectory to make any clinical difference. In addition the individuals studied were from an unselected population of COPD patients and in general the systemic TNF-α levels were low. It may be that a particular TNF-α dependent phenotype of COPD would be responsive to TNF-α blockade or that local delivery of anti-TNF-α therapy to the airways would be more appropriate. However, the potential risks of malignancy and infection in this group, raised as a concern in the aforementioned trials mean that there may be a reduced appetite for revisiting this issue.

1.5 **TNF-A**

1.5.1 Location of the TNF-A gene

TNF-A, the gene coding for the TNF-α protein is located on the short arm of chromosome 6 at position 6p21.3 (115) and lies within the class III region of the major histocompatibility complex (MHC) genes. Class III genes are found between the class I region, which codes for

human leukocyte antigen (HLA)-A, B and C antigens (antigen presenting molecules found on all nucleated cells and which present to CD8 T-cells) and the class II region, which codes for HLA-DP, DQ and DR antigens (antigen presenting molecules found on classical APCs such as dendritic cells and which present to CD4 T-cells). The MHC region of the chromosome measures 4 mega base pairs (bp) in length, has a high degree of genetic variation and is well known to undergo linkage disequilibrium, in which particular genes are not randomly separated at meiosis and hence are often co-inherited as an extended haplotype (115). Figure 1.2 shows the TNF-A locus.

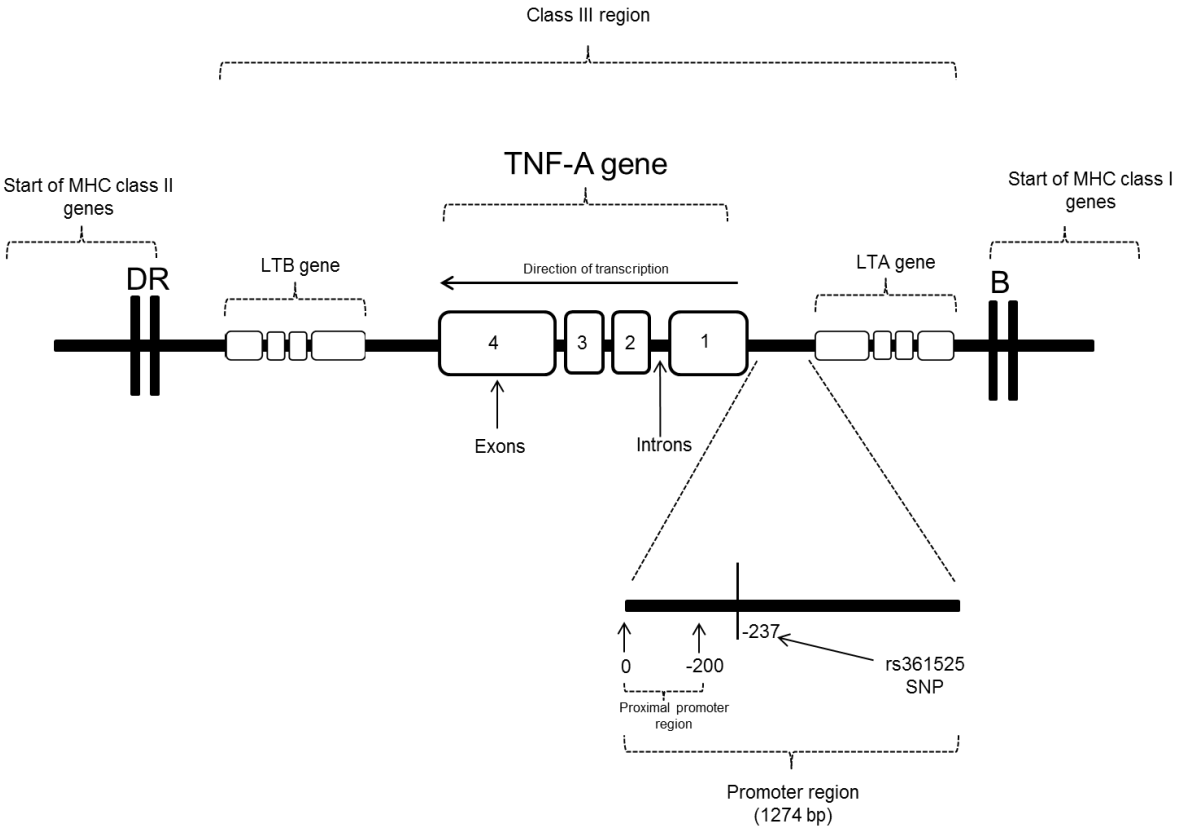

Figure 1-2 The TNF-A gene

The TNF-A gene is shown located between the lymphotoxin beta (LTB) and lymphotoxin alpha (LTA) genes (not to scale) within the class III region of the MHC genes. The TNF-A gene contains 4 exons and a promoter region, covering approximately 3 kilobase pairs. Exon 1 begins with nucleotides coding for the 5' untranslated region (UTR) of the gene and exon 4 ends with nucleotides coding for the 3' UTR, with the remaining exon nucleotides coding for the actual TNF-α protein. The expanded region highlights the promoter region of the gene. Position 0 relates to the first nucleotide in exon 1 and bp upstream of this in the promoter region are assigned negative numbers dependent on their distance from this nucleotide. Bp -1 to -200 comprise the proximal part of the promoter region. Position 237 has been highlighted and is the location of one particular SNP, the rs361525 polymorphism, studied in this thesis. Adapted from Posch *et al* (116).

1.5.2 Polymorphisms in the TNF-A gene

SNPs are substitutions of the usual nucleotide found at a position in a gene sequence by one of the other three possible nucleotides (A-adenine; T-thymine; C-cytosine; G-guanine). SNPs can affect either one (heterozygous) or both (homozygous) copies of the gene that an individual carries. As the MHC complex on chromosome 6 displays more genetic variation than any other chromosome (115) it is unsurprising that the TNF-A gene has been identified as having multiple SNPs. The majority (ten) of these are located in the promoter region of the gene. However, nine of these are situated beyond the highly conserved proximal promoter, upstream of bp -1 to -200, a region whose role in affecting gene transcription has been less well established. Others are located in the introns or exons and one is within the exon coding for the 3' UTR of the transcript (116). It has been speculated that SNPs may alter the binding capabilities of transcription factors, which bind to the promoter region and facilitate gene transcription, and hence may affect mRNA expression of the gene, either positively or negatively, and that this in turn may affect phenotypes of disease. To that end genetic association studies, either case-controlled or family based, and more recently genome-wide association studies (GWAS), have investigated many SNPs in a vast number of diseases. This thesis will in part concentrate on the investigation of one particular SNP in TNF-A, the rs361525 polymorphism, in A1ATD-related COPD.

1.6 COPD and the relevance of genetic variation

There has been a move in recent years to divide COPD into particular phenotypes, with the aim of being able to classify patients into groups that would provide a clearer idea about an individual's prognosis and response to available treatment (117). Phenotypes can be chosen based on clinical, radiological or physiological parameters. However, it is also important to consider the effect that an individual's genetic make-up might have on the clinical expression

of the disease as this may have a greater impact on designing effective tailored treatments than by considering clinical phenotypes alone. The only well characterised example of genotype influencing the development of COPD is that of defects within the serpinA1 gene in A1ATD.

It is possible that polymorphisms within other genes also contribute to COPD pathogenesis and might partly explain the heterogeneity of clinical expression of the disease between individuals and why only 25% of smokers develop clinically significant COPD (40). To this end genetic association studies have been performed investigating whether a wide range of SNPs are more frequent in COPD patients. A number of systematic reviews have attempted to collate results from these studies to determine which gene polymorphisms, (generally SNPs within inflammatory or antioxidant genes or genes involved in protease/anti-protease processes) are relevant to COPD, with conflicting results (118-122). There are a number of limitations with these case-control genetic association studies, including differences in clinical characteristics between cases and controls, methodological differences in defining COPD between studies and differences in the ethnicity and geographical location of groups within and between studies. These limitations make replication of results in other case-control populations and the combining of individual studies in meta-analyses a significant challenge. More recently we have witnessed the emergence of GWAS which have tested very large populations of individuals for a multitude of SNPs across the whole genome and then determined which of these confer susceptibility for particular diseases. Whilst GWAS importantly eliminate some of the issues observed with smaller case control or family based association studies there are still limitations, namely the dilution or loss of association of a SNP when a population is viewed globally. For example, SNPs causing A1ATD are not

shown to be associated with COPD when individuals of all ages were considered as opposed to a younger subset (123).

1.7 The rs361525 TNF-A polymorphism

The rs361525 polymorphism occurs at position -237 in the promoter region of the TNF-A gene (figure 1.2) whereby there is a substitution of the more common G nucleotide by the A nucleotide. The estimated allele frequency of the minor allele was 6.8% based on a small study in a healthy population (124). Evidence for its role in A1ATD-related COPD is considered here.

1.7.1 The rs361525 TNF-A polymorphism in A1ATD-related COPD case control studies

The importance of selecting the relevant population of patients when aiming to detect important associated SNPs is illustrated by a study by Wood *et al* (125). TNF-A gene polymorphisms have been studied in genetic association and laboratory based studies in a number of inflammatory diseases, including COPD (115, 118, 119). Wood *et al* studied four previously identified polymorphisms of the gene, including the rs361525 polymorphism, in a cohort of 424 unrelated patients with A1ATD-related COPD (125). Each patient was phenotyped based on the presence of emphysema and/or bronchiectasis and/or CB. The rs361525 allele was seen with greater frequency in subjects with CB (odds ratio of having the minor A allele in the CB group was 2.08, $p = 0.01$), independent of the presence of other phenotypes. No association was observed for the other polymorphisms. Previous meta-analyses of genetic association studies have not shown an association between the rs361525 polymorphism and usual COPD (118, 119). The study by Wood *et al* however is unique in that it identified an association between a TNF-A polymorphism and CB, a particular phenotype of COPD, specifically in A1ATD-related COPD.

1.7.2 The rs361525 TNF-A polymorphism in A1ATD-related COPD in-vitro studies

Sapey *et al* investigated this polymorphism further in a cohort of twelve A1ATD patients with COPD in in-vitro studies. Clinically, 83% of patients with the polymorphism (all heterozygotes with the AG genotype) were found to have a CB phenotype compared to 31% of patients with COPD without the polymorphism (GG) ($p<0.0001$), concurring with Wood *et al's* findings at case-control level (17). Affected patients also had a lower body mass index (BMI) and a greater decline in FEV1 over three years compared to the GG group, suggesting a more aggressive disease phenotype. In laboratory experiments a number of statistically significant results were obtained. Spontaneous sputum samples from ten AG patients were found to contain 100 times greater concentrations of TNF-α than sputum from ten matched GG patients (figure 1.3). There was also a 20 times greater concentration of CXCL8 and 10 times greater concentration of myeloperoxidase (MPO- a marker of neutrophil activation) than GG patients (figure 1.4). CXCL8 plays a key role in COPD as it is an important neutrophil chemo-attractant and is induced by TNF-α (79). However, no significant differences were observed in plasma concentrations of TNF-α between the two groups, indicating the importance of local production in the airways.

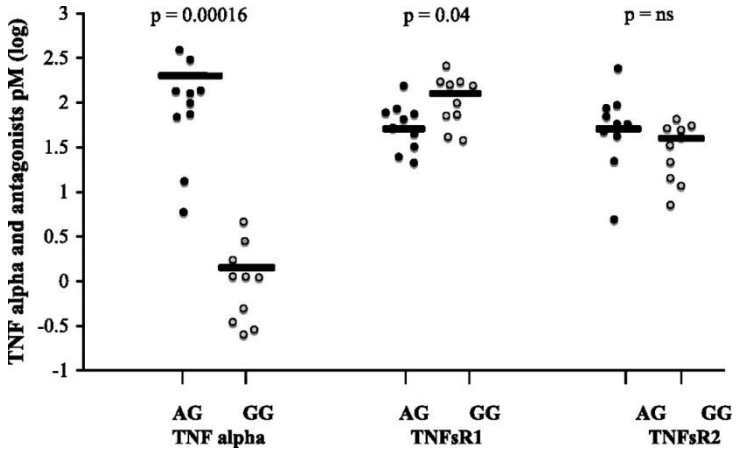

Figure 1-3 sTNF-α and receptors in sputum of AG and GG subjects

The graph shows the differences in mean logged concentrations of sTNF-α and soluble TNFR1 (sTNFR1) and sTNFR2 in the sputum of COPD patients with (AG) or without (GG) the rs361525 polymorphism. Each point equates to one subject's data. The mean is shown as a horizontal bar. Significant differences were observed in sTNF-α and sTNFR1 concentrations between the two groups. Reproduced from Sapey *et al* (17).

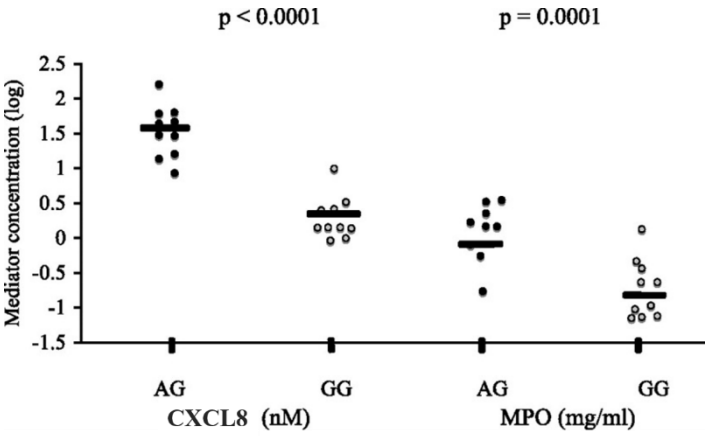

Figure 1-4 CXCL8 and MPO in sputum of AG and GG subjects

The graph shows the differences in mean logged concentrations of CXCL8 and MPO in the sputum of COPD patients with (AG) or without (GG) the rs361525 polymorphism. Each point equates to one subject's data. The mean is shown as a horizontal bar. Reproduced from Sapey *et al* (17).

These data show that patients carrying the rs316525 polymorphism have a far greater concentration of sTNF-α in their airways and slightly less sTNFR1 (but not sTNFR2) and hence there is more free sTNF-α to act upon other cell types and induce downstream inflammation as evidenced by increased CXCL8 and MPO. These data strongly suggest functionality of the SNP in altering TNF-α output by cells in the patients' airways.

The strongest evidence for an association of the rs316525 polymorphism with other disease is seen in psoriasis and psoriatic arthritis. A recent meta-analysis of a large number of case control studies showed an odds ratio of developing either psoriasis or psoriatic arthritis of 2.23 (95% confidence interval (CI) of 1.63-3.05) when patients carried the minor A allele. Again the results may be limited by heterogeneity of study populations and disease characteristics (126).

1.7.3 Assessing if the rs361525 TNF-A polymorphism is functional

Given the associations of SNPs with clinical disease in case control studies many authors have attempted to determine if the presence of a particular SNP, including the rs361525 TNF-A polymorphism, affects gene transcription and hence protein production, at a cellular level. A study conducted by Fong *et al* identified that the region of the promoter sequence of the TNF-A gene lying between bp -254 to -230 acts a repressor of TNF-α transcription. This was determined because replacement of this region in monocytic cell lines with DNA constructs lacking this section of the gene led to greater than usual output in reporter gene expression assays (127). This suggested that if the rs361525 polymorphism genuinely is functional it is occurring through loss of wild-type gene repression. In contrast, another more recent study, suggested that the presence of the A allele actually acts as a promoter of gene transcription (128).

Proving functionality of a SNP is clearly therefore difficult and as with other polymorphisms, studies examining the rs361525 polymorphism have shown conflicting results, as summarised in table 1.2. The methods used in investigating SNP functionality and their limitations are discussed below.

Chromatin immunoprecipitation (ChIP) assays can be used to detect preferential binding of RNA polymerase to the non-wild type allele in heterozygotes (129), with the inference therefore that the presence of the SNP affects gene transcription. Reporter gene assays can be used to transfect immortalised cell lines with an altered promoter sequence, attached to a gene which encodes for a measurable and quantifiable product. Examples include the chloramphenicol acetyltransferase (CAT) assay which measures acetylation of radioactively labelled chloramphenicol (127) and the luciferase assay which catalyses a reaction involving luciferin to emit light (130). Stimulation of transfected cells will lead to a quantifiable output from the assay dependent upon the function of the altered promoter sequence. Other authors have directly measured the mRNA or protein concentrations of TNF-α in plasma/serum or stimulated whole blood, monocytes or peripheral blood mononuclear cells (PBMCs-monocytes and lymphocytes) from patients carrying the SNP compared to wild-type subjects (131-140). With the exception of ChIP assays, all of these techniques have been used to investigate the rs361525 polymorphism (table 1.2).

There are limitations to all of these methods. Reporter gene assays may affect the complicated higher level structure that DNA forms with histone proteins to make nucleosomes. Slight changes in structure may therefore affect the binding capability of transcription factors and this may be wrongly attributed to an effect or lack of effect of a polymorphism. Measuring protein or mRNA content in serum might not reflect what is occurring within a particular organ system and indeed this was observed in the study by Sapey *et al* whereby a marked

increase in TNF-α concentration was seen in the rs361525 polymorphism group in the sputum but not in the plasma (17). Definitive conclusions from in-vitro work are also difficult to draw because of methodological differences, such as the cell type and stimulus employed, concentration of stimulant and time points measured post stimulation and the disease or ethnicity of the population studied. Ethnicity is potentially important as although the presence of the SNP under investigation can be easily identified it may be that linkage disequilibrium may vary between different populations and hence a SNP in one population may be inherited as part of an extended haplotype that is different to the extended haplotype in another population. If it is the inheritance of several SNPs together that affects functionality of a promoter region or inheritance of another gene in linkage disequilibrium with the SNP under investigation, then looking at an isolated SNP in one population may yield a different conclusion to that obtained from another. It is evident therefore that is important not to discount the relevance of a SNP based upon conflicting results from heterogenous studies but to concentrate instead on investigating the SNP within a single disease and homogenous population, as has been done by Wood *et al* (125) and Sapey *et al* (17) and presently in the current thesis, in A1ATD-related COPD.

Table 1-2 Studies investigating the cellular effects of the rs361525 TNF-A polymorphism

Study population	Healthy controls. N=50 10% AG; 90% GG
Ethnicity	Unspecified (North European study)
Methods	Monocytes- 4 hours stimulation mRNA quantified by RT-qPCR and protein by ELISA.
Stimulant	Basal; LPS
Outcome (AG vs GG)	No difference
Author/reference	Mekinian *et al* (131)
Study population	Immortal cell lines
Ethnicity	N/A
Methods	a) U937 and MonoMac6 cells (monocytic cells) - transfected with DNA construct and luciferase reporter gene. Stimulated for 4 hours. b) Jurkat (T-cell line) and Raji (B-cell line) cells - transfected with CAT reporter gene. 24 hours stimulation.
Stimulant	a) Basal ; LPS+/- PMA b) Basal; PMA+/- anti-CD3 mAb
Outcome (AG vs GG)	a) No difference b) No difference
Author/reference	Kaijzel *et al* (130)
Study population	Immortal (mouse) cell lines
Ethnicity	N/A
Methods	T-cell clone Ar-5 and B-cell lymphoma line A20. - transfected with DNA construct and CAT reporter gene.18 hours stimulation.
Stimulant	Basal; PMA and ionomycin
Outcome (AG vs GG)	No difference
Author/reference	Uglialoro *et al* (141)

Study population	Healthy controls and subjects with positive T. cruzi serology N=214; 22% AA; 16% AG; 62% GG
Ethnicity	Unspecified (South American study)
Methods	PBMCs. 48 hours stimulation. Protein measured by ELISA.
Stimulant	LPS; PHA; T. cruzi antigen
Outcome (AG vs GG)	In all patients- LPS induced slightly more TNF-α in combined AA/AG group vs GG group. In T.cruzi positive subjects- LPS and T.cruzi antigen induced more TNF-α in combined AA/AG group vs GG group.
Author/reference	Pissetti *et al* (132)
Study population	Psoriasis N=48 30% AG; 70% GG Immortal cell lines
Ethnicity	Unspecified (North European study)
Methods	PBMCs (from patients) - 24 hours stimulation. Protein measured by ELISA. Jurkat and Raji cells- transfected with DNA construct and luciferase reporter gene. Stimulated for 8 and 15 hours respectively. DNA constructs contained haplotypes of SNPs- -308G/-238A; -308A/-238G; -308G/-238G.
Stimulant	Basal ; LPS; PMA; antiCD3 mAb; strep antigen; PHA (PBMCs) Basal; Ionomycin and PMA (cell lines)
Outcome (AG vs GG)	PBMCs- AG subjects secreted less TNF-α than GG subjects if stimulated with antiCD3 mAb or streptococcal antigen. No difference with other stimuli. Jurkat cells- reduced activity in stimulated AG cells. Raji cells- reduced activity in basal and stimulated AG cells.
Author/reference	Kaluza *et al* (140)

Study population	Relatives of subjects with severe sepsis N=183 11% AG; 89% GG
Ethnicity	Unspecified (North European study)
Methods	Whole blood- stimulated ex-vivo for 6 hours. Protein measured by ELISA.
Stimulant	LPS
Outcome (AG vs GG)	No difference
Author/reference	Westendorp *et al* (133)
Study population	Healthy controls N=78
Ethnicity	Unspecified (North European study)
Methods	Monocytes- 18 hours stimulation. Protein measured by ELISA.
Stimulant	LPS
Outcome (AG vs GG)	No difference
Author/reference	Pociot *et al* (136)
Study population	Healthy controls (some families) N=752 1% AA; 12% AG; 87% GG
Ethnicity	Caucasian
Methods	Plasma. Protein measured by ELISA.
Stimulant	N/A
Outcome (AG vs GG)	No difference
Author/reference	Haddy *et al* (134)

Study population	Rheumatoid arthritis N=50 Healthy controls N=50
Ethnicity	Unspecified (South European study)
Methods	PBMCs- mRNA quantified by RT-qPCR. Plasma -protein measured by ELISA.
Stimulant	N/A
Outcome (AG vs GG)	No difference in healthy controls. GG subjects produced 2X as much *TNF-α* mRNA and1.3X as much protein in the plasma
Author/reference	Oregon-Romero *et al* (135)
Study population	Ankylosing spondylitis N=67 7% AG; 93% GG
Ethnicity	Chinese
Methods	PBMCs- mRNA quantified by RT-qPCR. Stimulated for 2 hours.
Stimulant	LPS
Outcome (AG vs GG)	No difference
Author/reference	Lu *et al* (137)
Study population	Healthy controls (including some families) N=179 12% AG; 88% GG
Ethnicity	Unspecified (North European study)
Methods	Whole blood- stimulated ex-vivo for 6 hours. Protein measured by ELISA.
Stimulant	LPS
Outcome (AG vs GG)	GG subjects produced 1.5X as much TNF-α if stimulated with 10 ng/ml of LPS (familial contribution controlled for). No difference observed with 1000 ng/ml LPS.
Author/reference	Huizinga *et al* (142)

Study population	Severe sepsis N=62 13% carried A allele (genotype unspecified); 87% GG
Ethnicity	Caucasian
Methods	PBMCs at 24 hours post admission- mRNA quantified by RT-qPCR. Plasma -protein measured by ELISA.
Stimulant	N/A
Outcome (AG vs GG)	No difference
Author/reference	O'Dwyer *et al* (138)
Study population	Sarcoidosis N=83; 4% carried A allele (genotype unspecified); 96% GG Healthy controls N=155; 5% carried A allele; 95% GG
Ethnicity	North Indian
Methods	Serum. Protein measured by ELISA.
Stimulant	N/A
Outcome (AG vs GG)	In the sarcoidosis subjects 23X greater TNF-α protein in the serum of AG group. No difference in the healthy control group.
Author/reference	Sharma *et al* (139)
Study population	Immortalised cell line (mouse)
Ethnicity	N/A
Methods	DNA constructs with either A or G allele and a luciferase reporter assay transfected into RAW 264.7 cells (murine macrophage-like cells)
Stimulant	LPS; lipoteichoic acid
Outcome (AG vs GG)	2.2 to 2.8 greater transcriptional activation in A-allele transfected cells.
Author/reference	Kiss-Toth *et al* (128)

Study population	COPD/A1ATD N=20 50% AG; 50% GG (purposely matched)
Ethnicity	Caucasian
Methods	Sputum and plasma
Stimulant	N/A
Outcome (AG vs GG)	100X greater TNF-α protein in the sputum of AG group than in GG group. No difference in plasma.
Author/reference	Sapey *et al* (17)

The table summarises the results of all studies investigating if the rs361525 TNF-A polymorphism affects TNF-α secretion by cells. For studies involving reporter gene assays- reporter genes were attached to DNA constructs encoding a portion of the TNF-A promoter region containing the -237 A allele or WT -237 G allele. A general critique of the methods used in these studies is provided in the text above.

CAT- chloramphenicol acetyltransferase; COPD- chronic obstructive pulmonary disease; DNA- deoxyribonucleic acid; ELISA: enzyme linked immunosorbent assay; LPS: lipopolysaccharide; ml: millilitre; mRNA: messenger RNA; ng: nanogram; PHA: phytohaemagglutinin; PMA: phorbol 12-myristate 13-acetate; RT-qPCR: real-time quantitative polymerase chain reaction; strep: streptococcus; T. cruzi: Trypanosoma cruzi

1.8 **Control of TNF-α production**

It is important to recognise that whilst binding of transcription factors or release of gene silencers at the promoter is vital, multiple other steps are also involved in the control of production of TNF-α, from transcription through to the post-transcriptional stages and processing of the protein itself. These are complex affairs, varying between cell types, in response to different stimuli and showing a high degree of redundancy (143-145).

Broadly, control mechanisms can be considered to act at specific stages: 1) through changes to chromatin structure allowing or preventing transcription factors access to the promoter region of a gene (epigenetic regulation), 2) binding of transcription factors to the promoter or

release of repressive factors allowing gene transcription, 3) alterations to the gene itself which may enhance or repress subsequent transcription (epigenetic regulation), 4) splicing of pre-mRNA transcripts into the final mRNA sequence 5) post-transcriptional stabilisation of the mRNA transcript prior to translation (epigenetic regulation), 6) cleavage of pro-TNF-α from the cell surface and 7) functional blockade of sTNF-α by soluble TNFR1 and TNFR2. Some examples of these mechanisms are considered below but are by no means exhaustive.

1.8.1 Control of TNF-A transcription

At the histone level acetylation by acetyltransferases can facilitate the binding of transcription factors to the promoter region by relaxing chromatin fibres and allowing access to DNA and conversely histone deacetyltransferases will repress this process (145-148). For example, an increase in acetylation of histone H4 at the TNF-A locus was associated with TNF-A transcription in human monocytes (149). In addition, these enzymes can regulate gene transcription in other ways, for example, histone deacetyltransferase 3 can decrease the phosphorylation of the enzyme MAPK11 leading to inhibition of activity of the transcription factor activating transcription factor 2 (ATF-2) with a resultant decrease in TNF-A transcription (150). Broadly when considering all cell types, histone methylation and phosphorylation are also believed to both promote and repress TNF-A transcription through changes to chromatin structure affecting the binding capabilities of transcription factors and may play a role in control of TNF-A transcription (146, 151). At the DNA level direct methylation of the TNF-A gene in monocyte cell lines represses gene transcription (146).

Following changes to chromatin structure, for genes to undergo transcription it is necessary for protein transcription factors to bind to specific areas of the gene DNA, usually in the promoter region and/or for gene silencers to detach themselves (10). TNF-α is secreted in response to a broad range of stimuli, including bacteria and bacterial products, other

cytokines, mitogens and viruses (144). It is unsurprising therefore that a large number of different transcription factors have been identified as being possible TNF-A gene activators and these may be cell and stimulus specific (144).

The region of the promoter lying between -1 to -200 bp has been most well investigated with respect to identifying binding sites and their complementary transcription factors. This area contains a TATA box, several cis-acting regulatory elements (CREs), six nuclear factor of activated T-cells (NFAT) binding sites, two specificity protein 1 (Sp1) binding sites, four E26 transformation-specific transcription factor (Ets) and ETS domain-containing protein (Elk) binding sites and an Early growth response protein (Egr) binding site (144). Members of the NFAT transcription factor family and the transcription factors ATF-2 and c-jun (the latter two acting in heterodimer form) bind separately to NFAT and CRE binding sites respectively but act in unison as an enhancesome. Of note the NFAT transcription factors are not believed to be involved in TNF-A transcription specifically in monocytes and macrophages (144).

In monocytes LPS induces TNF-A transcription by up-regulating the Extracellular-signal-regulated kinase (ERK) substrates ETS and Elk-1 which bind in conjunction with a number of other transcription factors, ATF-2, c-jun, Egr-1, and Sp1, and two co-activator proteins, cyclic AMP response element-binding protein (CREB) and p300, to the proximal promoter region of the gene and act as an enhancesome. Of interest the binding site for this complex is the same sequence of the TNF-A promoter region that usually binds NFAT transcription factors in T-cells upon T-cell receptor ligation by antigen presenting cells, demonstrating the cell and stimulus specific nature of TNF-A transcription (144).

Transcription factor binding sites (and their respective transcription factors) in the promoter region upstream of position -200, defined as the distal promoter and including the -237

position of the rs361525 SNP under study, are less well characterised. However, ChIP assays have implicated other transcription factors including NFκB members, particularly p65, in TNF-A transcription in LPS-stimulated monocytic cells (144) and that binding sites for these in the promoter region lie within the distal promoter (152, 153), making LPS an attractive stimulant to use in the studies in this thesis. The transcription factors involved in TNF-A transcription in monocytes in response to LPS are summarised in figure 1.5.

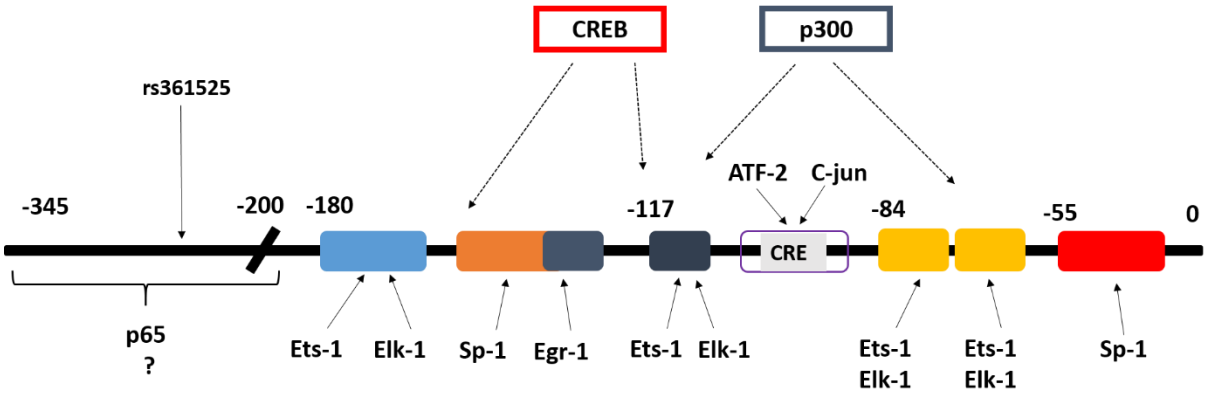

Figure 1-5 Transcription factors involved in the transcription of TNF-A in monocytes in response to LPS

The diagram illustrates the promoter region of the TNF-A gene. The proximal part of the promoter lies between 0 bp and -200 bp. Transcription factors bind to their respective binding sites (shown as coloured boxes) within the promoter, for example Ets-1 binds to Ets-1 binding site. ATF-2 and c-jun bind to a CRE. CREB and p300 are co-activator proteins that also bind within the proximal promoter, downstream of -200 bp, and altogether act as an enhanceosome to facilitate TNF-A transcription. The distal promoter lies upstream of -200 bp; the sequence containing the -237 position is shown. The only transcription factor identified via ChIP assays to bind in this region between -345 bp and -195 bp following LPS stimulation is the NFκB family member p65. The exact location of the binding site for p65 is unknown. Adapted from Falvo *et al* (144) and Suriano *et al* (152).

ATF-2: activating transcription factor 2; CRE: cis-acting regulatory element; CREB: cyclic AMP response element-binding protein; Egr-1: Early growth response protein 1; Ets: E26 transformation-specific transcription factor; Elk: ETS domain-containing protein; Sp1: specificity protein 1.

1.8.2 TNF-A transcript regulation

Once TNF-A has been transcribed the pre-mRNA is spliced to remove introns. Splicing of *TNF-α* mRNA transcripts is regulated in part by binding of protein kinase R (154). The mRNA transcript is then subject to post transcriptional regulation within the cytoplasm, without which the transcript rapidly degrades (155) . Modulation occurs at two locations: adenosyl-uridyl-rich elements (AREs) and microRNA binding sites, both located in the 3' UTR of the transcript. Up-regulation of p38 MAP kinase (MAPK) by the original stimulus, for example LPS, leads to the phosphorylation of two proteins, MAP kinase-interacting serine/threonine-protein kinase 1 (Mnk1) and MAPK-activated protein kinase-2 (MK-2), which subsequently bind to the ARE in the 3' UTR of the *TNF-α* mRNA. These proteins act either via deactivating constitutive repressor proteins or by functioning as enhancers (156). The end result is increased transcript stability and translation. MicroRNAs are short lengths of RNA which have no coding function but can bind approximately complementary nucleotide strands on mRNA transcripts and so affect stability of the mRNA (156).

1.8.3 Control of the TNF-α protein

Although active at the cell surface TNF-α is also cleaved and released into the circulation or peri-cellular environment. In AMs, cleavage of mTNF-α from the cell surface is controlled for the most part by the enzyme TACE, expressed on the cell surface and TNF-α has been demonstrated to regulate further TACE expression in a negative feedback loop. In addition, proteinase 3 secreted by neighbouring neutrophils was able to cleave mTNF-α from the surface of AMs by binding to the cell membrane (157). Lastly, soluble TNFR1 and TNFR2 also act as circulating inhibitors of sTNF-α (4) and the receptors are discussed further in 1.9.

1.9 **TNF-α receptors**

1.9.1 Overview

The two TNF-α receptors, TNFR1, a 55kDa protein and TNFR2, a 75kDa protein, are coded for on chromosomes 12 and 1 respectively (158). The receptors are composed of glycoproteins which span the cell membrane and have similar extracellular structure but different intracellular domains (159). Each receptor has four extracellular cysteine-rich domains (CRD) and TNF-α binds to CRD 2 and 3 (160). For binding to occur to either TNFR1 or TNFR2, both receptors must first form a trimer with two other receptors, creating a complex to which a TNF-α trimer can then bind. The domain on each receptor responsible for this is separate to the site for TNF-α ligation and is termed the pre-ligand-binding assembly domain (161). Lymphotoxin-alpha, secreted by lymphocytes, is the only other member of the TNF superfamily also able to bind both TNFR1 and TNFR2, but is thought to elicit its functions through alternative receptors (11, 162).

TNFR1 is expressed on most cell types in humans. In contrast TNFR2 is found only on the surface of immune cells and vascular endothelial cells (4). Each of the receptors can be cleaved from the cell surface to circulate freely and act as endogenous inhibitors of TNF-α (163). Both receptors have high affinity for soluble TNF-α with TNFR1 having greater affinity at physiological temperatures. Dissociation of TNF-α from TNFR1 is far slower than from TNFR2, with a half life time of 33.2 minutes versus 1.1 minutes respectively, when internalisation of the receptor-ligand complex is controlled for (163, 164). For these reasons soluble TNFR1 is likely to be the more effective inhibitor. The membrane form of TNF-α is also metabolically active, stimulating both TNF-α receptors (165, 166), in a paracrine and autocrine manner (166). However whilst sTNF-α and mTNF-α can bind to either receptor, only mTNF-α can activate TNFR2 (165, 167).

1.9.2 Role of TNFR1 and TNFR2 in physiological and pathological processes

Many studies have been conducted to investigate the relative roles of TNFR1 and TNFR2, mainly using animal models. Initial work suggested that TNFR2 did not directly trigger an intracellular signalling cascade but instead acted as a "ligand passer", concentrating sTNF-α at the cell surface as a result of its high affinity for binding followed by rapid dissociation, thereby making more of the cytokine available to bind to TNFR1 (163, 168). Subsequent investigation indicated this was unlikely to be correct for several reasons. Firstly, dissociation constants which suggested the presence of TNFR2 was needed to facilitate binding of sTNF-α to TNFR1 were calculated from experiments conducted at 0^{o}C (168). When repeated at physiological temperatures it became evident that in fact TNFR1 was actually the higher affinity receptor, thereby obviating the need for ligand passing (164). Secondly, many cell types express only TNFR1 and yet can still signal effectively (4).

The discovery that TNFR2 could only be activated by mTNF-α (165, 169) led to elegant studies showing that TNFR2 activation by agonist mAbs simulating the action of mTNF-α could in fact activate NFκB, leading to pro-inflammatory IL-6 secretion by an immortalised human cell line. However IL-6 was secreted to a far lesser extent than that induced by sTNF-α-TNFR1 signalling (169). Fascinatingly, whilst TNFR2 signalling only led to a modest NFκB effect, dual receptor ligation increased the apoptotic capability of TNF-α by 1000 fold compared to TNFR1 signalling alone and this was dependent on the presence of the adaptor molecule TNF receptor-associated factor 2 (TRAF2) binding to the intracellular portion of TNFR2 (169). Later work identified this to be due to TNFR2 mediated depletion of TRAF2 from the TNFR1 signalling complex rather than as a result of induction of downstream TNFR2 signalling pathways (see 1.9.3) but indicates the synergistic effect of both receptors in TNF-α induced apoptosis.

Table 1.3 outlines the results of studies that have attempted to define the roles of the two receptors further. In summary, data specifically from studying human cells are severely limited with most work having been conducted in animal models. The available evidence illustrates the complexity of differential TNFR1/2 roles, precluding a straightforward delineation into pro- versus anti-inflammatory signalling, at least in animal models. Both receptors clearly play a role in immune function, with TNFR2 perhaps being especially important in virus elimination and regulation of the immune response. Certainly its preferential expression on human CD4+FoxP3+ T-reg cells (a subgroup of T-reg cells which have a vital role in preventing excessive immune responses) over effector T-cells is important in controlling the function of the latter group of cells (170). Of note, in some animal disease models TNFR2 mediates an anti-inflammatory role (multiple sclerosis, rheumatoid arthritis) whereas in others its role is less certain or it contributes in part to pro-inflammatory effects (IBD, inflammatory lung diseases). Whilst animal studies are undoubtedly useful their findings may not bear close resemblance (in all cases) to human disease and global deletion or over-expression of the receptors in mice does not help identify particular cells which may be responsible for noted effects. Studies of TNFR2 especially in human cells are lacking to date.

Table 1-3 Evidence for the differential roles of TNFR1 and TNFR2 in health and disease

Immune system	**Details**	**Model**	**Ref**
TNFR1	Normal development of Peyer's patches, follicular dendritic cell clusters and germinal centres	Genetically modified mice (KO model)	(171)
	Mediates response to intracellular bacteria and effective granuloma formation	Genetically modified mice (KO models) +/- antagonist mAbs	(11, 12, 18)
	Mediates septic shock	Genetically modified mice (KO model); antagonist mAbs	(11, 12, 172)
TNFR2	T-cell proliferation; Memory T-cell clonal expansion; expansion and increased suppressive activity of foxP3+T-regs	Human thymic cells and agonist mAbs; genetically modified mice (KO models); human T-cells	(12, 173-175)
	Apoptosis of mature CD8 T-cells (not CD4 cells)	Genetically modified mice (KO model); antagonist mAbs	(176)
	Induction of adaptive immune responses (cross-talk between dendritic cells and NKCs)	Genetically modified mice (KO model)	(177)
	Mediates CD8 T-cell responses to hepatic viruses; viral clearance	Genetically modified mice (KO/over expression models); antagonist selective TNFR1 mAb	(178, 179)
	Protection against septic shock (?soluble TNFR2)	Genetically modified mice (KO model); antagonist mAbs	(11, 12, 172)
Lungs	**Details**	**Model**	**Ref**
TNFR1	Mediates neutrophil migration into lung	Genetically modified mice (KO model-response to Mycobacterium faeni)	(11)
	Contributes to development of inflammatory cell influx in response to cigarette smoke	Genetically modified mice (KO model)	(180)
TNFR2	Protects against neutrophil migration into lung	Genetically modified mice (KO model in response to Mycobacterium. faeni)	(11)
	Involved in neutrophil, lymphocyte, macrophage accumulation in BAL fluid; activates T-cells; drives weight loss and emphysema	Genetically modified mice (KO model)	(180)

Rheumatological system	**Details**	**Model**	**Ref**
TNFR1	Drives chronic inflammatory arthritis	Genetically modified mice (KO and over expression model); use of antagonist selective TNFR1 mAb	(179, 181)
	Increases osteoclast number	Genetically modified mice (KO model)	(182)
TNFR2	Suppression of development of chronic inflammatory arthritis	Genetically modified mice (KO and over expression model); use of antagonist selective TNFR1 mAb	(179, 181)
	Decreases osteoclast number	Genetically modified mice (KO model)	(182)
Intestine/Liver	**Details**	**Model**	**Ref**
TNFR1	Drives IBD	Genetically modified mice (KO models)	(181, 183)
	Involved in hepatitis and inducing fibrosis	Genetically modified mice (KO model) +/- antagonist selective TNFR1 mAb	(184, 185)
	Mediates liver regeneration	Genetically modified mice (KO model)	(186)
TNFR2	Drives IBD (in TNF-α over-expression model). Doesn't drive IBD in CD4+ transfer model of colitis. TNFR2 required for down-regulation of disease enhancing CD4+ cells	Genetically modified mice (KO models)	(181, 183)
Neurological system	**Details**	**Model**	**Ref**
TNFR1	Initiates multiple sclerosis-like pathology; drives TH-1/TH-17 infiltration	Genetically modified mice (KO models); antagonistic selective TNFR1 mAb	(187-189)
TNFR2	Protects against/resolves MS-like pathology. Allows oligodendrocyte regeneration	Genetically modified mice (KO models); antagonistic selective TNFR1 mAb	(187-189)

Cardiovascular system	Details	Model	Ref
TNFR1	Mediates contractile dysfunction after MI. Exacerbates post-MI remodelling, hypertrophy and inflammation leading to cardiac failure. Mediates oxidative stress and diastolic dysfunction (additive effect with TNFR2)	Genetically modified mice (KO and over expression models)	(190, 191)
TNFR2	Protects against post-MI myocardial remodelling, ventricular dilatation and inflammation. Mediates oxidative stress and diastolic dysfunction (additive effect with TNFR1)	Genetically modified mice (KO and over expression models)	(190, 191)
	Mediates E-selectin, VCAM-1 and ICAM-1 expression on vascular endothelium, facilitating leukocyte transmigration	Genetically modified mice (KO model)	(192)

The table summarises the available evidence, mainly from animal models, by body system.

BAL- bronchoalveolar lavage; IBD: inflammatory bowel disease; ICAM: intercellular adhesion molecule 1; KO: knock out: mAb: monoclonal antibody; myocardial infarction; mRNA- messenger RNA; MS- multiple sclerosis; NKC: natural killer cell; VCAM: vascular adhesion molecule

1.9.3 Intracellular signalling pathways for TNFR1 and TNFR2

A body of evidence accumulated from various cell lines, including monocytes in some studies, suggests that signalling via TNFR1 leads to increased gene transcription in three ways (9, 10, 193, 194), as illustrated in figure 1.6. The figure shows how transcription factors, activated downstream in the signalling cascade, translocate to the nucleus and bind to the gene of interest (point 8). With respect to CXCL8 gene transcription specifically, the evidence suggests that it is necessary for the two transcription factors, NFκB (p50/p65) and AP-1 to bind to the gene near to a molecule known as NFκB repressing factor (NRF), which in unstimulated cells suppresses CXCL8 transcription. Binding of these three molecules to the

gene forms an enhanceosome, believed necessary for promotion of gene transcription (10, 193).

There is a relative paucity of data regarding TNFR2 signalling, in particular in monocytes. Available data obtained from various human and murine cell lines suggests that mTNF-α signals through TNFR2 via two main pathways (4, 9, 167) as shown in figure 1.7.

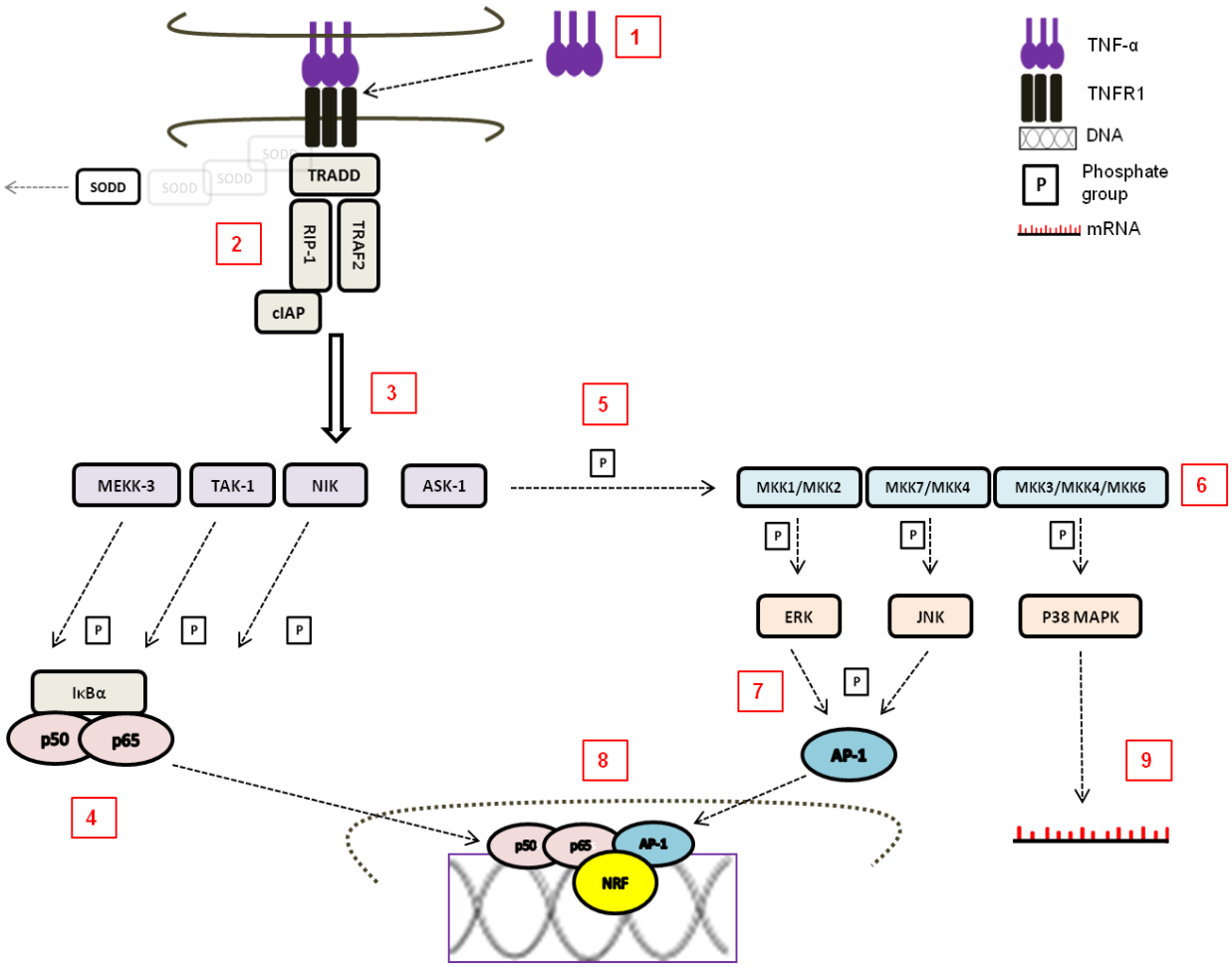

Figure 1-6 TNFR1 downstream signalling cascade activated by sTNF-α and mTNF-α

1) mTNF-α or sTNF-α binds to TNFR1. 2) TNF-α -receptor binding leads to release of SODD from the intracellular portion of TNFR1 enabling binding of an adaptor protein complex consisting of TRADD, RIP-1, TRAF2 and cIAP. 3) The adaptor protein complex activates several MAP3Ks. 4) Activated MEKK-3, TAK-1 and NIK phosphorylate IκBα leading to the release of NF-κB subunits p50 and p60 which are then free to translocate to the nucleus. 5) ASK-1 activates MAPKKs which 6) activate three MAPKs: ERK, JNK, P38 MAPK. 7) ERK and JNK activate AP-1 which translocates to the nucleus. 8) p50/p60, AP-1 and NRF form an enhancesome which leads to gene transcription. 9) p38 MAPK is able to act upon the subsequent mRNA transcript leading to transcript stabilisation.

AP-1: activating protein 1; ASK-1: apoptosis signal-regulating kinase 1; cIAP: cellular inhibitor of apoptosis; ERK: extracellular-signal-regulated kinase; IκBα: NFκB inhibitory protein; JNK: c-Jun N-terminal kinase; MAPK(K): MAP kinase (kinase); MAP3Ks: MAP kinase kinase kinases; MEKK-3: mitogen activated protein kinase kinase kinase; NIK: NF-kappa-B-inducing kinase; NRF: NFκB repressing factor; RIP-1: receptor activating protein 1; SODD: silencer of death domain; TAK-1: transforming growth factor-beta-activated kinase; TRADD: tumour necrosis factor receptor type 1-associated death domain; TRAF2: TNF receptor-associated factor 2.

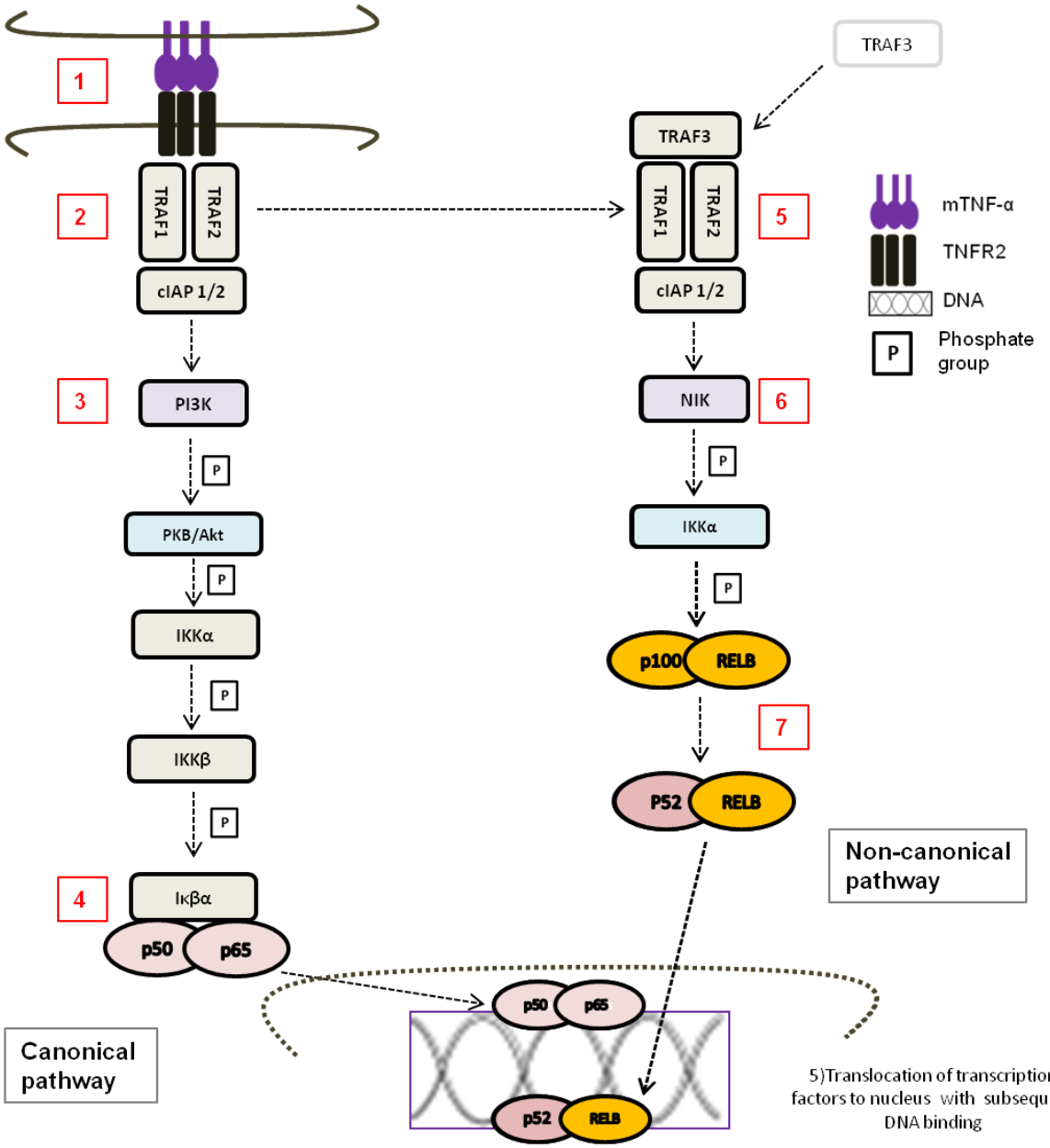

Figure 1-7 Intracellular signalling pathway activated upon TNFR2 ligation by mTNF-α

1) mTNF-α binds to TNFR2 on the surface of a TNFR2-bearing cell. 2) Upon TNF-α binding an adapter protein complex consisting of TRAF2, TRAF1 and cIAP1/2 forms, which binds the intracellular portion of the receptor. 3) The adaptor complex activates PI3K. 4) This initiates a downstream signalling cascade which leads to the release and translocation of NFκB p50/p65 subunits to the nucleus where it binds to DNA at its specific binding site (canonical pathway). 5) The TRAF2, TRAF1 and cIAP1/2 complex is also able to dissociate from the receptor and 6) activate NIK, 7) resulting in the conversion of p100/RELB NFκB dimer to p52/RELB which translocates to the nucleus to also act as a transcription factor (non-canonical pathway).

cIAP: cellular inhibitor of apoptosis; DNA: deoxyribonucleic acid; PI3K: phosphatidylinositide 3-kinase; TRAF: TNF receptor-associated factor

Apoptosis of cells as a result of TNF-α signalling occurs by the following mechanism. Release of SODD from the intracellular component of TNFR1 frees its death domain motif and allows the TRADD/RIP-1/TRAF2/cIAP complex to assemble with the receptor. This sets in motion the signalling pathways outlined previously which rapidly lead to NFκB release. Within an hour the TRADD/RIP-1/TRAF2/cIAP complex is released from TNFR1 into the cytoplasm whereby the death domain in TRADD can recruit FAS-associated death domain (FADD) which has the potential to go on to activate caspase-8, which in turn initiates apoptosis (20). However, much of the time apoptosis does not occur as the events in the apoptotic pathway occur more slowly over a period of several hours (in contrast with signalling induced by other apoptosis-inducing members of the TNF family such as Fas-ligand) allowing TNF-α induced NF-κB to up-regulate the anti-apoptotic protein FLICE-like inhibitory protein (FLIP) which switches off apoptosis (19). cIAP molecules are also anti-apoptotic (195). TNFR2 does not contain a death domain but may be able to influence apoptosis by depleting TNFR1 of TRAF2 and cIAP molecules which are needed to induce the pro-inflammatory signals which switch off apoptosis. However, the physiological circumstances and cell types in which that might occur are unclear (195).

It is unlikely that these proposed models of downstream TNFR1 and TNFR2 signalling apply to all cell types and stimuli employed, but they highlight potentially important broad differences in signalling pathways between the two receptors.

Another interesting area of research, at its early stages, is that of reverse signalling. Over-expression studies have suggested that soluble TNF-α receptors may be able to bind mTNF-α and activate reverse “outside-in” signalling, rather than just acting as inhibitors of mTNF-α. Whilst this may modulate cellular function (7) it is unlikely that the spectrum of downstream effects as a result of reverse signalling is as broad as those arising as result of classical

pathways, as otherwise binding of the receptor fusion protein, etanercept, would lead to a range of *pro*-inflammatory effects.

1.10 **Monocytes**

Monocytes are mononuclear phagocytic cells which comprise approximately 10% of the leukocytes circulating in human blood. They originate from precursor monoblast cells which themselves differentiate from a common granulocyte-macrophage progenitor, both of which reside in the bone marrow (196). The bone marrow is stimulated to produce monocytes by cytokine stimuli such as macrophage colony stimulating factor (M-CSF), granulocyte macrophage colony stimulating factor (GM-CSF) and IL-3 (multi-colony stimulating factor) (197). Monocytes are the principal secretors of TNF-α (3).

Monocytes are active cells, capable of phagocytosis and the release of cytokines and tissue damaging mediators such as ROS (198-200). At a microscopic level monocytes vary significantly in their diameter, granularity and nuclear appearance and much work has been conducted to characterise both murine and human monocyte subsets. Mouse monocytes are predominantly classified on the presence or absence of the murine-specific Ly6C (lymphocyte antigen 6C) cell surface marker. Models have suggested that the Ly6C -ve CXC3R1 ++ve monocytes form a minor population known as “patrolling” monocytes which due to a lack of the monocyte chemotactic protein 1 (MCP-1) chemokine receptor CCR2 do not generally leave the blood stream to travel to sites undergoing an infectious insult, but instead may be important in monitoring the vascular endothelium and can infiltrate tissues in the presence of endothelial damage (201). The Ly6C ++ve CCR2++ve monocytes are termed “inflammatory” as they *are* able to respond to a MCP-1 chemotactic gradient (202) and hence leave the circulation to traffic to sites of infection, where they release pro-inflammatory mediators and phagocytose bacteria (203).

1.10.1 Monocyte subsets

Human monocyte subsets can divided into three subsets: classical, intermediate and non-classical, based upon cell surface expression of two key markers, CD14 and CD16 (204). Classical monocytes comprise 90% of circulating monocytes and express CD14 but not CD16. These cells, like Ly6C ++ve murine monocytes, express CCR2 and so can respond to an MCP-1 chemoattractant gradient and leave the circulation. Their main roles are thought to be in responding to infectious insults as they are highly phagocytic and also in tissue repair (204). Although they can secrete pro-inflammatory cytokines such as TNF-α they are notably the main monocyte producers of the anti-inflammatory cytokine IL-10 (204). Intermediate monocytes express CD14 at a similar level to classical monocytes but also express CD16 at low levels. The final subset are termed non-classical and express little CD14 but high levels of CD16. Like Ly6C -ve murine monocytes they express CXC3R1, which can bind CXC3 anchored to vascular endothelial cells (205) and allow endothelial patrolling (206). They do not express CCR2. Evidence suggests that it is the non-classical subset which produces the most TNF-α in response to LPS, although all subsets do (204, 207). It is postulated that the three subtypes represent a progression of maturity from classical to intermediate to the non-classical phenotype (204). Table 1.4 summarises these subsets.

Name	% in circulation (size)	Distinguishing cell surface markers	Other key cell surface markers	Cytokine/chemokine profile (after LPS stimulation)	Mouse equivalent
Classical	90% (large)	CD14++CD16- (CD64+)	CCR2+; CXC3R1+ CD32++ CCR5++ MHC Class II+	**IL-6**; **IL-10**; **G-CSF**; **CCL2**; **RANTES**; TNF-α; IL-1β; CXCL8;	Ly6C++ CCR2++ CXC3R1-
Non-classical	10% (small)	CD14+CD16++	CXC3R1++ CCR5+ MHC Class II++	**IL-1β**; **TNF-α**; IL-10; RANTES; CXCL8; IL-6;	LyC6- CXC3R1++ CCR2-
Intermediate		CD14++CD16+ CD64+	MHC Class II++ CCR5++	IL-1β; TNF-α; IL-10; RANTES; CXCL8; IL-6	
References (203, 204)					

Table 1-4 Human monocyte subsets

The table shows the expression patterns of the most important cell surface markers delineating the three subtypes of human monocytes and their murine equivalents. Cytokine/chemokine profiles are based on work by Wong *et al* (204), whereby mediator concentrations were measured by enzyme linked immunosorbent assay (ELISA) 18 hours post stimulation with increasing concentration of LPS. Mediators shown in bold reflect the subset of monocyte which secreted most of that particular cytokine.

CD14 forms part of the LPS receptor; CD16 is also known as FcγRIII, (Fcγ are receptors for the Ig superfamily allowing induction of phagocytosis of opsonised bacteria); CD64 is also known as FcγRI; CCR2: C-C chemokine receptor type 2, binds MCP-1; CXC3R1: CXC3 chemokine receptor 1, binds CXC3; CD32 is also known as FcγRII; Ly6C: lymphocyte antigen 6C. RANTES: regulated on activation, normal T cell expressed and secreted; binds to CCR5.

+ indicates moderate expression; ++ indicates high expression; - indicates low or no expression.

1.10.2 Macrophages

Macrophages are considered in brief here, as they are a possible culprit cell for the findings in airway secretions of Sapey *et al's* study in rs361535 TNF-A polymorphism subjects (17) and in some circumstances may originate from blood monocytes (208).

Macrophages are found within tissues/organs throughout the body and as such play a role in many infection related and inflammatory diseases (208). They are essential for surveying their surroundings and reacting appropriately to maintain immune tolerance, clear undesirable material or initiate innate and adaptive immune responses and can survive several months (52). Alveolar macrophages (AMs) and interstitial macrophages (IMs) are specific to the lung, the former within the airways and the latter the lung interstitium (209). In general two subsets of macrophages have been identified, termed M1 and M2 macrophages, perhaps with a third type known as regulatory macrophages which predominantly produce IL-10. It is thought that M1 macrophages are pro-inflammatory, producing mediators such as TNF-α and IL-12 (which drive naïve TH-cells in a TH-1 direction and activate NKCs), IL-23 (which drives naïve TH-cells to become pro-inflammatory TH-17 cells) and nitric oxide, in-vitro. In contrast, in-vitro studies suggest M2 macrophages are anti-inflammatory and pro-repair (and possibly as a result, tumour promoting and pro-fibrotic), producing IL-10, transforming growth factor beta (TGF-β), platelet-derived growth factor, tissue inhibitors of metalloproteinases, and chemokines to attract T-regs. M2 macrophages also release chemo-attractants which attract TH-2 cells to drive anti-parasitic and allergic type eosinophilic inflammation (202). It is unlikely however that macrophage differentiation is so proscriptive in-vivo and indeed they show significant plasticity, with the ability to switch from a pro- to an anti-inflammatory phenotype (210, 211).

Historically it was believed that macrophage numbers could only be increased by recruitment of blood monocytes with subsequent differentiation. Recent reviews of available evidence have challenged this theory and propose instead that macrophages arise from precursor cells which populate the relevant organ during embryonic development (208, 212, 213). In addition macrophages can replicate themselves in situ and don't always require the recruitment of monocyte-derived macrophages (MDMs), although the latter can still occur in some organs under normal conditions such as the gut and skin (208). Specifically, fate-mapping studies in mice have shown that knock-out of monocytes, for example using Cre recombinase gene techniques, does not affect lung macrophage numbers (214, 215). Similarly parabiotic mice which have their circulation surgically joined for prolonged periods, display inevitable mixing of their circulating monocyte populations but do not show development of chimeric tissue macrophages, indicating that blood monocytes are not contributing to tissue macrophage numbers (215). At present it is still unclear if and to what extent MDMs might contribute to the pulmonary macrophage population during times of inflammation but experts believe this is likely to occur (208, 212). In keeping with this Desch *et al* have recently demonstrated for the first time the presence of five types of mononuclear phagocyte cells in non-diseased whole lung donated post-mortem (216). They identified that alveolar macrophages, isolated via bronchoalveolar lavage, differed from another mononuclear phagocyte with macrophage features but which shared surface markers in common with monocytes. They labelled the latter group "tissue monocytes" and hypothesised that this form of macrophage may be derived from circulating blood monocytes. These studies highlight the importance of interpreting studies using MDMs in-vitro with caution as data may not be applicable to macrophages in-vivo.

1.10.3 TNF-α autocrine feedback loops in monocytes

Surprisingly, given the wealth of evidence available concerning the effects of TNF-α on other cell types, there is a relative lack of data regarding the specific autocrine or paracrine effects of TNF-α on human monocytes/macrophages and particularly the differential roles of its two receptors. The importance of TNF-α and monocytes/macrophages in a range of acute and chronic inflammatory diseases suggests there is considerable value in determining how TNF-α acts upon its cells of origin.

In human MDMs and murine macrophages sTNF-α has been shown to induce transcription of the TNF-A gene and production of interferon-β, the latter feeding back to up-regulate transcription factors which influence late response inflammatory genes (217). TNF-α autocrine signalling also prolonged macrophage survival in murine macrophages stimulated with LPS (218). In a further study of bone-marrow derived murine macrophages, TNF-α acted in an autocrine manner to induce macrophage terminal differentiation (219). In human myelomonocytic cell lines TNF-α autocrine feedback augmented pre-existing expression of the HLA-DR gene (220). The complicated nature of TNF-α autocrine signalling effects on its own expression is highlighted in a study in which sTNF-α induced further TNF-α and also IL-1β gene expression, but in addition caused the up-regulation of nuclear factor (erythroid-derived 2)-like 2 (NrF2), a transcription factor activating anti-oxidant genes, which was also shown to have an inhibitory effect on TNF-α gene transcription (221). Lastly, TNF-α autocrine feedback has been shown to up-regulate the production of the predominantly anti-inflammatory cytokine IL-10 in monocytes (222-224).

1.11 **Conclusion and hypothesis**

In conclusion, given the importance of A1ATD as a cause of COPD, the special relevance of TNF-α in A1ATD and the findings of Sapey *et al's* work suggesting 100 fold greater TNF-α in the airways of affected subjects and a more aggressive disease trajectory (17) there was a clear rationale for investigating the rs361525 polymorphism further in A1ATD-related COPD, at a cellular level. Sapey *et al* identified a lower BMI in AG subjects (17), suggesting systemic effects of greater TNF-α production. As such the focus of this thesis was initially on studying monocytes, the principal TNF-α secreting cell type, before considering studying the effects of the polymorphism in MDMs or in macrophages harvested directly from the airways. As monocytes express both TNFR1 and TNFR2, studying this cell type afforded the potential benefit of considering the effects of excess TNF-α secretion on autocrine feedback loops, via its two receptors.

Therefore, the overarching hypothesis of this thesis was that the presence of the rs361525 TNF-A polymorphism would lead to greater TNF-α output by monocytes from affected A1ATD-related COPD subjects compared to matched controls and that this would lead to greater output of other pro-inflammatory mediators and have an enhancing effect on other monocyte/macrophage functions relevant to COPD, via an autocrine feedback loop occurring via TNFR1.

The primary component of this hypothesis was not proven using the current model of study, specifically monocytes from A1ATD-related COPD subjects with the rs361525 polymorphism did not produce more TNF-α. The possible reasons for this are discussed in chapter 4. However, a TNF-α autocrine feedback loop leading to enhanced CXCL8 production by monocytes from both groups was identified and as such further studies focussed on autocrine feedback loops in monocytes from healthy subjects, specifically

considering the relative roles of TNFR1 and TNFR2. The overall aims of the thesis in light of this change of focus are considered below. Hypotheses relevant to each area of study are covered in detail in each chapter along with specific objectives and strategies for addressing those objectives.

1.12 **Aims and structure of this thesis**

The aims were two-fold:

Firstly, to investigate the effects of the rs361525 TNF-A polymorphism in our cohort of A1ATD-related COPD patients at a cellular level and secondly to investigate the autocrine effects of TNF-α on monocytes via its two receptors.

Specifically, three key areas/questions were addressed.

1. Do monocytes (as the principal producers of TNF-α) of A1ATD-related COPD patients with the rs361525 TNF-A polymorphism produce more TNF-α than monocytes of matched wild-type subjects from the same cohort?

Chapter 3 examines exogenous mediators used to stimulate TNF-α production by monocytes from healthy subjects. Concentration response and time course experiments were conducted to determine optimum dosing of the chosen stimuli and optimum timing for harvesting of cell supernatants and mRNA from A1ATD subjects in subsequent experiments. Chapter 4 examines the expression of *TNF-α* and *CXCL8* mRNA and secreted protein in quiescent and activated monocytes in A1ATD-related COPD patients with and without the rs361525 TNF-A polymorphism.

2. Does TNF-α have an autocrine effect on monocytes?

Chapter 4 considers the effect of TNF-α blockade on CXCL8 output monocytes in A1ATD-related COPD patients with and without the rs361525 TNF-A polymorphism.

Chapter 5 examines the effect of TNF-α blockade on pro- and anti-inflammatory cytokine output from activated monocytes from healthy control subjects by measuring mRNA and secreted protein output. In addition, the autocrine effect of TNF-α on the expression of its own cell surface receptors on monocytes was assessed using flow cytometry.

3. What are the differential roles of TNFR1 and TNFR2 in TNF-α autocrine feedback loops in monocytes?

Chapter 5 also examines the effects of selective or dual blockade of TNFR1 and TNFR2 on pro- and anti-inflammatory cytokine output from activated monocytes from healthy subjects by measuring mRNA and secreted protein output. Lastly, the effect of selective receptor blockade on the expression of cell surface TNFR1 and TNFR2 was assessed using flow cytometry.

CHAPTER 2

MATERIALS AND METHODS

2 Materials and methods

2.1 Ethical approval

Ethical approval for the project was obtained from South Birmingham Research Ethics Committee (local research and ethics committee number- 3359a). All patients gave written informed consent to undergo physiological testing and peripheral blood sampling. Healthy control subjects gave verbal consent to donate blood samples.

2.2 Subject characteristics

The characteristics of patients with COPD and A1ATD are described in detail in chapter 4. All patients were homozygous for the Z variant of the serpinA1 gene (ZZ genotype) with a serum A1AT concentration below the putative protective level of 11 μM and the presence of COPD was diagnosed according to Global Strategy for Diagnosis, Management, and Prevention of COPD criteria (225). CB was defined as a cough productive of sputum for at least three months in each of two consecutive years (36). Patients in our cohort had previously undergone genotyping using TaqMan® genotyping technology to determine the allele they carried at position -237 on each copy of the TNF-A gene (125). We were subsequently able to match patients with and without the rs361525 polymorphism based on the following criteria: gender, age (within 10 years) and FEV1 (within 10% greater or less than the AG patient's FEV1), current smoking status, treatment with inhaled corticosteroids and where possible for the presence or absence of CB symptoms.

Healthy control subjects were non-smokers, free from any disease or symptoms and taking no medication at the time of the study. In total, 23 subjects donated peripheral blood samples (median age- 31 years, interquartile range (IQR-) 25 to 32.5 years; range- 21 to 45 years; 13 males).

2.3 **Pulmonary function testing**

Pulmonary function testing for subjects with COPD was conducted by trained respiratory physiologists in the Lung Function and Sleep Department at the Queen Elizabeth Hospital, Birmingham, according to national guideline standards (226). Patients performed post-bronchodilator spirometry, multiple breath helium dilution lung volume assessment, the single breath diffusing capacity test and underwent arterialised capillary blood gas sampling to determine the following measurements: forced expiratory volume in one second (FEV1), vital capacity (VC), effective alveolar volume (VA), total diffusing capacity of the lung for carbon monoxide (DLCO), transfer coefficient (DLCO/VA) and the partial pressures of oxygen (PaO_2) and carbon dioxide ($PaCO_2$) in the arterial circulation, measured in kilopascals (kPa). Table 2.1 summarises the interpretation of pulmonary function measurements commonly used in diagnosing and assessing the severity of COPD. All patients had undergone an HRCT scan either at their local hospital or our centre. The presence or absence of emphysema was determined by the reporting radiologist at the hospital where the scan took place.

Measurement	Classification		
FEV1/FVC % predicted	<70% = obstructive airways disease		
FEV1 % predicted	GOLD stage 1	Mild	FEV1 >/= 80% (with symptoms)
	GOLD stage 2	Moderate	FEV1 >/= 50%
	GOLD stage 3	Severe	FEV1 >/= 30%
	GOLD stage 4	Very severe	FEV1 < 30% (< 50% if respiratory failure present)
DLCO and DLCO/VA	Measurements less than 1.64 standardized residuals are indicative of reduced transfer of carbon monoxide. Reduced DLCO/VA suggests the presence of emphysema.		
Arterialized blood gas sample	Type I respiratory failure		PaO_2 < 8.0 kPa (hypoxia)
	Type II respiratory failure		PaO_2 < 8.0 kPa and $PaCO_2$ > 6 kPa (hypercapnia)

Table 2-1 Pulmonary function testing in COPD

On the basis of GOLD, COPD is diagnosed when the patient has an obstructive FEV1/FVC ratio (<70%) and one of the four FEV1 % predicted categories (225). FEV1/VC may be utilized as an alternative in order to minimize the risk of underestimating the degree of the obstructive ratio. This will occur if FVC is lower than VC as a result of early airways closure being exacerbated by a forced manoeuvre.

2.4 Isolation of human CD14+CD16- monocytes

A peripheral blood sample was obtained from each subject using a vacutainer system into lithium heparin-containing tubes (Becton Dickinson Vacutainer Systems, Franklin Lakes, USA). The monocyte extraction process was started within 30 minutes of obtaining the blood sample and was carried out in an ESCO class 2 biosafety cabinet. Whole blood was layered over Lymphoprep™ (Axis Shield, Dundee, UK) and centrifuged at 800*g* for 20 minutes at 3°C in a Hettich Rotina 46R centrifuge. As a result of centrifugation the blood components

separated into the following layers from top to bottom: plasma; buffy coat (containing mononuclear cells); Lymphoprep™; erythrocytes and granulocytes. The buffy coat was removed using a Pasteur pipette, the cells washed with sterile phosphate buffered saline (PBS) containing 2mM Ethylenediaminetetraacetic acid (EDTA) and 0.1% bovine serum albumin (BSA), hereafter referred to as PBS-1, in a sterile universal container and then centrifuged for 10 minutes at 1600*g* (3ºC). The cell pellet was then re-suspended in 20ml of PBS-1. A 10 microlitre (µl) sample of the suspension was mixed with trypan blue and the leukocytes were counted on a haemocytometer with improved Neubaur markings. The suspension was washed and centrifuged again as before.

The Dynabeads® Untouched™ Human Monocytes kit (Life Technologies Limited, Paisley, UK) was then used to isolate monocytes via a negative selection process, following the product protocol. The principle of this technique involves adding mouse IgG antibodies to the cell mixture which bind to specific leukocyte and erythrocyte cells surface markers (CD3, CD7, CD16, CD19, CD56, CDw123 and CD235a). The antibodies, bound to the unwanted cells, later bind to the magnetic Dynabeads® during a short incubation period. The CD14+ monocytes can then be separated from the Dynabeads®-cell complexes using a magnet, to leave the monocytes in suspension. In this technique the 10% of human monocytes that express CD16 on their cell surface (non-classical monocytes) are lost as it is critical for the antibody mixture to contain anti-CD16 antibodies in order to remove any neutrophils which may have contaminated the buffy coat layer. The benefit of the negative immune-selection technique however, is that it leaves the remaining 90% of monocytes "untouched" by any antibodies and hence unlikely to be activated by the isolation procedure.

In brief, the cell pellet was re-suspended in PBS-1. Blocking reagent and antibody mix supplied in the kit was then added to the suspension, each at a volume of 20 µl for every

$1x10^7$ mononuclear cells and the mixture was left to incubate at 2-8 ºC for 20 minutes. The cells were washed with PBS-1 as before and centrifuged for 6 minutes at 2000*g* at 3ºC. The cell pellet was re-suspended and mixed with Dynabeads® suspended in sterile PBS-1 (100 µl of beads for every $1x10^7$ mononuclear cells).The beads were first washed by adding PBS-1 and applying the tube to a magnet from which the PBS-1 was removed by pipette. The mixture was incubated for 15 minutes at 2-8 ºC with gentle agitation. The mixture was then applied to the magnet for 2 minutes at which time the supernatant was pipetted off into a sterile universal container. Further PBS-1 was added to the tube containing the beads and the process repeated. The cells in the supernatant were counted as before on a haemocytometer to determine the total number of monocytes retrieved. All cell suspensions were of greater than 95% viability as assessed by trypan blue exclusion. The mixture was centrifuged for 6 minutes at 2000*g* at 3ºC and the cell pellet re-suspended in sterile Roswell Park Memorial Institute 1640 medium (RPMI, Sigma-Aldrich Chemicals Ltd, Poole, UK) supplemented with 10% fetal bovine serum (FBS), 10% L-glutamine and 10% penicillinV and streptomycin, hereafter referred to as culture medium (CM).

2.5 **Tissue culture**

Experiments which required a period of culture were conducted in 12 or 24-well tissue culture plates (Costar, Sigma-Aldrich Chemicals Ltd, Poole, UK). Immediately following isolation monocytes were plated out at a concentration of between 0.25 and 0.45 million per ml of CM, as specified in individual experiments. The following stimulants were used in experiments: recombinant human TNF-α, IL-1β or MCP-1 (R and D Systems Ltd, Abingdon, UK), *Salmonella Enteritidis* derived LPS and phorbol 12-myristate 13-acetate (PMA) (both Sigma-Aldrich Chemicals Ltd, Poole, UK). A number of human mAbs were used in experiments, either as blocking antibodies, to prevent ligand binding to it receptor(s) or for flow cytometry

experiments where they were labelled with fluorophores, as listed in table 2.2. Written communication with R and D Systems Ltd (Abingdon, UK) confirmed that exact binding sites of the blocking mAbs to their specified ligands, TNF-α, TNFR1 and TNFR2, is not known. Antibodies are designed to bind to a single site on the TNF-α molecule or to the extracellular domain of receptors. All three blocking mAbs are able to neutralise the effect of TNF-α induced cytotoxicity in mouse fibroblasts, in a concentration dependent manner and presumably through competitive antagonism of the receptor(s) or TNF-α (direct communication with Dr E. Fioravanti, Scientific Coordinator, R and D Systems Ltd, 27th November 2015).

Culture plates containing cells incubated with blocking mAbs were gently agitated for 20 minutes prior to the addition of LPS. Cells were incubated for pre-determined time periods at 37 ^{0}C and in 5% CO_2. Monocyte supernatants were collected and then centrifuged in order to remove any cellular debris, before storing at -80^{0}C until analysed. Adherent cells were gently removed from the culture wells using a cell scraper (Sigma-Aldrich Chemicals Ltd, Poole, UK) and the cell pellet stored in RNA*later*® (Invitrogen, UK) at -80^{0}C for future use in real-time quantitative polymerase chain reaction (RT-qPCR) experiments.

Antibody	Clone	Fluorophore	Function	Manufacturer
Mouse IgG1TNF-α mAb	28401	N/A	Neutralisation	R and D Systems Abingdon, UK
Mouse IgG1 TNFR1 mAb	16805	N/A	Neutralisation	R and D Systems
Mouse IgG1 TNFR2 mAb	22210	N/A	Neutralisation	R and D Systems
Mouse IgG1 isotype control Ab	11711	N/A	Control	R and D Systems
Mouse IgG_1TNFR1 mAb	16803	Phycoerythrin (PE)	Flow cytometry	R and D Systems
Mouse IgG_{2A} TNFR2 mAb	22235	FITC	Flow cytometry	R and D Systems
Mouse IgG_1 control Ab	11711	PE	Flow cytometry	R and D Systems
Mouse IgG_{2A} control Ab	X39	Fluoroscein (FITC)	Flow cytometry	BD Biosciences, Oxford, UK
Mouse IgG_1 CD14 mAb	134620	Peridinin chlorophyll protein complex (PerCP)	Flow cytometry	R and D Systems
Mouse IgG_{2A} CD16 mAb	3G8	Allophycocyanin (APC)	Flow cytometry	Life Technologies, Paisley, UK
Mouse IgG_1 control Ab	11711	PerCP	Flow cytometry	R and D Systems
Mouse IgG_{2A} control Ab	PPV-04	APC	Flow cytometry	Life Technologies

Table 2-2 Antibodies used in the course of this thesis

2.6 **Measurement of soluble mediators**

The ELISA is used to detect and quantify the concentration of a protein of interest in a liquid sample. Figure 2.1 outlines the principles of this technique.

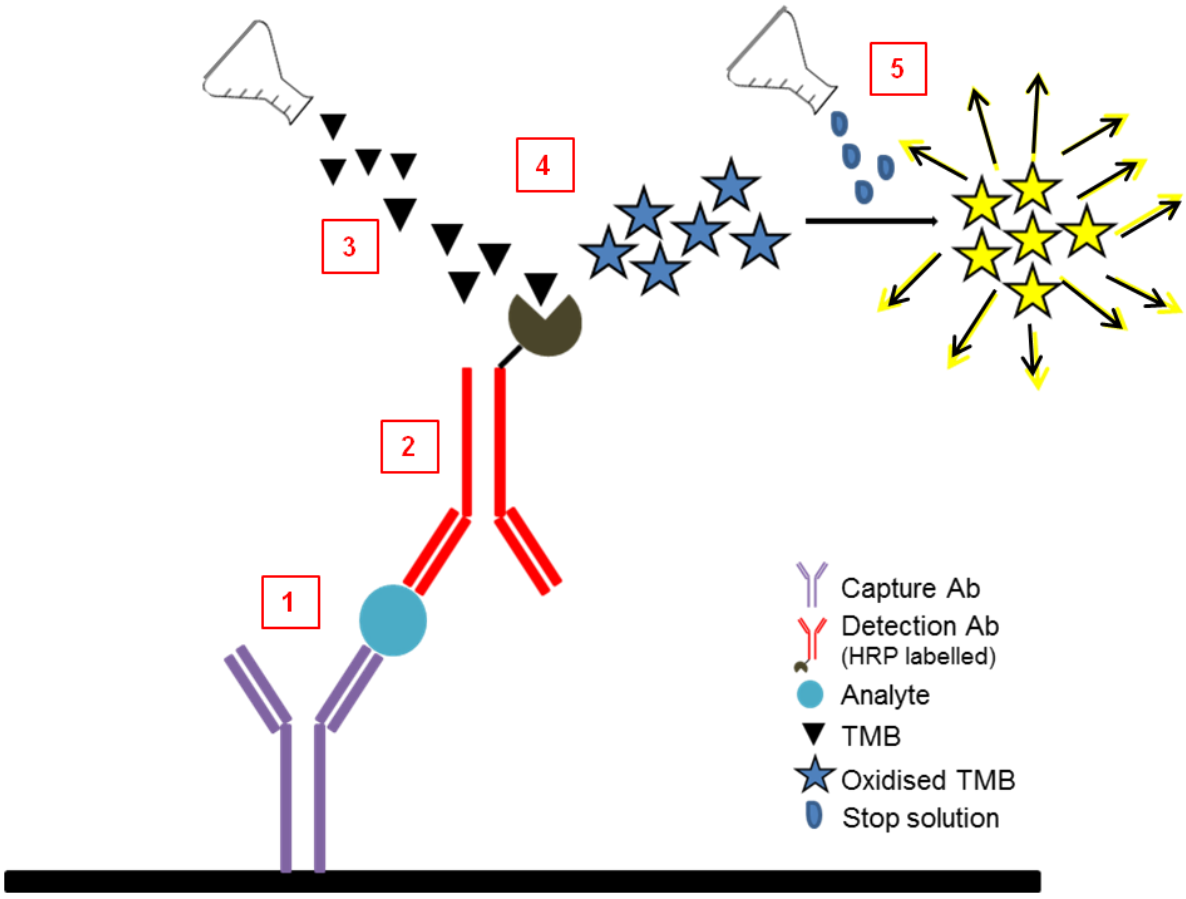

Figure 2-1 Principles of the ELISA

1) Cell-free supernatant is added to a 96-well plate pre-coated with a capture mAb capable of binding an epitope specific to the analyte of interest. The plate is then washed to remove unwanted molecules. 2) A detection (HRP-labelled) polyclonal antibody specific to different epitopes on the analyte of interest is added and will bind to any analyte. The detection antibody is labelled with HRP. 3) After a wash step to remove excess detection antibody, substrate solution is added, a mixture of stabilised hydrogen peroxide and stabilised chromogen (TMB). 4) TMB is oxidised by the HRP enzyme, using hydrogen peroxide as the oxidising agent to produce a blue colour. 5) The reaction is terminated at an assigned time point by the addition of stop solution (sulphuric acid) which changes the blue colour to yellow. The intensity of the colour is proportional to the quantity of analyte present in each well and is measured in a microplate reader. A standard curve produced by running known concentrations of analyte supplied in the assay kit is used to calculate actual concentrations of analyte by interpolation. Horse radish peroxidise- HRP; tetramethylbenzidine- TMB.

Table 2.3 shows the steps required for each of the ELISA kits used to measure the following mediators: TNF-α, CXCL8, TNFR1 and TNFR2. Each sample of cell-free supernatant, standard or control was run in duplicate and a mean reading taken. An Orbital Shaker S03 (Stuart Scientific, UK) set at 150 resolutions per minute was used to ensure adequate mixing for each incubation step. An LT-3500 microplate washer (Labtech.com, Uckfield, UK) was employed for each of the washing steps. The Synergy HT microplate reader (BioTek, Winooski, USA) read the optical density of each well at a set absorbance value and wavelength correction. The wavelength correction corrects for optical imperfections in the plate. The concentration of mediator in each sample was determined by using the forecast function in Excel (Microsoft Office 2010), which uses linear regression to calculate the concentration of mediator in a sample from the following values: the log value of the optical density of the sample and the log values of known standard concentrations and their optical densities. Values are given in picograms (pg)/ml and nanograms (ng)/ml.

Mediator	**TNF-α** R & D systems, UK	**CXCL8** R & D systems, UK	**TNFR1** Invitrogen, UK	**TNFR2** Invitrogen, UK
Step One	Add 50 µl assay diluent per well.	Add 100 µl assay diluent per well.		
Step Two	Add 200 µl of standard, control or sample per well (samples were diluted in calibrator diluent if necessary)	Add 50 µl of standard, control or sample per well (samples were diluted in calibrator diluent if necessary)	Add 50 µl of standard, control or sample per well	Add 50 µl of standard, control or sample per well
Step Three	Incubate 2 hours at room temperature	Incubate 2 hours at room temperature		
Step Four	Aspirate and wash 4 times (300 µl of wash buffer per well each wash)	Aspirate and wash 4 times (300 µl of wash buffer per well each wash)		
Step Five	Add 200 µl of anti-sTNF-α HRP-conjugate solution to wells	Add 100 µl of anti-sCXCL8 HRP-conjugate solution to wells	Add 200 µl of anti-sTNFR1 HRP-conjugate solution to wells	Add 200 µl of anti-sTNFR2 HRP-conjugate solution to wells
Step Six	Incubate 1 hour at room temperature	Incubate 1 hour at room temperature	Incubate 1 hour at room temperature	Incubate 1 hour at room temperature
Step Seven	Aspirate and wash 4 times (300 µl of diluted wash buffer per well each wash)	Aspirate and wash 4 times (300 µl of diluted wash buffer per well each wash)	Aspirate and wash 4 times (300 µl of diluted wash buffer per well each wash)	Aspirate and wash 4 times (300 µl of diluted wash buffer per well each wash)
Step Eight	Add 200 µl of substrate solution to each well, protect from light and incubate at room temperature for 20 minutes	Add 200 µl of substrate solution to each well, protect from light and incubate at room temperature for 30 minutes	Add 50 µl of substrate solution to each well, protect from light and incubate at room temperature for 15 minutes	Add 50 µl of substrate solution to each well, protect from light and incubate at room temperature for 15 minutes
Step Nine	Add 50 µl of stop solution to each well. Read optical density in microplate reader set to 450 nM with wavelength correction set to 570 nanometre (nm)	Add 50 µl of stop solution to each well. Read optical density in microplate reader set to 450 nM with wavelength correction set to 570 nm	Add 200 µl of stop solution to each well. Read optical density in microplate reader set to 450 nM with wavelength correction set to 630 nm	Add 200 µl of stop solution to each well. Read optical density in microplate reader set to 450 nM with wavelength correction set to 630 nm

Table 2-3 ELISA protocols

Figures 2.2 shows examples of standard curves generated for each of the four assays, with the linear regression equation and the correlation coefficient displayed. The lower and upper limits of quantification and the minimum detectable concentration for each of the assays are shown in table 2.4. The minimum detectable concentration of each measured mediator was determined by the manufacturers by adding two standard deviations to the mean optical density of twenty blank samples and from this calculating the corresponding concentration from the x-axis. The lower limit of quantification was equal to the minimum detectable concentration for the TNFR1 and TNFR2 assays which is deemed acceptable (227).

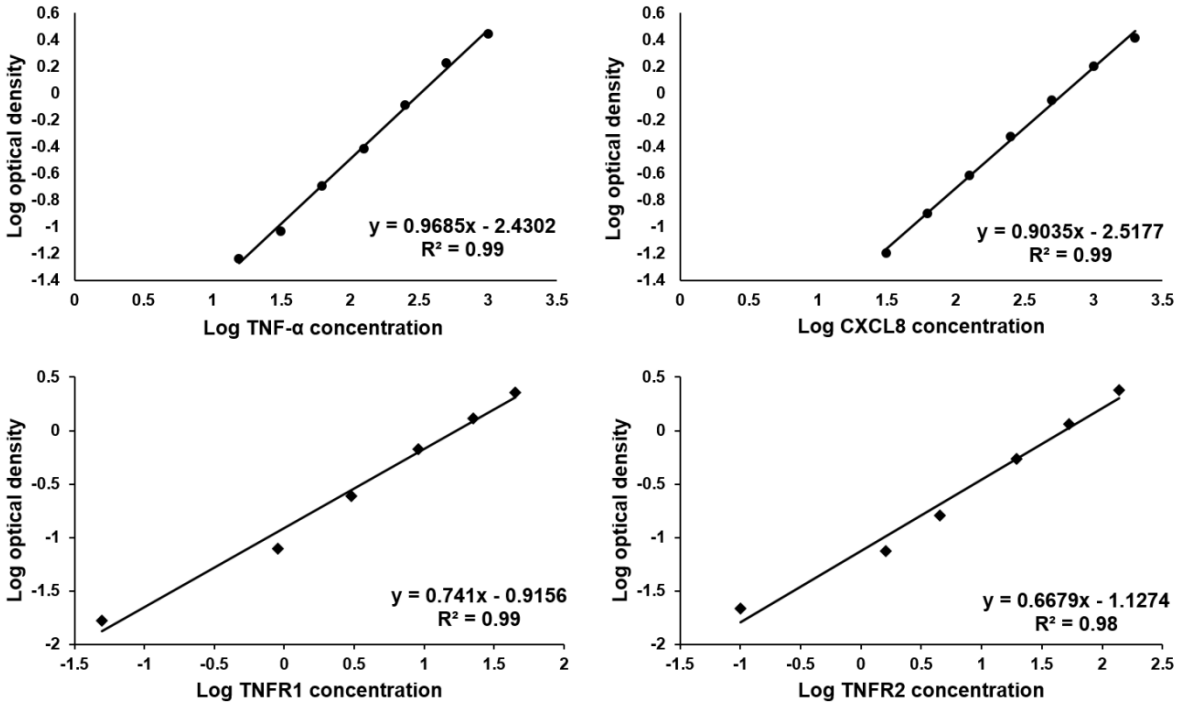

Figure 2-2 Standard curves for the TNF-α, CXCL8, TNFR1 and TNFR2 ELISAs

The graphs illustrate example standard curves with mean absorbance for each standard plotted on the y-axis against the concentration (pg/ml) on the x-axis, both displayed as logarithmic scales. A best fit curve is drawn through the points on the graph. The linear regression equation and R^2 values are shown.

Assay	Minimum detectable concentration	Lower limit of quantification	Upper limit of quantification
TNF-α	1.6 pg/ml	15.6 pg/ml	1000 pg/ml
CXCL8	3.5 pg/ml	31.3 pg/ml	1000 pg/ml
TNFR1	50 pg/ml	50 pg/ml	45000 pg/ml
TNFR2	100 pg/ml	100 pg/ml	138000 pg/ml

Table 2-4 Minimum detectable concentration and lower and upper limits of quantification of the ELISAs

The table outlines the sensitivity and limits of quantification of the four ELISAs used in this thesis.

2.7 Measurement of mRNA

2.7.1 RNA extraction

Messenger RNA was extracted from each thawed cell pellet using the Isolate RNA Minikit (Bioline, London, UK). The cells within a pellet were lysed using 450 µl of Lysis Buffer R, re-suspended by pipetting and then incubated at room temperature for 3 minutes. The lysis buffer inactivated any ribonuclease (RNAase) enzymes, protecting the released RNA from enzymatic breakdown. All further steps were performed on ice, unless otherwise specified. Each lysate was transferred to a Spin Column R1, spun at 10,000*g* for 2 minutes in a Stuart Microcentrifuge SCF2 within a collection tube and the filtrate saved. Any genomic DNA was thus removed from the lysate. An equal volume of 70% ethanol was added to the filtrate and the sample transferred to spin column R2. The spin column was spun at 10,000*g* for 2 minutes and the filtrate discarded. 500 µl of Wash Buffer AR (diluted with ethanol) was added to the spin column and spun at 10,000*g* for 1 minute. The filtrate was discarded and 700 µl of Wash

Buffer BR (diluted with ethanol) was added to the spin column and spun at 10,000*g* for 1 minute. The spin column was placed in a new collection tube and spun again at 10,000*g* for 3 minutes. These steps were necessary to wash the RNA bound to the silica membrane of Spin Column R2, removing any cellular debris. In the final step 50 µl of RNAase free water was added to the spin column, in a fresh collection tube, incubated for 1 minute at room temperature and then spun at 6000*g* for 1 minute, collecting the eluted RNA into an RNAase free eppendorph. Eppendorphs were stored at -80^{0}C for future use in RT-qPCR experiments.

2.7.2 Nucleic acid quantification and purity assessment

Prior to reverse transcription, the quantity and purity of extracted RNA in each sample was determined. This was done by measuring the absorbance of ultraviolet light at a wavelength of 260 nm, by 1 µl of each sample on a Nanodrop 2000c spectrophotometer. A one µl sample of RNA'ase free water was used in the first instance as a blank sample. Nucleic acids absorb ultraviolet light at this wavelength and hence the degree of absorption is proportional to the concentration of RNA in the sample. The purity of each sample was measured by calculation of the ratio of absorbance of light at 260 nm and 280 nm. Other molecules such as proteins may contaminate the RNA sample and absorb light better at the 280 nm wavelength. Ideally the 260/280 ratio for RNA should be between 1.8 and 2. A ratio lower than this may due to contamination of the sample with residual reagents from the extraction protocol or due to low concentrations of RNA (less than 10 ng/µl of nucleotide). A ratio higher than 2 indicates no contamination (228).

2.7.3 Reverse transcription

Once RNA had been extracted from the cells it was converted to complementary DNA (cDNA) for use in RTq-PCR. Figure 2.3 outlines the principles of reverse transcription.

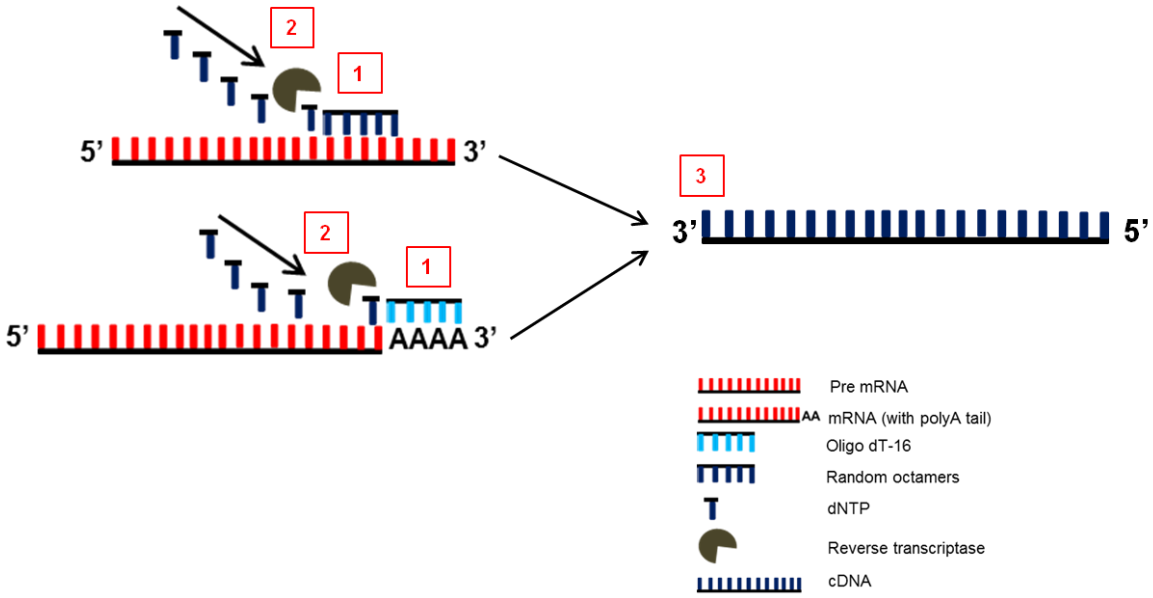

Figure 2-3 Reverse transcription of RNA to cDNA

1) Extracted RNA includes mRNA and pre-mRNA. mRNA is mature RNA which has undergone post transcriptional modification to aid stabilisation. This involves splicing, cleavage of the nucleotides at the 3' end of the molecule and addition of a polyadenine (poly-A) tail and also capping of the 5' end of the RNA molecule (229). The process of reverse transcription whereby single stranded cDNA is formed from RNA can occur from any type of RNA. Primers bind to sequences within an RNA transcript. Oligo dT-16 primers bind to the polyA tail of mature mRNA molecules. Random octamer primers are single strands of DNA consisting of every possible combination of 8 nucleotide bases, meaning there will be a complementary primer to bind to whichever sequences of RNA are present in the sample. 2) The primers act as templates for reverse transcriptase to begin assembling the complementary dNTPs in sequence. 3) This results in single stranded cDNA corresponding to all RNA transcripts present, both from immature and mature RNA. RNAase inhibitors are also present in the reaction to prevent inadvertent degradation of RNA (230) dNTPs: deoxyribonucleotide.

Reverse transcription of RNA to cDNA was achieved using a High Capacity RNA-to-cDNA™ Kit (Life Technologies, Paisley, UK). All components of the reaction were thawed on ice. Nine µl of a sample of RNA was added to 10 µl of 2x reverse transcriptase buffer mix (containing deoxyribonucleotide (dNTPs), random octamers, and oligo dT-16) and 1 µl of 20x enzyme mix (containing murine leukemia virus acting as the reverse transcriptase and also RNAase inhibitor protein). The sample, held in an RNA'ase free eppendorph, underwent reverse transcription in the Takara PCR Thermal Cycler Dice (Takara Bio, Otsu, Japan). The reaction mixtures were incubated at 37^{o}C for 60 minutes to allow reverse transcription to occur and the reaction terminated by heating to 95^{o}C. The samples were then cooled to 4^{o}C. Each sample containing cDNA was frozen at -28^{o}C for future analysis. A constant volume of 9 µl of each sample of RNA was added to each eppendorph for ease of setting up the reverse transcriptase reaction. As such the total weight (ng) of RNA in each reaction varied, but as each starting concentration was known it was then possible to calculate the volume of completed reverse transciptase reaction (cDNA) that would be needed in the subsequent RT-qPCR reaction to give an equivalent starting concentration of 1 ng of RNA per well of the RT-qPCR plate.

2.7.4 The real-time quantitative polymerase chain reaction

RT-qPCR relies on detection of fluorescence. In brief, addition of a primer designed to bind a specific sequence of cDNA (the gene of interest) and a DNA polymerase enzyme will lead to an exponential amplification of that sequence of DNA with each thermal cycle of the PCR machine. The process is illustrated in figure 2.4.

A thermal cycle involves heating the PCR plate containing the reaction mixture to a temperature of 95^{0}C to allow all double stranded DNA (dsDNA) to denature into two single strands. On the first cycle denaturation does not need to occur as only single stranded cDNA

is present. This is followed by a short period of lower temperature (usually 60^0C) in which the primer, specific to the gene of interest, binds to its complementary sequence on the relevant cDNA strand. DNA polymerase then catalyses the assembly of complementary dNTPs to begin the process of replicating each copy of the gene of interest during that cycle. The hydrolysis probe, also specific for the gene of interest, binds upstream of the primer. An MGB (minor groove binder) molecule attached to the 3' end of the hydrolysis probe is present in order to bind to a minor groove formed in the DNA upon probe binding. This stabilises probe-DNA binding. Attached to the probe are two fluorophore dyes. The reporter dye (green) has a shorter wavelength and hence higher energy of emission than the quencher dye (red). The three dimensional structure of the probe is such that the two dyes are close together and therefore as the green reporter dye fluoresces its energy is transferred to the red quencher dye, a process termed fluorescent resonant energy transfer (FRET).

DNA polymerase possesses 5' nuclease activity so that when it reaches the probe as it extends the newly formed DNA sequence it is able to cleave the probe from the original DNA strand. This leads to a change in the conformational structure of the probe and hence separation of the quencher and reporter dye, termination of FRET and emission of fluorescence from the reporter dye at a specific and detectable wavelength. The temperature of the reaction is raised to allow denaturation of the newly formed amplicon (dsDNA of interest) and the cycle is repeated. In subsequent cycles a reverse primer also binds to the antisense strand of the gene of interest so that both sense and antisense strands are doubled with each cycle.

Each duplication of the gene of interest is accompanied by an increase in fluorescence emission. The degree of fluorescence increases with each cycle (usually up to a total of 40-45 cycles) and crucially, increases sooner the greater the starting concentration of the gene of interest. A predetermined threshold for fluorescence detection is set by the machine and once

this is crossed for a particular sample the cycle threshold (CT value) is reached. The CT value is then used to quantify the original amount of gene of interest present using the relative quantification method, as described in 2.7.5.

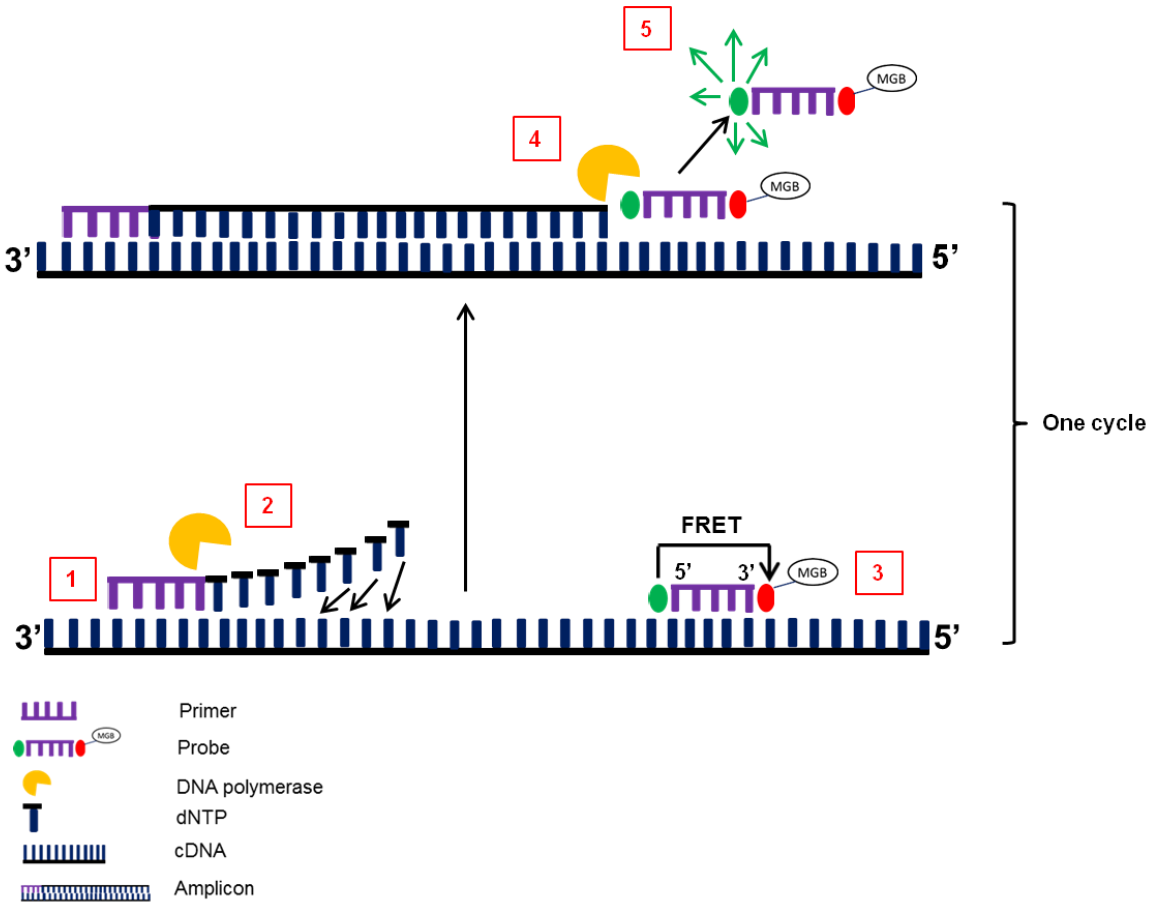

Figure 2-4 Cycle one of the real-time quantitative polymerase chain reaction using TaqMan® technology

1) A primer, specific to the gene of interest, binds to its complementary sequence on the relevant cDNA strand. 2) DNA polymerase catalyses the assembly of complementary dNTPs to replicate each copy of the gene of interest during that cycle. 3) A hydrolysis probe, specific for the gene of interest, binds upstream of the primer. Attached to the probe are two fluorophore dyes. The three dimensional structure of the probe is such that the two dyes are close together and therefore as the green reporter dye fluoresces its energy is transferred to the red quencher dye, a process termed FRET (fluorescent resonant energy transfer). 4) DNA polymerase cleaves the probe from the original DNA strand. 5) FRET is terminated leading to the emission of fluorescence from the reporter dye. The temperature of the reaction is raised to denature the newly formed amplicon and the cycle is repeated. In subsequent cycles a reverse primer also binds to the antisense strand of the gene of interest so that both sense and antisense strands are doubled with each cycle. MGB: minor groove binder.

For each sample, a volume of cDNA in solution, equivalent to 1.0 ng of starting mRNA unless otherwise specified, was added to PCR-grade water to a volume of 9 µl and mixed with 10 µl of Light Cycler 480 Probe PCR Master master mix (Roche Applied Science, Burgess Hill, UK) and 1 µl of the relevant TaqMan® gene expression assay, containing both primer and hydrolysis probe for the particular gene of interest (Life Technologies, Paisley, UK). The Light Cycler 480 Probe PCR Master mix contained FastStart Taq DNA Polymerase, capable of initiating PCR at high temperatures. In some cases where expression of some genes was low, for example in freshly isolated cells, a greater starting amount of cDNA was used, including in the wells carrying the reference gene expression assay.

This mixture, made up to a total volume of 20 µl, was added to duplicate wells of a clear 96-well PCR plate (Roche Applied Science, Burgess Hill, UK). A singleplex technique was used in which only one specific TaqMan® gene expression assay was used in any one duplicate set of wells. On each 96-well plate, control wells for each TaqMan® gene expression assay were run in which the cDNA was absent, replaced instead by PCR grade water as a non-template control. Detectable amplicon product in this control reflects the presence of contaminating completed PCR reaction product which can occasionally become aerosolised in the laboratory environment from previous finished reactions.

The RT-qPCR reaction was run on a Roche Lightcycler 480 PCR machine (Roche Applied Science, Burgess Hill, UK). The program was set to include a pre-incubation phase at 95^0C for 10 minutes, 40 amplification cycles at 95^0C for 10 seconds each, 60^0C for 30 seconds and 72^0C for 1 second, and lastly a cooling phase for 30 seconds. The following TaqMan® assays were used: Glyceraldehyde 3-phosphate dehydrogenase (GAPDH); TNF-α; CXCL8; IL-1β; IL-6; TGF-β1; IL-10 (Life Technologies, Paisley, UK). All assays were attached to the fluorophore dye, FITC. Details of each assay are given in table 2.5. Assays where the probe

and/or primer span an exon junction are less likely to amplify any contaminating genomic DNA. This is because genomic DNA contains introns lying between two exons, disrupting the sequence of nucleotides complementary to the primer/probe and hence preventing binding of the DNA to the primer/probe. The Isolate RNA Minikit (Bioline, London, UK) is designed to efficiently remove genomic DNA during the RNA extraction process. Examples of amplification curves for each assay are shown in figures 2.5 to 2.11. Figure 2.5 is annotated to show the different phases of a complete amplification curve.

Gene symbol	Assay-on-demand number	NCBI RefSeq transcript number	Amplicon length and position	Primer/probe position
GAPDH	Hs99999905_m1	NM_002046.5	122 bp; spans 3-3 exon boundary	Probe and one of the primers sit within one exon
TNF-α	Hs00174128_m1	NM_000594.3	80 bp; spans 3-4 exon boundary	Probe spans exon
CXCL8	Hs00174103_m1	NM_000584.3	101 bp; spans 1-2 exon boundary	Probe spans exon
IL-1β	Hs01555410_m1	NM_000576.2	91 bp; spans 3-4 exon boundary	Probe spans exons
IL-6	Hs00985639_m1	NM_000600.3	66 bp; spans 2-3 exon boundary	Probe spans exons
TGF-β	Hs00998133_m1	NM_000660.4	57 bp; spans 6-7 exon boundary	Probe spans exons
IL-10	Hs00961622_m1	NM_000572.2	74 bp; spans 4-5 exon boundary	Probe spans exons

Table 2-5 TaqMan® gene expression assays

The table highlights the identification numbers of each assay, the NCBI RefSeq (National Center for Biotechnology Information reference sequence) database numbers of the DNA transcripts produced in the PCR reaction, the length and position of those transcripts, and the binding position of the primers and/or probes.

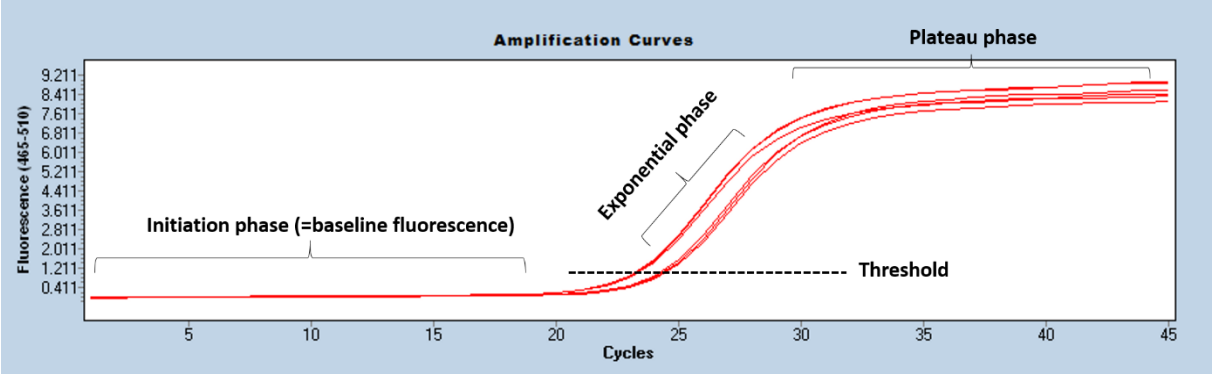

Figure 2-5 CXCL8 RT-qPCR amplification curves

The figure shows amplification curves for six separate wells containing RNA and other RT-qPCR reagents, including the TaqMan® CXCL8 assay. Initiation phase- the PCR reaction is occurring but fluorescence is not yet great enough to be distinguished from background fluorescence. Exponential phase- PCR product and hence fluorescence doubles with each cycle. Plateau phase- reagents are exhausted and hence no further increase in fluorescence occurs with each cycle. A threshold level is set by the Roche Lightcycler 480 PCR machine. The CT value is determined from the point at which fluorescence from each well exceeds this threshold.

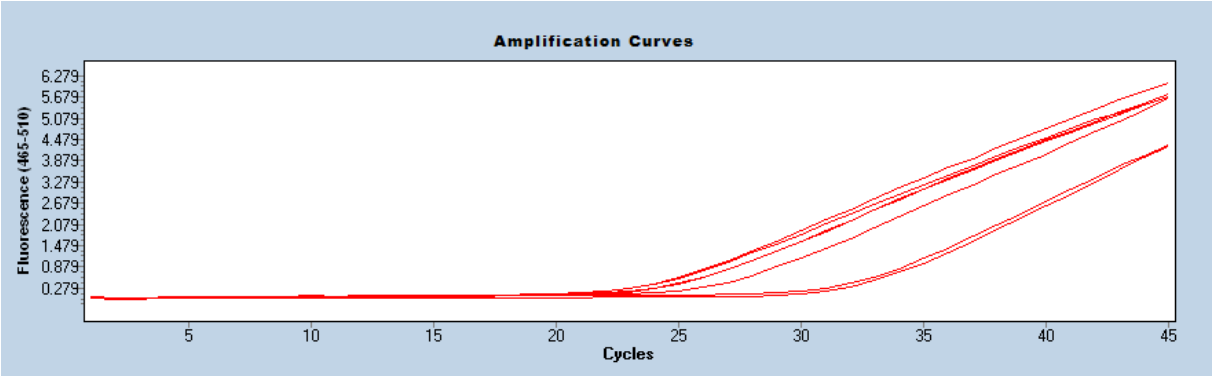

Figure 2-6 TNF-α RT-qPCR amplification curves

The figure shows amplification curves for six separate wells containing RNA and other RT-qPCR reagents, including the TaqMan® TNF-α assay. Plateau phase has not been reached by 45 cycles.

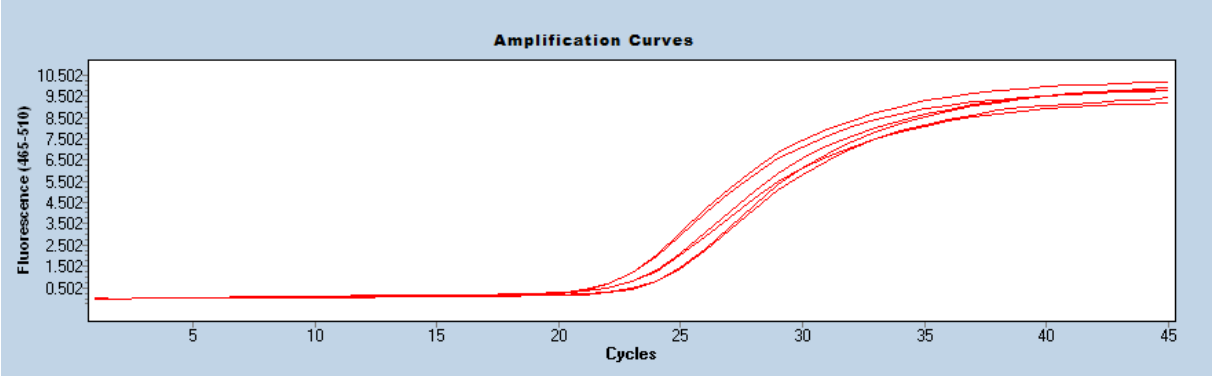

Figure 2-7 IL-1β RT-qPCR amplification curves

The figure shows amplification curves for six separate wells containing RNA and other RT-qPCR reagents, including the TaqMan® IL-1β assay.

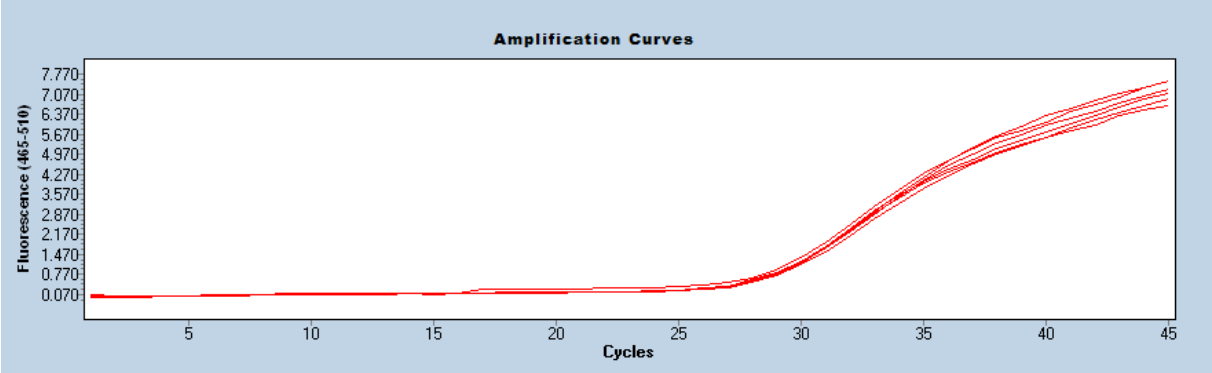

Figure 2-8 IL-6 RT-qPCR amplification curves

The figure shows amplification curves for six separate wells containing RNA and other RT-qPCR reagents, including the TaqMan® IL-6 assay. Plateau phase has not been reached by 45 cycles.

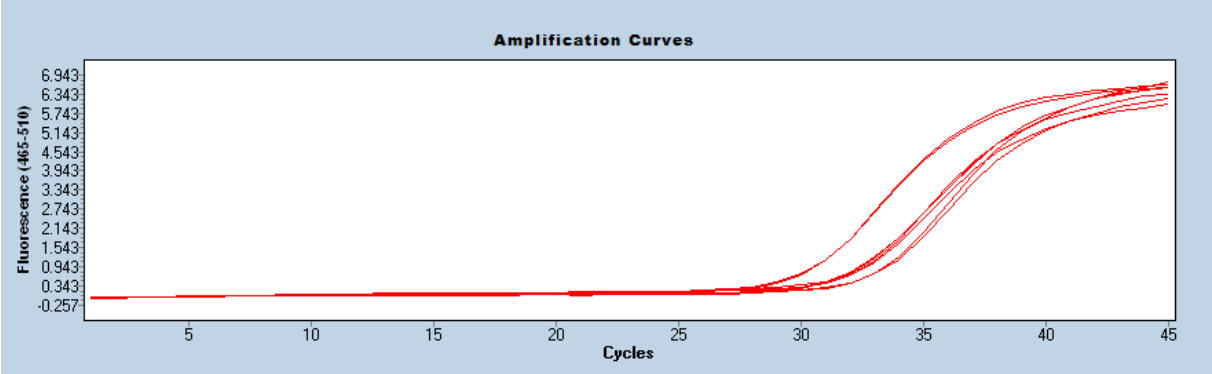

Figure 2-9 IL-10 RT-qPCR amplification curves

The figure shows amplification curves for six separate wells containing RNA and other RT-qPCR reagents, including the TaqMan® IL-10 assay.

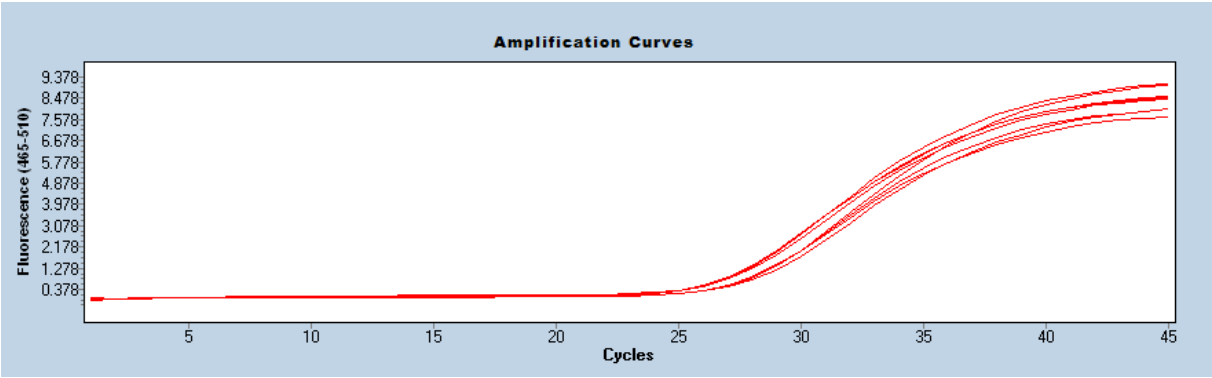

Figure 2-10 TGF-β RT-qPCR amplification curves

The figure shows amplification curves for six separate wells containing RNA and other RT-qPCR reagents, including the TaqMan® TGF-β assay.

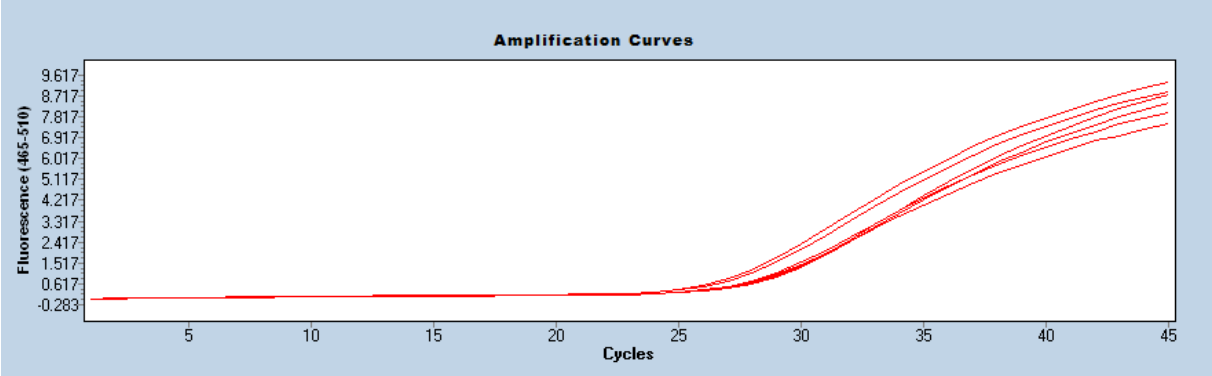

Figure 2-11 GAPDH RT-qPCR amplification curves

The figure shows amplification curves for six separate wells containing RNA and other RT-qPCR reagents, including the TaqMan® GAPDH assay. Plateau phase has not been reached by 45 cycles.

2.7.5 Relative quantification method

The CT value is used in the relative quantification method, which negates the need for calculating the precise copy number of the amplicon. In this method any errors in the obtained CT value for the gene of interest, which might have arisen as a result of a number of potential factors (such as reverse transcription inefficiency or minor differences between efficiency of PCR reactions in different plates), are corrected for by subtracting the CT value for a stably expressed reference gene obtained from another well using the same cDNA sample. This is known as the ΔCT value. The fold change in expression of the gene of interest relative to that reference gene is then calculated using the equation $2^{-\Delta CT}$. This fold change can then be compared as a number against results obtained from other subjects' samples or different experimental conditions in the same subject, as the CT value for the reference gene should not be affected by these different experimental conditions or between subjects, making differences in fold changes between subjects/conditions genuine rather than reflecting experimental error. Alternatively a further step can be added in which the ΔCT value of an

unstimulated baseline sample from the same subject (known as a calibrator sample), is subtracted from the first ΔCT value. The fold change in expression of the gene of interest in a particular sample relative to its own baseline is then calculated using the equation $2^{-\Delta\Delta CT}$ (231). This number can again be compared with other subjects or experimental conditions. Examples are shown below in tables 2.6 and 2.7. Each sample was run in duplicate and the mean of two CT values taken. GAPDH was used as the reference gene in these studies. All genes of interest and GAPDH were run in singleplex reactions with equal starting quantities of cDNA.

Gene of interest (mean of 2 CT values)	Reference gene (mean of 2 CT values)	ΔCT $=CT^{\text{gene of interest}} - CT^{\text{reference gene}}$	Fold change compared to GAPDH $=\text{power}(2^{-\Delta CT})$
21.6	26.2	-4.6	24.7

Table 2-6 Example of the $2^{-\Delta CT}$ relative quantification method

The table outlines an example calculation of gene of interest mRNA expression relative to the normalising gene, GAPDH.

ΔCT of stimulated sample $=CT^{\text{gene of interest}} - CT^{\text{reference gene}}$	ΔCT of calibrator (e.g.unstimulated) sample $=CT^{\text{gene of interest}} - CT^{\text{reference gene}}$	ΔΔCT $= \Delta CT^{\text{stimulated sample}} - \Delta CT^{\text{calibrator sample}}$	Fold change compared to calibrator sample $=\text{power}(2^{-\Delta\Delta CT})$
-4.6	0.8	-5.4	42.2

Table 2-7 Example of the $2^{-\Delta\Delta CT}$ relative quantification method

The table outlines an example calculation of the fold change of a gene of interest mRNA from baseline expression, relative to the normalising gene, GAPDH.

2.8 **Analysis of cell surface markers using flow cytometry**

Flow cytometry was used to confirm the purity of monocyte isolates obtained by the Dynabeads® Untouched™ Human Monocytes kit (Life Technologies Limited, Paisley, UK), to detect and quantify the expression of cell surface TNFR1 and TNFR2 on monocytes under various experimental conditions and to detect apoptotic cells. Figure 2.12 outlines the principles of flow cytometry.

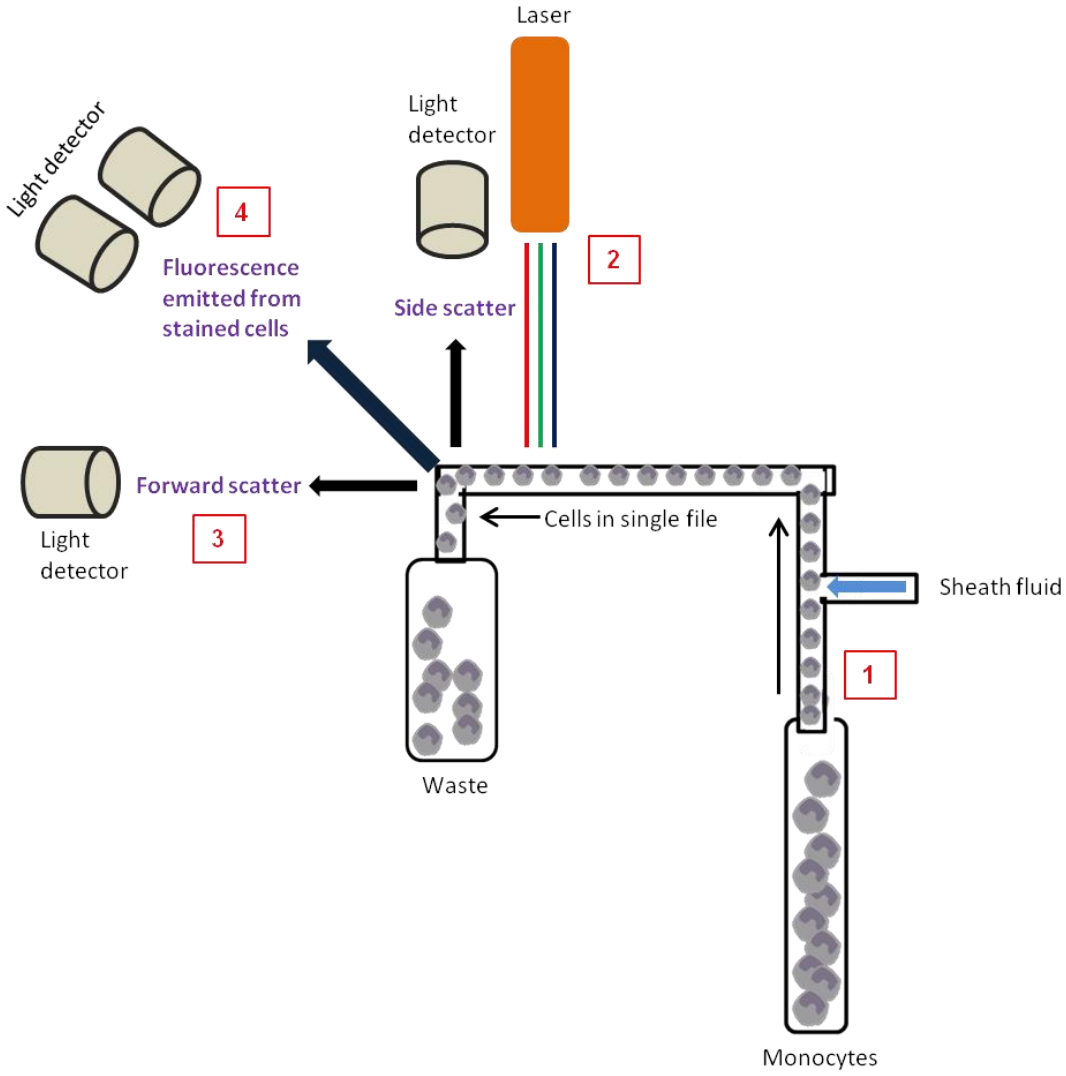

Figure 2-12 Principles of flow cytometry

1) Isolated cells suspended in PBS-1 are streamed through the flow cytometer in single file. 2) Each cell individually passes through a laser beam. As the light hits each cell it is scattered in different directions. The intensity of forward scatter is approximately proportional to the diameter of the cell and the intensity of side scatter is approximately proportional to the degree of granularity and complexity of the intracellular contents of the cell type in question. 3) The scattered light is detected by light detectors and the intensity converted to a voltage pulse. 4) Cells under study can also be labelled with mAbs to a particular cell surface marker. In turn, the antibody is pre-labelled with a specific fluorophore. The fluorophore is excited by absorption of light from the laser. On return to its ground state energy level the fluorophore emits light (fluoresces) at a wavelength specific to the fluorophore chosen. The emitted light is detected by a detector capable of sensing that particular wavelength of light (a band pass filter). The intensity of light detected is proportional to the number of cell surface receptors labelled with the mAb. A range of fluorophores, emitting light at different wavelengths can be utilised in order to detect different surface markers.

Monocytes (0.25 x 10^6 per sample) underwent flow cytometry immediately after isolation or after a period in culture. Cells in culture plates were first gently de-adhered by removing the culture media and replacing it for 20 minutes with 750 µl of Accutase® solution (Sigma-Aldrich Chemicals Ltd, Poole, UK). Accutase® solution contains non-mammalian and non-bacterial sources of enzymes to de-adhere cells and is marketed as being a more gentle method than trypsin or collagenase, preserving most epitopes for subsequent flow cytometry studies (232).

Monocytes were washed and re-suspended with sterile PBS-1. 10 µg of human IgG was added per 1 x 10^5 cells as an Fc-receptor blocking step for 15 minutes, followed by incubation in the dark for 30 minutes at room temperature, with 10 µl per 1 x 10^6 monocytes of each fluorophore-labelled mAb to the cell surface markers under study, as per product protocols. A maximum of two mAbs per sample were used. Samples were then washed twice with PBS-1 before re-suspending in 300 µl of PBS-1 for final flow cytometric analysis. Samples were kept on ice throughout.

Control samples labelled with equivalent volume of isotype matched control Abs were run simultaneously to identify any binding to Fc-receptors, despite the use of a blocking step earlier in the protocol, or binding to non-specific cell surface targets. These samples were used in the gating process as described in 2.8.1 and in presenting fluorescence intensity data. Positively-labelled samples were run in duplicate; control samples and unstained cells were not, due to limitations to available cell numbers. Where possible, approximately 10000 events within the gate set over the monocyte population were collected per sample. In some cases this was not possible with cells which had been de-adhered from culture plates at later time-points, as a proportion of these cells were shown to undergo apoptosis over time and hence less viable cells were available for gating and analysis. Of 138 positively labelled samples

which underwent analysis of TNFR1 and TNFR2 expression the median number of monocytes gated per plot was 9914 and the IQR was 5560 to 10684. All results were included in analyses. The limitations of this are discussed in chapter 5.

The following antibodies were used in experiments, as previously outlined in full in table 2.2: mouse anti-human IgG_1 TNFR1 mAb; mouse anti-human IgG_{2A} TNFR2 mAb; mouse IgG_1 isotype control Ab; mouse anti-human IgG_1 CD14 mAb; mouse anti-human IgG_1 control Ab (all R and D Systems, Abingdon, UK); mouse IgG_{2A} control Ab (BD Biosciences, Oxford, UK); mouse anti-human IgG_{2A} CD16 mAb and mouse anti-human IgG_{2A} control Ab (2 µl of each) (Life Technologies, Paisley, UK). Fluorescence was recorded using a BD Accuri™ C6 flow cytometer (BD Biosciences, UK). Excitation of the fluorochromes FITC, PE and PerCP was achieved using an argon laser at 488 nm and at 640 nm for APC. Fluorescence emitted from each fluorophore was detected through different band pass filters: 530 nm for FITC, 585 nm for PE, 670 nm for PerCP and 675/25 nm for APC.

Flow cytometry data was analysed using BD Accuri C6 software (BD Biosciences, Oxford, UK). Data was recorded as both median fluorescence intensity (MFI), an average of the brightness of each cell labelled with a specific receptor mAb, and as percentages of cell surface marker positive monocytes. MFI results are presented as a ratio of the MFI for the positively labelled cells, to the MFI of the negative control cells incubated with fluorophore-labelled isotype controls.

Colour compensation was set for each group of experiments prior to data analysis, to correct for any fluorescence spillover. This occurs when the emission spectra of two fluorophores overlaps slightly and hence a band pass filter detecting one may also detect a degree of fluorescence emitted by the other fluorophore (conjugated to a different cell surface receptor

mAb) and hence cause inaccuracy in the results obtained. The degree of colour compensation of each band pass filter in use was determined by running one subject's samples, labelled separately with each flow cytometry mAb and using the MFI values from the two detectors for these separate samples to determine an appropriate percentage correction for each filter. An example is shown in table 2.8.

	MFI in PE band pass filter (585nm)	MFI in FITC band pass filter (530nm)
Unstained cells	342*	732*
Cells labelled with a TNFR2 mAb (conjugated to FITC)	1012**	5748
Correction factor= (1012-342)/(5748-732)=0.134 **The 585nm (PE) band pass filter is corrected by subtracting 13.4% of the total signal detected in that filter.** *due to autofluorescence **due to unwanted spillover		

Table 2-8 An example of colour compensation

The table shows the MFI values of unstained monocytes and monocytes labelled with a TNFR2 mAb conjugated to FITC in band pass filters that detect FITC or PE. Any fluorescence detected in the PE band pass filter is as a result of autofluorescence and/or spillover. The four values can be used to determine what percentage of the signal must be subtracted from the PE filter in future experiments to correct for spillover.

2.8.1 Gating strategy

For each set of experiments a forward versus side scatter plot was created on a sample of unstained cells to identify all events and a gate was placed around the isolated monocyte population. Each dot represents an individual event/cell. Most events are complete cells but debris is often present and this is identified to the bottom left of the plot, indicating its low size and low internal complexity. An example plot is shown in figure 2.13.

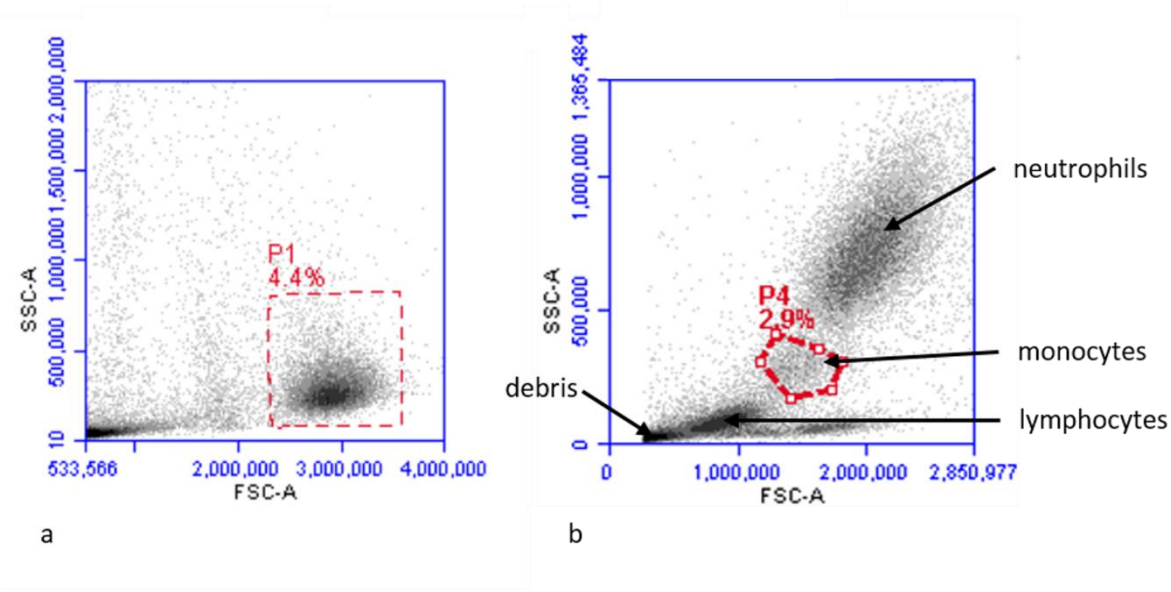

Figure 2-13 Gating around the monocyte population

a) A forward scatter (x-axis) versus side scatter (y-axis) plot is shown. The monocyte population extracted by negative immunoselection is shown in gate P1 (in this example equals 10,457 events). b) A forward scatter versus side scatter plot of whole blood from a different young healthy control subject is shown for comparison. Monocytes are shown in gate P4.

A pulse-width versus forward scatter area plot was created in order to exclude any doublet events, whereby two cells clump and pass through the flow cytometer together rather than in succession. This plot works on the principle that the time taken for a light signal to pass through two cells clumped together will be longer, i.e. a greater voltage pulse width. Two clumped cells may also have a greater diameter and hence higher forward scatter. For this reason, as shown in figure 2.14, cells with high pulse width and of a forward scatter equal or greater than the majority of cells can be identified and excluded as these are likely to represent doublet events (233).

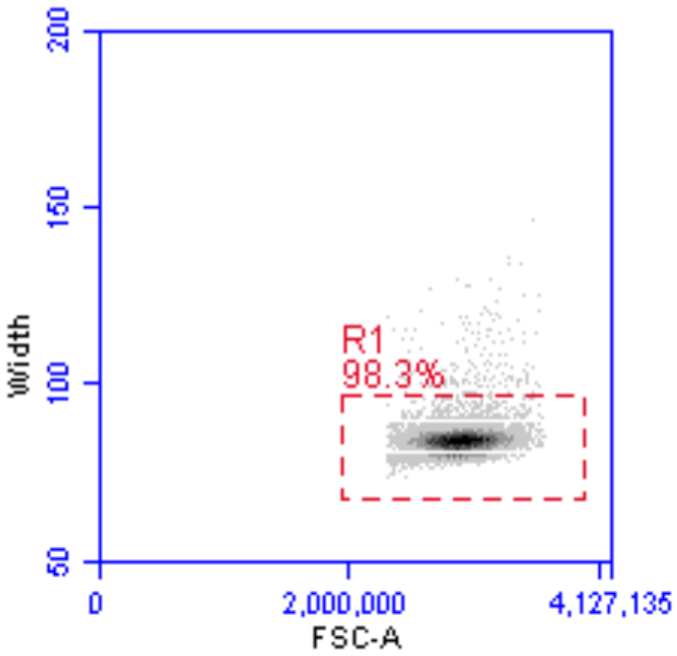

Figure 2-14 Pulse width versus forward scatter plot.

R1 shows a gate around singlet events/cells. Events with high pulse width are shown as blue dots above gate R1 and represent excluded doublet events.

Next, quadrant scatter plots were created of the previously gated cells, comparing intensity of one cell surface receptor of interest on the x-axis against another on the y axis, for example TNFR2 against TNFR1, as shown in figure 2.15. Quadrant gate setting is shown in the figure.

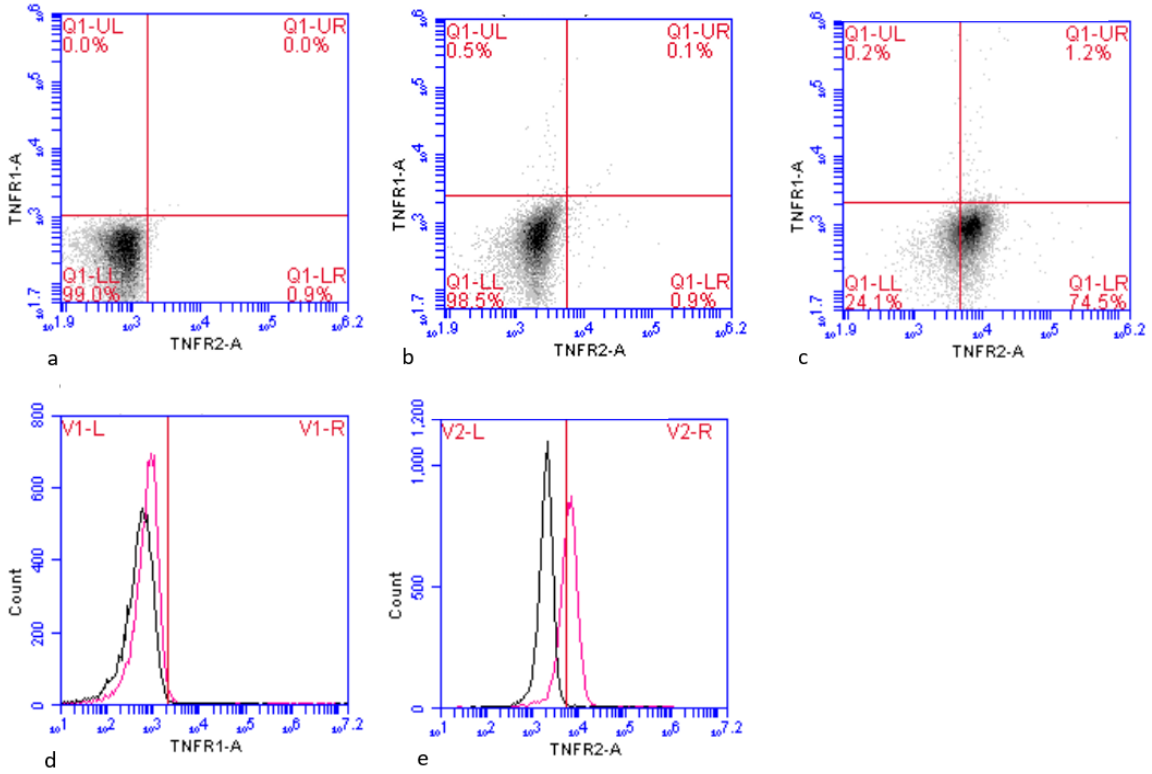

Figure 2-15 Further gating of monocytes

a) Quadrant plot showing autofluorescence of unstained monocytes, detected in the band pass filters for TNFR1 (y-axis) and TNFR2 (x-axis). A quadrant gate has been set. b) Quadrant plot showing fluorescence emitted from cells from the same experiment incubated with fluorophore labelled isotype control Abs (negative control). The quadrant gate has been moved to the right to exclude the additional fluorescence from non-specific and Fc-receptor binding. This is the final gate for later analysis of cells labelled with the antibodies of interest. c) Quadrant plot showing fluorescence emitted from cells labelled with TNFR1 and TNFR2 flow cytometry mAbs. Some cells have moved beyond the limits of the previously set quadrant gate, reflecting genuine receptor-mAb binding. Shown are percentages of monocytes that were positive for neither receptor (left lower quadrant), both (upper right quadrant), TNFR1 only (upper left quadrant) or TNFR2 only (lower right quadrant). d) Data from the same subject as c, shown as a fluorescence histogram for TNFR1 intensity, demonstrating that very few cells (pink histogram) had greater fluorescence than the negative control cells (black histogram). The red marker is set to delineate positive from negative cells. e) Data from the same subject as c, shown as a fluorescence histogram for TNFR2 intensity, demonstrating that

many cells (pink histogram) had greater fluorescence than the negative control cells (black histogram). The red marker is set to delineate positive from negative cells.

2.9 **Apoptosis assay**

It was observed that in some subjects' samples, flow cytometry plots for monocytes incubated for longer periods showed a reduction in the size (corresponding to less forward scatter) and in some cells increased granularity (increased side scatter) also. To investigate if this change was due to apoptosis of some of the cells, the PE- Annexin V Apoptosis Detection Kit I (BD Biosciences, Oxford, UK) was used to test isolated monocytes from one healthy subject. This assays works on the principle that as cells begin the process of early apoptosis the membrane phospholipid, phosphatidylserine, is translocated from the inner to the outer aspect of the plasma membrane. Annexin V, a calcium dependent phospholipid-binding protein is able to bind to this and fluoresce if labelled with PE (234). Cells in the later stages of apoptosis, or those undergoing necrosis, lose the impermeability of the cell membrane and hence allow a dye, 7-Amino-Actinomycin (7-AAD), to enter the cell. The 7-AAD dye is only visible once within a damaged cell when it undergoes a spectral shift once associated with DNA (235). The apoptosis assay protocol (236) used does not involve a washing step post addition of the annexin V and 7-AAD as any bound 7-AAD would be washed away, therefore some annexin V might bind non-specifically at low levels even in the absence of any early apoptosis (direct communication with BD Biosciences Scientific Support, March 2013). Product literature therefore recommends incorporating a positive control, in which monocytes are induced to undergo apoptosis, with which to compare the extent of Annexin V or 7-AAD binding. Camptothecin (Sigma-Aldrich Chemicals Ltd, Poole, UK), an inhibitor of DNA replication and commonly used inducer of apoptosis (237) was used as per the assay protocol (236).

Isolated monocytes from one healthy subject (1 x 10^5 per condition and in duplicate) were treated in the following ways: freshly isolated untreated cells; cells treated with camptothecin to a final concentration of 20 µM for 20 hours (as recommended in the assay protocol (236)); cells treated with LPS to a final concentration of 100 ng/ml for 20 hours. Monocytes treated for 20 hours were incubated at 37 ^{0}C and in 5% CO_2.

Cells in culture plates were first gently de-adhered by removing the culture media and replacing it for 20 minutes with 750 µl of Accutase® solution (Sigma-Aldrich Chemicals Ltd, Poole, UK). Monocytes were washed twice in sterile PBS-1 and re-suspended in 1X binding buffer, provided in the commercial assay. 100 µL of the binding buffer, containing approximately 1 x 10^5 monocytes was transferred to each flow cytometry tube. Cells were then either left unstained, stained with 5 µl of PE-labelled Annexin V or 5 µl of 7-AAD or with both. The flow cytometry tubes were gently vortexed and incubated for 15 min at room temperature in the dark, following which 400 µl of 1X binding buffer was added to each tube. Fluorescence was recorded using the BD Accuri™ C6 flow cytometer (BD Biosciences, Oxford, UK). Excitation of PE and 7-AAD was achieved using an argon laser at 488 nm. Fluorescence emitted from each fluorophore was detected through the following band pass filters: 585 nm for PE and 670 nm for 7-AAD. A 4.5% correction was applied to the 585 nm band pass filter and 19.6% to the 670 nm band pass filter to correct for those percentages of spillover into those filters. Flow cytometry data was analysed using BD Accuri C6 software (BD Biosciences, Oxford, UK). Gating was applied as previously outlined in 2.8.1. In some analyses further gates were applied to exclude debris and this strategy is outlined in detail in figure 3.11.

2.10 **Statistical analysis**

Data is presented as median and range/IQR in chapters 4 and 5, due to small sample sizes, with the exception of data presented as percentages which is displayed as means and standard deviation (SD). Data is presented as mean and SD or median and range/IQR in chapter 3. Non-parametric testing was used throughout. Individual comparisons were made using a Wilcoxon signed-rank test for dependent data and a Mann Whitney U test for independent data. Friedman's test was used to detect any overall difference in multiple related medians, with post-hoc all pairwise multiple comparisons testing if the Friedman's test result allowed rejection of the null hypothesis of there being no overall difference. SPSS provides adjusted significance levels for the post-hoc pairwise comparisons using the Dunn-Bonferroni correction, whereby the unadjusted significance values are multiplied by the number of comparisons, setting the value to 1 if the product is greater than 1. In some analyses all possible comparisons were not relevant, for example time course experiments in which the comparisons of interest were each time-point specifically with time zero. In these cases an adjusted p-value was determined by multiplying the unadjusted p-value only by the number of comparisons of interest. Area-under-the curve (AUC) values were calculated according to the trapezium rule. Statistical significance was set at $p<0.05$ with two-tailed significance if there was no prior hypothesis regarding the direction of difference between two groups and one-tailed significance if the direction of difference was predicted due to previous experiments or published data, as suggested (238). Use of one-tailed p-values are specified in the text where used. Data was analysed using the SPSS statistical program (version 22.0 Chicago, USA). All statistical analyses were discussed with a medical statistician.

CHAPTER 3

VALIDATION EXPERIMENTS

3 Validation experiments

3.1 Introduction and aims

The main aim of this chapter was to describe the initial experiments that were undertaken in order to thoroughly prepare for the investigation of the effects of the rs361525 polymorphism on monocytes from patients with A1ATD-related COPD in chapter 4. In addition, validation results of the various assays and experimental techniques used throughout the thesis are also described. Lastly, findings from the PE- Annexin V Apoptosis Detection Kit I (BD Biosciences, Oxford, UK) are presented. This assay was used to investigate the hypothesis that the change in monocyte size and granularity that was first noted in later stages of the thesis was due to apoptosis of monocytes.

3.2 Results

3.2.1 Purity of monocyte isolates

Immunostaining with CD14 and CD16 mAbs and subsequent flow cytometric analysis of monocyte isolates from three healthy control subjects was performed to determine the purity of isolates obtained using the Dynabeads® Untouched™ Human Monocytes kit (Life Technologies Limited, Paisley, UK). Fluorescence spill-over was detected in the 675/25 band pass filter and an 18.4 % correction factor applied to compensate for this.

Figure 3.1 shows a representative plot from one subject, illustrating that the majority of gated monocytes were CD14 positive and CD16 negative, although unexpectedly a proportion were CD14 and CD16 positive.

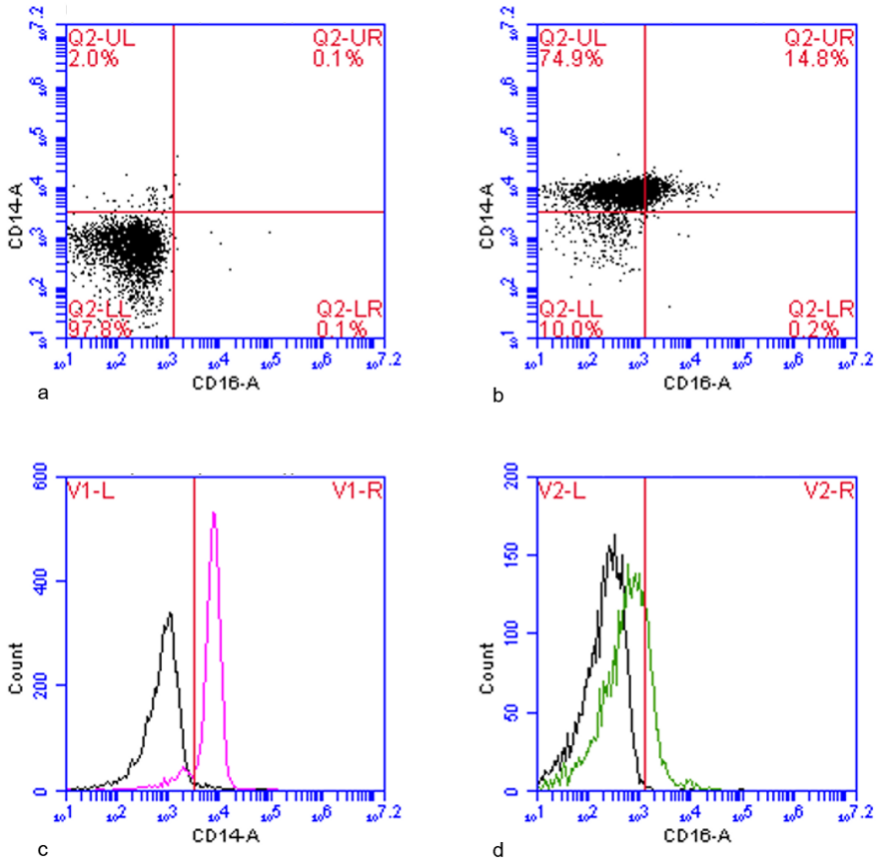

Figure 3-1 Example flow cytometry plot illustrating CD14/CD16 status.

Representative quadrant plot and fluorescence overlay histograms from one subject. a) A quadrant marker is set around the main body of monocytes incubated with an isotype control antibody. b) Monocytes labelled with CD14 and CD16 mAbs. The 2-parameter dot plot is split into 4 quadrants: bottom left- CD14 and CD16 negative; top left- CD14 positive only; top right- CD14 and CD16 positive; bottom right- CD16 positive only. b) Two histograms are shown, with fluorescence intensity in the PerCP channel on the x-axis (logarithmic scale) and cell count on the y-axis. The black histogram represents monocytes incubated with a PerCP-labelled isotype control antibody. The pink histogram represents monocytes labelled with PerCP-CD14 mAb. c) The black histogram represents monocytes incubated with an APC-labelled isotype control antibody. The green histogram represents monocytes labelled with APC-CD16 mAb. Red vertical markers are shown on both figures to delineate fluorescence due to specific binding of mAbs to the cell surface receptor of interest (to the right of the set marker) from that due to non-specific binding of flow cytometry antibodies (to the left of the marker).

Table 3.1 shows the percentages of monocytes which were CD14+CD16-, CD14+CD16+, CD14-CD16+ and CD14-CD16- in each of the three healthy subjects tested.

Subject	CD14+CD16-	CD14+CD16+	CD14-CD16+	CD14-CD16-	Total
One	74.3	14.6	10.9	0.2	100.0%
Two	63.9	29.9	6.1	0.1	100.0%
Three	64.6	30.3	5.0	0.1	100.0%

Table 3-1 Purity of monocyte isolates in three healthy subjects

CD14 and CD16 cell surface marker expression was measured in monocyte isolates from 3 healthy subjects extracted using the Dynabeads® Untouched™ Human Monocytes kit. Positively labelled samples were run in duplicate and the percentages shown are the mean of 2 results.

3.2.2 Validation of enzyme linked immunosorbent assays

The precision of an assay is determined by how reproducible a result is within one ELISA plate (intra-assay validation) and across multiple ELISA plates (inter-assay validation). Intra-assay validation of the TNF-α, CXCL8, TNFR1 and TNFR2 ELISA assays was conducted as follows and the coefficient of variation percentage (CV%) values are shown in table 3.2: for each of the four assays one known concentration of the relevant mediator wa prepared from the supplied standard. These solutions were then run in 10 wells for each known concentration to allow determination of the intra-assay variability. Each result was determined by interpolation from the standard curve using the forecast function in Excel (Microsoft Office 2010). The mean and SD of the results of the 10 wells was calculated and from this the CV% was determined.

Assay	TNF-α	CXCL8	TNFR1	TNFR2
CV %	5.8	3.2	9.8	9.1

Table 3-2 Intra-assay validation of ELISAs

The table shows CV% values for the four ELISAs used in this thesis, when a known concentration of the relevant mediator was run in 10 wells of the same assay plate.

Multiple TNF-α and CXCL8 ELISA plates were used in the studies for this thesis. It was therefore necessary to conduct inter-assay validation of the assays used for these mediators, and the CV% values are shown in table 3.3. For both assays one known concentration of the relevant mediator was prepared from the supplied standard and then run once on each of ten consecutive plates. Each result was determined by interpolation from the standard curve using the forecast function in Excel (Microsoft Office 2010). The mean and SD of the results of the 10 wells was calculated to determine the CV % value.

Assay	TNF-α	CXCL8
CV %	14.8	15.5

Table 3-3 Inter-assay validation of ELISAs

The table shows CV% values for the two ELISAs used in this thesis where multiple plates over time were required. A known concentration of each mediator was run in one well on each of ten assay plates.

3.2.3 Determining quantity and purity of extracted RNA

The median 260/280 ratio of 396 RNA samples was 2.1 (IQR 1.8-2.4). The concentration of RNA in all samples was less than 10 ng/µl. All samples were used in ongoing experiments and the reasons for this are discussed in 3.3.

3.2.4 Validation of GAPDH as a reference gene

It is important when choosing a reference gene that the gene is validated for an individual experimental model. This means that its expression must be shown to remain unaffected by a particular experimental condition and must be the same between subjects, otherwise calculated differences in expression of the gene of interest will be inaccurate (239). Ideally, each gene of interest should be normalised against multiple reference genes but this is costly and impractical in cases where limited RNA/DNA is available (240). Alternatively, experts have stated that where an individual reference gene can be shown to be stably expressed in the model under study then it is acceptable to use only that one, particularly when any slight genuine variability in reference gene expression is outweighed by much greater changes in the gene of interest between samples (239, 240). For example, a 10 fold variability in expression of the reference gene is less important if changes in the gene of interest are 100 fold (239). Dedha *et al* compared the expression of a panel of commonly used reference genes in whole blood and PBMCs under a variety of conditions and subject characteristics. They classified stable reference genes as those in which the average fold change of that gene from the mean expression was less than 2 and the maximum variability in fold change less than 5 (240).

The suitability of GAPDH for use as a reference gene in this thesis was tested by performing RT-qPCR on samples from five of the COPD patients (three with the rs361525 polymorphism and two without), each containing a volume of cDNA in solution equivalent to 0.9 ng of starting mRNA. This equated to 64 CT values. Each of the 64 values was an average of a

sample run in duplicate. The samples represented a range of experimental conditions (unstimulated; stimulated with LPS or PMA; stimulated with LPS in the presence of TNF-α mAb) and had been harvested at varying time-points between 0 and 24 hours. The results of this validation experiment are shown in table 3.4 and highlight the stability of expression of GAPDH across a large number of samples from different patients and under a variety of experimental conditions. The results are expressed as a mean fold change from the mean CT value.

Mean (median) CT value for GAPDH in 64 samples	27.1 (27.0) cycles
Standard deviation of the mean CT value	0.8 cycles
Mean fold change from the mean CT value	1.7
Standard deviation of fold change from the mean CT value	0.6
Maximum fold change from the mean CT	4.6
75^{th} percentile fold change from the mean CT	1.8
25^{th} percentile fold change from the mean CT	1.2

Table 3-4 Validation of GAPDH as a reference gene

The table shows the mean (SD) CT value for GAPDH in 64 different samples and the mean (SD) fold change from this mean value. This demonstrates the stability of GAPDH across a broad range of samples.

3.2.5 Intra-assay and inter-assay validation of the RT-qPCR reaction

The three most frequently studied genes in this thesis, TNF-α, CXCL8 and GAPDH, were chosen to determine an estimate of the intra-assay and inter-assay variation in results obtained using TaqMan® gene expression assays. To determine intra-assay variation RT-qPCR was performed using equal quantities of cDNA from one subject in eight wells per gene expression assay of one PCR experiment. To determine inter-assay validation RT-qPCR was performed using equal quantities of cDNA from one subject in one well per gene expression

assay for eight PCR experiments. The results, shown in table 3.5, are expressed as a SD of the mean CT value obtained for each of the three assays and CV% values.

	TNF-α		CXCL8		GAPDH	
	Intra-assay	Inter-assay	Intra-assay	Inter-assay	Intra-assay	Inter-assay
Mean CT value	30.2	29.6	23.4	23.0	26.7	26.5
SD of CT value	0.1	0.3	0.06	0.2	0.04	0.2
CV%	0.3%	1.0%	0.3%	0.9%	0.1%	0.8%

Table 3-5 RT-qPCR intra-assay and inter-assay validation

The table shows the mean, SD and CV% values of CT values for three genes of interest. Intra-assay variation was determined by measuring the expression of each gene (expressed as as a CT value) using cDNA from one subject in eight replicates per gene during one RT-qPCR experiment. Inter-assay variation was determined by measuring the expression of each gene using cDNA from one subject in one well per gene for eight separate PCR experiments.

3.2.6 Identifying stimulants of TNF-α secretion by monocytes

In order to determine if monocytes from A1ATD-related COPD subjects with the rs361525 polymorphism produced more TNF-α than cells from wild-type subjects it was necessary first to identify a mediator which would elicit a TNF-α response, the optimum concentration of that mediator to elicit a maximum response and the peak time point of TNF-α secretion at which to harvest supernatants in these later experiments. Unless otherwise specified, 0.45 million monocytes per well were used, each time point or condition was conducted in duplicate and a mean result taken. Results for each pre-specified time point or concentration of mediator were determined by collecting supernatants from separate wells.

Time course profiles of sTNF-α were conducted using monocytes cultured in the absence of an exogenous stimulant (unstimulated) or in the presence of LPS, IL-1β or MCP-1 (figure 3.2). Although indirect comparisons between different subjects' monocytes, LPS elicited the

greatest response. Similar time course profiles (not shown) were observed using 1 ng/ml or 10 ng/ml of the relevant stimulant. All time course profiles demonstrated that the concentration of sTNF-α decreased back towards to baseline after 20 hours of culture.

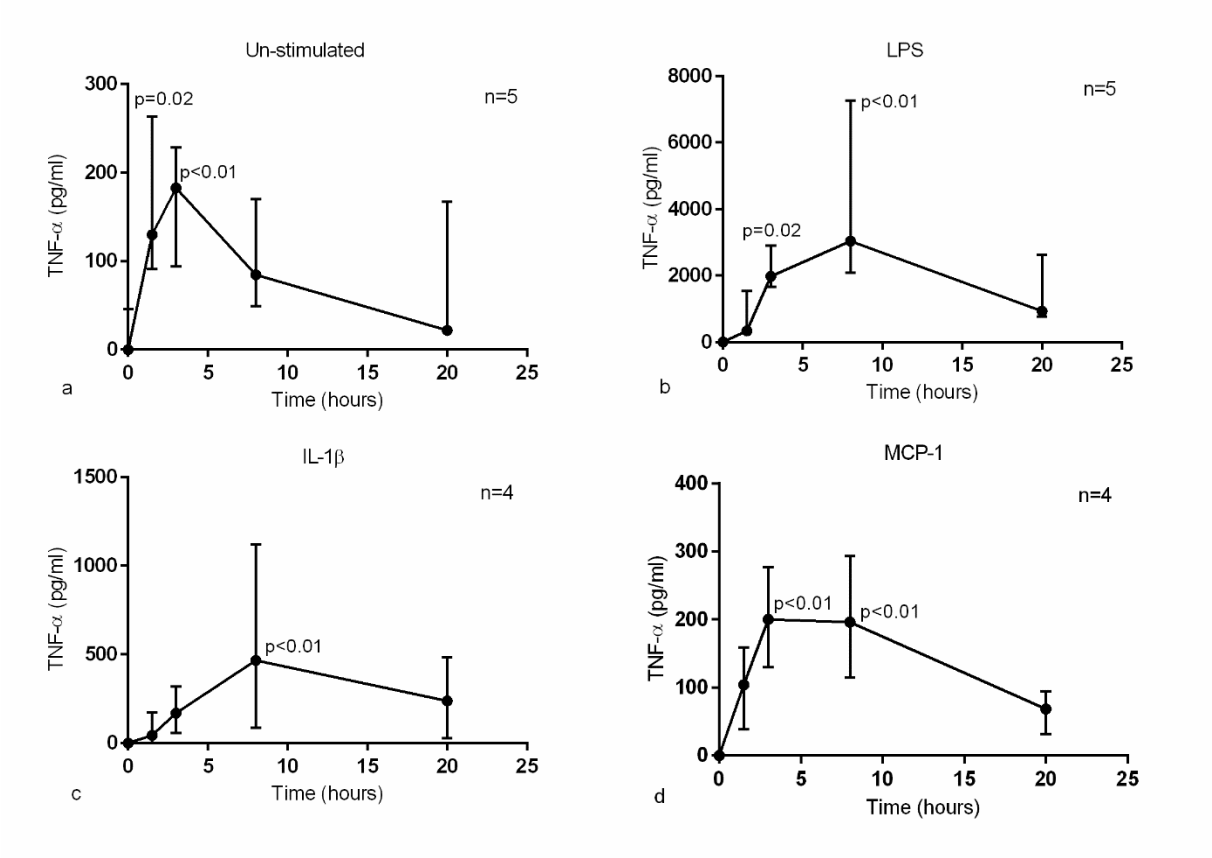

Figure 3-2 Time course profile of sTNF-α in the supernatant of monocytes

Time course profiles for sTNF-α concentration in response to different stimuli are shown. Each datum point is the median value (with range). Friedman's testing where significant was followed by post-hoc pairwise comparisons of each time-point to time zero (unadjusted p-values were first corrected by multiplying by 4 and where significant are shown on the graphs at the relevant time-points). a) No exogenous stimulus: Friedman's test $p<0.01$. b) 100 ng/ml of LPS: Friedman's test $p<0.01$. c) 100 ng/ml of IL-1β: Friedman's test $p=0.01$ d) 100 ng/ml of MCP-1: Friedman's test $p=0.01$.

Monocytes were stimulated for 8 hours with increasing concentrations of each stimulus, up to a maximum of 100 ng/ml of the mediator. Figure 3.3 shows that 100 ng/ml of LPS or IL-1β increased sTNF-α concentration over that produced by monocytes cultured without an

exogenous stimulus. MCP-1 had no effect on sTNF-α concentration at any concentration. Higher concentrations of LPS were not tested as these were likely to be supra-physiological and hence less clinically relevant (241).

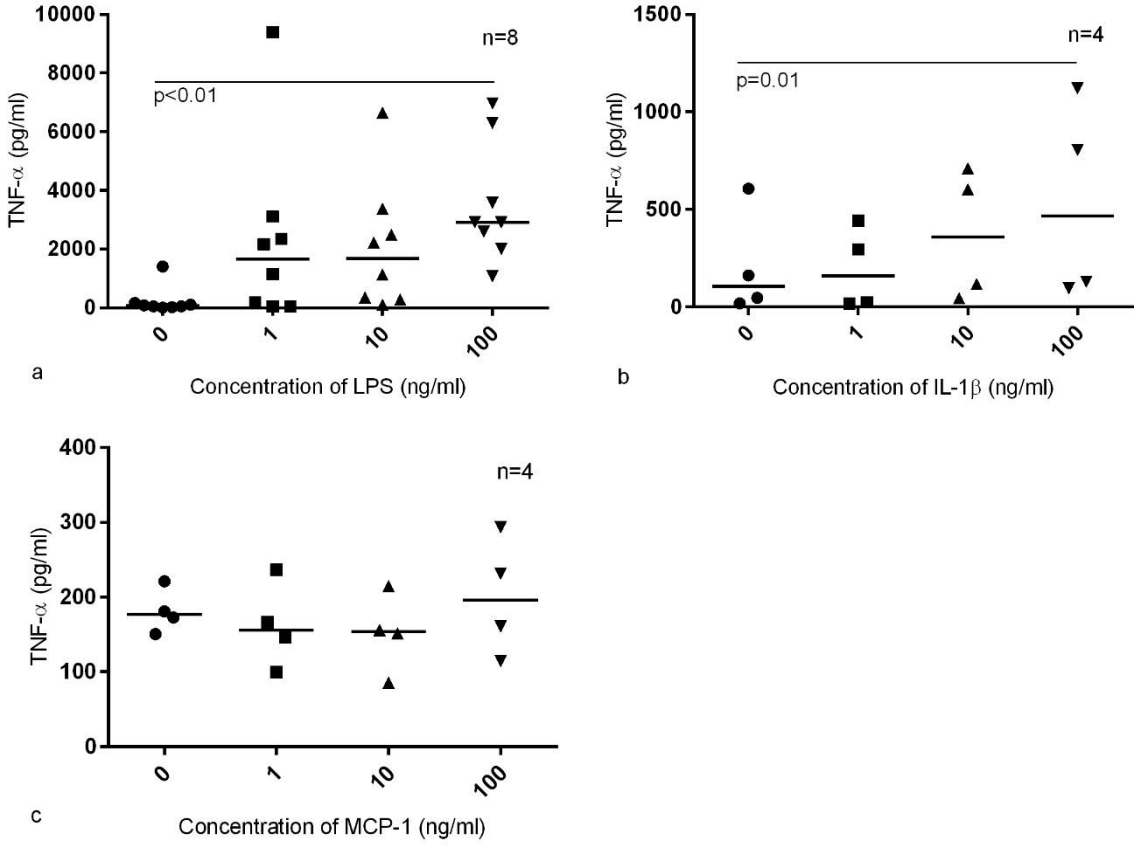

Figure 3-3 sTNF-α production by monocytes stimulated with increasing concentration of stimulant

Monocytes were stimulated for 8 hours with an increasing concentration of each stimulant. Individual subject data is shown with median values displayed as bars. Friedman's testing where significant was followed by post-hoc pairwise comparisons of each concentration to 0 ng/ml of stimulant (unadjusted p-values were first corrected by multiplying by 3 and where significant are shown on the graphs at the relevant time-points). a) LPS: Friedman's test $p<0.01$ b) IL-1β: Friedman's test: $p=0.01$ c) MCP-1: Friedman's test non-significant.

3.2.7 Optimal timing for cell supernatant collection

The monocyte extraction process takes approximately four hours to carry out making detailed time course experiments difficult to achieve if conducted on the same day as extraction. Further time course experiments were therefore conducted in cells which had been allowed to incubate overnight, again using 0.45 million monocytes per well and in duplicate. This permitted a greater number of time-points to be tested throughout the course of a day. 100 ng/ml of LPS was employed as the monocyte stimulant as this had elicited the greatest sTNF-α response in concentration response experiments (figure 3.3). After incubating overnight the cell culture medium was changed prior to stimulating the monocytes with LPS, to remove any cytokines which had been secreted prior to this and which would affect subsequent measurements.

Figure 3.4a shows the time course profile following stimulation with LPS. In a separate time course profile it was not possible to detect any sTNF-α at any time-point in the supernatants of monocytes which had been incubated overnight and then left without any exogenous stimulation.

The concentration of CXCL8 was also measured in the same samples. Figure 3.4b shows that even without the addition of an exogenous stimulus monocytes which have been incubated overnight remain able to produce CXCL8 and that this accumulates in the supernatant with time, eventually levelling off after approximately 12 hours. In contrast, monocytes incubated overnight and then stimulated with LPS continue to secrete CXCL8 into the supernatant at 24 hours (figure 3.4c).

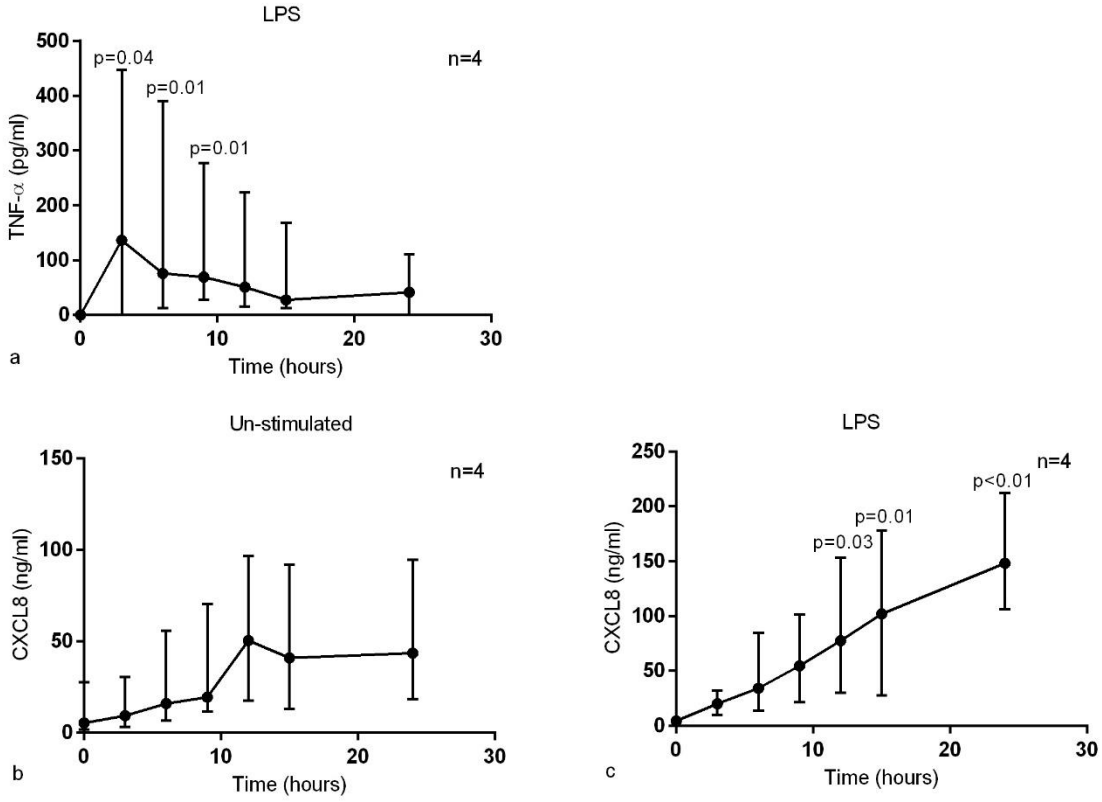

Figure 3-4 Time course profile of sTNF-α and CXCL8 in the supernatant of monocytes rested overnight prior to stimulation with 100 ng/ml of LPS

Time course profiles for sTNF-α and CXCL8 concentration are shown. Each datum point is the median value (with range). Friedman's testing where significant was followed by post-hoc pairwise comparisons of each time-point to time zero (unadjusted p-values were first corrected by multiplying by 6 and where significant are shown on the graphs at the relevant time-points). a) sTNF-α concentration in LPS-stimulated monocytes: Friedman's test p=0.01 b) CXCL8 concentration in unstimulated monocytes: Friedman's test p=0.02 c) CXCL8 concentration in LPS-stimulated monocytes: Friedman's test p<0.01.

Despite the comparison of time course profiles between monocytes stimulated immediately and those left overnight prior to stimulation being indirect (different healthy subjects donated monocytes to each), it was observed that there was a marked reduction in the concentration of sTNF-α detectable at each time-point in response to LPS stimulation in the latter experiment. The original experimental design intended for use in the A1ATD patient group had been to

extract monocytes on day 1 and stimulate them on day 2 as this would be more practical from an organisational perspective. However it became clear that should monocytes produce less sTNF-α on day 2 this would not be a feasible strategy. A further experiment was therefore designed in which monocytes from 6 subjects were stimulated for 8 hours either immediately after the extraction process was completed or the following morning (figure 3.5). This demonstrated, as hypothesised, that the concentration of sTNF-α was significantly lower in cells which had been allowed to incubate overnight prior to stimulation. It was determined therefore that experiments conducted in the A1ATD patient group would need to occur on the day of monocyte isolation, immediately following the extraction process.

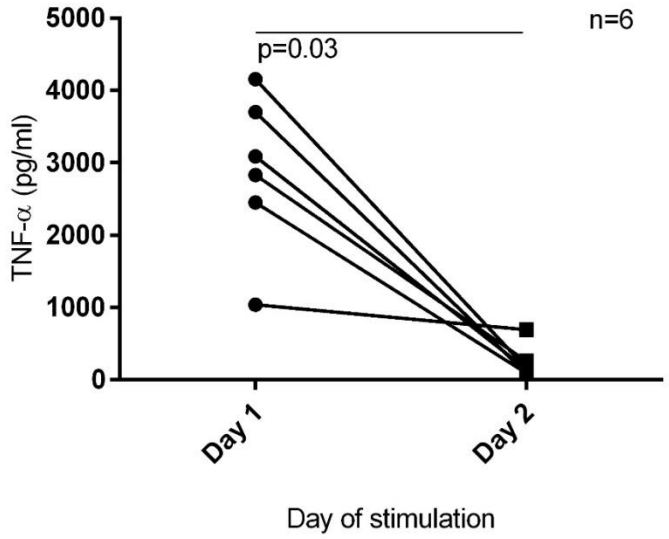

Figure 3-5 Concentration of sTNF-α in the supernatant of monocytes stimulated for 8 hours with 100 ng/ml of LPS immediately after monocyte extraction (day 1) or after incubating overnight (day 2)

Paired data is shown for monocytes stimulated on day 1 or day 2 after isolation. Differences between experimental conditions were tested with a Wilcoxon Signed Ranks test.

3.2.8 Effect of experimental replication on coefficient of variation

In order to determine if increasing the number of replicate samples for each experimental condition reduced the variation in results obtained, expressed as a CV% value, the following experiment was conducted: 5 replicate preparations of monocytes per subject were stimulated for 8 hours with 100 ng/ml of LPS and the concentration of sTNF-α in the supernatant measured. Each sample of supernatant was run in duplicate on the ELISA plate as described earlier. CV% values were calculated for each subject using sequential results, so that values were obtained for variation using 2, 3, 4 and 5 replicates. It was hypothesised that increasing the number of replicates would significantly reduce the CV%, however, as this was not the case statistical testing was not performed (figure 3.6). A pragmatic approach was therefore taken in future experiments in A1ATD patients and 3 replicates of each condition were conducted for each experimental condition/time-point.

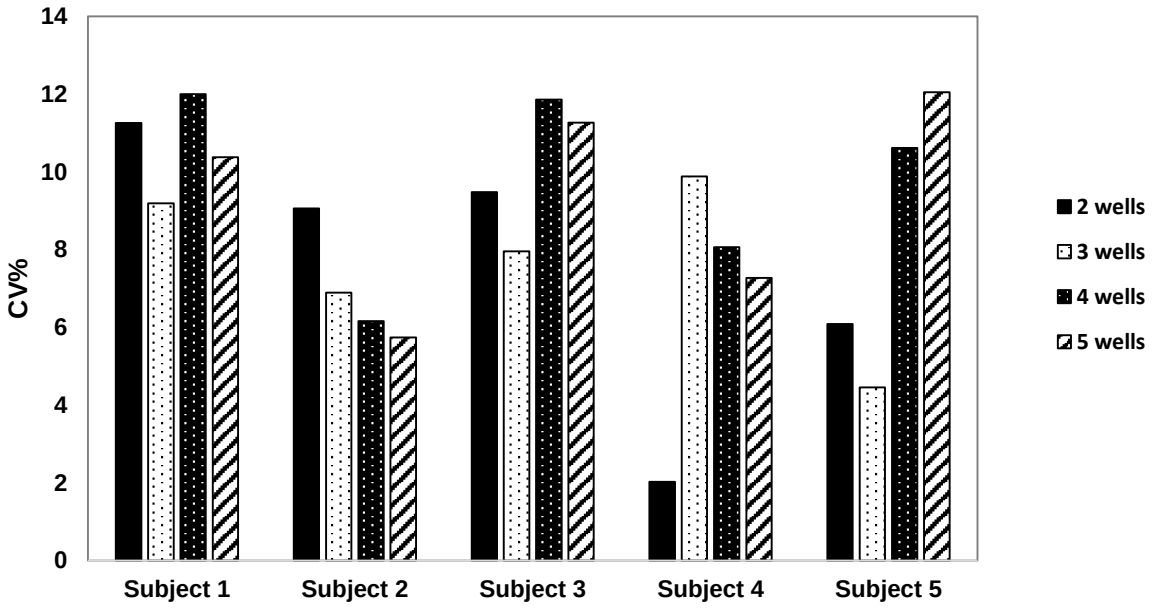

Figure 3-6 Effect of experimental replication on intrasubject variation in results obtained for TNF-α concentration in the cell-free culture supernatant

For each subject four columns are shown. Columns represent the CV% value of TNF-α concentration in the cell culture wells of monocytes exposed to 100 ng/ml of LPS for 8 hours, using 2, 3, 4 or 5 replicate wells.

3.2.9 Soluble TNF-α stimulates CXCL8 production

One hypothesis of this thesis was that increased production of TNF-α by monocytes from A1ATD-related COPD patients with the rs361525 polymorphism would lead to an enhanced effect on those monocytes by the excess TNF-α, specifically, they would produce more of the neutrophil chemoattractant CXCL8, and that blocking the TNF-α with a mAb would abrogate the effect. It was therefore necessary to show that monocytes can produce CXCL8 in response to sTNF-α and that a commercially available anti-TNF-α mAb could reduce this. Monocytes from 4 healthy subjects were stimulated in duplicate with increasing concentrations of exogenous sTNF-α for 24 hours and the concentration of CXCL8 measured by ELISA (figure

3.7a). No difference in CXCL8 concentration compared to unstimulated monocytes was observed until 1000 pg/ml of sTNF-α was used.

It was necessary to determine if the TNF-α mAb used was inhibitory, i.e. its binding to sTNF-α prevented sTNF-α from activating its receptors, rather than purely preventing its detection by a commercial ELISA and also to exclude any non-specific effect of an IgG1 antibody. Monocytes from 4 subjects were stimulated in duplicate with 100 pg/ml of sTNF-α alone, sTNF-α plus 10 µg/ml of TNF-α mAb (IgG1) or sTNF-α plus 10 µg/ml of IgG1 control isotype antibody (figure 3.7b). It was hypothesised that the presence of a TNF-α mAb would lead to a reduction in CXCL8 output by the monocytes compared to those stimulated with sTNF-α, whereas there would be no change in the presence of an irrelevant antibody. A trend was observed for CXCL8 concentration to reduce in the presence of the TNF-α mAb but this did not reach statistical significance. However, there was less CXCL8 in the presence of this mAb compared to the isotype control antibody ($p=0.01$) and no significant difference between the monocytes incubated with the control antibody and those stimulated with sTNF-α. From this it can be inferred that the isotype control antibody was having no clinically relevant effect on the interaction of sTNF-α with its receptors, whereas the TNF-α mAb was.

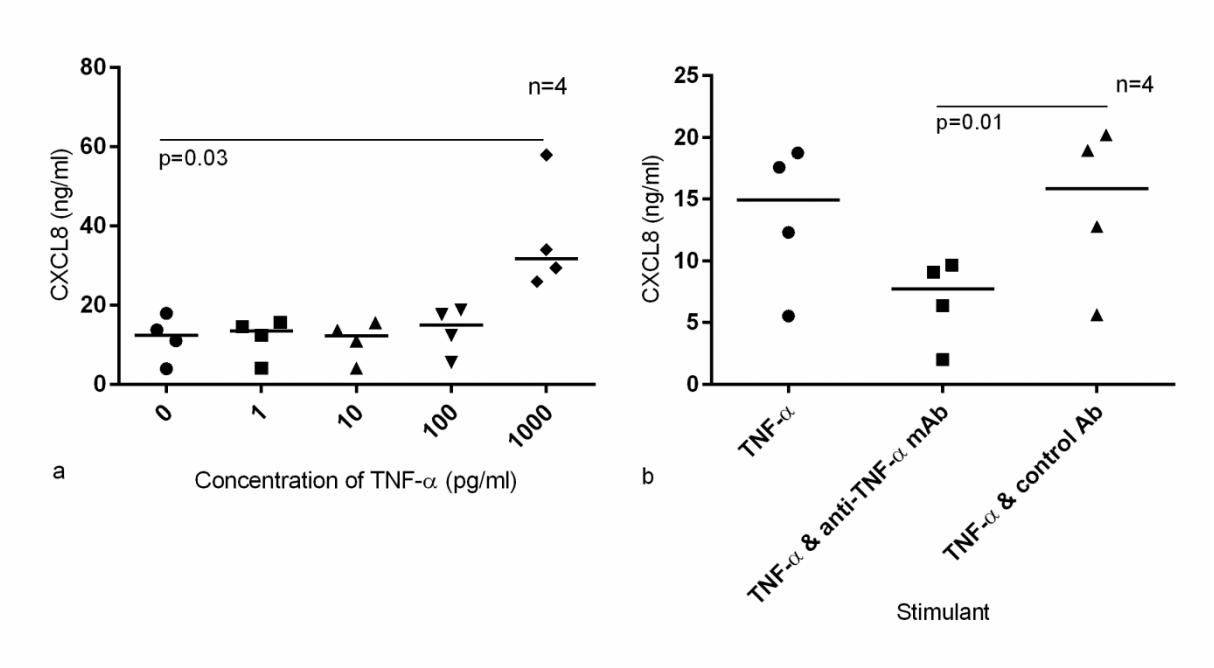

Figure 3-7 sTNF-α induces CXCL8 secretion by monocytes and a TNF-α mAb prevents this

a) Monocytes were stimulated with an increasing concentration of sTNF-α for 24 hours. Individual subject data is shown with median values displayed as a bar. Friedman's test p=0.01. Significant post hoc pairwise comparisons of stimulating sTNF-α concentrations to 0 ng/ml sTNF-α are shown on the graph (unadjusted p-values were first corrected by multiplying by 4). b) Monocytes were stimulated with 100 pg/ml of sTNF-α, alone or in the presence of a TNF-α mAb or an isotype control Ab, for 24 hours. Individual subject data is shown with median values displayed as a bar. Friedman's test p=0.02. Significant post hoc pairwise comparisons are shown on the graph (a Dunn-Bonferroni correction was applied to unadjusted p-values).

3.2.10 Selecting an optimum concentration of TNF-α mAb

In order to determine an estimate of the optimum concentration of the TNF-α mAb required to block sTNF-α produced by monocytes, an experiment was conducted in which 10 ng/ml of sTNF-α was added to each of 14 culture wells, containing 0.45 million monocytes per well, from one healthy control. 10 ng/ml was chosen as an appropriate concentration of sTNF-α to use as this exceeded the maximum concentration of sTNF-α detected in early validation experiments using LPS as a stimulant (approximately 8 ng/ml). Increasing concentrations of

the TNF-α mAb, ranging from 0 to 40 μg/ml had first been added to each well and the culture plate gently agitated prior to incubation for either 1 or 24 hours. At the end of these pre-specified time periods, detectable sTNF-α was determined in the cell-free supernatants using ELISA. In this way it was possible to determine the concentration of the TNF-α mAb required to neutralise the effect of 10 ng/ml of sTNF-α. The time-points of 1 and 24 hours were chosen to show that binding of the TNF-α mAb is both rapid and remains in steady state. Figure 3.8 illustrates that a concentration of 5 μg/ml of TNF-α mAb was sufficient to bind 98.2% of 10 ng/ml of exogenous sTNF-α (plus any produced by the monocytes themselves). As the output of sTNF-α by monocytes from A1ATD-related COPD patients with the rs361525 polymorphism was at this stage unknown this concentration was doubled to 10 μg/ml for use in future experiments.

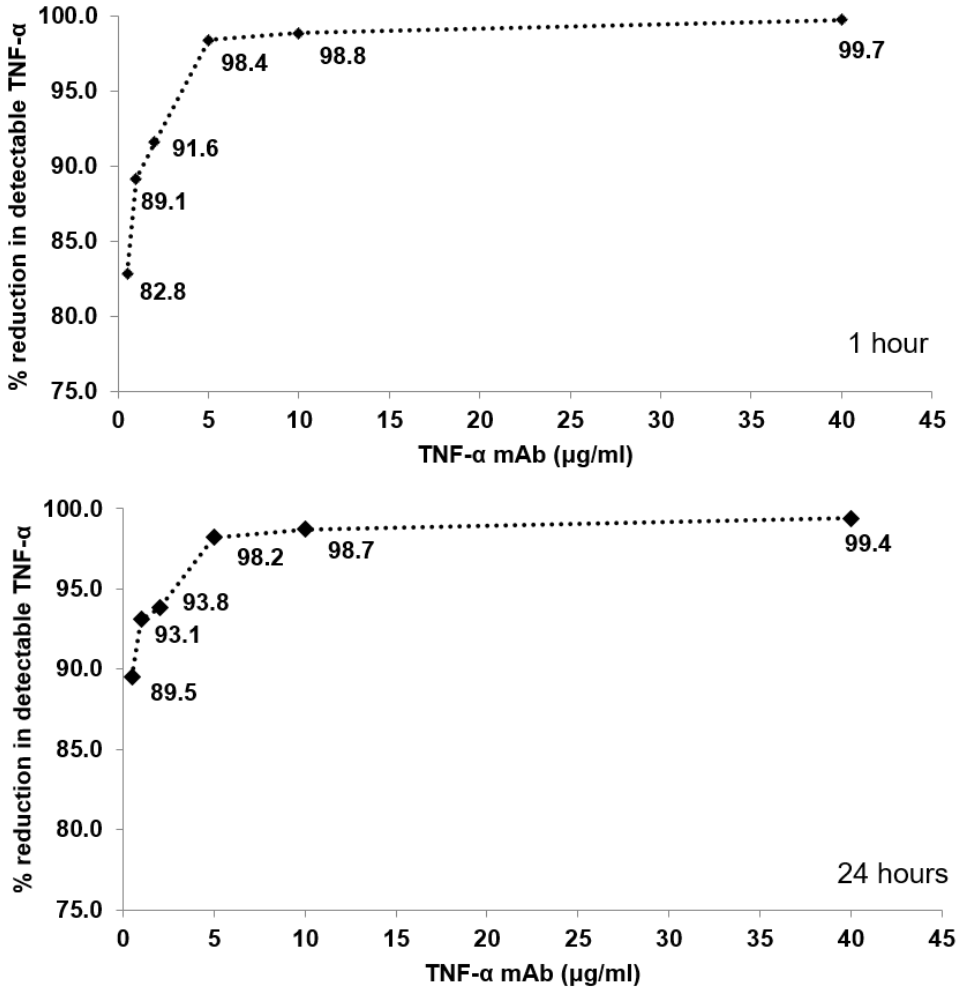

Figure 3-8 Concentration of a TNF-α mAb required to prevent detection of 10 ng/ml of sTNF-α

Each datum point represents the ability of each concentration of the TNF-α mAb to bind 10 ng of sTNF-α, expressed as a percentage reduction in detectable sTNF-α by ELISA. Cell-free supernatants were removed from culture plates at 1 and 24 hours post incubation to illustrate that antigen-mAb binding occurs rapidly and remains in steady state.

3.2.11 Apoptosis of monocytes

It was noted that some subjects' monocytes when incubated for 6 or 24 hours were undergoing changes to their size and internal complexity, as shown by changes to forward and side scatter respectively. This is illustrated in figures 3.9 and 3.10, whereby freshly isolated monocytes appear as a discrete population (figure 3.9a) but after 20 hours of culture in the presence of LPS there appears to be two populations of cells (figure 3.10a), one occupying the same position as freshly isolated monocytes and the other much smaller. Some cells in both of these populations also had greater side scatter than freshly isolated monocytes.

In order to determine if the population of monocytes which became smaller was undergoing apoptosis and hence should be gated out during further analysis of cell surface receptor expression (see chapter 5), the PE- Annexin V Apoptosis Detection Kit I (BD Biosciences, Oxford, UK) was employed, using monocytes from one healthy subject. Figure 3.9 illustrates a sample of freshly isolated unstained monocytes. Annexin V binding was observed in the majority of cells, suggesting possible early apoptosis even in freshly isolated monocytes. 1.6% of monocytes were both Annexin V and 7-AAD positive, indicating late apoptosis/cell death.

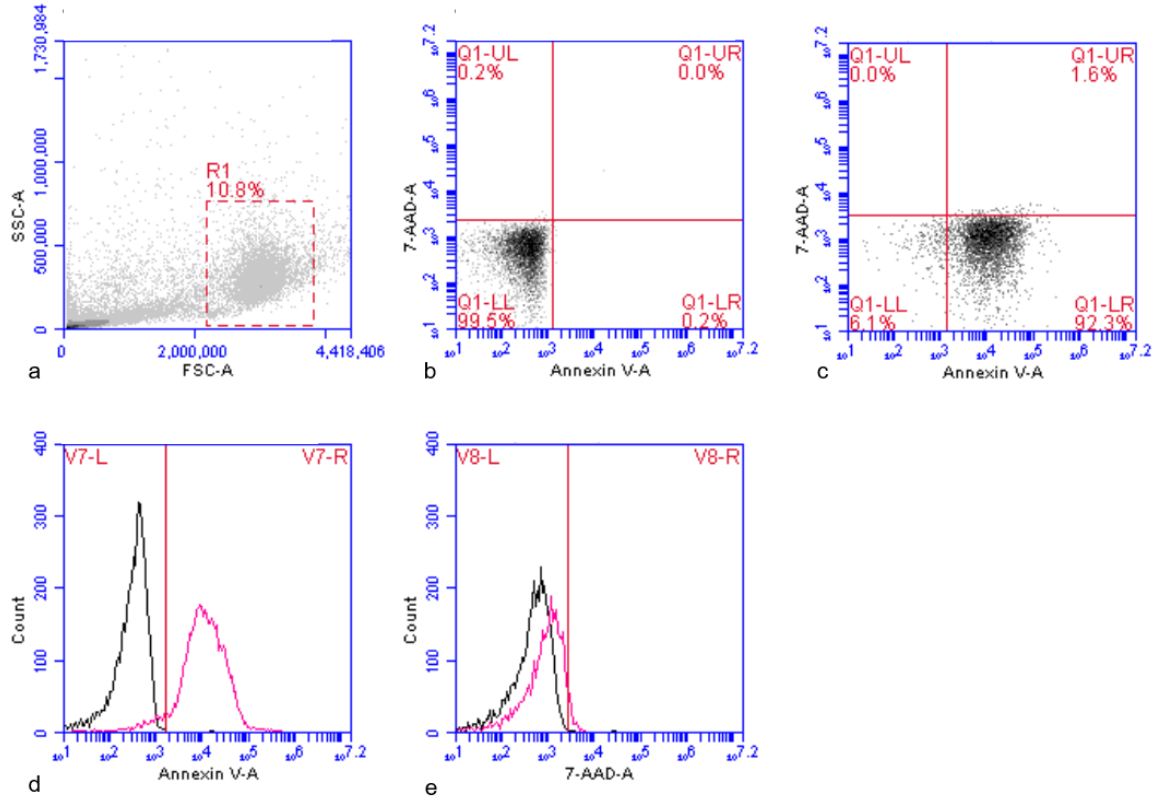

Figure 3-9 The PE-Annexin V Apoptosis Detection Assay in freshly isolated monocytes

a) Freshly isolated monocytes were gated as shown on the forward-side scatter plot. Doublet events were then excluded (not shown). b) Quadrant gates were set from unstained gated monocytes. c) The quadrant plot shows that the majority of monocytes were Annexin V positive. d) The black histogram represents autofluorescence of gated unstained monocytes and the pink histogram, monocytes labelled with PE-Annexin V. The shift in fluorescence to the right of the red marker indicates Annexin V binding. e) The black histogram represents autofluorescence of gated unstained monocytes and the pink histogram, monocytes incubated with 7-AAD. Minimal shift in fluorescence to the right of the marker was observed with only 1.6% of monocytes staining positive for 7-AAD.

Figure 3.10 shows monocytes which had been stimulated with LPS for 20 hours. When gated over the monocytes which remained in approximately the same position on the forward-side scatter plot as freshly isolated monocytes it was evident that again the majority of cells were Annexin V positive (with a similar MFI to that of freshly isolated monocytes). A minority of monocytes were also 7-AAD positive, indicating late apoptosis/cell death.

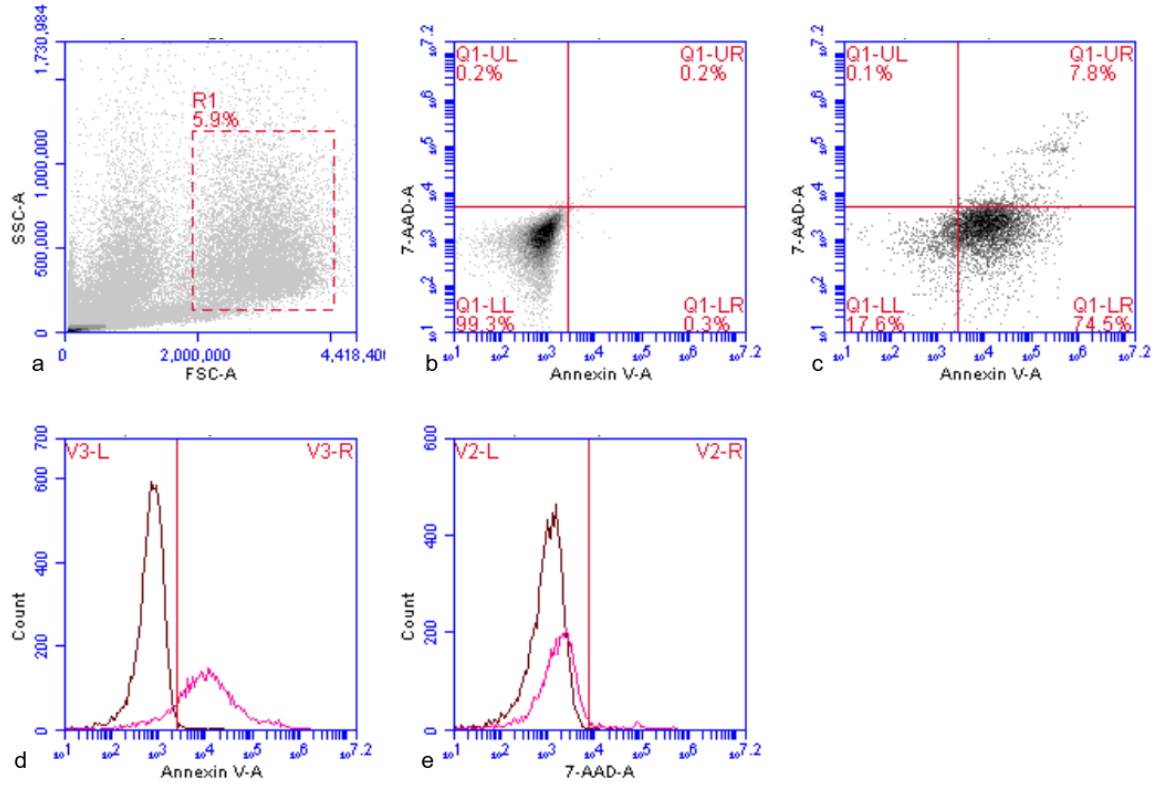

Figure 3-10 The PE-Annexin V Apoptosis Detection Assay in monocytes stimulated with LPS for 20 hours (one)

a) Monocytes cultured for 20 hours with LPS were gated as shown on the forward-side scatter plot. Doublet events were then excluded (not shown). b) Quadrant gates were set from unstained gated monocytes. c) The quadrant plot shows that the majority of gated monocytes were Annexin V positive and 7.8% were Annexin V and 7-AAD positive. d) The black histogram represents autofluorescence of unstained monocytes and the pink histogram, monocytes labelled with PE-Annexin V. The shift in fluorescence to the right of the red marker indicates Annexin V binding. e) The black histogram represents autofluorescence of gated unstained monocytes and the pink histogram, monocytes incubated with 7-AAD. Low numbers of cells with varying degrees of fluorescence secondary to 7-AAD binding can be seen, to the right of the red marker (7.9% of monocytes 7-AAD positive).

Figure 3.11 shows the same monocytes stimulated with LPS for 20 hours, but gated over the population of cells lying to the left of the forward-side scatter plot. As many of the events in this area of the plot represent debris rather than cells, further gates were applied to exclude these non-cellular events, as described in the figure legend (gating advised by Mr Yoav Altman, director of the Flow Cytometry Shared Resource, Sanford Burnham Prebys Medical Discovery Institute, USA, direct communication, 13th November 2015). The majority of these monocytes were in late apoptosis and the fluorescence intensity of Annexin V positive cells was for most cells greater than in earlier examples. However, it should be noted that some 7-AAD positive cells had a similar degree of Annexin V binding as freshly isolated monocytes, suggesting the Annexin V binding observed in freshly isolated cells may have been a genuine phenomenon, indicative of early apoptosis.

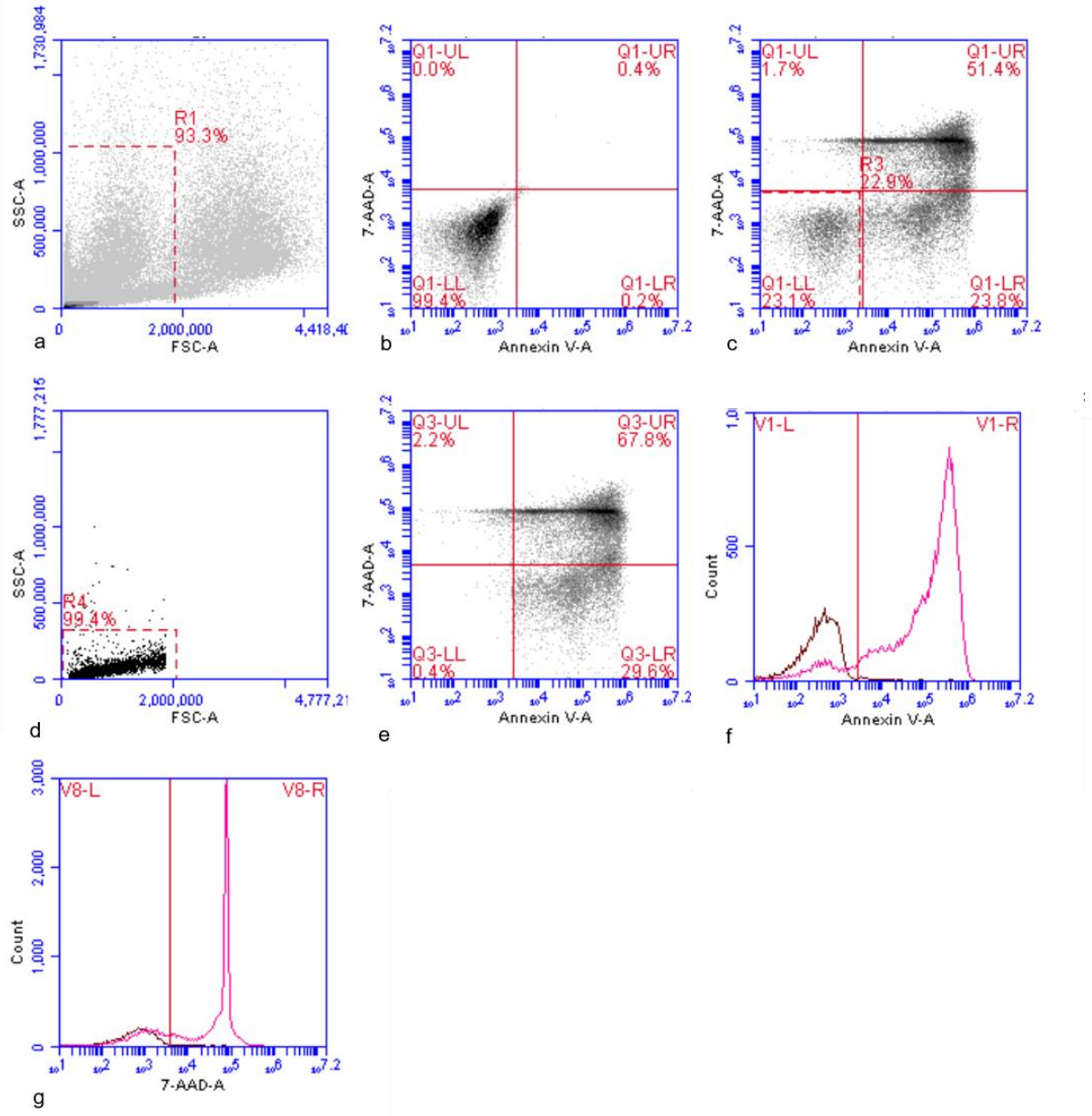

Figure 3-11 The PE-Annexin V Apoptosis Detection Assay in monocytes stimulated with LPS for 20 hours (two)

a) Monocytes which had been cultured for 20 hours with LPS were gated as shown on the forward-side scatter plot. Doublet events were then excluded (not shown). b) Quadrant gates were set from unstained gated monocytes. c) A quadrant plot of the gated stained monocytes is shown. A further gate (R3) was placed around the double negative population d) R3 events are shown on a forward-side scatter plot. These events occupied a position on the plot consistent with debris (low forward and side scatter). These events were gated (R4) and excluded from further analysis. e) The final quadrant plot shows 68% of monocytes were Annexin V and 7-AAD positive and 30% Annexin V positive only f) The black histogram represents autofluorescence of gated unstained monocytes and the pink histogram monocytes labelled with PE-Annexin V. The shift in fluorescence to the right of the red marker indicates

Annexin V binding. f) The black histogram represents autofluorescence of gated unstained monocytes and the pink histogram monocytes incubated with 7-AAD. Most cells were 7-AAD positive.

As a positive control monocytes were induced to undergo apoptosis using camptothecin, an inhibitor of DNA replication and commonly used inducer of apoptosis (237) as advised by the assay manufacturers (236). Figure 3.12 shows that most of the monocytes had less forward scatter than freshly isolated monocytes, consistent with apoptosed cells and were all either Annexin V positive or Annexin V and 7-AAD positive, indicating early or late stage apoptosis respectively. Gating was conducted as decribed in figure 3.11. Only the salient figures are shown in this example.

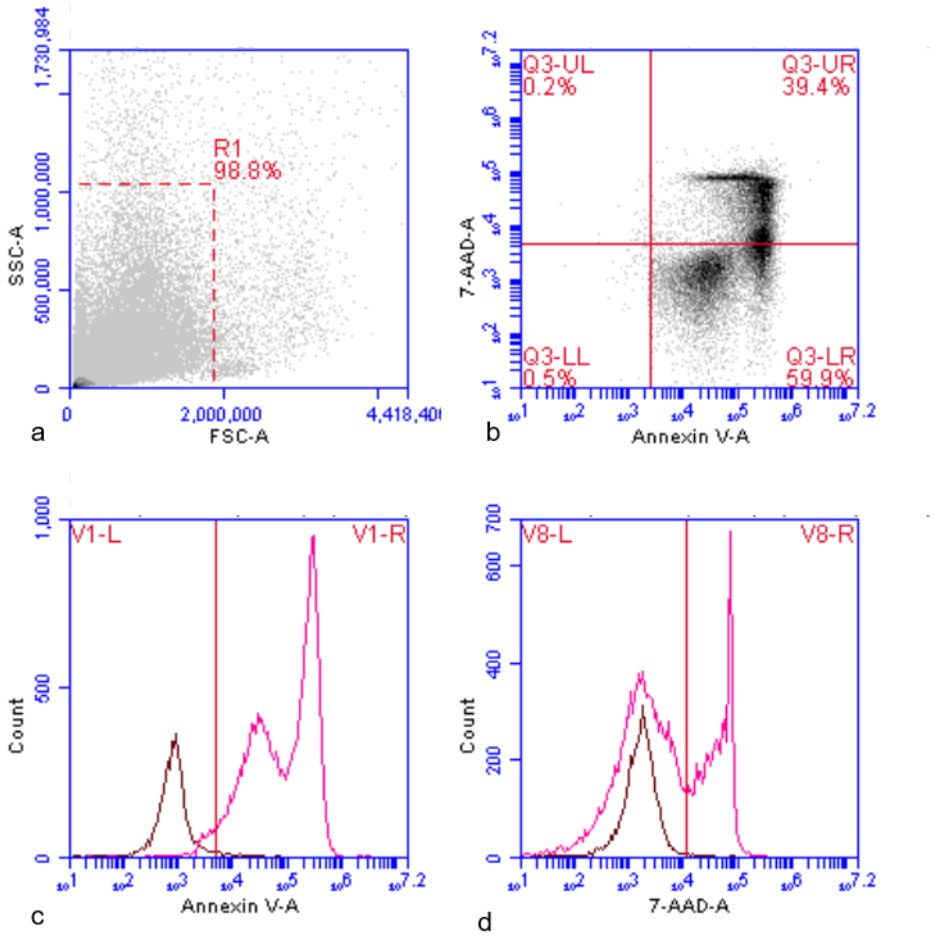

Figure 3-12 The PE-Annexin V Apoptosis Detection Assay in monocytes incubated with camptothecin for 20 hours

a) Monocytes which had been cultured for 20 hours with camptothecin were gated as shown on the forward-side scatter plot. Further gating was as described in figure 3.11. b) The quadrant plot shows 39% of monocytes were Annexin V and 7-AAD positive and 60% Annexin V positive only f) The black histogram represents autofluorescence of gated unstained monocytes and the pink histogram monocytes labelled with PE-Annexin V. The shift in fluorescence to the right of the red marker indicates Annexin V binding, with two populations evident). f) The black histogram represents autofluorescence of gated unstained monocytes and the pink histogram monocytes incubated with 7-AAD. The shift in fluorescence to the right of the red marker indicates a population of monocytes positive for 7-AAD.

3.3 **Discussion**

In the current study the CD14+CD16- purity of monocytes obtained from PBMC preparations, using the Dynabeads® Untouched™ Human Monocytes kit (Life Technologies Limited, Paisley, UK) varied between 64% and 74%. Product literature supplied by Life Technologies Limited states that purity is 94% but this is based purely on categorising isolated cells on the presence or absence of CD14 on the cell surface (242). In this respect, the isolates obtained in this study were between 89 and 95% pure, close to that specified by the commercial data. However, it is clear from data presented here that a percentage of cells obtained were also CD16+. This possibly reflects either that not all of the CD16+ cells were bound by the anti-CD16 mAbs in the isolation kit or antibody bound cells were not effectively cleared by the magnet separation step. The latter is less likely as final cell preparations had no brown discolouration visible to the naked eye, suggestive of magnetic bead contamination. It is unlikely that the cell preparations were contaminated with significant numbers of other cell types such as lymphocytes or CD16+ neutrophils, as the forward-side scatter plots of all isolated monocyte preparations showed one distinct population of cells (as illustrated in figure 3.9). Hence it is most likely that the CD16+ cells were CD14+CD16+ monocytes. In one sense it is of no great concern that some CD14+CD16+ monocytes were included in the final cell preparations as this thesis aimed to study monocytes in general. However it must be borne in mind that it is likely that the two different monocyte subsets react differently to stimulants such as LPS or indeed TNF-α (243, 244), and the CD16+ monocytes may or may not have had anti-CD16 mAbs bound to them which could have caused inadvertent stimulation. Alternatively these findings could be explained by changes to CD14 and CD16 expression patterns during the extraction process. Skinner *et al* demonstrated in whole blood that the percentage of CD16+ monocytes doubled from 5 to 10% only two hours following LPS

stimulation and that TNF-α stimulation could also drive this change in monocyte phenotype (244). It is possible therefore that TNF-α secretion by the monocytes during the extraction process may have been causing up-regulation of CD16 and that this was being expressed at the cell surface after the negative isolation process had finished. In support of this theory it was observed that the CD16+ monocytes had similar intensity of expression of CD14 as that of the greater CD16– population, indicative of these cells being intermediate monocytes, with far less non-classical CD14– CD16+ non-classical monocytes. As monocyte subsets are thought to possibly progress from CD14+CD16– (classical) to CD14+CD16+ (intermediate) to CD14–CD16+ (non-classical) (204) it is possible that that process was being observed in the isolated monocytes in the current studies.

Classical monocytes were studied in this thesis for a number of reasons. Firstly, this monocyte subset constitutes 90% of circulating monocytes (204) and hence a greater proportion of cells could be utilised from donated blood (of which only 10% of blood leukocytes are monocytes (196)). Secondly, whilst it is recognised that they may secrete less TNF-α than non-classical monocytes they are still able to produce TNF-α (204, 207, 243) (as demonstrated in the present experiments) and it was deemed important to isolate the cells using a negative selection technique that would ideally avoid inadvertent cell stimulation. An alternative method of isolation from whole blood or the Buffy coat layer, such as using a flow cytometry cell sorter, could be used in future, although this theoretically might lead to cell activation. This would permit study of all monocyte subsets together or separately. In addition each tube of cells could be run as a multi-colour experiment, whereby cells are labelled with CD14, CD16, CD64, TNFR1 and TNFR2 mAbs. This would allow assessment of TNF-α receptor status to be further considered in the context of monocyte subsets.

Other improvements to flow cytometry experiments should also be incorporated. A viability dye could be included as a marker in each tube to gate out dead cells from analysis, for example, 7-AAD. Dead cells are a particular problem as they may exhibit increased autofluorescence, reducing the sensitivity of each assay for low levels of cell surface marker expression, as gates are adjusted to compensate (245). In addition, multicolour experiments are subject to a risk of fluorescence spillover into individual channels as a result of combined fluorescence from multiple fluorophores and this is not corrected for by colour compensation corrections made when considering only pairs of fluorophores. Employing fluorescence-minus-one controls, whereby control tubes contain all flow cytometry mAbs, except the mAb conjugated to one of the fluorophores, can be used to set more accurate gates and exclude events that are due to spillover into a particular channel (246, 247). This is repeated for each mAb-fluorophore conjugate used in the experiment. Lastly, some authors argue that quantitation beads may be a superior way of expressing cell surface marker numbers per cell than comparing MFI ratios (of the MFI of sample labelled with mAb of interest to the MFI of sample incubated with its isotype control) (246). Beads labelled with a known quantity of fluorophore molecules can be used to calibrate the flow cytometry machine on each run (to correct for day to day variation in laser performance for example) and can also be used as a standard to calculate and compare the numbers of cell surface markers between subjects and experimental conditions. This may be preferable to presenting MFI ratios as the latter relies on the assumption that the background level of unwanted Fc-receptor binding is equivalent between the specific mAb and its isotype control and that binding of both are affected equally by the experimental conditions imposed on the cells (247), which may not be the case.

The present study confirmed that intra-assay variability of the TNF-α and CXCL8 ELISA assays agreed with that quoted by the manufacturers (R and D systems Ltd, Abingdon, UK) at

less than 10% (248). However, inter-assay variability of the two assays was slightly higher than 10% (table 3.2 and 3.3). Inter-assay variability is unavoidable to a degree as the reagents across ELISA kits for the same protein can vary slightly and even slight differences in timing of the ELISA stages can have a small effect. As this could have affected conclusions drawn regarding differences in TNF-α and CXCL8 output between monocytes from A1ATD-related COPD patients with and without the rs361525 polymorphism, in chapter 4 one CXCL8 ELISA was conducted in which samples from LPS-stimulated monocytes at one time-point from all 18 patients with and without the polymorphism were run on the same plate. This showed no major difference in the conclusions drawn compared to results that had been obtained from a number of CXCL8 ELISA plates (see chapter 4). This issue could also be addressed in future studies by running the same low, medium and high standard on each ELISA plate and using this as a correction factor if needed.

The intra-assay variability of the TNFR1 and TNFR2 ELISAs was higher in the current study than that quoted by the manufacturer (Invitrogen, UK) (249, 250), said to be between 1.7 and 6.5% for TNFR1 and 2.1 and 3.7% for TNFR2. However, the intra-assay variability obtained for these assays was still 10% or less, in keeping with general ELISA performance and the TNF-α and CXCL8 assays studied here and so was deemed acceptable (table 3.2). The R^2 value for the regression equations for the TNF-α, CXCL8 and TNFR1 assays was 0.99 which is considered a good fit (251) and for the TNFR2 assay, close to this at 0.98.

RNA from centrifuged cell pellets was isolated using the Isolate RNA Minikit (Bioline, UK). The kit is designed to allow isolation of highly pure RNA, uncontaminated with proteins or genomic DNA. Ideally the 260/280 ratio for RNA should be between 1.8 and 2. A ratio lower than this may due to contamination of the sample with residual reagents from the extraction protocol or due to low concentrations of RNA (less than 10 ng/µl of nucleotide). A ratio

higher than 2 is not indicative of a problem (252). The majority of samples obtained in this study (82%) had a 260/280 ratio of 1.8 or higher. In the current study a large number of experimental conditions had to be carried out using the monocytes isolated from each healthy subject or A1ATD patient and a considerable volume of blood was necessary to be able to do this (60 ml). The monocyte yield from blood samples is much less than that for other leukocytes such as neutrophils because they compromise a smaller proportion of the circulating leukocyte pool (196). Therefore a consequence of this limitation is that only 0.25 million monocytes per culture plate well could be used for mRNA time course experiments and hence low final concentrations of total RNA were obtained for each sample (less than 10 ng/µl of nucleotide). As described, this can lead to an erroneously low 260/280 ratio value. For this reason and because there was no clear pattern to samples where ratios were out of the desired range (i.e. samples run simultaneously using the same kit did not uniformly have low values suggestive of contamination) and because the majority of RNA samples had an acceptable 260/280 ratio of greater than 1.8, all RNA samples were included in ongoing RT-qPCR experiments. To support the assertion that some 260/280 ratios were erroneously low rather than because of poor quality it should be noted that the direction of results for mRNA expression in chapter 4 matched those of the protein expression obtained by ELISA.

The CV% values for intra-assay and inter-assay variability of the three most frequently studied genes undergoing RT-qPCR were acceptable, having a CT standard deviation value of less than or equal to 0.3 in all (table 3.5). Some authors suggest it is preferable to express inter-assay variability as a CV% of actual DNA copy number generated for one sample across multiple runs (253). This is because CT values will always be subject to a small but unavoidable variability between runs whereas differences in copy number of amplicon will reflect true inter-assay variability. This technique was not possible in the current studies as

use of a DNA amplicon to generate a standard curve for each plate requires preparation of the samples under a specialised PCR hood (not available) to prevent inadvertent release of DNA template into the laboratory which could contaminate future PCR reactions as they are being set up. Despite this, the SDs of the mean CT values across multiple plates for the three sample genes were all 0.3 or less and thus deemed acceptable (240).

A key principle of the relative quantification method is that it relies on the TaqMan® assay for both the normalising gene and the gene of interest having equal efficiencies. Efficiency refers to the ability of the primer, probe, other PCR reaction components and the PCR thermal cycler to allow a doubling in quantity of the DNA template with each thermal cycle. When this occurs efficiency is 100%. Differences in efficiency between the assays for the normalising gene and gene of interest would introduce error into the relative quantification calculation at higher CT values (253). Efficiency can be determined for each assay by producing serial dilutions of a chosen sample (5 to 6 log dilution ideally) and then plotting the log cDNA concentration against acquired CT values. An expected slope for a dilution series of template cDNA is –3.32 if the efficiency is equal to 100%. The major limitation of conducting efficiency experiments occurs when the starting copy number of mRNA for the studied genes is low, for example as in this study whereby extracted RNA concentration was necessarily low due to limits on the number of monocytes which could be isolated from each subject. This makes even a 1 to 2 log dilution series difficult and it has been shown that without a broad range of concentrations of cDNA, starting with a high concentration, then efficiency calculations are extremely inaccurate (253). To this end, the manufacturer of TaqMan® assays specifically recommend not testing the efficiencies of their assays as this has been conducted extensively in-house and all are stated to have efficiencies close to 100%. Of course, it is possible to amplify a cDNA sample generated from a previous RT-qPCR

reaction in order to produce enough cDNA to generate a 5 to 6 log series dilution, but this carries with it the significant risk of contaminating the laboratory with completed PCR product. Therefore, in the current study, equal and near 100% efficiency of all assays was assumed and efficiency testing was not carried out. However, it must be noted that the example PCR amplification curves shown in figure 2.5 to 2.11 illustrate that although curve shape was consistent within assays, the TNF-α, IL-6 and GAPDH PCR curves were shallower in comparison to the other assays, suggesting reduced efficiency of the reaction, and did not reach plateau phase. Possible reasons for reduced efficiency, real or apparent, include differences in fluorescence intensity of different fluorophores (apparent), primer-dimerisation when target sequence concentration is low, amplicon length greater than 100 bp possibly reducing the likelihood of doubling each cycle, or inadequate concentration of reagents in the sample (228). In the current experiments the same fluorophore, FITC, was used for all assays. Primer-dimerisation or inadequate reagent concentration are unlikely as other assays, for example, IL-6 and IL-10, routinely had later CT values and yet produced classic sigmoidal shaped amplification curves. The amplicon length for GAPDH was 122 bp which may have adversely affected efficiency but TNF-α amplicon length was only 80 bp. Whilst a simple explanation for the disparity in amplification curve shape between assays is not apparent it must be considered that there may have been differences in PCR efficiency between assays.

Non-template controls for each of the assays used were run on each plate. The non-template control contained PCR-grade water as a replacement for an RNA sample. These wells sometimes produced a CT value of between 35 and 40. A positive non-template control suggests possible contamination by and amplification of previous PCR product which has been aerosolised into the laboratory. It is likely however that these results are erroneous as firstly CT values of 35 and above are at the very limits of the sensitivity of the thermal cycler

and hence are suspect (253) and secondly in many cases the shape of the PCR curve was not in keeping with a genuine result. Even in the scenario of possible contamination such low levels of expression (these CT values are likely to reflect only one to two copies of a gene) are unlikely to affect validity of results obtained from other samples where the gene was expressed at much higher levels. As such, PCR plates containing positive non-template controls with CT values of 35 or above were not rejected.

It should be highlighted that the GAPDH TaqMan® assay, despite being labelled as spanning an exon-exon boundary (denoted by the suffix m1), does in fact sit within an exon of the GAPDH gene. (Data regarding assays changes from time to time as more details regarding the genome are obtained -clarified via direct communication with Life Technologies, April 10th 2014). This increases the risk that should any genomic DNA be present in an RNA sample, which is unlikely with the RNA extraction kit used in the current study, then it could be amplified by the assay during the PCR reaction. This is unlikely to have occurred however as table 3.4 details the stability of GAPDH across a wide range of samples, which would have been adversely affected should a number of samples have been contaminated with genomic DNA containing extra GAPDH.

Several potential stimulants of TNF-α secretion by monocytes were selected for initial time course and concentration-response experiments. IL-1β is an early phase cytokine which stimulates the transcription of inflammatory cytokines including TNF-α within monocytes and macrophages in COPD (79). MCP-1 is a principally a monocyte chemo-attractant but was used here in stimulation experiments to determine if it also has a role in up-regulation of TNF-α production (79). LPS is a component of the cell membrane of gram-negative bacteria which when bound to the serum factor, LPS binding protein (254), is able to bind to CD14 (255) on the monocyte/macrophage cell surface and activate toll-like receptor 4 (TLR4),

leading to activation of multiple transcription factors and subsequent transcription of pro-inflammatory genes including the TNF-A gene (256). The endotoxin is internalised by the monocyte/macrophage within 5 minutes (257).

Whilst most of the transcription factors up-regulated by LPS act at the proximal TNF-A promoter (144) studies have demonstrated binding of NFκB members, particularly p65, up-regulated by LPS, to the distal portion of the promoter where the rs361525 polymorphism lies (152, 153, 258) and other authors have shown that LPS can up-regulate reporter gene expression in macrophage cell lines expressing the A-allele at position -237 (128). These reports support the use of LPS as a stimulant in the current studies. LPS is also a component of cigarette smoke, making it a relevant stimulant in COPD subjects (259, 260).

Although limits to the number of monocytes which could be extracted per individual precluded direct comparison, the results of these time course and concentration-response experiments suggested that LPS induced the most TNF-α secretion (figure 3.2), with MCP-1 inducing no response. It was noted that the intersubject variation in TNF-α secretion was wide, in keeping with previous studies (261, 262). In order to maximise the possibility of seeing a difference in TNF-α secretion by monocytes between A1ATD-related COPD patients with and without the rs361525 polymorphism, LPS was therefore selected as the most appropriate stimulant to use in ongoing experiments. As the exact properties of LPS are known to vary considerably between type and strain of mutant bacteria (255), one batch of LPS, reconstituted and divided into aliquots, was used throughout the current study. Deciding upon the concentration of LPS was a more challenging decision as it is unclear what the local concentrations of inhaled LPS at the lung mucosal surface might be in smokers and hence the concentration that monocytes/macrophages are exposed to. LPS is implicated in the pathogenesis of COPD and is frequently used in models of lung inflammation (241, 263).

Korsgren *et al* showed that inhaled LPS at a dose of 5 µg and 50 µg elicited a marked increase in induced sputum TNF-α concentration and neutrophil cell activity (260). Hasday *et al* demonstrated that the tobacco and filter tip components of light cigarettes contained on average 27 µg and 0.7 µg of LPS respectively. The mainstream and side stream smoke produced upon mechanical smoking of these cigarettes contained 45 ng and 75 ng of LPS per cigarette with an estimated 2400 ng delivered to the lungs after smoking one pack. The authors also measured the concentration of circulating LPS in 15 healthy smokers and 16 age-matched non-smoking controls and found no statistically significant difference in serum concentration. Serum concentrations were much lower than that found in inhaled cigarette smoke, at approximately 67 pg/ml in each group (259). Even in patients with septic shock, circulating LPS concentrations have been found to be only 300 pg/ml on average (264). Hence it would seem that the burden of inhaled LPS as a result of cigarette smoking, occupational exposure (e.g. cotton textile workers) or even domestic exposure from dust and pets is largely dealt with by mechanisms within the lungs (241) and it is probable that monocytes/macrophages with their abundance of CD14 expression contribute significantly to this. It remains challenging to accurately estimate the concentration of LPS that patrolling macrophages in the airways and alveoli of the lung may be exposed to. However it can be surmised that it is likely to be higher than that found in the serum. It was decided therefore to use 100 ng/ml in further experiments with monocytes as this was shown in the current studies to elicit greater TNF-α secretion than 10 ng/ml, whilst not using higher concentrations that were unlikely to reflect those present during pathological insults.

However, in retrospect it may have been preferable to have used the EC80% (effective concentration of LPS that elicits 80% of the maximum response) as this would allow one to observe TNF-α output on the linear part of a sigmoidal concentration response curve rather

than at plateau as occurs with a maximum concentration of stimulant. This is potentially important when interpreting experiments presented in chapter 4. If the position of the linear phase of a sigmoidal concentration response curve for AG monocytes lies to the left of that of GG monocytes they would produce more TNF-α at lower concentrations of stimulant and a difference between the two groups would be seen. By using higher concentrations of LPS it is possible that any differences between the AG and GG monocytes would have been missed as both may have reached (the same) plateau at 100 ng/ml of LPS. However, even using the average EC80% is subject to limitations. Specifically, when the LPS concentration-response curve (shown in figure 3.3) was considered as individual curves for each of the eight subjects (not shown) there was considerable variation in EC80% and ECmax between subjects. Therefore, the mean/median EC80% may not actually be the concentration that elicits 80% of the maximum response for some subjects' monocytes.

This early validation work demonstrated that peak sTNF-α concentration in the cell culture supernatant occurred at approximately 8 hours post stimulation with LPS, decreasing thereafter (figure 3.2b). It was hypothesised that the decrease in detectable sTNF-α may be due to autocrine binding of sTNF-α to its receptors and this was subsequently investigated in chapter 5. CXCL8 concentration continued to rise up to 24 hours post LPS stimulation despite the latter experiment having been conducted in monocytes rested overnight, which had lost their ability to produce TNF-α (figure 3.4). The production of low concentrations of sTNF-α by freshly isolated unstimulated monocytes (figure 3.2a) may have been due to a degree of activation of the monocytes as a result of their adherence to the culture plate (265).

From these studies it was determined that cell culture supernatants from monocytes from A1ATD-related COPD patients would need to be harvested at approximately 6 to 8 hours and at 24 hours post isolation and stimulation to capture maximum sTNF-α and CXCL8 output

respectively. It should be noted however that choosing these peak-time points relies upon the assumption that time course profiles in monocytes from healthy subjects match those of monocytes from A1ATD-related COPD subjects with and without the rs361525 polymorphism. If they differ then comparing individual time-points could lead to erroneous conclusions regarding differences in sTNF-α output by both groups. For this reason full time course profiles of both mRNA expression and protein concentration may have been preferable (although difficult to practically carry out due to time limitations), with data expressed as differences between AUC values. Conversely, AUC calculations are subject to potential error as they rely on the inclusion of enough time-points to generate accurate shaped curves. This issue is discussed further in chapter 4.

It must be noted that the apoptosis assay confirmed that some monocytes were undergoing apoptosis by 20 hours which may have partly contributed to the reduction in TNF-α secretion observed in rested cells (figure 3.4a). Another contributing factor may be that the low level of sTNF-α secreted by freshly isolated monocytes in the absence of any stimulant may have directly or indirectly exerted a negative feedback effect on the monocytes, preventing subsequent sTNF-α secretion in response to LPS, as has been observed in LPS-treated mice pre-treated with low concentrations of TNF-α (266). Alternatively, the reduction in response may reflect changes to the expression of CD14 and/or TLR4 on the monocyte surface as a consequence of overnight incubation in CM without an exogenous stimulus. As CD14 and TLR4 form the receptor for LPS (255, 256) any down-regulation of receptors would decrease the cellular response to LPS. In keeping with this, Gantner *et al* demonstrated CD14 decreased on the surface of monocytes when cultured in human serum for 6 days and that twenty times higher concentrations of LPS were required to stimulate TNF-α secretion than in freshly isolated monocytes (267).Whilst not directly comparable, for example monocytes in

the current studies were incubated with CM containing FBS rather than human serum and overnight rather than for six days, these data suggest that changes to CD14 might be occurring overnight prior to the addition of LPS. Furthermore, Tsai *et al* demonstrated that TNF-α can down-regulate TLR4 on the surface of human monocytic THP-1 cells (268) and as freshly isolated monocytes have been shown here to produce TNF-α in the absence of an exogenous stimulus (figure 3.2a) it is possible that this TNF-α was down-regulating TLR4 expression on the monocyte surface and hence abrogating the response to LPS the following day.

Although it was not possible to know the range of concentrations of sTNF-α that would be observed in the patient group a suitable concentration of blocking TNF-α mAb was estimated from the current studies. The nature of the function of the mAbs used in this thesis and subsequent limitations are discussed in full in chapter 5. The experiment presented in figure 3.7b, whereby the blocking effect of the TNF-α mAb was studied could be improved in future by repeating it with a greater number of samples and a negative control well measuring CXCL8 secretion in monocytes cultured without any sTNF-α present. This would determine whether the addition of the TNF-α mAb prevented all sTNF-α induced CXCL8 secretion, back to baseline levels.

It was necessary to take a pragmatic approach when deciding upon the number of replicate culture wells for each experimental condition/time-point to conduct as there was no evidence to suggest that using greater than three replicates reduced variation. It is evident from the data shown in figure 3.6 that even when using three replicates the results for some individuals produced CV% of greater than 9%. It is clear that intrasubject variation can be significant even when suspensions of monocytes are inverted several times prior to pipetting equally among culture wells, the same concentration of stimulant is employed and the results are analysed using the same ELISA assay. Althought suspensions of monocytes were inverted

gently to allow equal distribution of cells throughout the CM it is possible that small air bubbles in the suspension may have affected final cell numbers in wells of the culture plates and this may have contributed to the CV% values observed. How variation between experimental replicates might be affected by different stimulants or when considering the measurement of cytokines other than TNF-α was not considered here.

The final studies in this chapter addressed the issue of the changing morphology of the isolated monocytes over time, as observed by the change in the forward-side scatter flow cytometry plots of the cultured cells compared to those of freshly isolated monocytes. This was confirmed to be due to apoptosis of a proportion of the monocytes. It is well recognised that monocytes cultured in the absence of serum will undergo apoptosis and that pro-stimulant factors such as LPS or TNF-α can induce resistance to programmed cell death (269, 270). Despite the presence of serum, LPS and TNF-α in the current experiments, apoptosis still occurred to an extent and it was important to recognise this in order to identify viable cells at later time-points for gating purposes. Many cells which stayed approximately the same diameter never-the-less displayed increased side-scatter reflective of increased granularity and intra-cellular complexity. This may reflect monocytes which were beginning the process of differentiating into macrophages (271).

Surprisingly, Annexin V binding was also observed in freshly isolated monocytes from the healthy donor. This may reflect early apoptosis occurring as a result of the extraction process and cell handling, despite efforts to minimise cellular activation by keeping the cells on ice between steps of the protocol. In support of these findings reflecting genuine early apoptosis was the observation that in camptothecin treated 7-AAD positive monocytes the extent of co-existent Annexin V binding (as expressed by fluorescence intensity) varied considerably. Some of the monocytes in this late apoptotic state had similar low degrees of Annexin V

binding as that observed in freshly isolated monocytes and yet must have been in apoptosis given they were also 7-AAD positive. Similarly, low level Annexin V binding is unlikely to be completely explained by possible exposure of PS on the cell surface as a result of removal of adherent cells as it was observed in freshly isolated monocytes in suspension as well as adherent stimulated monocytes. Whilst Accutase® solution (Sigma-Aldrich Chemicals Ltd, Poole, UK) was recommended in the apoptosis assay protocol (236) to gently remove adherent cells prior to addition of Annexin V it remains a possibility that de-adherence may lead to PS exposure on the cell surface.

It also remains possible that some of the Annexin V binding may have been non-specific (although not via Fc receptor binding as Annexin V is not an antibody). To control for this in future a number of experimental modifications could be made. Firstly, as Annexin V binding is calcium dependent a control tube with the addition of EDTA to sequester calcium ions, as has been described previously (272) could be added. Any Annexin V binding observed in this tube would be consistent with non-specific binding (direct communication with Mr Yoav Altman, director of the Flow Cytometry Shared Resource, USA, 13th November 2015). Secondly, although the assay protocol used in the current experiments did not include a washing step, this could be added between the addition of Annexin V and then 7-AAD, using the binding buffer to wash (direct communication with Mrs. A. Berasategi, BD Biosciences Scientific Support Europe, 12th November 2015). However, non-specific binding, should it occur, may not necessarily be affected by washing the cells.

Conversely, the relative lack of freshly isolated monocytes undergoing late stage apoptosis goes against the hypothesis that these monocytes were all undergoing early apoptosis as one might expect some of the cells to be in a later stage of the apoptotic process at the point of performing the assay. Interestingly, Appelt *et al* reported that PS is expressed on the surface

of non-apoptotic monocytes leading to Annexin V binding, both immediately after isolation and after 24 hours of culture and that the degree of Annexin V binding was one to two orders of magnitude lower than that on monocytes induced to undergo apoptosis (272). They confirmed the viability of those monocytes by determing the absence of caspase activity, the presence of an intact mitochondrial membrane potential and lack of nuclear morphological changes. These findings would suggest that at least some of the Annexin binding observed in freshly isolated monocytes in particular was due to the presence of PS on the cell surface membrane in intact viable cells.

Alternative methods of assessing if apoptosis was occurring in freshly isolated monocytes should also be used in future, for example, staining cells with acridine orange and ethidium bromide, followed by fluorescence microscopy, as has been previously used in monocytes (273). Live cells are shown by the uptake of acridine orange (green fluorescence) and exclusion of ethidium bromide (red fluorescence). Apoptotic cells can be discriminated from necrotic cells by the perinuclear condensation of chromatin stained by ethidium bromide in the former or the generalised cell staining with ethidium bromide in the latter (273).

3.4 **Conclusions**

This chapter has described the initial experiments undertaken in order to optimise studies conducted in chapter 4. Validation results of the various assays and experimental techniques used throughout the thesis have also been described and any limitations of and challenges arising from these techniques addressed.

CHAPTER 4

THE EFFECTS OF THE RS361525 TNF-A POLYMORPHISM IN PATIENTS WITH A1ATD AND COPD

4 The effects of the rs361525 TNF-A polymorphism in patients with A1ATD and COPD

4.1 Brief Introduction

Previous work from our research group has shown that the presence of the rs361525 polymorphism, a G to A substitution at position -237 in the promoter region of the TNF-A gene, conferred an increased relative risk of having CB, a specific phenotype of COPD, in patients with A1ATD (125). In addition, sputum from A1ATD patients with CB and the polymorphism (AG heterozygotes) had one hundred times greater TNF-α concentration compared to those with the wild type gene (GG homozyogotes) (17), suggesting that presence of the polymorphism leads to increased local production of the protein, most likely through increased gene transcription given its location in the promoter region. Their sputum also contained more CXCL8, suggesting the greater concentration of free TNF-α was exerting an exaggerated pro-inflammatory effect on CXCL8 producing cells found in the airway. The sputum contained approximately 50% less soluble TNFR1 (although no difference in concentration of TNFR1 in the plasma was seen), the reason for which is unknown in the context of this polymorphism, but theoretically might relate to a reduction in TNFR1 cleavage from cell surfaces by TACE or reduction in receptor production, as a result of greater TNF-α in the pericellular environment. If the former were the case this could potentially enhance the pro-inflammatory phenotype of the cells from rs361525 subjects even further, as illustrated by the uncommon inherited TNF-receptor associated periodic febrile syndrome, in which sufferers have excess TNFR1 on the cell surface, thereby making them more susceptible to TNF-α-TNFR1 mediated effects (274).

As Sapey *et al* found that patients with the polymorphism had a lower BMI (17), suggesting that increased TNF-α production was associated with a systemic effect (as observed in other

studies (98, 99, 108)), it was concluded that there was a strong rationale for initially studying the polymorphism further at a cellular level in blood-derived cells rather than airway derived cells. Monocytes as the principal producers of TNF-α (3) and cells which are relatively simple to isolate were therefore chosen for study in the first instance.

Based upon these findings the primary hypotheses of this chapter were:

Hypothesis one: monocytes from A1ATD patients with COPD and the rs361525 TNF-A polymorphism would produce more TNF-α than monocytes from matched A1ATD patients with COPD and the wildtype allele.

Hypothesis two: secreted TNF-α would lead to autocrine up-regulation of pro-inflammatory cytokine production and the effects of this would be greater in monocytes with the rs361525 TNF-A polymorphism as a result of there being more TNF-α secreted into the pericellular environment.

The secondary hypotheses in this chapter were planned to be investigated should the primary hypothesis be met and were as follows:

Hypothesis three: Greater TNF-α production in monocytes with the rs361525 TNF-A polymorphism would exert a greater autocrine effect on the monocytes, leading to increased pro-inflammatory cytokine output occurring specifically via TNF-α binding to TNFR1.

Hypothesis four: Increased TNF-α production in the rs361525 monocytes would have an autocrine effect on the monocytes affecting other monocyte functions such as ROS production and phagocytotic ability (in an unknown direction).

To investigate the primary hypotheses, the following objectives and strategies to meet those objectives were set:

- Determine if TNF-α production was greater in monocytes from subjects with A1ATD-related COPD with the rs361525 polymorphism than in monocytes from matched subjects with the wild type gene. This was conducted by using LPS and PMA (or no exogenous stimulus) to stimulate TNF-α production and then measuring cytokine mRNA expression with RT-qPCR and secreted protein by ELISA.
- Determine if CXCL8 production was greater in monocytes from subjects with A1ATD-related COPD with the rs361525 polymorphism than in monocytes from matched subjects with the wild type gene, presumed to be as a result of an enhanced TNF-α autocrine feedback loop. This was conducted by using LPS and PMA (or no exogenous stimulus) to stimulate TNF-α production and then measuring *CXCL8* mRNA expression with RT-qPCR and secreted protein by ELISA.
- Determine if the production of CXCL8 was affected by TNF-α autocrine feedback loops. This was conducted by using LPS to stimulate TNF-α production, in the presence or absence of a TNF-α mAb and then measuring *CXCL8* mRNA expression with RT-qPCR and secreted protein by ELISA.

0.45 million cells per ml of CM were used for culture experiments (in triplicate) where cell-free supernatants were to be collected to measure protein concentration by ELISA. All RNA experiments at the culture stage were conducted singly (as a large number of time-points for each experimental condition was examined this precluded duplication due to limits to cell numbers available) and using 0.25 million cells per ml of CM. Messenger RNA samples from each experimental condition underwent RT-qPCR in duplicate and the mean result was taken.

4.2 **Subject characteristics**

Table 4.1 shows the characteristics of the 18 A1ATD subjects included in the studies for this chapter. Patients were matched as closely as possible based upon: presence of COPD, age, FEV1, transfer coefficient of carbon monoxide (KCO) and gender. Other clinical characteristics were compared after the matching process had taken place. Data from mRNA experiments in only eight subjects in each group could be used due to a technical issue affecting RNA extraction for one subject's samples, hence that pair was removed. No significant differences were observed between groups, before and after removal of one pair's data. One subject in the rs361525 group was homozygous for the A allele (AA). Hereafter, the groups are referred to as AG and GG. All patients with COPD were studied rather than just those with CB as although the minor allele was expressed at a clinical level in CB subjects (125) (possibly suggesting specific CB-related stimuli are important in-vivo) it was hypothesised that the rs361525 polymorphism would exert a pro-TNF-α effect at an individual cell level in monocytes from all A1ATD/COPD subjects. This permitted a greater number of subjects from our cohort of patients to partake in the studies.

Blood samples from all patients in our A1ATD cohort had previously undergone genotyping. This was carried out using a TaqMan® SNP genotyping assay (Life Technologies, UK) on an ABI7900 HT PCR machine. The assay included two allele-specific TaqMan® MGB probes conjugated to different fluorescent dyes and a PCR primer pair to detect the SNP targets (the A allele and the more common G allele). The plates included appropriate negative controls.

Characteristic		rs361525 +ve (AG/AA)	rs361525 -ve (GG)	P value
N		9 (8 AG/1 AA)	9	
Presence of COPD		9/9	9/9	
Age in years		51 (50-65)	60 (49-61)	0.8
Male		7 (77.8%)	7 (77.8%)	
A1ATD level (µM)		3.6 (2.9-4.6)	4 (2.8-4.9)	0.9
BMI		21.2 (21.0-23.8)	23.2 (22.0-26.0)	0.3
Smoking hx	**Current**	1	0	
	Ex/never	7/1	8/1	
Pack years		22 (10-28)	22 (9-30)	0.9
FEV1 (L)		1.5 (1.2-1.7)	1.4 (1.0-1.7)	0.3
FEV1 % predicted		37.7 (33.4-43.4)	33.6 (32.6-54.6)	0.9
FEV1/FVC		32.0 (28.0-34.0)	32.2 (23.0-33.0)	0.5
KCO % predicted		52 (44-58)	56 (50-64)	1.0
Emphysema on HRCT		8/9	9/9	
CB phenotype		4/9	5/9	
Bronchiectasis on HRCT		4/9	5/9	
Inhaled steroids		8/9	9/9	
Average of median exacerbations per year per patient		1.0 (1.0-2.0)	0.5 (0-1.0)	0.3

Table 4-1 Characteristics of study subjects

The table shows key characteristics of subjects with (AG/AA) and without (GG) the rs361525 TNF-A polymorphism. Subjects were matched as closely as possible. Data is given as median (IQR). A Mann Whitney U test was used to detect any difference between groups.

4.3 **Results**

4.3.1 *TNF-α* mRNA expression and protein secretion is not increased by the presence of the rs361525 TNF-A polymorphism

Messenger RNA was extracted from the cell pellets of monocytes freshly isolated from AG and GG subjects. Figure 4.1 demonstrates that there was no significant difference in constitutive *TNF-α* mRNA expression observed between the subject groups, although there was a trend for greater expression in the AG group. Culture experiments were conducted singly for mRNA measurement and in triplicate for protein measurement.

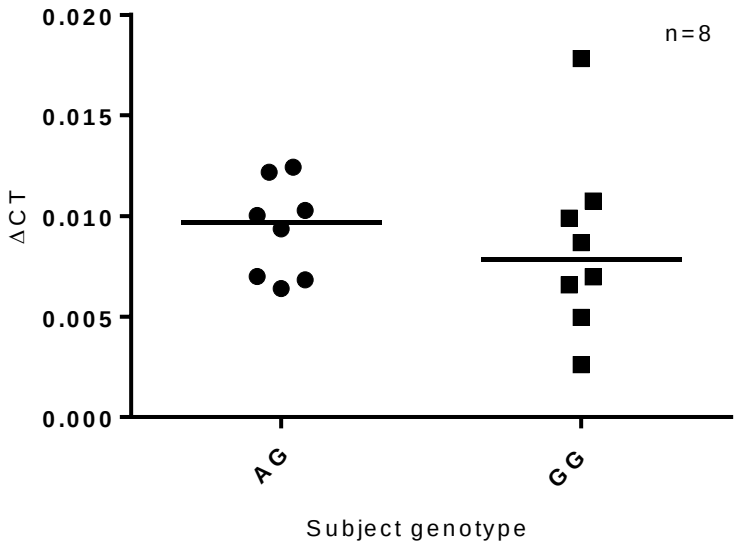

Figure 4-1 Baseline expression of *TNF-α* mRNA in unstimulated monocytes from patients with and without the rs361525 TNF-A polymorphism

TNF-α mRNA expression in freshly isolated monocytes from AG and GG subjects is shown. Individual data points for each subject are illustrated with median displayed as a horizontal line. Differences between subject groups were assessed with a Mann Whitney U test. No significant difference was observed.

Monocytes were also cultured for increasing time periods over 24 hours, unstimulated or stimulated with 100 ng/ml of LPS. *TNF-α* mRNA expression is displayed as time course curves as multiple time-points were measured. However, it should be noted that all AUC calculations in this chapter were restricted to data from time 0 to 6 hours. This was done due to the long gap between the last two time-points (6 hours and 24 hours), meaning that the shape of curves beyond 6 hours should be interpreted with some caution. Figure 4.2 shows that in monocytes cultured in the absence of an exogenous stimulus there was no difference in *TNF-α* mRNA expression or protein concentration between the two groups. The median AUC for AG monocytes was 5.87 ΔCT.hours (range 1.41 to 18.0) versus 4.16 ΔCT.hours (range 2.26 to 11.27) in GG monocytes.

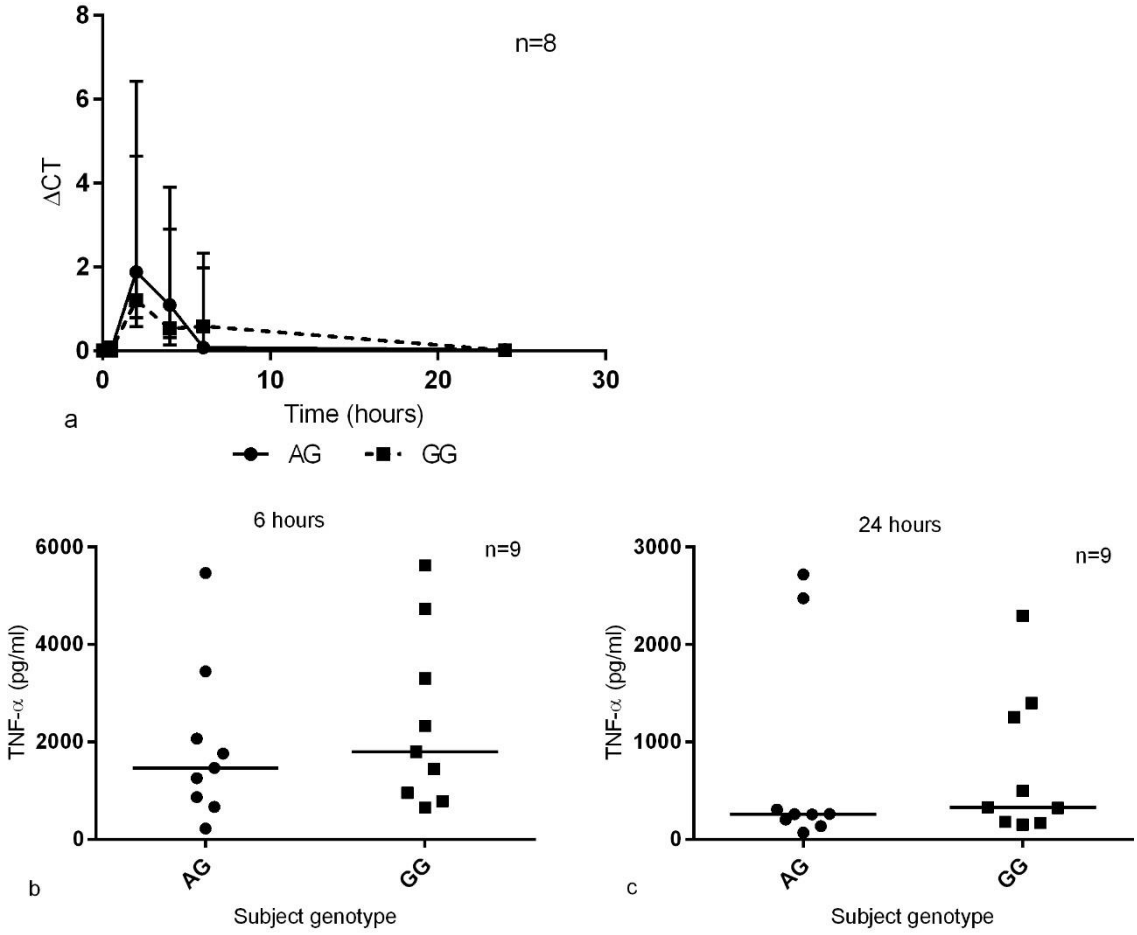

Figure 4-2 *TNF-α* mRNA and protein production by unstimulated monocytes from patients with and without the rs361525 TNF-A polymorphism

a) A time course curve is shown of *TNF-α* mRNA expression over 24 hours. Data points are shown as median and range values. No significant difference in AUC (calculated from data up to the 6 hour time-point only) between groups was observed. The concentration of TNF-α in the CM was measured at 6 hours (b) and 24 hours (c). Individual data points for each subject are illustrated with the median displayed as horizontal lines. No significant difference in TNF-α concentration was observed. Data tested with a Mann Whitney U test.

Figure 4.3 illustrates that in monocytes stimulated with LPS there was no significant difference in *TNF-α* mRNA expression between groups. The median AUC (calculated up to 6 hours post stimulation) for AG monocytes was 13.97 ΔCT.hours (range 4.14 to 20.81) versus 12.71 ΔCT.hours (range 6.48 to 29.64) in GG monocytes. However it should be highlighted here that there was a divergence in the shape of the time course curves for both groups at 6 hours (and to a lesser extent within the unstimulated monocytes in figure 4.2), with the AG monocyte *TNF-α* mRNA expression time course having reached plateau and decreased back towards baseline by 6 hours whereas GG monocyte *TNF-α* mRNA expression had not reached plateau by 6 hours post stimulation. The shape of the curve suggests that GG monocyte *TNF-α* mRNA expression may have actually been greater than AG monocyte *TNF-α* mRNA expression, the opposite of the findings observed in the sputum (17), but cannot prove this given the need for further time-points between 6 and 24 hours. In keeping with this figure 4.3c showed that TNF-α concentration in the CM was greater in the GG group at 24 hours with a trend for it also to be higher at 6 hours (p=0.07) (figure 4.3b).

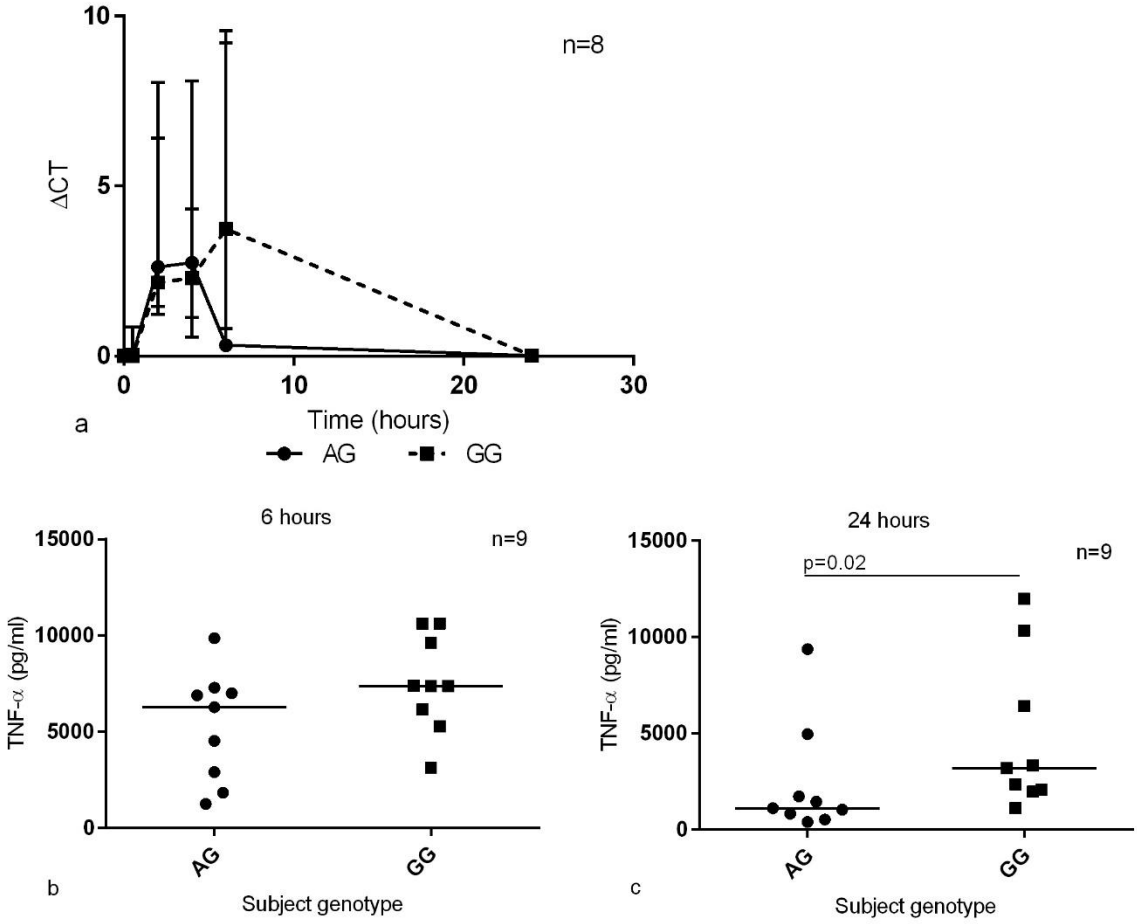

Figure 4-3 *TNF-α* mRNA and protein production by LPS-stimulated monocytes from patients with and without the rs361525 TNF-A polymorphism

a) A time course curve is shown of *TNF-α* mRNA expression over 24 hours. Data points are shown as median and range values. No significant difference in AUC (calculated from data up to the 6 hour time-point only) between groups was observed. The concentration of TNF-α in the CM was measured at 6 hours (b) and 24 hours (c). Individual data points for each subject are illustrated with the median displayed as horizontal lines. A higher concentration of TNF-α was observed in the GG group at 24 hours. Data tested with a Mann Whitney U test.

In all subjects there was a small excess of monocytes for the number of planned experiments. Therefore, monocytes were also stimulated for 6 and 24 hours with 3 ng/ml of the potent stimulant PMA. PMA is an activator of protein kinase C and hence of NF-κB which will induce TNF-α gene transcription (275). Whilst full time course and concentration response

profiles of *TNF-α* mRNA expression and protein secretion for PMA had not been performed in preliminary experiments it was deemed worthwhile to use a second known inducer of TNF-α, at a concentration known to induce production. Figure 4.4 shows that at 6 and 24 hours post stimulation there was no statistically significant difference in *TNF-α* mRNA expression or protein concentration between AG and GG subjects, although there were trends for production to be greater in the GG monocytes.

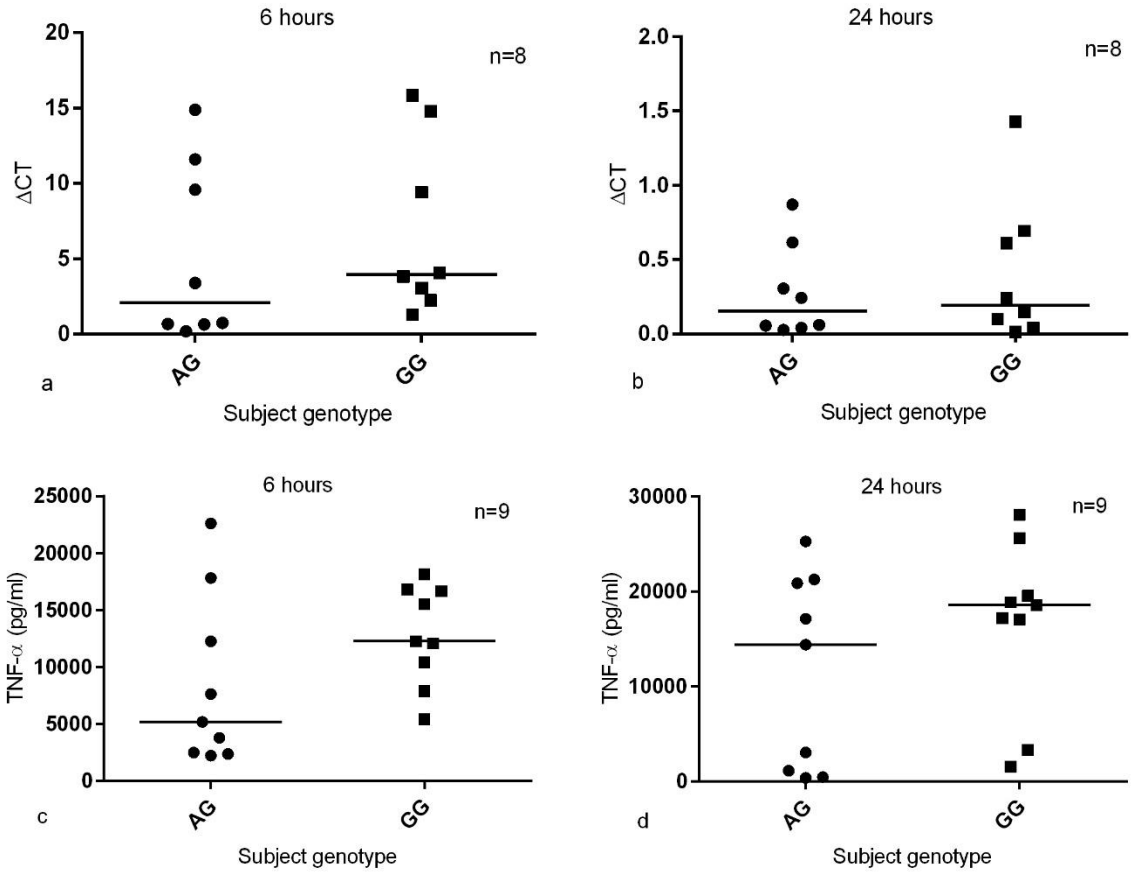

Figure 4-4 *TNF-α* mRNA and protein production by PMA-stimulated monocytes from patients with and without the rs361525 TNF-A polymorphism

Individual data points for each subject are illustrated with the median displayed as horizontal lines. *TNF-α* mRNA expression is shown at 6 hours (a) and 24 hours (b) post stimulation with PMA. TNF-α concentration in the CM is shown at 6 hours (c) and 24 hours (d) post stimulation with 3 ng/ml of PMA. No significant differences were observed between AG and GG groups. Data tested with a Mann Whitney U test.

4.3.2 *CXCL8* mRNA expression and protein secretion is not increased by the presence of the rs361525 TNF-A polymorphism

Sapey *et al* demonstrated a 20 times greater concentration of CXCL8 in the sputum of A1ATD-related COPD patients with the rs361525 polymorphism, likely as a result of more free TNF-α acting on local cells in the airway, such as epithelial cells and macrophages, to up-regulate production of the chemokine (17). It was hypothesised that this would also be observed in the monocytes from AG subjects and that this would be as result of greater TNF-α autocrine feedback up-regulating CXCL8 production.

In freshly isolated monocytes there was no difference in *CXCL8* mRNA expression between the two groups, although there was a trend for greater CXCL8 expression in the AG group (figure 4.5).

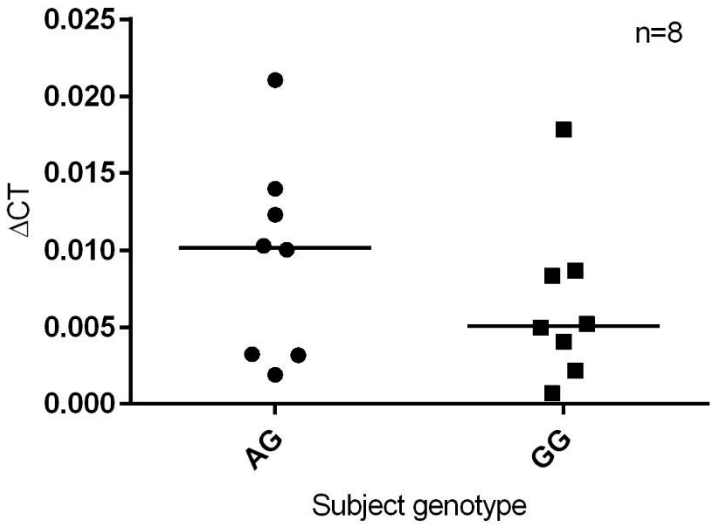

Figure 4-5 Baseline expression of *CXCL8* mRNA in unstimulated monocytes from patients with and without the rs361525 TNF-A polymorphism

CXCL8 mRNA expression in freshly isolated monocytes from AG and GG subjects is shown. Individual data points for each subject are illustrated with median values displayed as horizontal lines. No significant difference in *CXCL8* mRNA expression was observed, assessed with a Mann Whitney U test.

In unstimulated monocytes no significant differences in CXCL8 output at mRNA or protein level were observed between the two groups over time (figure 4.6). However, there was a trend for *CXCL8* mRNA expression as measured by AUC to be greater in the GG monocytes. Median AUC for GG monocytes was 99.57 ΔCT.hours (range 44.37 to 138.12) versus 80.83 ΔCT.hours (range 26.63 to 209.03) for AG monocytes (p=0.75). Similarly there were trends for CXCL8 protein concentration at both time points to be greater in the GG group.

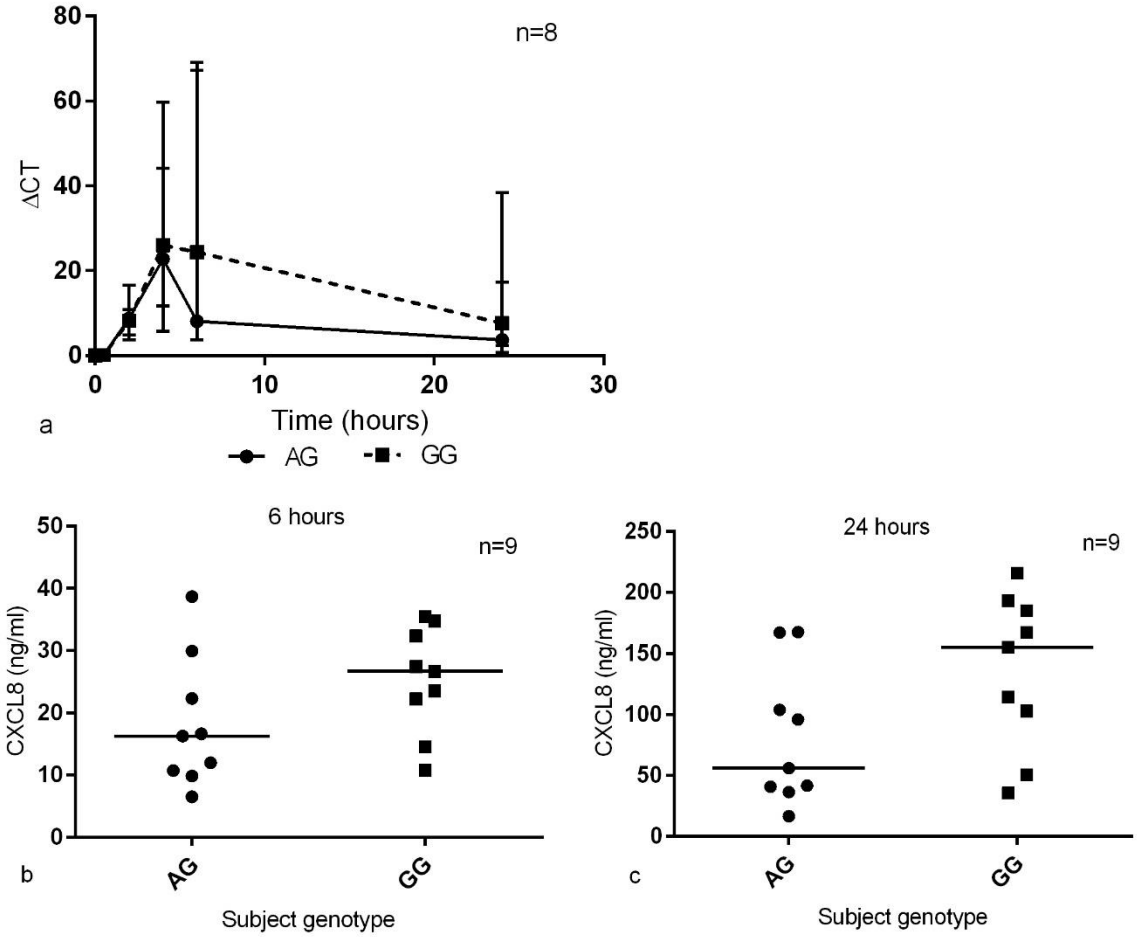

Figure 4-6 *CXCL8* mRNA and protein production by unstimulated monocytes from patients with and without the rs361525 TNF-A polymorphism

a) A time course curve is shown of *CXCL8* mRNA expression over 24 hours. Data points are shown as median and range values. No significant difference in AUC (calculated from data up to the 6 hour time-point only) between groups was observed. The concentration of CXCL8 in the CM was measured at 6 hours (b) and 24 hours (c). Individual data points for each subject are illustrated with median values displayed as horizontal lines. No significant difference in CXCL8 concentration was observed. Data tested with a Mann Whitney U test.

In LPS-stimulated monocytes there was a trend for the AUC for GG monocyte *CXCL8* mRNA expression to be greater than that for AG monocytes (figure 4.7). Median AUC for the GG monocytes was 292.39 ΔCT.hours (range 147.77 to 367.54) versus 190.89 ΔCT.hours

(range 98.49 to 261.82) in the AG monocytes (p=0.05). CXCL8 protein concentration was significantly higher at 24 hours post stimulation in the GG monocyte supernatant.

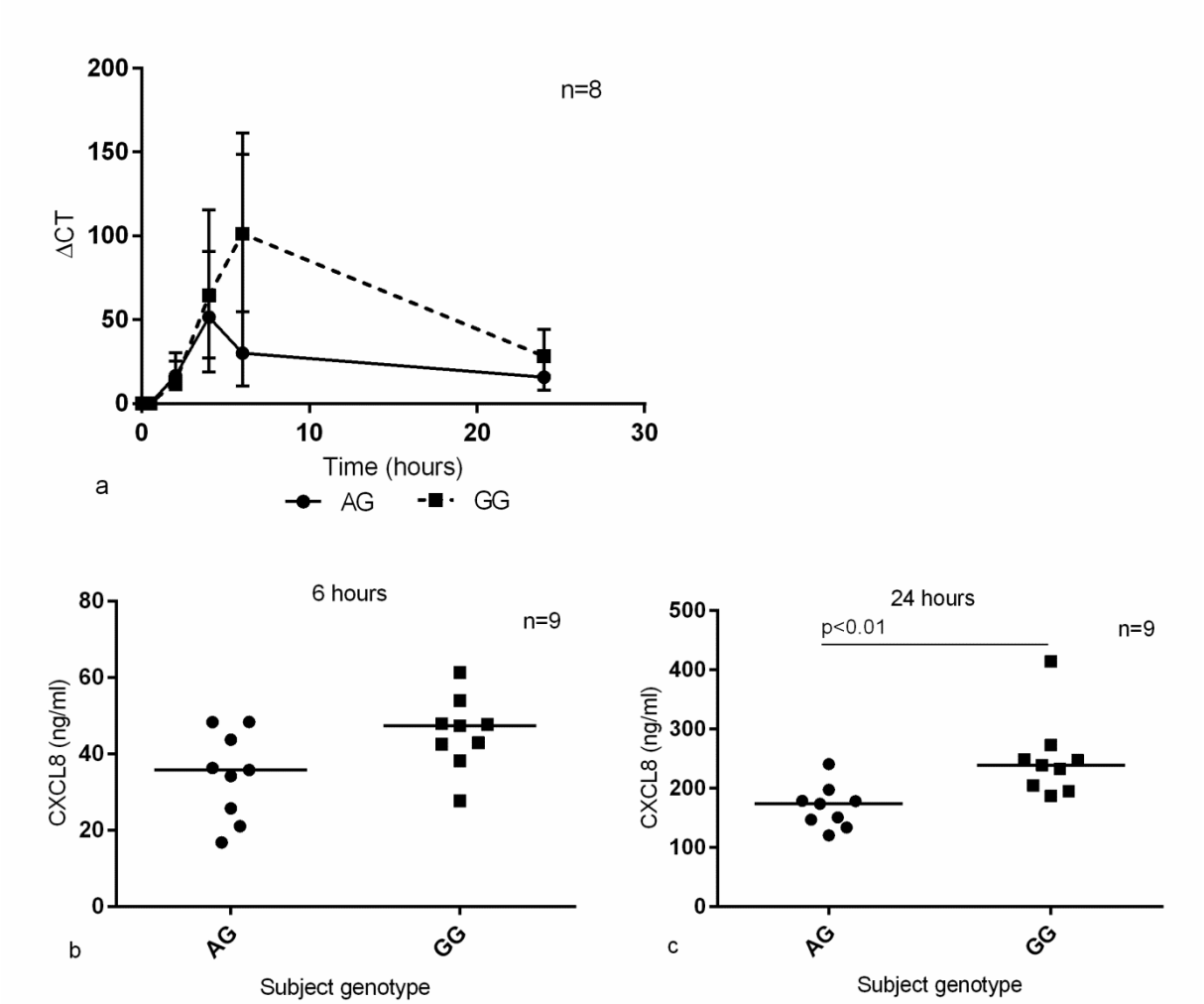

Figure 4-7 *CXCL8* mRNA and protein production by LPS-stimulated monocytes from patients with and without the rs361525 TNF-A polymorphism

a) A time course curve is shown of *CXCL8* mRNA expression over 24 hours. Data points are shown as median and range values. No significant difference in AUC (calculated from data up to the 6 hour time-point only) between groups was observed. The concentration of CXCL8 in the CM was measured at 6 hours (b) and 24 hours (c). Individual data points for each subject are illustrated with median values displayed as horizontal lines. Higher CXCL8 concentration in the GG monocytes at 24 hours post stimulation was observed. Differences between subject groups were assessed with a Mann Whitney U test.

In PMA stimulated monocytes there was a trend at both time-points for both *CXCL8* mRNA expression and protein concentration to be greater in the GG monocytes with a statistically significant difference in the protein concentration at 6 hours (figure 4.8).

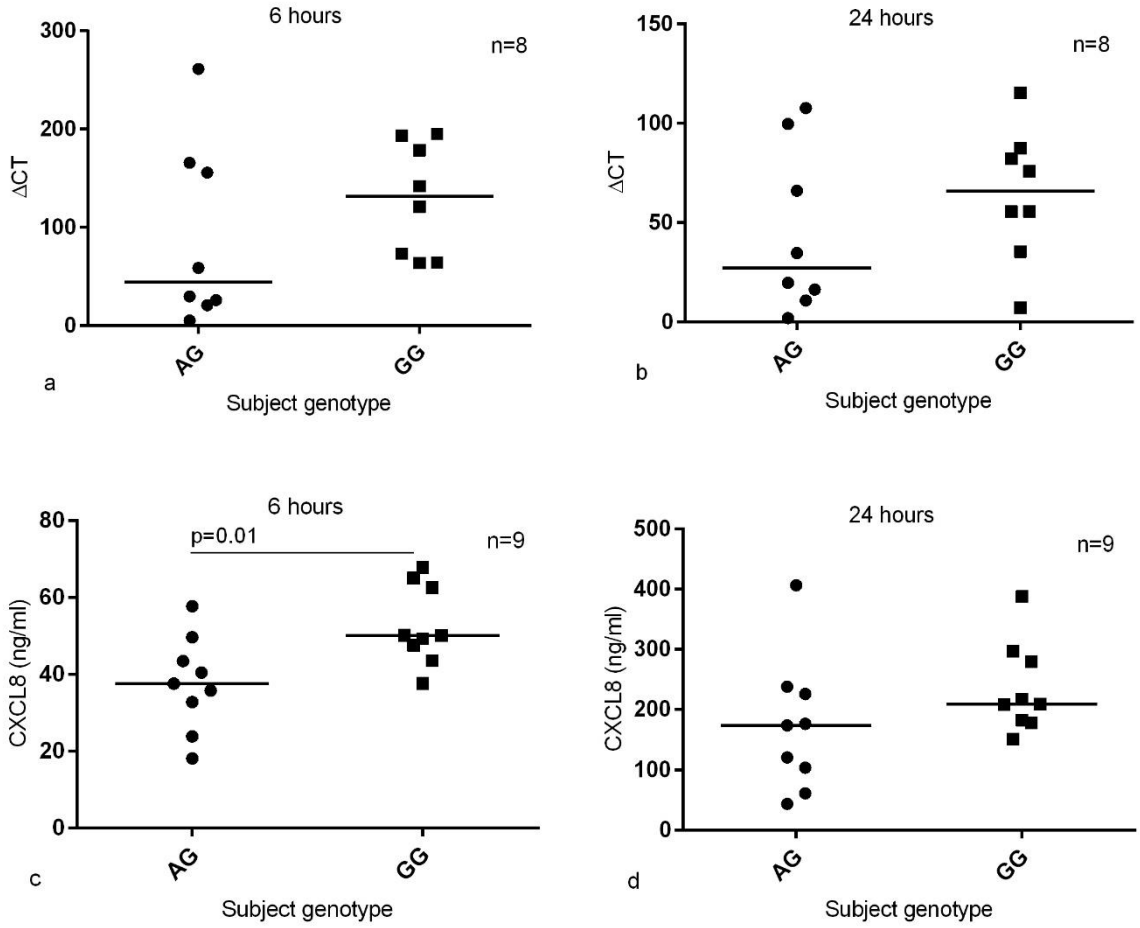

Figure 4-8 *CXCL8* mRNA and protein production by PMA-stimulated monocytes from patients with and without the rs361525 TNF-A polymorphism

Individual data points for each subject are illustrated with median values displayed as horizontal lines. *CXCL8* mRNA expression is shown at 6 hours (a) and 24 hours (b) post stimulation with PMA. CXCL8 concentration in the CM is shown at 6 hours (c) and 24 hours (d) post stimulation with PMA. Higher concentration of CXCL8 was observed in the GG monocyte CM at 6 hours post stimulation. Data tested with a Mann Whitney U test.

A large number of samples were collected during the course of these experiments resulting in the use of many ELISA plates. As the CV% for inter-assay variation had been shown to be greater than 10% (chapter 3) it was necessary to determine if inter-assay variation had any effect on the results obtained. Therefore, samples collected at 24 hours post LPS stimulation hours from both subject groups were re-run on one CXCL8 ELISA plate (figure 4.9). A similar absolute result to that shown in figure 4.7 was obtained. Ideally, samples for individual time points and experimental conditions from the two subject groups would have been tested on one ELISA plate, however this was not feasible as on many occasions samples had to be re-run with different dilution factors and overall many more ELISA plates would have been required.

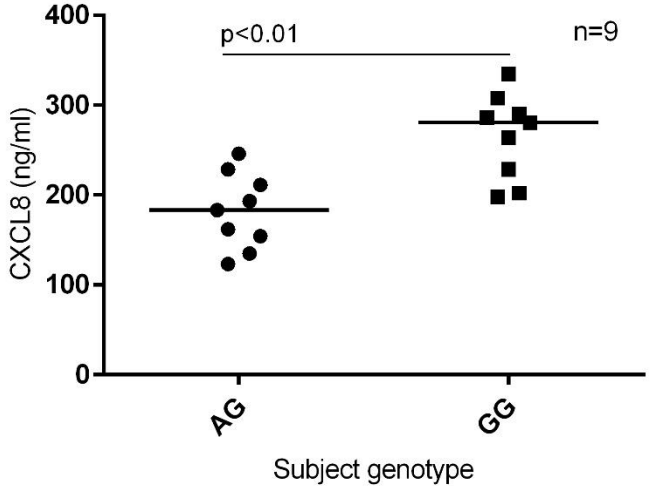

Figure 4-9 Concentration of CXCL8 in the supernatant of LPS-stimulated monocytes in patients with and without the rs361525 TNF-A polymorphism at 24 hours

The concentration of CXCL8 in the CM was measured at 24 hours. Individual data points for each subject are illustrated with median values displayed as horizontal lines. Higher CXCL8 concentration in the GG monocytes at 24 hours post stimulation was observed, assessed with a Mann Whitney U test. All samples of supernatant were tested using the same ELISA plate to eliminate the effect of inter-assay variation.

4.3.3 The autocrine effect of TNF-α

To investigate whether TNF-α was involved in an autocrine feedback loop to up-regulate CXCL8 production, monocytes stimulated with LPS for 6 and 24 hours were also incubated with 10 μg/ml of TNF-α mAb. Cell-free supernatants were collected for analysis of protein content and the cells de-adhered for RNA extraction. Data from both subject groups were combined.

Figure 4.10 shows that blockade of TNF-α had no effect on its own expression in this model at 6 hours post LPS-stimulation, but there was a significant increase in *TNF-α* mRNA expression at 24 hours in the monocytes incubated with TNF-α mAb. The absolute difference was small however, as shown in the table in figure 4.10.

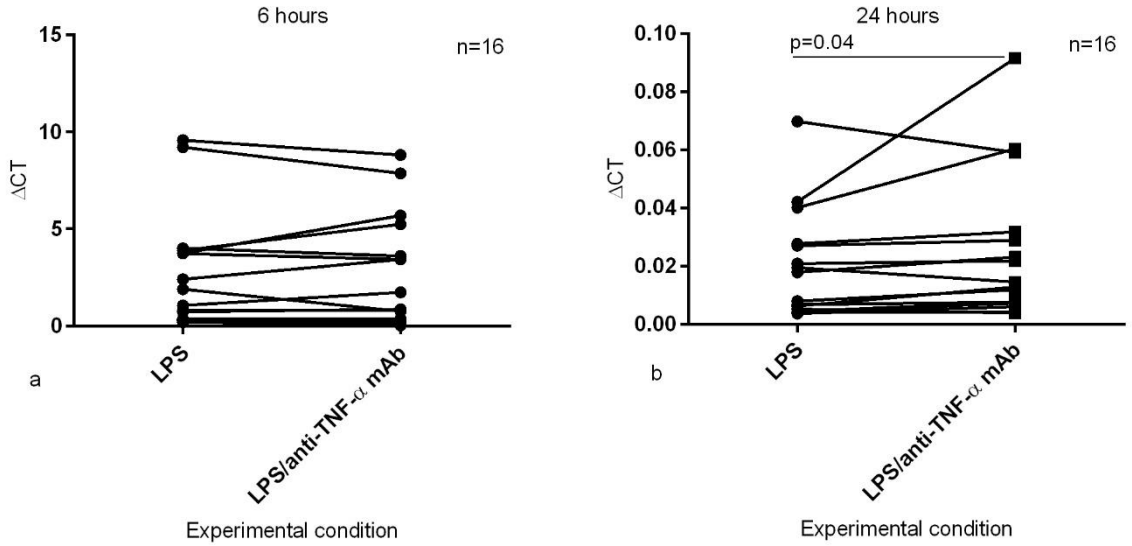

Time (hours)	LPS- median ΔCT (range)	LPS and anti-TNF-α mAb- median ΔCT (range)	P value
6	1.48 (0.19-9.58)	1.29 (0.03-8.82)	
24	0.013 (0.004-0.07)	0.014 (0.004-0.09)	p=0.04

Figure 4-10 *TNF-α* mRNA expression in monocytes stimulated with LPS in the presence or absence of a TNF-α mAb

Paired data is shown for *TNF-α* mRNA expression at a) 6 hours and b) 24 hours. Each pair of data is connected by a line and shows mRNA expression for that subject's monocytes in the presence or absence of a TNF-α mAb. Results from AG and GG subjects were combined. Median data is shown in the table. Differences were tested with a Wilcoxon Signed Ranks test and p values where significant are shown in the table/figure.

Figure 4.11 shows that *CXCL8* mRNA expression and protein concentration in the supernatant were decreased at 24 hours in the presence of a TNF-α mAb. Messenger RNA expression had almost halved at 24 hours but the absolute difference was slight in the protein concentration, suggesting a later time-point would need to have been tested to see this translate through to the protein level.

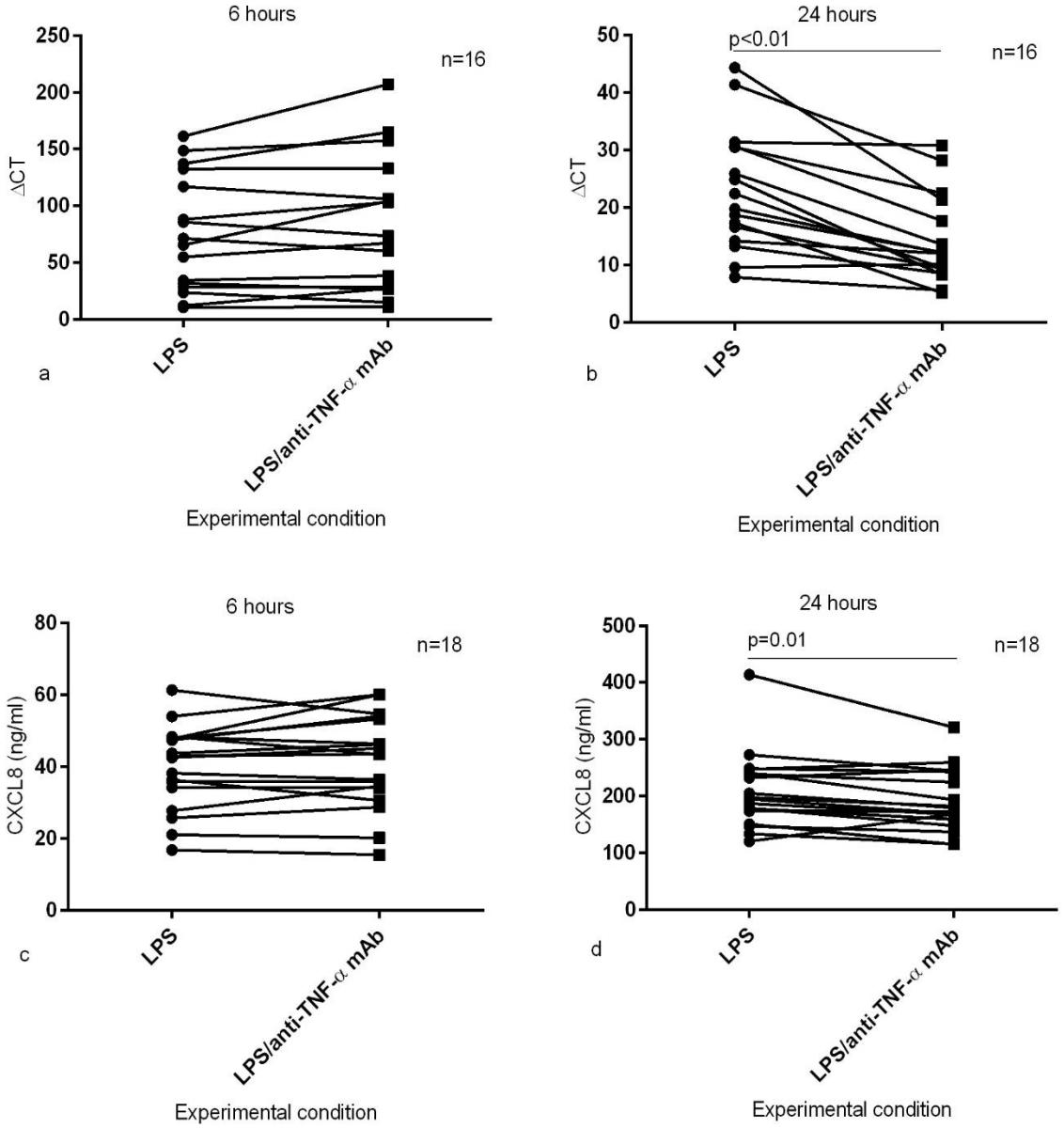

Time (hours)	LPS- median ΔCT (range)	LPS and anti-TNF-α mAb- median ΔCT (range)	P value
6	68.42 (10.56-161.5)	70.35 (10.85-207.2)	
24	21.08 (7.84-44.32)	12.0 (5.13-30.80)	p<0.01
Time (hours)	**LPS- median concentration ng/ml (range)**	**LPS and anti-TNF-α mAb- median concentration ng/ml (range)**	**P value**
6	42.71 (16.78-61.33)	43.41 (15.44-60.06)	
24	196.1 (120.1-414.1)	176.4 (114.7-321.0)	p=0.01

Figure 4-11 *CXCL8* mRNA expression in monocytes stimulated with LPS in the presence or absence of a TNF-α mAb

Paired data is shown for *CXCL8* mRNA expression at a) 6 hours and b) 24 hours and for protein concentration in the CM at c) 6 hours and d) 24 hours. Each pair of data is connected

by a line and shows mRNA expression/protein concentration for that subject's monocytes in the presence or absence of a TNF-α mAb. Results from AG and GG subjects were combined. Median data is shown in the table. Differences were tested with a Wilcoxon Signed Ranks test and p values where significant are shown in the table/figure.

The median concentration of detectable TNF-α in the supernatant of LPS-stimulated monocytes at 6 hours was significantly higher than that in the supernatant of monocytes stimulated with LPS in the presence of a TNF-α mAb (6080.0 pg/ml versus 42.7 pg/ml in the AG group ($p<0.01$) and 7157.3 pg/ml versus 58.7 pg/ml in the GG group ($p<0.01$)), indicating that almost all of the secreted TNF-α had been successfully bound by the mAb.

4.3.4 Intrasubject variation in TNF-α secretion over time

It was hypothesised that one possible cause for not having confirmed greater *TNF-α* mRNA expression and protein secretion at a cellular level in AG subjects was that TNF-α production by monocytes might vary significantly over time, making comparisons between single measurements unreliable. To test this monocytes from 3 healthy subjects were isolated twice weekly (3-4 days apart) for 3 weeks, stimulating them in duplicate with 100 ng/ml of LPS and measuring sTNF-α concentration in the cell-free supernatant at 3 hours. Figure 4.12 shows the values over time for each subject. CV% values for subjects one to three were 26.9%, 48.4% and 17.7%.

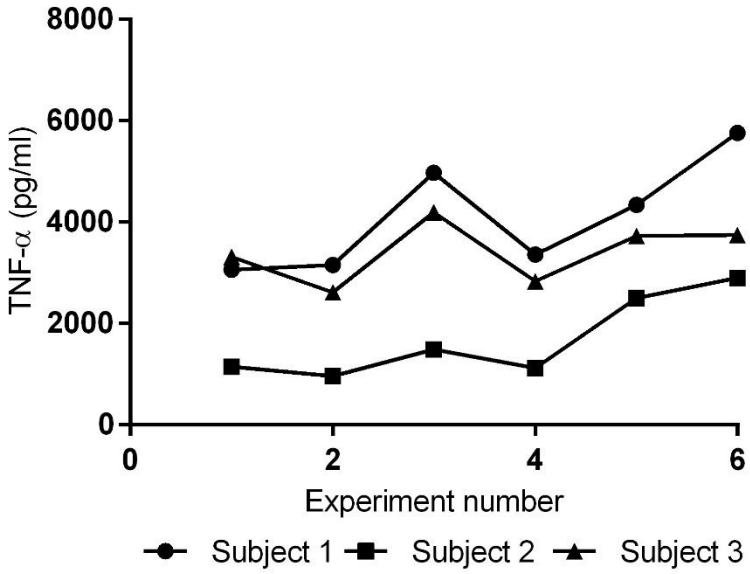

Figure 4-12 TNF-α secretion by LPS-stimulated monocytes over three weeks

Monocytes from 3 healthy subjects (2 female) were isolated twice weekly for 3 weeks and stimulated in duplicate with 100 ng/ml of LPS for 3 hours. TNF-α concentration in the cell-free supernatant was measured using ELISA.

With the assistance of a medical statistician these data were used to estimate the numbers of patients in each of the AG and GG groups that would be needed to demonstrate a true 20% difference in sTNF-α concentration in the monocyte-free supernatants with varying levels of power. For the 6 hour data with a sample size of 40 per group the achieved power would be 83%. For the 24 hour data with a sample size of 140 per group the achieved power would be only 62%.

4.4 **Discussion**

The results from this study did not support the primary hypothesis that monocytes with the rs361525 polymorphism express more *TNF-α* mRNA or secrete more sTNF-α protein than monocytes with the wild type gene. In fact, when cells were stimulated with LPS it was the monocytes from GG subjects that produced more TNF-α protein at later time points (figure 4.3). This was an unexpected finding given the 100 times greater concentration of TNF-α protein detected in the sputum of AG subjects compared to GG subjects in Sapey *et al's* work (17), studying COPD patients from the same A1ATD cohort. The second hypothesis, that a TNF-α autocrine feedback loop would exist, leading to greater CXCL8 production above that due to LPS stimulation alone was found to be partially true, in that blocking the TNF-α produced by monocytes with a commercial mAb had a negative effect on CXCL8 output (figure 4.11). However, the greater CXCL8 output was observed in the GG rather than AG monocytes (figure 4.7), likely to be in keeping with those monocytes having produced more TNF-α when stimulated with LPS, leading to a more pronounced autocrine effect. A very small but significant increase in *TNF-α* mRNA was observed in the presence of the TNF-α mAb (figure 4.10) suggesting that TNF-α autocrine feedback negatively affects its own production. However, the same finding was not observed in TNF-α time course profiles in figure 5.9 in chapter 5.

As the primary hypothesis was not found to be true, further investigation of the other hypotheses, investigating the possible effects of the polymorphism on other monocyte functions and the role of TNFR1 in the autocrine feedback loop were not studied.

The current studies raise interesting questions regarding the significance of this SNP. Specifically, can it be concluded that monocytes from subjects with the rs361525 TNF-A polymorphism do not produce more TNF-α under any circumstance than those from subjects

without the polymorphism and in fact do monocytes from the latter produce more TNF-α than those with the polymorphism? The answer is probably not a simple yes or no and the results obtained here likely reflect both limitations of the studies and the inherent complexity of the effect of SNPs within different cell types and diseases and in response to different stimuli. These issues are considered below.

4.4.1 Patient factors

The subjects in the two groups were matched as closely into pairs, based on as many relevant criteria as possible (age, gender, FEV1, KCO and diagnosis of COPD) and no statistically significant differences between the two groups were found when comparing other characteristics after matching. However, several limitations may have had a bearing on the results. Firstly, although overall the number of patients with the phenotype of CB was similar in the two groups it was difficult to match each individual pair for this particular criterion, whilst still meeting as many other matching criteria as possible, as only 40% of patients in our A1ATD cohort have CB. This may have affected the results obtained in the current studies as Wood *et al* found an association of the polymorphism specifically with the CB phenotype of COPD (125) and Sapey *et al's* findings in the sputum were obtained solely from patients with CB (17). Interestingly Sapey *et al* also noted that after matching their A1ATD/CB patients on a number of criteria, the BMI of patients was significantly lower in the rs361525 polymorphism group (18 versus 24 kg/m^2) (17). In conjunction with a faster decline in FEV1 over 3 years this led the authors to propose that the excess TNF-α in this group was associated with a more aggressive disease phenotype. The current studies focussed on cellular work rather than clinical features but it is important to note that this finding was not replicated in the current studies as there was no significant difference in BMI between the two groups (AG-

21 and GG- 23 kg/m^2). This may again relate to the fact that not all patients studied had CB and that individual subject pairs could not always be matched for this.

In addition, there was a non-statistically significant but potentially clinically relevant difference in age between the AG and GG subjects, as the AG subjects were on average ten years younger. Whether age affects in-vitro production of TNF-α specifically by monocytes is unclear as a review of studies addressing this question described conflicting results (276), but this is certainly a possibility.

One AG subject was a current smoker and the rest of the subjects were mostly ex-smokers in equal proportions. Airway inflammation is known to persist in ex-smokers (277) but all of the patients studied by Sapey *et al'* (17) were also ex-smokers so this should not have been a confounding factor in the current studies, although with only 9 subjects per group it is possible that the one current smoker may have affected the results obtained from peripheral blood monocytes. As smoking is recognised to accelerate the onset and progression of COPD in individuals with A1ATD (42) and hence increase the likelihood of presentation to a specialist A1ATD clinic it is unsurprising that most of the subjects studied here were ex-smokers. Although our cohort also includes non-index cases these are fewer and usually have better preserved lung function meaning that separating groups by current or previous smoking status and then matching for the rs361525 polymorphism and lung function was not feasible. To address this in part a further set of initial TNF-α time course experiments could have been conducted in healthy control smokers in order to determine whether smoking status affects TNF-α output by monocytes.

All of the patients in the original study (17) were taking inhaled steroids (which might modulate monocyte function even in the circulation) as were all of the subjects in the current

study with the exception of one patient in the AG group, which potentially may have a confounding effect on the results.

Despite these possible limitations matching was carried out as closely as possible. Although other authors have found that the GG group in their studies produced more TNF-α than the AG group or vice versa (table 1.2), the subjects in those experiments were not individually matched and hence it is difficult to exclude another cause for differences observed between groups in those studies (133, 135).

Linkage disequilibrium, whilst a potential issue when combining the results of the effects of a SNP on disease expression in case-control studies from different populations, is unlikely to explain the discordance between results presented here and those seen in sputum (17) as our patient samples were all Northern European and taken from the same cohort.

4.4.2 Stimulant factors

Extensive validation experiments were first conducted in monocytes from healthy subjects prior to recruiting patients with the rs361525 TNF-A polymorphism, as presented in chapter 3. LPS was identified as the most potent inducer of TNF-α, of the stimulants tested and peak time-points for measuring TNF-α (6-8 hours) and CXCL8 (24 hours) were chosen.

Ideally it would have been preferable to perform more detailed time course experiments for mRNA work and also for protein measurement by ELISA in the A1ATD patients, as this would have allowed calculation of AUC values in every case rather than comparing one-off time-points, providing a more detailed picture of TNF-α/CXCL8 production over time. However, comparing AUC values is also subject to limitations too, namely the need for close time-points in order to produce as accurate curves as possible. In this chapter, AUC values were only calculated for mRNA time course curves up to and including 6 hours as the gap

between this and the final time-point of 24 hours was too long to produce a meaningful curve beyond 6 hours. The practicalities of performing a detailed 24 hour time course experiment in each case would have been challenging as patients in our cohort live throughout the UK rather than locally, meaning that blood sampling, monocyte extraction and the start time of experiments varied greatly.

Lack of prior determination of peak-time-points and concentration response experiments is a clear limitation with respect to the data gathered from PMA-stimulated monocytes, in which studies suggested trends for slightly greater TNF-α production by GG monocytes, but with no statistically significant difference between the two groups. Never-the-less as all subjects had a small number of excess monocytes it was determined that using a second stimulant was worthwhile.

PMA is a plant phorbol ester which replicates the action of diacylglycerol, a membrane bound secondary messenger found in human cells, which in conjunction with calcium ions activates the intracellular messenger protein kinase C (278). In-vivo, diacylglycerol is formed as a result of hydrolysis of phosphatidylinositol 4,5-bisphosphate following ligand binding to G-protein coupled receptors on the cell surface (279). PMA is able to bypass this by passing across cell membranes and directly activating protein kinase C. Protein kinase C, of which there exists several isoenzymes, is then able to up-regulate TNF-α production in monocytes through divergent downstream signalling pathways that activate NFκB transcription factors and via ERK (a MAP kinase), the transcription factor AP-1 (279, 280). As the opportunity to perform concentration response experiments was not available for PMA the concentration of 3 ng/ml (equivalent to 5 nM) was chosen based upon experience of using this stimulant in monocytes in our laboratory (direct communication with Dr Gillian McNab, ADAPT Project).

PMA has been shown to induce TNF-α by cells in whole blood up to a maximum concentration of 50 ng/ml (281).

LPS acts on monocytes by binding to TLR4 and CD14 on the cell surface, along with lipid binding protein. This switches on multiple intracellular signalling pathways that lead to the rapid up-regulation of numerous transcription factors responsible for pro-inflammatory cytokine gene transcription, such as NFκB, AP-1 and members of the interferon regulatory factor family of transcription factors, among others (282). The transcription factors that switch on TNF-α in monocytes and macrophages in response to LPS have been outlined in detail in 1.8.1. Of relevance to the rs361525 TNF-A polymorphism is work suggesting that NFκB family members, in particular p65, bind to the distal portion of the promoter of the TNF-A gene including the region in which the SNP lies (152, 258). Therefore LPS and PMA are both potentially relevant stimuli as they up-regulate NFκB family members and hence could allow any differential effects of binding of these transcription factors to this area of the promoter in AG and GG monocytes.

However, whilst LPS-induced TNF-α induction has been shown to occur independently of the protein kinase C pathway (283) both LPS and PMA induce intra-cellular signalling pathways that will subsequently activate some of the same transcription factors, meaning that using both these stimuli may offer no benefit in the current studies over using one or the other. In support of this, the differences observed for PMA and LPS-stimulated monocytes were similar, whether trends or statistically significant. In addition, a further negative aspect of using LPS and PMA is their ability to induce a wide variety of transcription factors which might be a disadvantage should those acting at the proximal promoter predominate with respect to affecting TNF-A transcription and thus dilute any effects of differential transcription factor binding in the distal promoter at position -237 between AG and GG monocytes. Never-the-

less as another study using DNA constructs with either the A or G allele and a luciferase reporter assay transfected into RAW 264.7 murine macrophage-like cells showed that LPS up-regulated reporter gene ouput (128) it was still reasonable to use LPS as the primary stimulus. In addition, even if the functional effect of the polymorphism is dependent on binding of one specific transcription factor, the effects of the polymorphism observed in airway secretions would argue against any significant dilutional effect of other transcription factors as multiple potential stimuli will be present in the lungs of a patient with COPD (284) and yet a 100 fold difference in TNF-α between groups was still observed (17).

As the cytokine milieu within the airways of COPD subjects is complex (79) it may be other, multiple exogenous and/or endogenous stimulants which drove the differences observed by Sapey *et al* (17). In keeping with this, a recent study by Kiss-Toth e*t al* (128) showed that expression of a reporter gene encoding for the AG variant of the TNF-α promoter in murine macrophages led to increased gene activity in response to LPS and interestingly this was potentiated by binding of thyroid hormone receptor to the A allele but not the G allele. This indicates that there are multiple steps which may affect the functionality of a SNP and it may be that in the airways other co-factors or epigenetic mechanisms were present which led to 100 times greater TNF-α concentration in the sputum from the polymorphism group (17). Although LPS is found in cigarette smoke and dust and has been shown to induce neutrophilic airways inflammation (241, 285), this may not have been the optimum stimulant, particularly in A1ATD patients who are more likely to have ceased smoking.

The concentration of LPS chosen for use in the experiments was 100 ng/ml, based upon this eliciting the greatest TNF-α response of the concentrations tested, by monocytes from healthy subjects. However, as previously discussed in chapter 3 it may have been preferable to have used the EC80%. If the position of the linear phase of a sigmoidal concentration response

curve for AG monocytes lies to the left of that of GG monocytes they would produce more TNF-α at lower concentrations of stimulant and a difference between the two groups would be seen. By using higher concentrations of LPS it is possible that any differences between the AG and GG monocytes were missed as both may have reached plateau at 100 ng/ml of LPS.

4.4.3 Cellular factors

There are other possible reasons why the results obtained did not support those of Sapey *et al* (17). The primary objective of this thesis was to study the effects of the rs361525 polymorphism at a cellular level. The monocyte was chosen as the cell of interest for several reasons: it is simple to isolate in comparison to airway macrophages or epithelial cells, is the principal producer of TNF-α and as a cell found predominantly in the circulation may have played a role in the possible systemic effect of the polymorphism (3), whereby AG subjects had a lower BMI (17). The objective was to show that in this particular patient population the polymorphism is associated with increased TNF-α production at a cellular level. Although this technique could not prove actual functionality of the SNP this is of less importance as even if the polymorphism is only a marker of increased TNF-α production it could still be used to identify patients who might have have a more aggressive disease phenotype. Despite sound reasons for choosing this cell type there are limitations. It is possible that the polymorphism is only active in other cell types relevant to the airways and alveoli of COPD patients, for example, bronchial epithelial cells or macrophages and indeed Sapey *et al* observed no difference in TNF-α concentration in the plasma between the two groups suggesting blood monocytes may not be the relevant cell type (17). Alternatively the monocyte subset studied may have affected the conclusions reached from the current studies. Whilst results presented in chapter 3 demonstrate that cell preparations inadvertently contained some CD14+CD16+ monocytes, either through experimental limitations or changes

to monocytes during the extraction process, very few CD14-CD16+ monocytes were present. Although this subset is in the minority of circulating monocytes they are believed to be the more pro-inflammatory type (208) and hence may have been the more relevant monocyte to study.

An interesting explanation for the findings might be related to reduction in the cleavage of pro-TNF-α in an in-vitro system. Regulation of TACE, the cell bound enzyme which cleaves both TNF-α and TNFR1 from the cell surface is incompletely understood (286). It is possible that in the airways of A1ATD-related COPD patients there exists a number of mediators that increase TACE activity, leading to the increased concentration of sTNF-α observed in bronchial secretions, and that these mediators might not be present in a culture system containing only monocytes, LPS and CM. If that were the case the supernatant of the AG monocytes may not contain higher concentrations of sTNF-α but there may still be greater production of TNF-α as a result of the rs361525 polymorphism in the form of greater numbers of mTNF-α per cell. Arguing against this theory is the lack of difference in TNF-α expression at the mRNA level. This could be addressed in future studies using flow cytometry.

Lastly, with respect to cell factors is the issue of cell viability. Studies performed later in this thesis and described in chapters 3 and 5 identified that a degree of monocyte apoptosis was occurring over time, particularly in unstimulated cells. The possible effects of this on the results presented here are largely unknown. In some circumstances TNF-α can induce apoptosis, via TNFR1 (287-289), so it is possible that the rs361525 monocytes did produce more TNF-α but conversely were undergoing more extensive and rapid apoptosis as a result. Loss of a greater number of cells to apoptosis, in the absence of in-vivo factors that might maintain their viability, would then mean there were less live cells to contribute to further TNF-α production, giving the appearance that AG monocytes produced less TNF-α. Of note,

GAPDH expression was stable at all time-points, as discussed in chapter 3 and can therefore be assumed not to be affected by early and late stages of apoptosis.

Other factors related to apoptosis might also be relevant. For example, when surrounding phagocytes (in this case live monocytes within the culture wells) are overwhelmed by the number of apoptotic cells and fail to effectively clear them via phagocytosis a process known as programmed necrosis may occur. The apoptotic cell membrane loses its integrity and intracellular contents such as DNA are released into the peri-cellular environment (287). These mediators can elicit pro-inflammatory effects. If this was occurring in the LPS-stimulated monocytes and to varying degrees between subjects' samples then these pro-inflammatory mediators may have affected the outcomes obtained by influencing inflammatory pathways within live monocytes. Lastly, as monocytes themselves act as phagoctyes (290, 291) it is likely that some of the live monocytes were phagocytosing the apoptotic monocytes which may also have activated them and altered their function, influencing the results obtained.

4.4.4 Factors relating to study power

A further possible explanation for the unexpected results obtained in the current study is the intrasubject variation in TNF-α production observed over time. The data obtained from studies over three weeks in healthy subjects clearly showed that monocytes vary in their TNF-α secretion over time, the reasons for which are beyond the scope of this thesis. This phenomenon may be less of a concern when sampling secretions from the lungs as the protein content of sputum should reflect the accumulation of cytokine over more than one day and from large cell numbers and cell types. Subsequent statistical analysis demonstrated that large numbers of patients would be required to show a true 20% difference in TNF-α protein production between AG and GG groups using a one-off monocyte study with sufficient

power. To recruit eighty or more patients from our cohort, or alternatively to perform multiple replicate experiments over time in a smaller sample, is unlikely to be feasible. It was challenging to recruit eighteen subjects as patients reside throughout the UK and often find it difficult and time consuming to attend, particularly if they are limited by their disease. In addition, these power calculations were based on results from healthy subjects. The intrasubject variation in monocyte TNF-α protein production in COPD subjects may be even greater and hence much larger numbers of patients could be needed than estimated.

There was a trend for greater *TNF-α* mRNA expression in freshly isolated monocytes (figure 4.1) and hence one might argue that with greater sample sizes this may have become statistically significant. However, in light of the subsequent finding of intrasubject variation over time, even should this be the case, it would remain unwise to conclude from one-off studies that monocytes from AG subjects do in fact secrete more TNF-α under certain circumstances. This may be a major limitation of many of the in-vitro monocyte studies described in table 1.2.

4.4.5 TNF-α autocrine feedback loop

The experiments presented in this chapter have shown that TNF-α was involved in an autocrine feedback loop to increase production of CXCL8. By 24 hours after LPS stimulation, monocytes co-incubated with a TNF-α mAb had significantly reduced *CXCL8* mRNA expression (by almost half). A small but significant reduction in CXCL8 protein was also observed at 24 hours (figure 4.11). It is likely that if the time-points were extended beyond 24 hours for protein measurement then a greater absolute reduction in CXCL8 protein concentration would be observed. The presence of an autocrine feedback loop also likely explains why greater *CXCL8* mRNA expression and protein secretion was seen in the stimulated GG group monocytes, as this group produced more TNF-α in response to LPS.

One limitation of these particular experiments was the lack of control wells whereby LPS-stimulated monocytes should have been incubated with a matched isotype control antibody at the same concentration as the TNF-α mAb. This would have ruled out a non-specific effect of the TNF-α mAb unrelated to its blocking effect of the TNF-α molecule due to specific epitope binding, such as binding of the immunoglobulin Fc portion to Fc receptors on the monocyte.

4.4.6 Refining study methodology

The main implications of this work are that either the rs361525 polymorphism is not relevant in monocytes from the systemic circulation or that methodological factors have influenced the results. In some respects it is not surprising that the results did not agree with those found in the airways as the studies outlined in table 1.2 show the available evidence for functionality of this polymorphism at a cellular level is conflicting.

A number of further experiments could be conducted to expand upon the findings (discussed in detail in chapter 6), however it would first be important to repeat the current experiments using a refined methodology to address some of the issues that arose during this work.

All cell culture experiments should have included the use of a viability assay to measure the degree of cell loss between the AG and GG monocytes, time-points and experimental conditions. Several different viability assays are available for this purpose (292). The adenosine triphosphate (ATP) assay works on the principle that only viable cells contain ATP (in dead cells ATP is no longer synthesised and any existing ATP is rapidly degraded). In the presence of the luciferase enzyme ATP will react with luciferin to generate luminescence which can be quantified with a plate reader. ATP assays contain a detergent to lyse the cells so this assay can only be used after the cell supernatant has been removed for ELISA and not for cells which are being harvested for later RT-qPCR. The benefit of this assay is that is does

not require a long period to allow colour change to occur (292). Alternatively a protease viability marker assay could be used, such as the CellTiter-Fluor™ Cell Viability Assay (Promega, Wisconsin, United States). Glycylphenylalanyl-aminofluorocoumarin, a cell permeable fluorogenic protease substrate is added to culture wells and only live cells will possess protease activity able to catalyse conversion of the substrate to fluorescent aminofluorocoumarin. The degree of fluorescence is proportional to the number of live cells (292). The strengths of this assay are that cells do not undergo lysis and further assays can be conducted afterwards, such as removing the supernatant for ELISA or harvesting the adherent cells for RNA extraction. Validation experiments would need to be conducted to ensure that the protease viability assay did not affect the results of ELISA and RT-qPCR experiments. Standard curves for both assays can be generated using values from serial dilutions of viable cells or alternatively results can be expressed as a percent change in luminescence/fluorescence relative to an experimental control. The benefit of these assays is that they allow normalisation of results relative to the number of live cells in each culture well.

To overcome intrasubject variation greater numbers of patients would be required (or a similar number of subjects but giving blood on multiple days to allow experiments to be repeated). Monocytes could be extracted from whole blood using a flow cytometer to sort cells for culture experiments. This would allow monocytes to be further sorted on the basis of CD14/CD16 status. The expression of mTNF-α at baseline and over time in response to stimuli could also be measured in the AG and GG monocytes. A flow cytometry viability marker such as 7-AAD should also be used routinely to gate out non-viable cells.

Lastly, a wider range of stimuli could be used to induce TNF-α production, following validation experiments to determine EC80% values and both mRNA and protein time courses could be conducted, using unstimulated cells cultured in CM as an appropriate negative control.

4.5 **Conclusions**

In the current studies the presence of the rs361525 TNF-A SNP in A1ATD patients with COPD was not found to be associated with greater TNF-α production by monocytes and this may have been due to factors such as the high intrinsic intrasubject variation in TNF-α secretion. Alternatively it may be the cell type or specific A1ATD/COPD phenotype (i.e. CB) studied or the interplay of complex patterns of inflammation on many downstream pathways that results in a positive relationship between the rs361525 polymorphism and TNF-α expression. TNF-α was demonstrated to up-regulate production of the chemokine CXCL8 via an autocrine feedback loop. Given the practical limitations of recruiting enough subjects in each group to overcome the issue of intrasubject variation in TNF-α production over time, a decision was reached to focus further studies in this thesis on TNF-α autocrine feedback loops in monocytes from healthy subjects.

CHAPTER 5

THE AUTOCRINE EFFECTS OF TNF-α ON MONOCYTES FROM HEALTHY SUBJECTS

5 The autocrine effects of TNF-α on monocytes in healthy subjects

5.1 Brief Introduction

Monocytes are the principal producers of TNF-α and yet surprisingly little is known about the autocrine or paracrine effects of TNF-α on this cell type in humans (hereafter referred to as autocrine only for simplicity) and the differential roles of its two receptors. Monocytes are believed to be central in many diseases, including IBD, inflammatory arthropathies and septic shock (3, 9). Monocytes are also one of the few cells that express both TNF-α receptors; TNFR1 is expressed on most human cells whereas TNFR2 is found only on immune cells and vascular endothelial cells (4). TNFR2 has clearly been shown to play a predominantly anti-inflammatory role in another important human immune cell, the CD4+FoxP3+ T-reg cell, as these cells preferentially express TNFR2 compared to effector T-cells and their suppressive function is enhanced by mTNF-α binding to TNFR2 (170). The role of TNFR2 in human monocytes has not yet been established.

The importance of characterising the respective roles TNFR1 and TNFR2 is being increasingly recognised. If TNFR1, ubiquitously expressed on almost all cell types, is the "pro-inflammatory" receptor, with TNFR2 responsible for a more immunomodulatory role this could make selective TNFR1 blockade a more beneficial concept. Indeed, a phase one study of Atrosab, a humanized mAb that specifically blocks TNFR1 has demonstrated an acceptable safety profile and phase two proof-of-concept trials in rheumatoid arthritis and psoriasis are planned for 2016 (293). In addition, another mAb targeting the TNFR1 receptor, GSK1995057, has been tested in healthy volunteers with an associated reduction in pro-inflammatory mediators in BAL fluid in response to LPS (to simulate acute lung injury) (294).

The work carried out for this thesis investigating the effects of the rs361525 TNF-A polymorphism in A1ATD patients, as described in chapter 4, revealed a TNF-α autocrine feedback loop, shown by the addition of the TNF-α mAb to LPS-stimulated monocytes attenuating the production of CXCL8. Characterising these autocrine effects further and the differential roles of the two receptors in monocytes from healthy subjects was therefore felt to be important. Several hypotheses were formed relating to the role of TNF-α autocrine feedback loops in monocytes and are shown below. All experiments presented in this chapter were conducted using monocytes from healthy control subjects (23 subjects, median age- 31 years, IQR- 25 to 32.5 years; range- 21 to 45 years; 13 males)) rather than A1ATD patients with the rs361525 polymorphism.

Hypothesis one: TNF-α produced by monocytes is involved in autocrine feedback loops to up-regulate both pro and anti-inflammatory cytokine production.

Hypothesis two: TNF-α autocrine feedback loops in monocytes occur via TNFR1 for pro-inflammatory cytokine production and via TNFR2 for anti-inflammatory cytokine production.

Hypothesis three: the decrease in measurable sTNF-α over time in the supernatant of monocytes in culture (as observed in figure 3.2) is due to autocrine binding to one or both of its receptors.

Hypothesis four: TNF-α autocrine feedback loops in monocytes play a role in influencing the expression of the two TNF-α receptors, TNFR1 and TNFR2.

To investigate these hypotheses the following objectives and strategies to meet these objectives were set:

- Determine if the production of other pro-inflammatory and anti-inflammatory cytokines in addition to CXCL8 was affected by TNF-α autocrine feedback loops. This was conducted by using LPS to stimulate TNF-α production, in the presence or absence of a TNF-α mAb and then measuring cytokine mRNA expression with RT-qPCR and secreted protein by ELISA.
- Examine the relative involvement of the two TNF-α receptors in autocrine feedback loops influencing cytokine production. This was conducted by using LPS to stimulate TNF-α production in the presence or absence of TNFR1 mAb or TNFR2 mAb or both receptor mAbs and then measuring cytokine mRNA expression with RT-qPCR.
- Measure sTNF-α in the supernatant of LPS-stimulated monocytes incubated in the presence or absence of TNFR1 mAb or TNFR2 mAb or both mAbs to determine if receptor blockade increases sTNF-α concentration.
- Characterise the expression pattern of the TNF-α receptors on the surface of monocytes at baseline and over time and determine if change in receptor density was due in any part to TNF-α autocrine feedback loops. This was done by measuring TNFR1/TNFR2 expression on LPS-stimulated monocytes incubated in the presence or absence of a TNF-α mAb or TNFR1/TNFR2 mAbs.

5.2 **Results**

5.2.1 LPS induces cytokine mRNA expression by monocytes

Prior to investigating the autocrine effects of TNF-α it was necessary to determine the time course profiles of pro and anti-inflammatory cytokines in response to LPS. As it was previously accepted that LPS induces cytokine secretion (295) one-tailed testing was used to test the hypothesis that LPS induced greater production of TNF-α, IL-6, CXCL8, IL-1β, TGF-β and IL-10 over time than that by unstimulated monocytes.

Monocytes at a concentration of 0.25 million per ml of CM were cultured in the presence or absence of 100 ng/ml of LPS for pre-specified time periods over 48 hours and the RNA extracted from harvested cell pellets. Culture experiments were conducted singly. Messenger RNA samples from each experimental condition underwent RT-qPCR in duplicate. Comparison of AUC values for time course curves demonstrated that stimulating healthy monocytes with LPS induced expression of a number of pro-inflammatory cytokines, greater than that observed in unstimulated monocytes (figure 5.1 to 5.4). This data is in keeping with established knowledge regarding the effect of LPS on pro-inflammatory cytokine mRNA transcription (295, 296).

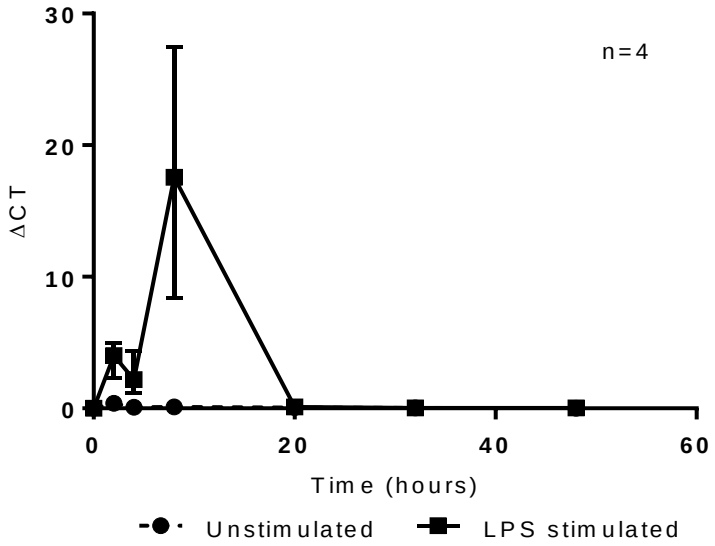

Time (hours)	0	2	4	8	20	32	48	AUC (ΔCT.hours)
ΔCT Unstimulated	0.01	0.38 (p<0.01)	0.09	0.12 (p=0.03)	0.07	0.03	0.02	**3.91** (3.31- 4.10)
ΔCT LPS-stimulated	0.01	4.01 (p=0.01)	2.18 (p=0.03)	17.55 (p<0.01)	0.11	0.03	0.03	**159.34** (85.58-232.56)

Figure 5-1 Effect of LPS on *TNF-α* mRNA expression by monocytes over 48 hours

Data points are shown for unstimulated and LPS-stimulated monocytes. Data points represent median values (with range), also supplied in the table. Friedman's testing was conducted for individual time course experiments and post-hoc pairwise comparison p-values of each time-point to time zero are shown in the table, where significant (unadjusted p-values were first corrected by multiplying by 6). AUC was calculated for each time course curve and the two values compared with a Wilcoxon Signed Ranks test (one-tailed p=0.04).

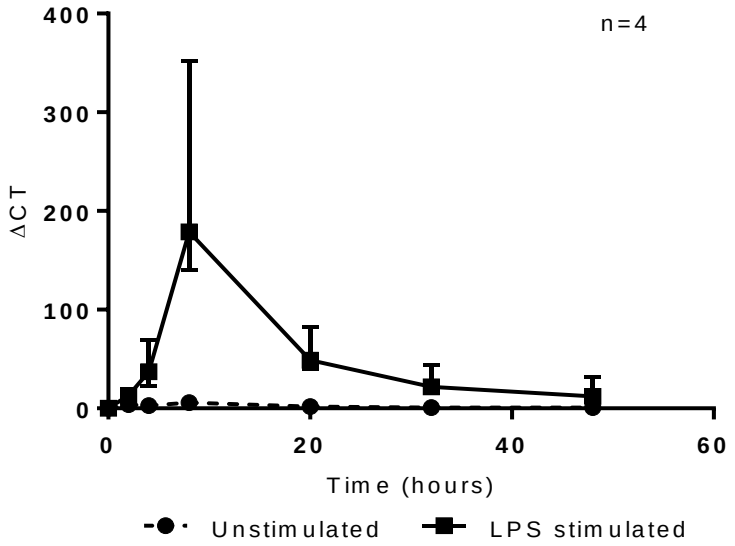

Time (hours)	0	2	4	8	20	32	48	AUC (ΔCT.hours)
ΔCT Unstimulated	0.03	3.95 (p=0.01)	2.92 (p=0.03)	5.69 (p<0.01)	1.92	0.92	0.70	**110.09** (62.72-168.84)
ΔCT LPS-stimulated	0.03	13.11	37.24 (p=0.03)	178.81 (p<0.01)	49.00 (p=0.01)	21.98	12.07	**3049.63** (2169.80-3696.88)

Figure 5-2 Effect of LPS on *CXCL8* mRNA expression by monocytes over 48 hours

Data points are shown for unstimulated and LPS-stimulated monocytes. Data points represent median values (with range), also supplied in the table. Friedman's testing was conducted for individual time course experiments and post-hoc pairwise comparison p-values of each time-point to time zero are shown in the table, where significant (unadjusted p-values were first corrected by multiplying by 6). AUC was calculated for each time course curve and the two values compared with a Wilcoxon Signed Ranks test (one-tailed p=0.04).

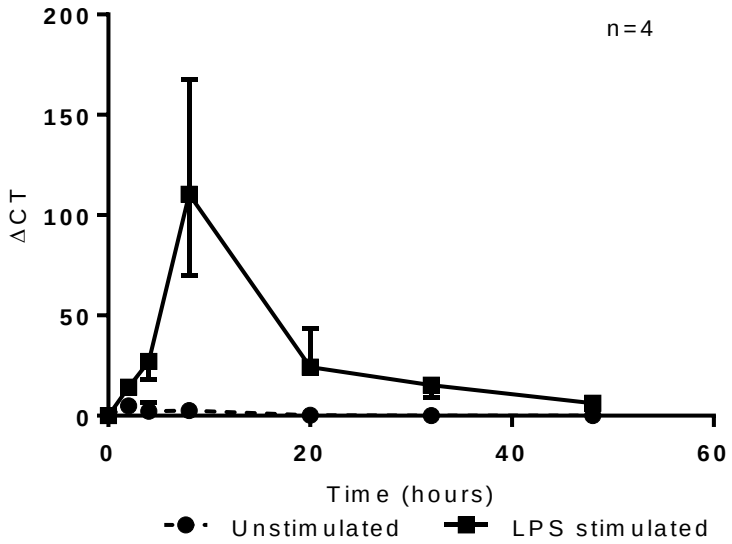

Time (hours)	0	2	4	8	20	32	48	AUC (ΔCT.hours)
ΔCT Unstimulated	0.01	4.94 (p<0.01)	2.25 (p=0.01)	2.56 (p=0.01)	0.29	0.06	0.03	**40.26** (26.93-79.93)
ΔCT LPS-stimulated	0.01	14.18	27.02 (p=0.02)	110.50 (p<0.01)	24.19 (p=0.02)	15.28	6.20	**1571.21** (1436.36-1890.55)

Figure 5-3 Effect of LPS on *IL-1β* mRNA expression by monocytes over 48 hours

Data points are shown for unstimulated and LPS-stimulated monocytes. Data points represent median values (with range), also supplied in the table. Friedman's testing was conducted for individual time course experiments and post-hoc pairwise comparison p-values of each time-point to time zero are shown in the table, where significant (unadjusted p-values were first corrected by multiplying by 6). AUC was calculated for each time course curve and the two values compared with a Wilcoxon Signed Ranks test (one-tailed p=0.04).

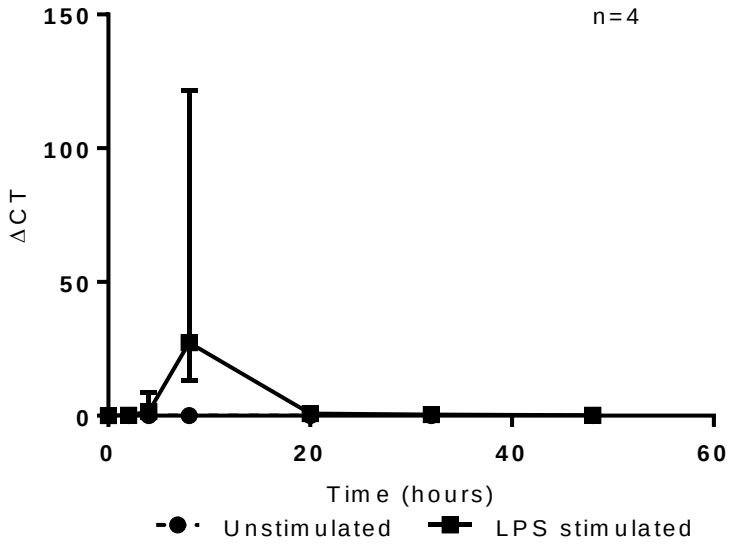

Time (hours)	0	2	4	8	20	32	48	AUC (ΔCT.hours)
ΔCT Unstimulated	0.00	0.02 (p=0.01)	0.03 (p=0.01)	0.02	0.00	0.00	0.00	**0.29** (0.16-0.38)
ΔCT LPS-stimulated	0.00	0.14	1.58 (p=0.01)	27.31 (p<0.01)	0.78	0.43	0.17	**241.73** (120.37-1021.56)

Figure 5-4 Effect of LPS on *IL-6* mRNA expression by monocytes over 48 hours

Data points are shown for unstimulated and LPS-stimulated monocytes. Data points represent median values (with range), also supplied in the table. Friedman's testing was conducted for individual time course experiments and post-hoc pairwise comparison p-values of each time-point to time zero are shown in the table, where significant (unadjusted p-values were first corrected by multiplying by 6). AUC was calculated for each time course curve and the two values compared with a Wilcoxon Signed Ranks test (one-tailed p=0.04).

The expression of mRNA of two predominantly anti-inflammatory cytokines, IL-10 and TGF-β (297) over 48 hours, was also measured in response to LPS and in unstimulated cells. LPS induced significantly greater *IL-10* mRNA expression than unstimulated monocytes (figure 5.5). In contrast, there was no difference in TGF-β expression in LPS-stimulated monocytes compared to unstimulated cells (figure 5.6).

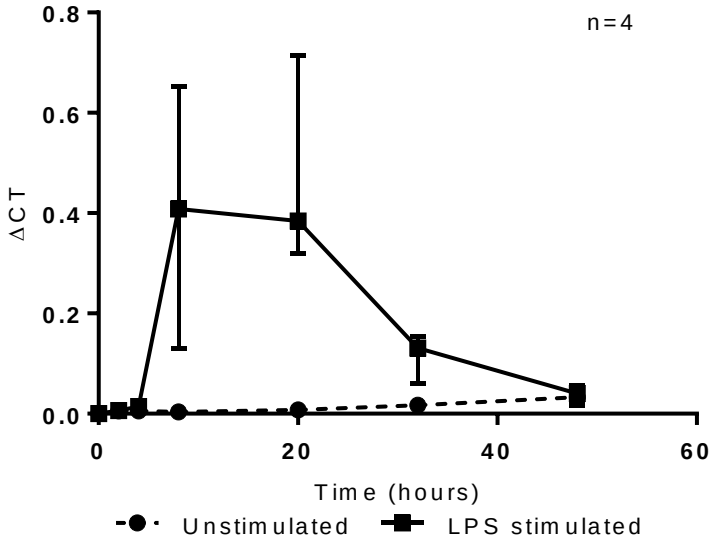

Time (hours)	0	2	4	8	20	32	48	AUC (ΔCT.hours)
ΔCT Unstimulated	0.00	0.01	0.01	0.00	0.01	0.02 (p=0.01)	0.03 (p<0.01)	**0.69** (0.39-1.11)
ΔCT LPS-stimulated	0.00	0.01	0.01	0.41 (p<0.01)	0.38 (p<0.01)	0.13	0.04	**10.85** (8.28-12.53)

Figure 5-5 Effect of LPS on *IL-10* mRNA expression by monocytes over 48 hours

Data points are shown for unstimulated and LPS-stimulated monocytes. Data points represent median values (with range), also supplied in the table. Friedman's testing was conducted for individual time course experiments and post-hoc pairwise comparison p-values of each time-point to time zero are shown in the table, where significant (unadjusted p-values were first corrected by multiplying by 6). AUC was calculated for each time course curve and the two values compared with a Wilcoxon Signed Ranks test (one-tailed p=0.04).

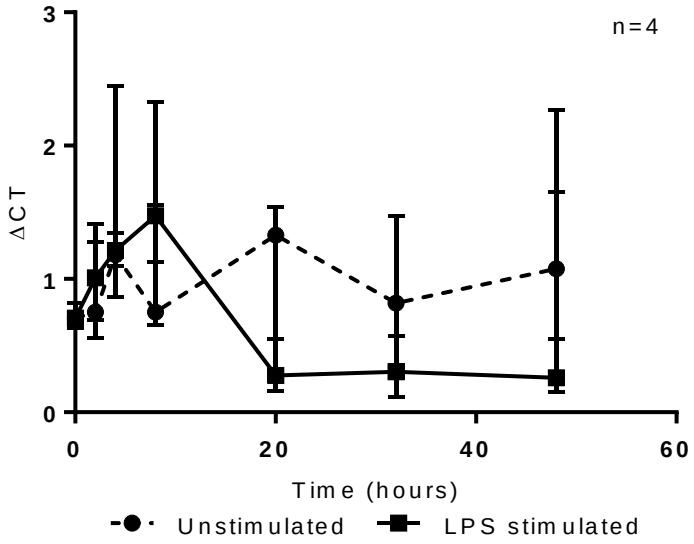

Time (hours)	0	2	4	8	20	32	48	AUC (ΔCT.hours)
ΔCT Unstimulated	0.71	0.75	1.18	0.75	1.33	0.82	1.08	**51.39** (22.47-64.76)
ΔCT LPS-stimulated	0.71	1.01	1.21	1.47	0.28	0.30	0.26	**32.57** (21.28-50.13)

Figure 5-6 Effect of LPS on *TGF-β* mRNA expression by monocytes over 48 hours

Data points are shown for unstimulated and LPS-stimulated monocytes. Data points represent median values (with range), also supplied in the table. No significant post-hoc pairwise comparison of each time-point to time zero were found. AUC was calculated for each time course curve and the two values compared with a Wilcoxon Signed Ranks test (non-significant).

5.2.2 Autocrine binding of soluble TNF-α may occur predominantly via TNFR2 in monocytes cultured in isolation

Cell free supernatants were collected from monocytes cultured in the presence of LPS over a 20 hour period (figure 5.7a), at a concentration of 0.45 million cells per well/ml. An increase in sTNF-α was observed until 8 hours post LPS stimulation, following which the concentration of detectable sTNF-α decreased.

The TNF-α ELISA used detects both free and soluble receptor-bound cytokine indicating that the fall in detectable sTNF-α was not due to binding to its soluble receptors but could instead be due to degradation of the protein or binding to one or both of its cell surface receptors, excluding the cytokine from the supernatants collected. To test the latter hypothesis monocytes from 7 individuals were stimulated in duplicate, with LPS, for 20 hours in the presence or absence of a mAb to one or both TNF-α receptors (10 μg/ml). Soluble TNF-α in the cell free supernatant was subsequently measured (figure 5.7b). Blockade of TNFR2 led to a significant increase in detectable sTNF-α with a trend for a small increase in the presence of TNFR1 blockade. This suggests that a significant proportion of the decrease in sTNF-α in the cell culture supernatant by 20 hours was due to binding to TNFR2.

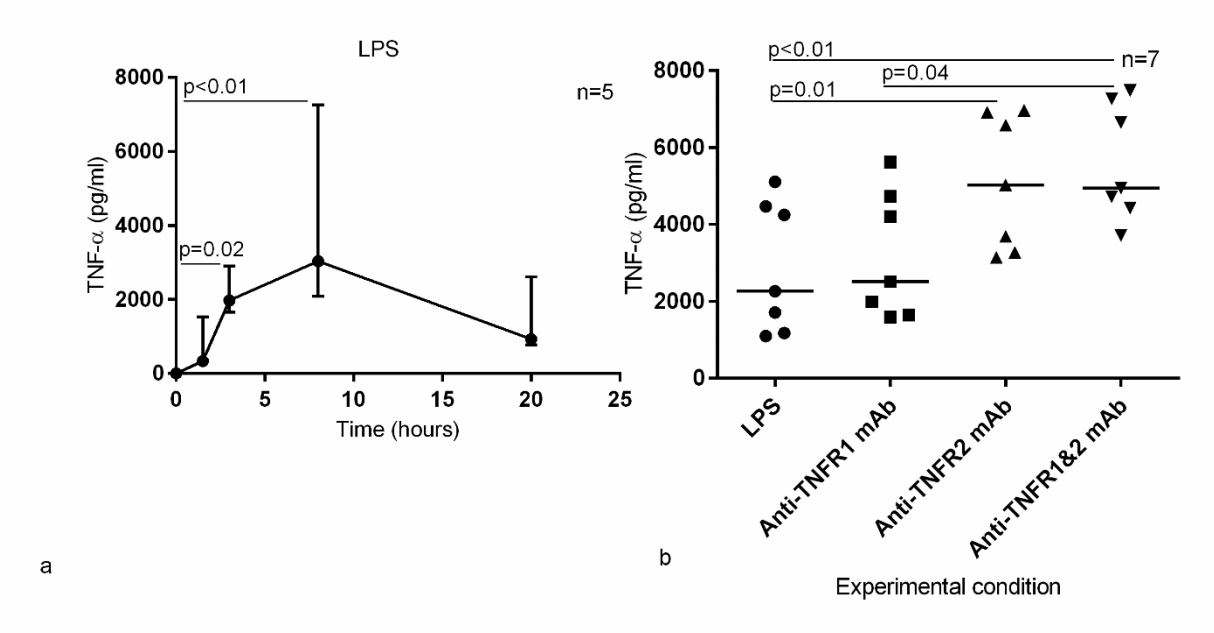

Figure 5-7 Autocrine binding of sTNF-α secreted by LPS-stimulated monocytes

a) A time course profile for sTNF-α concentration in response to LPS stimulation is shown. Each datum point is the median value (with range). Friedman's testing was significant ($p<0.01$) and post-hoc pairwise comparison p-values of each time-point to time zero are shown on the figure where significant (unadjusted p-values were first corrected by multiplying by 4). b) Monocytes were cultured with LPS for 20 hours, with or without the addition of 10 µg/ml of TNF-α R1 mAb or TNF-α R2 mAb or both mAbs. Each experimental condition shows individual data points with median values displayed as horizontal lines. Overall differences between experimental conditions were assessed with a Friedman's test ($p<0.001$). Post hoc Dunn-Bonferroni adjusted pairwise comparisons where significant are shown on the figure.

A further experiment was conducted to determine if sufficient concentration of each receptor antibody had been used to block TNFR1 and TNFR2 on the monocyte surface. Monocytes from one subject were cultured (0.45 million cells per well) under four conditions: stimulated with LPS, stimulated with LPS in the presence of increasing concentration of either TNFR1 mAb, TNFR2 mAb or both receptor mAbs. Cells were incubated with the relevant mAbs for 30 minutes, with gentle agitation, prior to addition of LPS. This was done to ensure blockade of cell surface receptors prior to the release of TNF-α by the monocytes in response to LPS.

The concentration of receptor mAb ranged from 1 ng/ml (log 0) to 10 μg/ml (log 4). After 24 hours the concentration of sTNF-α in the cell free supernatants was measured by ELISA. The concentration of sTNF-α at 24 hours in control cells stimulated with LPS in the absence of either mAb was 1842.5 pg/ml. Figure 5.8 illustrates that as the concentration of TNFR2 mAb increased logarithmically there was a steady increase in the concentration of sTNF-α in the supernatant, suggesting that an increasing number of TNFR2 receptors on the cell surface were being prevented from binding any sTNF-α, thereby displacing it into the supernatant to be detected by the ELISA. The concentration response curve indicated that 1 μg /ml of TNFR2 mAb was sufficient to block the cell surface receptors on 0.45 million monocytes. However, to be sure this was the case an excess of TNFR2 mAb was used in further experiments, at a concentration of 10 μg/ml.

In contrast, no detectable increase in sTNF-α was observed with increasing concentrations of TNFR1 mAb. This was unlikely to be due to insufficient concentration of the receptor mAb. Product datasheets for the antibodies outline that the concentration of TNFR1 mAb required to prevent 50% of sTNF-α induced cytotoxicity in mouse fibroblasts is at most two to four times greater than for TNFR2 mAb (298, 299). As TNFR2 ligation by mAb was beginning to occur with concentrations as low as 100 ng/ml of mAb, displacing sTNF-α, then it is impossible based on product characteristics that concentrations of TNFR1 mAb two orders of magnitude greater would not be ligating TNFR1. The same concentration of TNFR1 mAb (10 μg/ml) was therefore chosen for all future experiments. An alternative method to determine optimum concentrations of receptor mAbs required to block receptors such as using flow cytometry was not used. This was because the location of binding of fluorophore labelled flow cytometry antibodies to the receptors could not be confirmed with the manufacturers as epitope locations for mAb binding are not characterised in detail (direct communication with

Dr E. Fioravanti, R and D Systems, 27th November 2015). If the flow cytometry TNFR mAbs bind at an alternate epitope of the receptor to the functional blocking mAbs then using this method to assess optimal concentration would be not be accurate in determining the proportion of TNF-α receptors blocked by mAb.

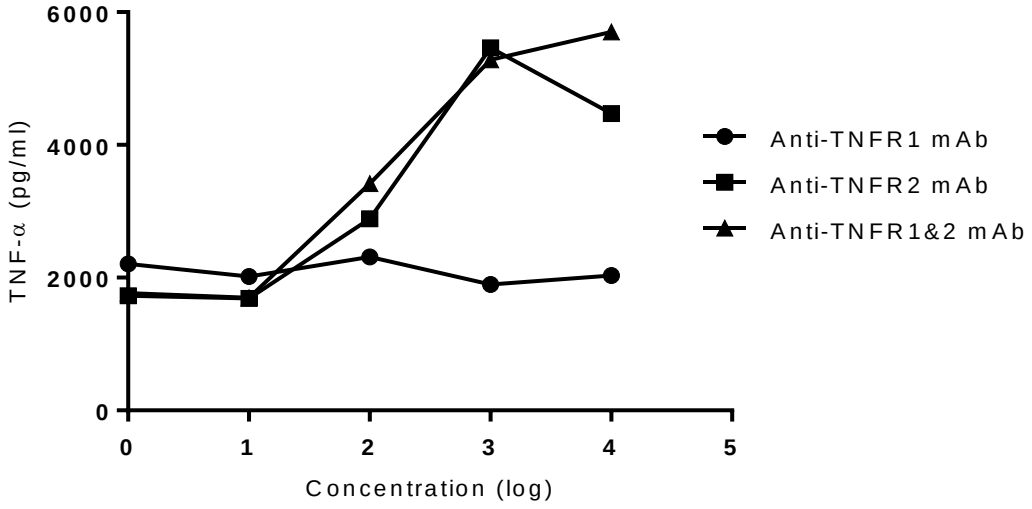

Figure 5-8 Determining the concentration of TNFR1 and TNFR2 mAb needed to prevent TNF-α binding to its cell surface receptors

The graph shows monocytes from one subject stimulated for 24 hours with LPS in the presence of increasing concentrations of either TNFR1 mAb, TNFR2 mAb or both. The concentration of mAbs required to occupy all of either of the receptors was estimated indirectly by measuring the concentration of secreted sTNF-α prevented from binding to its receptor and hence detectable by ELISA. A concentration-response curve was observed for TNFR2 mAb but not TNFR1 mAb. Starting concentration of TNFR1/TNFR2 mAb= 1 ng/ml (0 on logarithmic x-axis). The concentration of sTNF-α at 24 hours in cells stimulated with LPS in the absence of either mAb was 1842.5 pg/ml.

5.2.3 TNF-α induces cytokine mRNA expression in monocytes via a positive feedback loop

To determine whether autocrine binding of TNF-α has a positive feedback effect, cells from 4 subjects were stimulated with LPS in the presence or absence of TNF-α mAb and the supernatants and monocytes were collected separately at 0, 2, 4, 8, 20, 32 and 48 hours post stimulation (0.25 million cells per well). As experiments presented in chapter 4 had already demonstrated an autocrine feedback loop leading to reduction in CXCL8 output (figure 4.11) the following statistical tests were applied as one-tailed tests.

Messenger RNA expression of TNF-α, CXCL8, IL-1β, IL-6, IL-10 and TGF-β was quantified at each time point and presented as time course curves with calculated AUC values (figure 5.9). *TNF-α* mRNA expression was not affected by blockade of secreted TNF-α, however CXCL8, IL-1β, IL-6 and IL-10 expression was reduced in the presence of TNF-α mAb. *TGF-β* mRNA was not affected by the blockade of secreted TNF-α, indicating that TNF-α did not affect its regulation as it has been shown to do in other cell types (300). TGF-β is constitutively expressed in human tissues (301) and the data in figure 5.6 suggested that LPS may actually down-regulate its expression by human monocytes over time. Using LPS as a model of natural TNF-α secretion was therefore determined not to be useful in assessing the effect of TNF-α on *TGF-β* mRNA expression by monocytes. TGF-β as an example of an anti-inflammatory cytokine was therefore not studied further in this thesis.

Figure 5-9 Effect of the TNF-α mAb on pro- and anti-inflammatory cytokine mRNA expression in LPS-stimulated monocytes

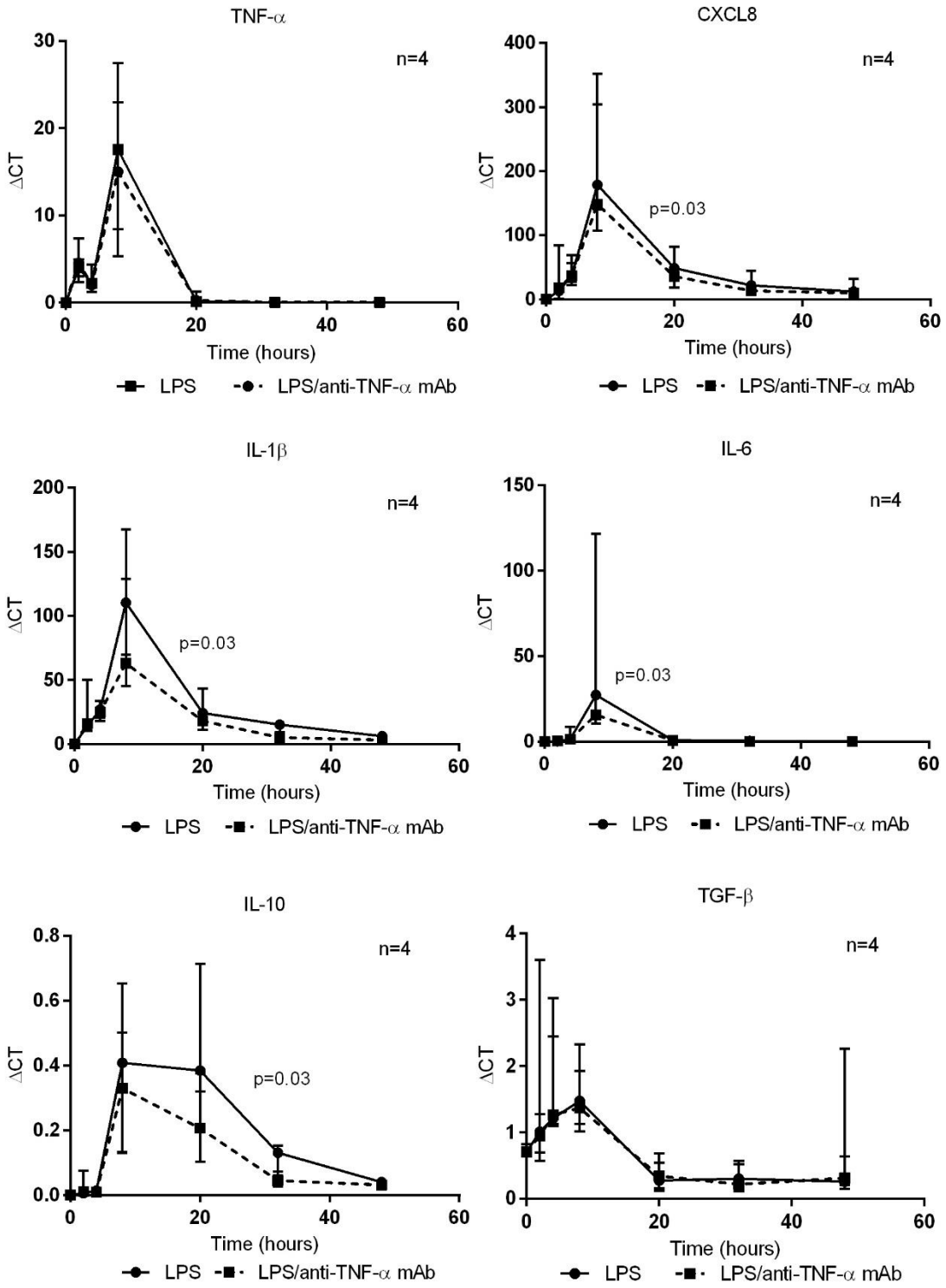

	TNF-α	**CXCL8**	**IL-1β**	**IL-6**	**IL-10**	**TGF-β**
LPS- median (range) AUC (ΔCT.hours)	**159.34** (85.58-232.56)	**3049.63** (2169.80-3696.88)	**1571.21** (1436.36-1890.55)	**241.73** (120.37-1021.56)	**10.85** (8.28-12.53)	**32.57** (21.28-50.13)
LPS/anti-TNF-α mAb- median (range) AUC (ΔCT.hours)	**152.11** (54.26-197.02)	**2247.92** (1678.88-2988.08)	**940.22** (885.30-1394.20)	**144.08** (92.66-234.90)	**5.78** (3.84-9.64)	**29.09** (18.40-48.81)
One-tailed p-values		p=0.03	p=0.03	p=0.03	p=0.03	

Each figure illustrates a time course experiment showing cytokine mRNA expression by monocytes stimulated with LPS, in the presence or absence of the TNF-α mAb. Data points are expressed as median (range). AUC was calculated for each subject's time course profiles and the two values compared using the Wilcoxon Signed Rank Test as shown in the table**.** P-values are one-tailed.

To confirm that TNF-α blockade would also influence the secreted protein, the concentration of one of the cytokines, CXCL8, was determined in the cell-free supernatants at each time point by ELISA (each condition was run in duplicate). This is illustrated in figure 5.10. Significantly less CXCL8 was secreted in the presence of TNF-α mAb, however the absolute differences were small.

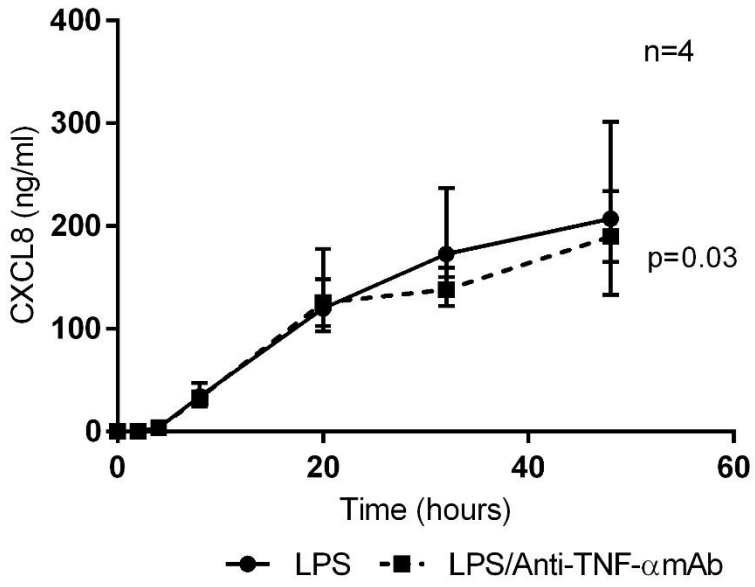

Figure 5-10 Effect of TNF-α mAb on CXCL8 in the cell-free supernatant of LPS-stimulated monocytes.

The figure illustrates a time course experiment showing CXCL8 protein secreted by monocytes stimulated with LPS, in the presence or absence of TNF-α mAb. Data points are expressed as median (range). AUC was calculated for each subject's time course profiles and AUC values compared using the Wilcoxon Signed Rank Test**.** P-values are one-tailed. A significantly lower AUC value in the presence of TNF-α mAb was observed (5222.21 ng.hour.ml^{-1} versus 5771.49 ng.hour.ml^{-1} ;one tailed p=0.03).

5.2.4 TNF-α induced pro-inflammatory cytokine expression may be induced via TNFR1 and anti-inflammatory cytokine expression via both TNFR1 and TNFR2

To determine the role of individual TNF-α receptors following autocrine binding of TNF-α, monocytes from 7 subjects (0.25 million cells per well) were cultured for 20 hours following stimulation with 100 ng/ml of LPS in the presence or absence of 10 μg/ml of TNF-α R1 mAb or TNF-α R2 mAb or both. Figure 5.11 shows that significant reductions in expression of IL-1β and *IL-10* mRNA were observed when both receptors were blocked. A trend was observed across all the cytokines (with the exception of TNF-α) for TNFR1 blockade to reduce cytokine mRNA expression. For IL-1β and IL-10 this fell just short of reaching statistical significance (both p=0.05). A trend was also observed for TNFR2 blockade to reduce *IL-10* mRNA expression (p=0.09). This suggests but does not prove that TNF-α induced pro-inflammatory cytokine expression may be induced via TNFR1 and anti-inflammatory cytokine expression via both TNFR1 and TNFR2. As expected from the studies using TNF-α blockade with a TNF-α mAb (figure 5.9), there was also no significant effect of blocking either receptor on *TNF-α* mRNA in this experimental system.

Figure 5-11 Effect of selective TNF-α receptor blockade on cytokine mRNA expression

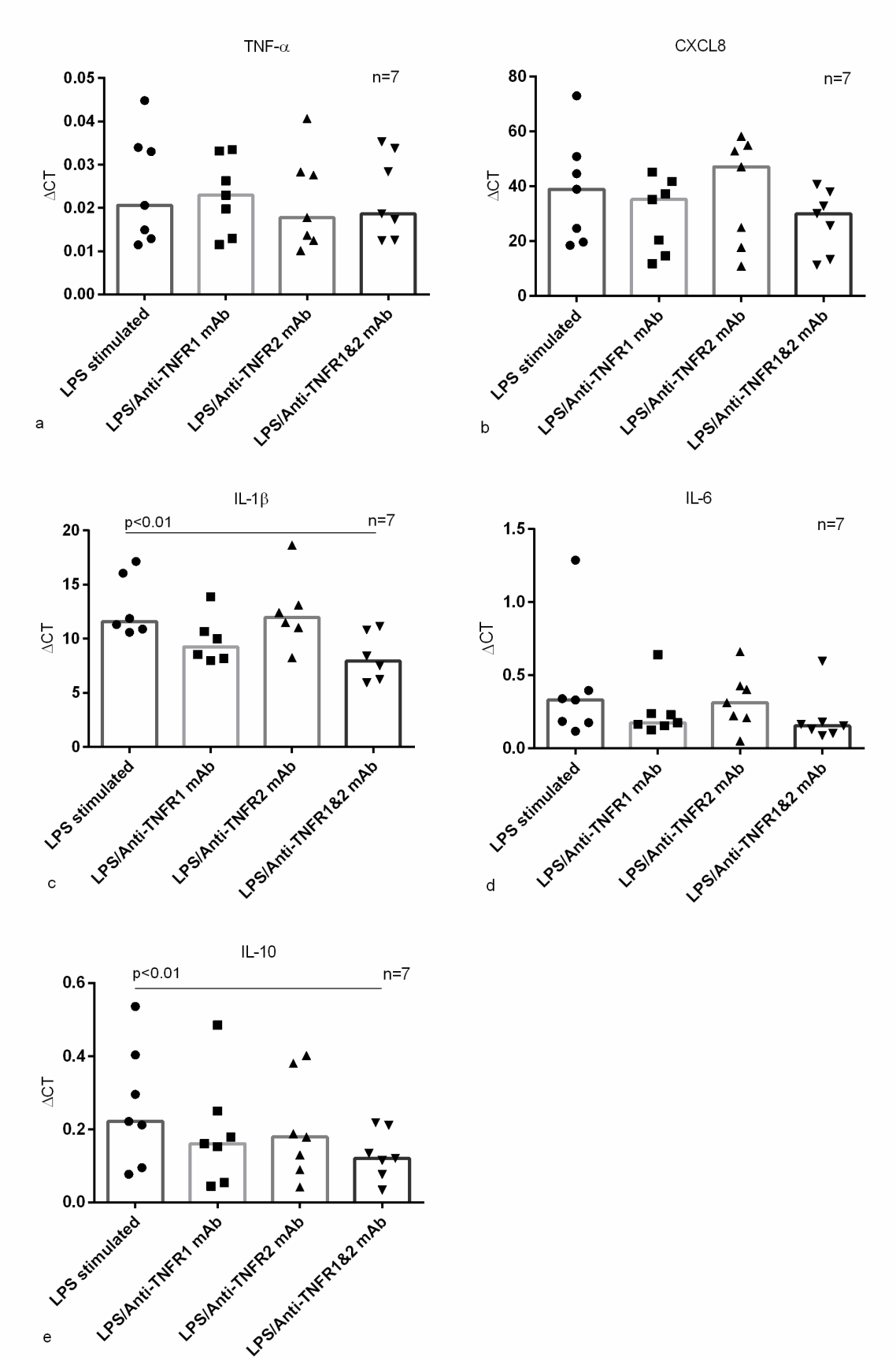

Monocytes were stimulated with LPS (positive control) for 20 hours, alone or in the presence of TNFR1 or TNFR2 mAb or both, and cytokine mRNA expression measured. Each experimental condition shows individual data points with median values shown as bars. Overall differences between experimental conditions for each cytokine were assessed with a Friedman's test and post hoc pairwise comparisons with the positive control conducted if appropriate (unadjusted p-values were first corrected by multiplying by 3 and are shown on the figures where significant) a) TNF-α: Friedman's test non-significant b) CXCL8: Friedman's test $p=0.03$. c) IL-1β: Friedman's test $p<0.01$ d) IL-6: Friedman's test non-significant e) IL-10: Friedman's test $p<0.01$.

5.2.5 TNFR1 and TNFR2 surface expression on monocytes and in response to LPS

Next the expression of TNFR1 and TNFR2 was examined on the monocyte surface. Flow cytometry was conducted as described in 2.8. Fluorescence spillover was detected in both band pass filters. 13.4% and 3.7% of signal was deducted from the PE (TNFR1) filter and the FITC (TNFR2) filter respectively to compensate for spillover into these channels.

Figure 5.12 shows the distribution of the pattern of receptor expression on freshly isolated monocytes (time zero) and monocytes stimulated with LPS for 22 hours. Monocytes differed in their cell surface expression of the receptors, some expressing TNFR1 alone, TNFR2 alone, both receptors, or neither receptor. Experimental conditions were conducted in duplicate from time 3 onwards. Unfortunately because of intersubject variation encountered in the number of monocytes isolated from the same extracted volumes of blood, four subjects whose samples were taken on the same day did not have enough monocytes to conduct each time point in duplicate. A decision was reached to run time zero experiments (in which the issue of cell loss due to apoptosis reducing viable gated events would not be an issue) only once in order that later time points could be conducted in duplicate. Example overlay histograms are shown in figure 5.13.

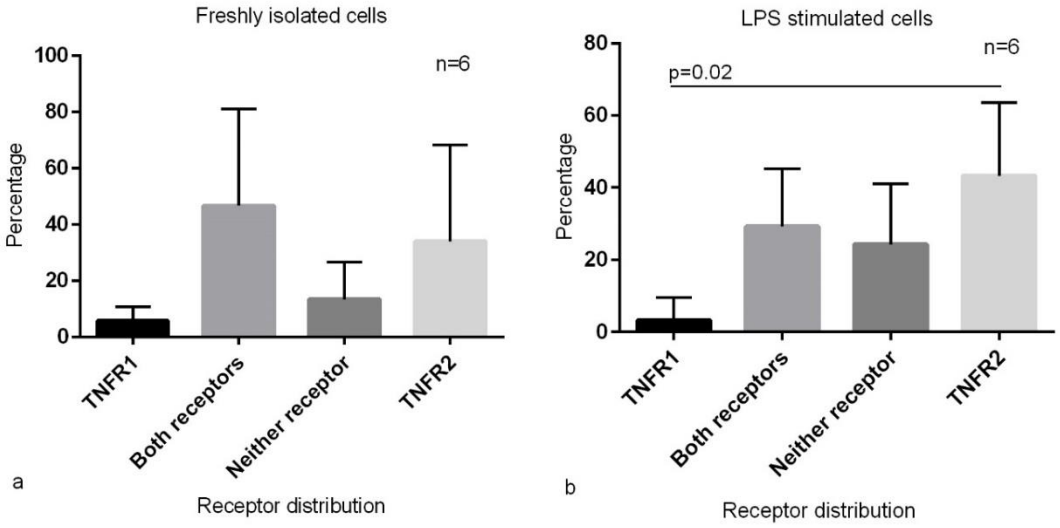

Freshly isolated monocytes	**TNFR1 only (%)**	**Both receptors (%)**	**Neither receptor (%)**	**TNFR2 only (%)**
Subject one	0	1	22	76
Subject two	9	45	36	10
Subject three	1	20	7	72
Subject four	4	42	12	42
Subject five	6	87	3	4
Subject six	14	84	1	1

Figure 5-12 Pattern of TNF-α receptor expression on monocytes

Each column shows the mean percentage of monocytes (with SD bars) expressing each of the four possible cell surface receptor combinations from 6 subjects. Differences between experimental conditions for each cytokine were assessed with a Friedman's test and post hoc pairwise comparisons conducted if appropriate (a Dunn-Bonferroni correction was applied to unadjusted p-values). Significant differences are shown as horizontal lines. a) Freshly isolated unstimulated monocytes. Friedman's test non-significant (p=0.09). b) Monocytes stimulated for 22 hours with LPS. Friedman's test p=0.02. The table shows the raw data for freshly isolated monocytes for each of the six subjects.

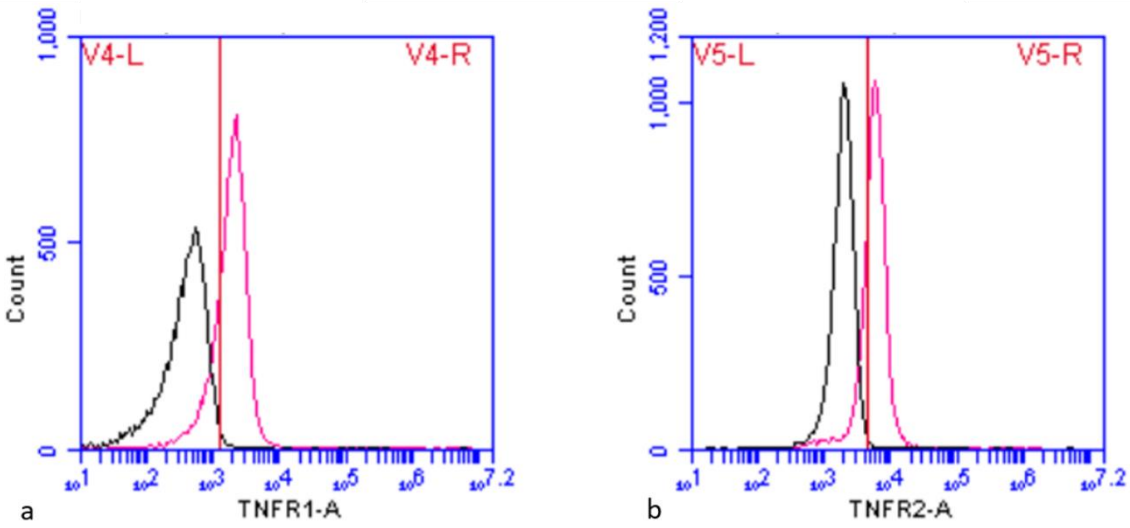

Figure 5-13 TNF-α receptor expression on freshly isolated monocytes- an example of overlay histograms

Overlay histograms are shown for gated monocytes from one subject. a) Two histograms are shown with fluorescence intensity in the PE channel on the x-axis (logarithmic scale) and cell count on the y-axis. The black histogram represents monocytes incubated with a PE-labelled isotype control antibody. The pink histogram represents monocytes labelled with PE-TNFR1 mAb. b) The black histogram represents monocytes incubated with a FITC-labelled isotype control antibody. The pink histogram represents monocytes labelled with FITC-TNFR2 mAb. Red vertical markers are shown on both figures to delineate fluorescence due to specific binding of mAbs to the cell surface receptor of interest (to the right of the set marker) from that due to non-specific binding of flow cytometry antibodies and autofluorescence (to the left of the marker).

Next the expression of TNFR1 and TNFR2 on LPS-stimulated monocytes was examined over time. MFI results are expressed as a ratio of the positively labelled monocytes to the MFI of monocyte samples incubated with the immunoglobulin isotype control Ab. Figure 5.14 shows that TNFR1 expression reduced by 6 hours post LPS stimulation with a trend for a subsequent increase by 22 hours post stimulation back to baseline expression. No post-hoc significant differences in TNFR2 expression were observed over time when comparing with time zero, although there was a trend for expression to increase by 22 hours post stimulation. Example quadrant dot plots and overlay histograms are shown in figure 5.15.

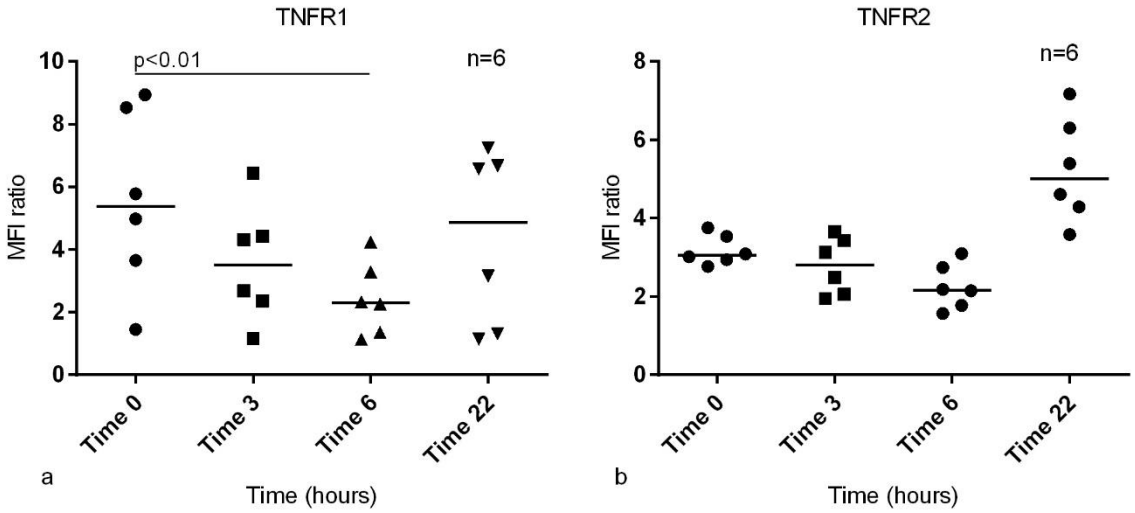

Figure 5-14 Changes to TNF-α receptor cell surface expression over time

Each time-point shows individual subjects' MFI ratios, of the MFI of monocytes labelled with TNFR1/TNFR2 flow cytometry mAbs to the MFI of monocytes labelled with isotype control Ab. Median values are displayed as horizontal lines. Differences between time-points were assessed with a Friedman's test with post hoc pairwise comparisons as appropriate, comparing to time 0 (unadjusted p-values were first corrected by multiplying by 3 and are shown on the figure where significant). a) TNFR1 expression: Friedman's test ($p<0.01$) b) TNFR2 expression: Friedman's test ($p<0.01$).

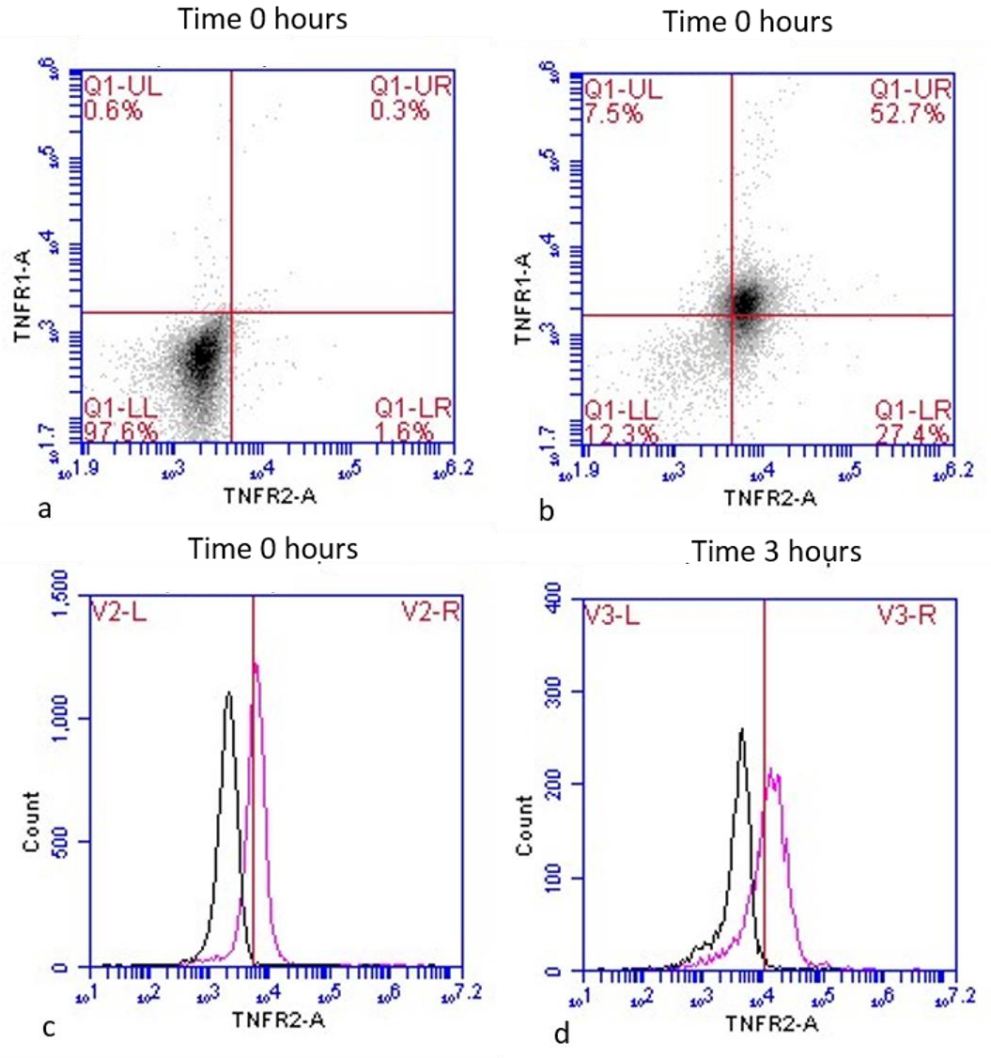

Figure 5-15 Changes to TNF-α receptor cell surface expression over time- an example of quadrant plots and overlay histograms

An example quadrant dot plot and overlay histograms are shown for gated monocytes from one subject. a) The dot plot illustrates freshly isolated (time 0) monocytes incubated with an isotype control flow cytometry Ab. A quadrant gate is set from these cells as shown by the red markers. b) The dot plot shows the percentage breakdown of freshly isolated monocytes by TNFR1 and TNFR2 status: TNFR1 only (upper left quadrant), TNFR2 only (lower right quadrant), both receptors (upper right quadrant) and neither receptor (lower left quadrant). c) Two histograms are shown, with fluorescence intensity in the FITC channel on the x-axis (logarithmic scale) and cell count on the y-axis. The black histogram represents freshly isolated monocytes incubated with a FITC-labelled isotype control Ab. The pink histogram represents monocytes labelled with FITC-TNFR2 mAb. d) The black histogram represents monocytes which had been stimulated for 3 hours with LPS, incubated with a FITC-labelled isotype control Ab. The pink histogram represents monocytes labelled with FITC-TNFR2 mAb. Red vertical markers are shown on both figures to delineate fluorescence due to specific binding of mAbs to the cell surface receptor of interest (to the right of the set marker) from

that due to non-specific binding of flow cytometry antibodies and autofluorescence (to the left of the marker). Note the slight shift in fluorescence of control Ab labelled cells to the right (comparing black histograms in c and d) suggesting greater non-specific binding occurring at this later time-point, which illustrates the importance of presenting MFI ratios.

5.2.6 The autocrine effect of TNF-α on cell surface TNFR1 and TNFR2

Further experiments investigated the hypothesis that changes to TNFR1 and/or TNFR2 expression over time were in part mediated by autocrine feedback loops. Monocytes from 6 subjects (0.25 million cells per condition, in duplicate) were stimulated with LPS for 20 hours with and without an excess of TNF-α mAb (to attempt to ensure that all sTNF-α and mTNF-α was blocked). Twenty five μg/ml of TNF-α mAb was used. Figure 5.16 shows that blockade of sTNF-α/mTNF-α led to a trend for a decrease in the expression per cell of TNFR1 (non-significant p=0.05). A trend for reduction was also observed if TNFR2 specifically was blocked rather than the TNF-α molecule itself (non-significant p=0.05), suggesting that TNFR1 expression is in part driven by TNF-α signalling via TNFR2. Conversely, a slight increase in TNFR2 expression was observed when TNF-α was blocked (median MFI ratio 7.41, range 4.05 to 10.26 compared to 7.70, range 4.82 to 11.54; p=0.03). No difference was observed when TNFR1 was blocked rather than the TNF-α molecule itself. Figure 5.17 shows an example of flow cytometry histograms from one subject.

Figure 5-16 Effect of TNF-α blockade on TNF-α receptor cell surface expression

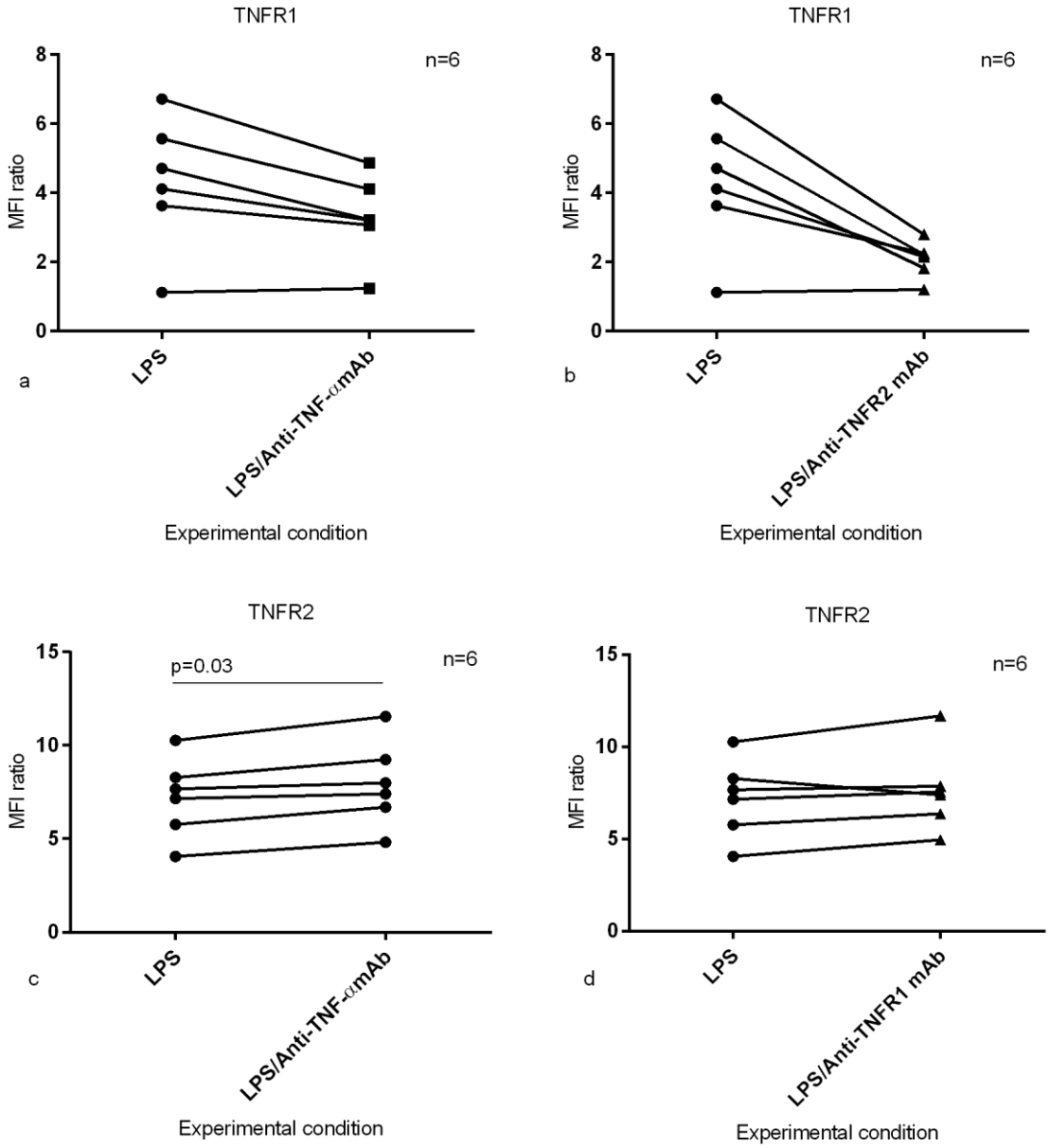

TNFR1 median MFI ratio (range)	**LPS**	**LPS and anti-TNF-α mAb**	**LPS and anti-TNFR2 mAb**	**P value**
	4.41 (1.12-6.72)	3.22 (1.24- 4.86)		p=0.05 (non-significant)
	4.41 (1.12-6.72)		2.18 (1.20-2.80)	p=0.05 (non-significant)
TNFR2 median MFI ratio (range)	**LPS**	**LPS and anti-TNF-α mAb**	**LPS and anti-TNFR1 mAb**	**P value**
	7.41 (4.05- 10.26)	7.70 (4.82- 11.54)		p=0.03
	7.41 (4.05- 10.26)		7.47 (4.95- 11.68)	p=0.17 (non-significant)

Each figure shows individual subjects' paired MFI ratios (of the MFI of positively labelled samples to the MFI of cells labelled with isotype control flow cytometry Ab). Differences between LPS stimulated cells and other experimental conditions were assessed using a Wilcoxon Signed ranks test. Significant differences are shown with horizontal lines. a) The effect of global TNF-α blockade on TNFR1 expression. b) The effect of selective TNFR2 blockade on TNFR1 expression. c) The effect of global TNF-α blockade on TNFR2 expression. d) The effect of selective TNFR1 blockade on TNFR2 expression. Monocytes were stimulated for 20 hours. Median and range values are supplied in the table.

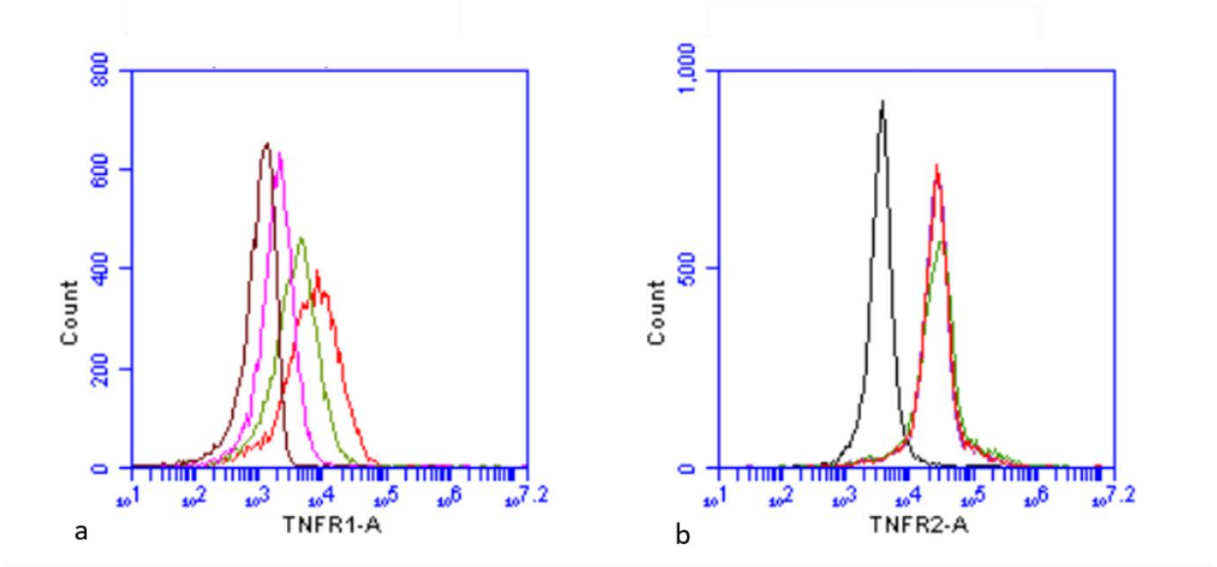

Figure 5-17 Effect of TNF-α blockade on TNF-α receptor cell surface expression- an example of overlay histograms

Overlay histograms are shown for gated monocytes from one subject. a) Four histograms are shown, with fluorescence intensity in the PE channel on the x-axis (logarithmic scale) and cell count on the y-axis. The black histogram represents LPS-stimulated monocytes incubated with a PE-labelled isotype control Ab. The red histogram represents monocytes stimulated with LPS and labelled with PE-TNFR1 mAb. Green and pink histograms represent LPS-stimulated monocytes incubated in the presence of TNF-α mAb or TNFR2 mAb respectively and then labelled with PE-TNFR1 mAb. b) Four histograms are shown, with fluorescence intensity in the FITC channel on the x-axis and cell count on the y-axis. The black histogram represents LPS-stimulated monocytes incubated with a FITC-labelled isotype control antibody. The red histogram represents monocytes stimulated with LPS and labelled with FITC-TNFR2 mAb. Green and pink histograms represent LPS-stimulated monocytes incubated in the presence of TNF-α mAb or TNFR1 mAb respectively and then labelled with FITC-TNFR2 mAb (in this example none of the experimental conditions had an effect on TNFR2 expression). Each of the three experimental conditions were conducted alongside samples subjected to the same conditions but incubated with an isotype control flow cytometry antibody. As all isotype control histograms overlaid each other only one of three is shown in each figure for ease of visualisation.

Next it was determined if the addition of a TNF-α mAb to LPS-stimulated monocytes had any effect on the concentration of soluble TNFR1 or TNFR2, in particular to investigate whether the reduction in cell surface TNFR1 was due to increased shedding of the receptor into the peri-cellular environment, rather than an alternative mechanism such as decreased intra-

cellular manufacture and expression at the cell surface. The cell free supernatants from previously outlined experiments whereby monocytes were stimulated with LPS with and without a TNF-α mAb present for 22 hours were harvested to detect any TNFR1/TNFR2 shedding, using ELISAs able to detect both free and TNF-α-bound receptors. Blockade of TNF-α using TNF-α mAb showed trends only for a small increase in soluble TNFR1 and TNFR2 in the supernatant (figure 5.18).

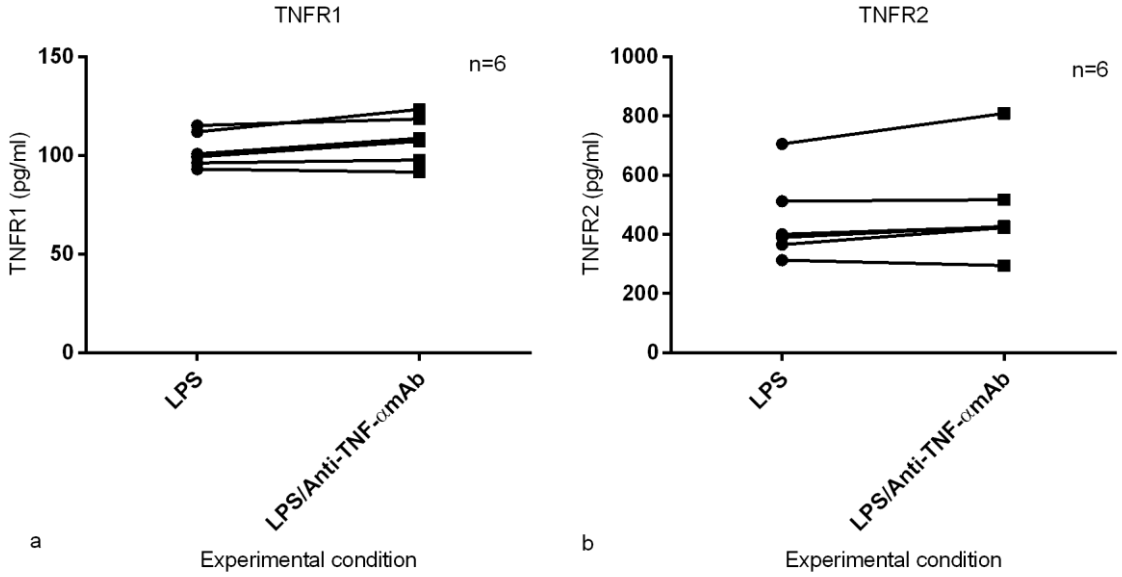

	LPS	**LPS and TNF-α mAb**	**P-values**
Soluble TNFR1 (pg/ml)	100.08 (93.11- 115.16)	107.95 (91.58- 118.43)	p=0.05 (non-significant)
Soluble TNFR2 (pg/ml)	395.16 (313.16- 705.58)	426.20 (294.24- 809.11)	p=0.08 (non-significant)

Figure 5-18 Effect of TNF-α blockade on the concentration of soluble TNFR1 and TNFR2 in the supernatant of LPS-stimulated monocytes

The figures show paired data for each subject. Differences between LPS stimulated monocytes and monocytes co-incubated with TNF-α mAb were assessed using a Wilcoxon Signed Ranks test. Median and range values are shown in the table. Monocytes were stimulated for 22 hours.

5.3 **Discussion**

Although it is well recognised that TNF-α can signal in an autocrine fashion (3, 166, 302), relatively little is known about the autocrine effect of this cytokine specifically on its major source, monocytes. The studies in this chapter provide evidence to support some of the stated hypotheses and further understanding of TNF-α autocrine feedback loops and the roles of TNR1 and TNFR2 in human monocytes.

Firstly, time course experiments were conducted to determine if LPS was an appropriate stimulant of a number of pro-and anti-inflammatory cytokines. All cytokines, with the exception of TGF-β were up-regulated by LPS stimulation compared to monocytes cultured in the absence of an exogenous stimulus (figures 5.1 to 5.6). Blockade of secreted and membrane bound TNF-α in this LPS model led to significant reductions in the mRNA output over time of CXCL8, IL-1β, IL-6, and IL-10 (figure 5.9) as hypothesised (hypothesis one). The degree of reduction varied between cytokines, for example only a slight reduction was observed for CXCL8. The clinical significance of the degree of reduction and whether this variation was stimulus specific is unknown. A statistically significant reduction in CXCL8 protein concentration supported the hypothesis that reduction in cytokine production as a result of prevention of TNF-α autocrine binding translated through to the protein level (figure 5.10).

The second hypothesis that TNF-α autocrine feedback loops in monocytes occur via TNFR1 for pro-inflammatory cytokine production and via TNFR2 for anti-inflammatory cytokine production was not found to be true (figure 5.11). Trends for reduction in the pro-inflammatory cytokines IL-1β, CXCL8 and IL-6 and anti-inflammatory IL-10 when TNFR1 alone was blocked were observed but did not reach statistical significance. A trend for reduction in IL-10 when TNFR2 alone was blocked and for additive reduction in the face of

dual receptor blockade suggests that IL-10 pathways are switched on by TNF-α activating either of its receptors, in contrast to the other cytokines. This requires further study with a larger sample size. That IL-10 was also produced by monocytes in response to LPS as previously shown (303), with an additional positive feedback effect of TNF-α on *IL-10* mRNA expression is in keeping with data from previous studies in monocyte/monocyte-derived cells (222, 224, 302) and human and animal studies (266, 304). This illustrates the inherent complexity of the feedback loops of many cytokines as IL-10 itself plays a role in down regulating TNF-α (223, 305). If in repeat experiments IL-10 is shown to be up-regulated by both TNFR1 and TNFR2 this could have important clinical implications as IL-10 is a key immunoregulatory cytokine with anti-inflammatory effects in many diseases (306). Monocytes, in particular the dominant CD14+ CD16- monocyte and other cells of the monocyte lineage, are a major source of IL-10 (307). By blocking the TNF-α molecule itself, some autocrine up-regulation of IL-10 as result of TNF-α binding might be lost, disrupting the pro-inflammatory/anti-inflammatory balance. Thus selective blockade of TNFR1 in a clinical setting could ameliorate the pro-inflammatory effects of TNF-α, whilst allowing on-going synergistic effects of the predominantly anti-inflammatory IL-10. This might be especially relevant in diseases in which monocytes and/or macrophages play an important role, for example, inflammatory arthropathies, psoriasis, IBD and multiple sclerosis (308-312).

An experiment was conducted to investigate the third hypothesis that the decrease in measurable sTNF-α over time in the supernatant of LPS-stimulated monocytes was due to autocrine binding to its receptors. This confirmed that blockade of TNFR2 led to a large increase in detectable sTNF-α as hypothesised (figure 5.7). The role of this possible extensive sTNF-α binding to TNFR2 is uncertain as only mTNF-α activates TNFR2 (165, 167). It is possible that the TNF-α-TNFR2 complex is internalised as shown previously (313) and the

cytokine degraded. This concept requires further study as the current experiments studied monocytes in isolation and hence did not assess competition for TNFR1 on other cell types.

Alternative explanations for the rise in sTNF-α are also possible. For example, by blocking the receptor the TNFR2 mAb may have prevented mTNF-α from inducing intra-cellular signalling pathways that switch off further TNF-α production and/or secretion into the supernatant. As a result sTNF-α would be detected at higher concentration in the supernatant. In isolation this hypothesis does not explain why in figure 5.7 sTNF-α is observed to decrease with time rather than reach a plateau. A second explanation, such as protein degradation within the CM would also have to occur. In addition, the data presented in figure 5.11a do not support the hypothesis that mTNF-α acting via TNFR2 down-regulates further *TNF-α* mRNA production as blockade of TNFR2 had no significant effect on *TNF-α* mRNA expression. However, it remains theoretically possible that mTNF-α signalling via TNFR2 could negatively affect later steps in TNF-α production, such as translation, post-translational modification or cleavage from the cell surface membrane, and therefore blockade of TNFR2 would lead to a rise in detectable sTNF-α. It must also be considered that the apoptotic monocytes present might be responsible for the reduction in sTNF-α over time, for example, if TNFR1 or TNFR2 increased at the cell surface during early apoptosis this might provide enhanced sTNF-α clearance from the supernatant. If TNF-α signalling via TNFR2 increased monocyte apoptosis then blocking this receptor could explain the increase in sTNF-α in the supernatant (figure 5.7) as reduced apoptosis of monocytes would occur. This seems an unlikely explanation though as Dreschers *et al* have recently shown that TNF-α driven monocyte apoptosis occurs specifically via TNFR1 ligation and endocytosis, rather than TNFR2 (289).

The final hypothesis in this chapter concerned the cell surface expression of TNFR1 and TNFR2, specifically that TNF-α autocrine feedback loops would influence their expression. The alternative hypothesis was only met in part. Figure 5.12 and the table of raw data provided show that there was a large intersubject variation in receptor expression pattern in freshly isolated (and LPS-stimulated) monocytes. This made showing a statistically significant difference in expression pattern difficult with a sample size of six. Certainly there was a trend for the least frequent phenotype to be that of monocytes expressing TNFR1 only. Figure 5.14a showed that the density of TNFR1 receptors per monocyte (as expressed by suurogate marker MFI ratio) decreased over the first 6 hours with a trend for a subsequent increase by 22 hours post LPS stimulation. This decrease may be due to internalisation of the TNF-α-TNFR1 complex that has been shown to occur in monocytes infected with bacteria (289) rather than a decrease in production of the receptor. Although no statistically significant comparisons with time 0 were observed, the density of TNFR2 receptors per monocyte showed a trend to increase by 22 hours (figure 5.14b).

To determine if TNF-α autocrine feedback loops were involved in influencing expression density of either receptor, LPS-stimulated monocytes were incubated with TNF-α mAb or a mAb to TNFR1 or TNFR2. Subsequent comparison of receptor expression was determined and showed a trend for blockade of the TNF-α molecule itself to reduce TNFR1 expression by 27% and selective TNFR2 blockade by 51% (figure 5.16). This supports but does not prove the hypothesis that TNF-α autocrine feedback loops contribute to some of the expression of TNFR1 at the monocyte surface in LPS-stimulated cells and that this occurs via TNFR2 activation. Given the trend for greater reduction in TNFR1 expression when TNFR2 only is blocked one can hypothesise further that autocrine feedback via TNFR1 may either down-regulate its own production or perhaps lead to greater internalisation of TNF-α-TNFR1

complexes with resultant decrease in cell surface expression. This would require further study. A 4% increase in TNFR2 expression was observed when TNF-α was blocked but the clinical significance of this is unknown (figure 5.16). Similarly, the trend observed of a slight increase in sTNFR1 in the supernatant of LPS stimulated monocytes incubated with TNF-α mAb (figure 5.18) is unlikely to reflect an autocrine feedback loop preventing TNFR1 cleavage, at least not enough to explain the 51% reduction in surface TNFR1 when TNF-α autocrine binding to TNFR2 was prevented. Therefore, it remains more likely that TNF-α autocrine feedback via TNFR2 leads to greater production of TNFR1 or expression of it at the cell surface. However, this experiment was limited by being able to measure sTNFR1 and TNFR2 at one time-point only rather than as part of a time-course profile.

The results presented in this chapter support other authors' work regarding the function of both receptors. Both TNF-α receptors have high affinity for sTNF-α (164). Dissociation of TNF-α from TNFR1 is far slower than from TNFR2 and thus it had been assumed that most downstream effects occurred through the stable TNF-α-TNFR1 complex. TNFR2 has high "on-off" kinetics with the ligand moving on and off the receptor repeatedly due to its reasonable affinity and fast dissociation rates (163, 164). It was initially suggested that the purpose of the high on-off kinetics of TNFR2 was to create a peri-cellular environment in which soluble TNF-α is abundant at the cell surface and hence more readily available to bind to TNFR1, mediating downstream effects (ligand-passing) (163, 168). The data presented here argues against this and agrees with other authors (164, 169), as selective TNFR2 blockade did not down-regulate IL-1β, CXCL8 or *IL-6* mRNA expression (figure 5.11), which would be expected were sTNF-α ligand-passing by TNFR2 necessary for activation of TNFR1 pathways. The current experiments cannot differentiate TNFR1 pathway activation

due to mTNF-α from that due to sTNF-α binding, but sTNF-α is believed to be the main activator of TNFR1 (165, 167).

Taken together, the studies presented here suggest that TNF-α autocrine feedback loops occur in monocytes and that pro-inflammatory cytokine up-regulation occurs via TNFR1 with both receptors allowing up-regulation of IL-10. In addition TNF-α autocrine feedback loops likely drive some of the expression of TNFR1 at the monocyte surface and this occurs via TNFR2 autocrine feedback. Lastly, the studies suggest that much of the TNF-α secreted into the CM may bind back to the monocyte surface, via TNFR2. This may reflect a previously unrecognised homeostatic mechanism for clearing TNF-α from the peri-cellular environment as sTNF-α is not thought to activate intra-cellular signalling pathways (165). However, the presented data must be interpreted with caution due to a number of experimental limitations and the need for future experiments to verify these findings and/or eliminate alternative explanations. Strengths and limitations of the studies are considered further below and areas for future study are considered in detail in chapter 6.

There are some limitations to the studies. For example, many of the experiments were conducted with insufficient control arms. Specifically, all experiments involving TNF-α or TNFR1/2 mAbs should have been run with an additional condition whereby the cells were exposed to the same experimental conditions but the mAb replaced with a matched isotype control at the same concentration (e.g. an IgG1 irrelevant antibody should be used alongside an IgG1 mAb binding TNF-α). This would rule out any effect of the mAb unrelated to its specific ligand binding effect, for example binding of the antibody to the monocyte Fc receptors via its Fc region. Although an early experiment (figure 3.7) had shown that an isotype control Ab did not reduce TNF-α induced CXCL8 secretion, compared to the presence of a TNF-α mAb, it would still be vital in future studies to include this negative control in

each experiment. The experiment in which TNFR1 and TNFR2 expression was considered over time in response to LPS (figure 5.14) should have had a negative control using CM without LPS, as without an unstimulated control arm to the experiment it is impossible to conclude that any effects observed are due to LPS rather than other factors within the culture process. This experiment would also have benefitted from the addition of further time-points between 6 and 22 hours. With respect to flow cytometry it would be optimal in future to purchase matched mAbs and isotype controls from a supplier that ensures the fluorophore to protein ratio are equal for both (and provides information on this). If the fluorophore to protein ratios vary then calculated MFI ratios may be erroneous.

A further limitation in this chapter was the small sample sizes. Whilst trends were observed many results did not reach statistical significance and clearly greater numbers of subjects should be studied in future to determine if these trends were genuine, particularly where multiple comparisons were taking place with subsequent correction to p-values. Whilst corrections such as the Dunn-Bonferroni correction are important to reduce the incidence of type one statistical errors that can occur through multiple testing they will conversely reduce the power of a study and increase the chance of making a type two error (314). However, the results presented in this thesis can be considered preliminary and useful in powering future studies.

Several limitations must be considered with respect to the accuracy of the flow cytometry data showing the proportions of monocytes bearing each combination of TNF-α receptor (figure 5.12). Although it was possible to collect 10000 gated events for monocytes which had just been isolated, there was noted to be a considerable intersubject variation in the breakdown of expression patterns, and most commonly (but not always) it was cells expressing TNFR1 or neither receptor which fell into the category of rare events, in some cases making up only 0.1

to 5% of total monocytes in the gate. Expert opinion suggests that to obtain a CV% of 5% for positive events occurring with a frequency of only 1 in 20 it is necessary to collect 8000 events, for 1 in 100, 40000 events and for 1 in 1000, 400000 events (315). It was not feasible to attempt to gate more than 10000 monocytes in the current study as even with freshly isolated cells it would require a considerable extra volume of blood to be taken from each subject. In addition, as previously discussed there was a notable loss in viable cells over time, the degree of which varied between subjects. This made the time taken to run each sample through the flow cytometer quite lengthy as the apoptosed cells, apoptotic bodies and debris had to be counted as well, before finally gating over the viable population of monocytes. To achieve 40000 viable monocyte events would therefore require large volumes of blood and time. The fastest flow cytometers (not available in our laboratory) can now process up to 100,000 events per second, so should this equipment be available it would be useful to focus on this area of differential receptor expression patterns in more detail and repeat all experiments with more cells.

CD14+CD16- monocytes were chosen to be studied in isolation as the CD14+CD16- subset constitutes 90% of total circulating monocytes, is capable of producing TNF-α and is also the subset that produces the greatest quantity of IL-10 (204). Results presented in chapter 3 showed that the cell isolates may have been contaminated with CD14+CD16+ monocytes, which may or may not have been activated by bound anti-CD16 mAbs during the extraction process or alternatively some monocytes may have actually become CD16+. How this would affect the results is unknown as functional differences between monocyte subsets is currently an emerging research field. In redesigning these experiments it would be preferable to extract monocytes from whole blood using a flow cytometry cell sorter. This would allow a quicker

extraction process and permit the monocytes to be subdivided based upon CD14 and CD16 status.

Previous authors studying the respective roles of the two receptors in monocytes have been limited by the use of exogenous sTNF-α which can bind but not fully activate TNFR2 (165). Alternatively they have used mutant forms of TNF-α which can activate TNFR2 and/or commercially available cell lines where mTNF-α has been over-expressed (165, 316, 317). Whilst useful, these models may not bear close resemblance to the events occurring with naturally occurring mTNF-α. In the present experimental system LPS was used as a potent inducer of TNF-α (318) which overcomes this particular issue, as in order to release sTNF-α, mTNF-α must first be produced, hence providing confidence that activation of receptors could occur through both forms of the cytokine. The same batch of LPS, diluted and stored frozen in aliquots to reduce freeze thaw cycles to one per experiment, was used throughout this thesis as it is recognised that the properties of LPS can vary between bacterial sources and even between separate batches from the same strain (255) and this may introduce error into the results.

The initial experiments demonstrated that the expression of pro-inflammatory cytokines in monocytes was up-regulated by autocrine binding of TNF-α (figure 5.9). No effect of TNF-α autocrine feedback on its own expression was observed, which contrasts with other studies that have shown that exogenous TNF-α can induce TNF-α gene transcription (217, 221). This may be one drawback of using LPS as a stimulant. As LPS is known to have wide ranging effects (296) it is possible that this observed lack of effect (and that in TGF-β expression also) is because other pathways activated by LPS ligation switch off TNF-α signalling after time, preventing further up-regulation by autocrine binding of secreted TNF-α. Despite this

accepted limitation, it is clear using the current model that TNF-α was having a number of autocrine effects on monocytes.

It was common at later time-points, particularly in monocytes incubated in CM without LPS for varying proportions of the cells to be undergoing early or late stage apoptosis (as has been shown in other studies (319, 320)). The presence of apoptotic monocytes resulted in a number of technical issues, principally reduced numbers of viable cells to gate over and longer transit time of samples through the flow cytometer to achieve as many events within the monocyte gate as possible (presumably due to apoptotic bodies increasing the overall numbers of events). What remains unknown is the possible effects of the presence of apoptotic monocytes on the results of the presented experiments. Although generally apoptosis does not induce a pro-inflammatory environment in some cases this can occur. When the surrounding phagocytes (in this case live monocytes) are overwhelmed by the number of apoptotic cells and fail to effectively clear them via phagocytosis a process known as programmed necrosis may occur whereby the apoptotic cell membrane loses its integrity and intracellular contents such as DNA and heat shock proteins are released into the peri-cellular environment (287). These mediators can elicit pro-inflammatory effects. If this was occurring in the LPS-stimulated monocytes and to varying degrees between subjects' samples then these pro-inflammatory mediators may have affected the outcomes obtained by influencing inflammatory pathways within live monocytes. Gating over the area on the forward-side scatter plot that contained debris and monocytes in late apoptosis (to the left of the plot as shown in figure 3.11a) demonstrated that these cells were still binding the TNFR1 and TNFR2 flow cytometry mAbs. As these monocytes were not concurrently labelled with markers of apoptosis one cannot know if monocytes in early or late apoptosis have a higher density of TNFR1 or TNFR2 than live monocytes and if so whether that might play a specific

role in removing sTNF-α from the cell culture supernatant. Lastly, as monocytes themselves act as phagoctyes (290, 291) it is likely that many of the live monocytes were phagocytosing the apoptotic monocytes which may also have activated them and altered their function, influencing the results obtained.

Lastly it must be considered that limited information is available regarding the binding sites and possible effects of the mAbs used in this thesis, both the blocking mAbs and those used to bind TNFR1/2 in flow cytometry experiments. Exact binding sites to the epitopes in question are not characterised and the only information regarding the function of the blocking antibodies is from neutralisation experiments determining the concentration-dependent neutralising effect of the TNF-α and TNFR1/2 mAbs on TNF-α induced cytotoxicity in mouse fibroblasts (direct communication with Dr E. Fioravanti, Scientific Coordinator, R and D Systems, 27th November 2015). Whilst they are marketed for their general neutralising effect it is unknown whether they might inadvertently exert positive effects, for example through reverse signalling via binding to mTNF-α or by acting as partial agonists. Whilst other authors have shown that a soluble TNFR2:Ig receptor construct could induce TNF-α production by binding to mTNF-α and causing reverse signalling (321) the commercial anti-TNF-α mAb used in this thesis is unlikely to have had the same effect as *TNF-α* mRNA expression was unaffected in its presence. In addition, as full characterisation is unknown it is possible that the presence of blocking mAbs bound to their ligand might interfere with subsequent binding of one of the receptor flow cytometry mAbs. For example, it is possible that occupation of a TNFR2 receptor by TNFR2 mAb might impair binding of the TNFR1 flow cytometry mAb to an adjacent TNFR1 receptor. If this were the case then it would be incorrect for example to assume that the reduction in TNFR1 expression in LPS-stimulated monocytes incubated with TNFR2 mAb (figure 5.16) was due to interruption of autocrine feedback via TNFR2. It would

therefore be important to investigate receptor function using other methods to determine the validity of the data, for example using small interfering RNA molecules to knock out receptor expression and function.

5.4 **Conclusions**

In conclusion the studies presented here show that autocrine feedback loops do occur in monocytes and suggest that TNFR1 and TNFR2 have differential roles. Whilst TNFR1 may be the receptor through which pro-inflammatory cytokine production is up-regulated, with TNFR2 playing no role, both receptors may be able to up-regulate the anti-inflammatory cytokine IL-10 with an additive effect. A case for clear delineation into pro versus anti-inflammatory roles for TNFR1 and TNFR2 in monocytes though cannot be made from the current studies as flow cytometry experiments suggested that TNF-α-TNFR2 binding led to up-regulation of TNFR1.

The experiments presented here should be repeated with appropriate power analysis using the current preliminary data to do so, with adequate negative controls and using additional methods to verify findings (discussed in detail in chapter 6). It is generally accepted that in susceptible individuals TNF-α plays a key role in the pathogenesis of a number of chronic inflammatory diseases. TNFR1 is a ubiquitous receptor and as a result its ligation by the TNF-α molecule has widespread pro-inflammatory effects, whereas TNFR2 expression is limited in the main to leukocytes and its function in humans has been less clear. Further studies should assist in clarifying the roles of the two receptors in monocytes and help to determine therefore if selective TNFR1 blockade might be a viable clinical treatment in diseases in which monocytes play a key role.

CHAPTER 6

GENERAL DISCUSSION

6 General Discussion

6.1 Summary of results

The overarching hypothesis of this thesis was firstly that monocytes from A1ATD patients with COPD and the rs361525 TNF-A polymorphism (AG) would produce more TNF-α than monocytes from matched A1ATD patients with COPD and the wildtype allele (GG) and secondly that this increased TNF-α secretion would lead to greater autocrine up-regulation of pro-inflammatory cytokine production in the AG monocytes through an autocrine feedback loop occurring via TNFR1.

The first component of the hypothesis was not found to be true, in fact in LPS-stimulated cells it was monocytes from GG subjects that secreted more TNF-α and CXCL8, although the validity of this finding is called into question when the high intrasubject variability of TNF-α secretion by monocytes over several weeks is considered. The results from these pilot experiments were used in power calculations to determine the numbers of patients that would be needed in repeat experiments to show a genuine difference between the groups, should this exist. The numbers required were prohibitive and as such the second component of the hypothesis was not investigated and further studies focussed on the autocrine effects of TNF-α in monocytes from healthy subjects.

There are many possible explanations for why the primary hypothesis was not met and an overview of these has been considered in chapter 4. However, it is worth considering some of these in greater detail.

Firstly, the process beginning with a gene being transcribed and ending with the secretion of a final protein product is tremendously complex. Whilst the presence of a SNP in the promoter region of the gene may well affect transcriptional regulation of the coding portion of the gene

this might be confounded by the presence or absence of other regulatory steps under different circumstances.

One example of this would be epigenetic processes, which are well recognised to affect TNF-A transcription and post transcriptional modification of mRNA and these vary between cell types and in response to different stimuli. One form of epigenetic regulation which is being increasingly characterised is the effects of non-coding RNA transcripts, transcribed RNA but with no protein coding potential (145). For example, microRNA molecules have been demonstrated to suppress TNF-α output by LPS-stimulated monocytes through binding to complementary RNA in the TNF-α transcript, presumably by adversely affecting transcript stability (322, 323). In a further example of how microRNAs can negatively regulate TNF-α, microRNA-346 has been shown to inhibit Bruton's tyrosine kinase expression in LPS-stimulated THP-1 (monocytic cells) leading to increased tristetraprolin expression, a protein which inhibits TNF-α synthesis through binding to AU rich elements of *TNF-α* mRNA (324). In recent years there has been great interest in another type of non-coding RNA known as long-non coding RNAs (lncRNAs) which are more than 200 nucleotides in length. The full spectrum of mechanism of action of lncRNAs remains to elucidated but a number of authors have shown their repressive or stimulatory function in the control of pro-inflammatory cytokine gene expression in monocytes (325, 326). In monocyte cell lines, stimulated with LPS or PMA, knockdown of characterised lncRNAs upstream of the TNF-A gene led to increased *TNF-α* mRNA output, indicating a repressive function. Furthermore in this instance the transcribed lncRNAs were bound to chromatin and determined to work by binding a well known repressor protein, LRRFIP1, acting together as a complex to repress TNF-A transcription (325). Conversely, knockdown of lncRNA 1992 in stimulated THP-1 macrophages strongly suppressed TNF-α production. The lncRNA was found to increase

TNF-α mRNA output by forming a complex with heterogenous nuclear ribonucleoprotein L which bound to the promoter region of the TNF-A gene to induce expression (327).

These examples and other regulatory steps previously discussed in section 1.8 demonstrate that multiple processes, including epigenetic mechanisms, are involved in the control of TNF-α production and it is likely that a large degree of cell and stimulus specificity and redundancy in these mechanisms exists. As such it is perhaps unsurprising that an association of the rs361525 polymorphism with high TNF-α output was not observed in monocytes from the systemic circulation in response simply to LPS or PMA, as an additional co-factor or epigenetic mechanism may need to be present to act in tandem with any change in transcription factor binding at the TNF-A polymorphism site to increase TNF-α output.

Secondly, the effects of the rs361525 polymorphism may be specific to the airways rather than the systemic circulation and as such the monocyte may not have been the relevant cell to study. Many different cell types in the lungs are capable of secreting TNF-α, for example, macrophages (328), T-cells (144), neutrophils (75), epithelial cells (329) and vascular endothelial cells (78) and the effects of the polymorphism might be specific to one or more of these. Certainly, as monocytes and tissue macrophages are now recognised to have separate developmental pathways (208) it is likely that intra-cellular signalling pathways differ and this might apply to control of TNF-A transcription and hence possibly explain the lack of expected effect of the rs361525 polymorphism in blood monocytes, if its effects are only relevant in lung macrophages. A review of work conducted in human and murine monocytes and macrophages and monocyte/macrophage immortalised human cell lines does consider monocytes and macrophages largely as a single entity with respect to control mechanisms of TNF-A transcription (144, 145), however it is likely that there are differences in TNF-α pathways. For example, Lee *et al* showed that MDMs secreted more TNF-α than monocytes

and that this was partly dependent on epigenetic differences, specifically greater histone acetylation near to the promoter region in the macrophages, allowing transcription factor binding to the TNF-A promoter in a greater number of cells (147). As recent work in murine macrophages has shown, the effect of the rs361525 SNP is potentiated by multiple factors, in this case binding of transcription factors up-regulated by external stimuli but also binding of the thyroid hormone receptor preferentially to the A-allele (128). It is possible therefore that the polymorphism is relevant only in macrophages (or another cell type) in A1ATD subjects where other unknown co-factor molecules are present.

Thirdly, it was the CB phenotype specifically that was shown to be associated with the rs361525 polymorphism by Wood *et al* (125) and it was spontaneous sputum samples from CB patients with and without the polymorphism that were studied by Sapey *et al* (17). It became evident after inital searching for suitable patients that matching individual pairs based on the presence or absence of the CB phenotype as well as other criteria would be difficult given that this is not the predominant phenotype in A1ATD (125). It is possible however that the polymorphism is only relevant within this phenotype of COPD, perhaps due to other interacting biological mediators present only in the CB phenotype which may interact with the polymorphism to affect TNF-α production. Should this be the case then matching would have been inadequate in the current studies.

The second half of this thesis focused on investigating TNF-α autocrine feedback loops in monocytes from healthy subjects and the respective roles of TNFR1 and TNFR2. The studies for the most part were underpowered and hence many results could only be reported as trends. Never-the-less a number of the findings were interesting and warrant further study with greater subject numbers to determine if trends reflect true differences and the current studies

could be used to power these appropriately. In addition other experimental techniques should be used to corroborate the current findings and are described where appropriate.

Whilst the first hypothesis that TNF-α autocrine feedback loops up-regulated the production of a number of cytokines was found to be true, the second, that pro-inflammatory cytokine production occurred via TNFR1 and anti-inflammatory cytokines via TNFR2, was not. As expected blocking TNFR2 had no effect on pro-inflammatory cytokines but there was a trend for reduction in IL-10 output. However, although TNFR1 blockade showed trends for reduction in pro-inflammatory cytokine output, it also demonstrated a trend for reduced IL-10 suggesting that activation of TNFR1 pathways can not be clearly proscribed as having only pro-inflammatory effects.

The third hypothesis that the decrease in measurable sTNF-α over time in the supernatant of cultured monocytes was due to autocrine binding to one or both of its receptors was suggested by the presented studies but not proven, and will require further study. Should this hypothesis be proven it is possible that differential TNF-α receptor expression on the surface of monocytes from A1ATD patients with and without the rs361525 polymorphism might be responsible for the findings in chapter 4. Specifically, should TNFR2 expression be greater on the surface of AG monocytes then any increased sTNF-α secretion may be negated in-vitro by an increase in its clearance from the supernatant by greater numbers of cell-bound TNFR2. Sapey *et al* reported differences in the concentration of TNFR1 in the sputum of AG patients (17) so it is possible that the increased TNF-α output in these patients may be influencing TNFR1 and/or TNFR2 pathways by some mechanism.

The final hypothesis that TNF-α autocrine feedback loops in monocytes played a role in influencing the expression of TNFR1 and TNFR2 was suggested but not proven by the

current studies. TNF-α blockade and selective TNFR2 blockade led to trends for lower TNFR1 expression at the monocyte surface, falling short of statistical significance, suggesting that TNF-α autocrine feedback loops, occurring via TNFR2, positively affect TNFR1 expression.

Taken together these data suggest that the roles of TNFR1 and TNFR2 in monocytes cannot be clearly delineated into pro versus anti-inflammatory roles.

In advancing the work from this thesis it would first be important to optimise current experimental protocols and address the issue of statistical power. Detailed discussion of experimental optimisation has been covered in individual chapters but are considered in brief here.

Firstly, a cell sorting flow cytometer could be used to isolate monocytes, rather than the negative immunoselection bead-based kit used (330). This would be efficient, allow both classical, intermediate and non-classical monocytes to be studied and overcome the issue of possible contamination of isolates with CD14+CD16+ monocytes.

Secondly, all experiments should include appropriate negative controls, for example, the use of isotype control antibodies as a negative control when studying the effect of TNF-α or TNF-α receptor blockade on cytokine output by monocytes. This would control for any effect of binding of the Fc portion of a mAb to Fc receptors on the cell surface rather than that observed from targeted binding by the highly specific antigen binding fragment to an epitope on the cytokine or its receptor.

Thirdly, flow cytometry work could be improved by running each set of cells as a multi-coloured experiment, whereby cells are labelled with CD14, CD16, TNFR1 and TNFR2 mAbs, allowing assessment of TNF-α receptor status to be further considered in the context of

monocyte subtypes. A viability dye should also be included as a marker in each tube to gate out dead cells from analysis.

Finally, the data collected from the current experiments could be used to appropriately power future studies. The power of a study is affected by three factors, the sample size, the magnitude of true difference between the two groups and the SD of the group means (331). Sapey *et al* demonstrated a two log magnitude of difference in TNF-α concentration in the sputum of AG subjects with A1ATD and CB compared to GG subjects (17) but no preliminary data was available from AG and GG monocytes from A1ATD subjects with COPD. The data presented in chapter 4, in conjunction with that from studies of intrasubject variation in TNF-α secretion over a 3 week period by healthy subjects' monocytes can therefore be considered as pilot data, useful in determining the sample size needed to power future studies in AG/GG monocytes. The sample sizes required to repeat these studies are prohibitive in terms of resources and practicality and as such would indicate that further investigation of the rs361525 polymorphism in A1ATD or usual COPD patients should not focus specifically on monocytes. Many of the data presented in chapter 5 from healthy subject monocytes showed trends rather than statistically significant differences and although these trends clearly cannot be assumed to reflect genuine differences the data could be used to perform power calculations to determine necessary sample sizes to show true differences (should these exist) with predetermined power level set at 80%.

6.2 **Future direction of work**

6.2.1 The rs361525 TNF-A polymorphism in A1ATD and COPD

Future studies of A1ATD subjects with the rs361525 polymorphism should focus on cells retrieved from the airways. For example, bronchial epithelial cells and airway macrophages could be harvested bronchoscopically, cultured and stimulated with a variety of stimuli, including pooled airway secretions to simulate in-vivo conditions, in order to investigate if the polymorphism is associated with increased TNF-α production at mRNA and protein level. In addition, cell surface expression of mTNF-α and TNFR1 and TNFR2 could be studied using flow cytometry to determine at which stages in TNF-α processing the polymorphism is most relevant and how increased TNF-α production might affect cell surface expression of its receptors. Other methods could also be employed, such as ChIP assays, whereby cell nuclear material is extracted and undergoes immunoprecipitation to determine if RNA polymerase preferentially binds to the A allele over the G allele. Detailed clinical characterisation of the A1ATD patients with the polymorphism could also be conducted and compared to all GG subjects within the available cohort, given that the difference in BMI between groups noted in Sapey *et al's* work (17) was not observed in the current studies.

A recently published GWAS of several large cohorts of COPD subjects and healthy controls identified six SNPs associated with the presence of either moderate or severe COPD (332). The rs361525 polymorphism was not one of the identified loci, nor it should be noted was any other TNF-A SNP. Whilst this would suggest that this polymorphism is not relevant to usual COPD that may not be the case. Wood *et al* (125) showed that the rs361525 polymorphism was associated with a particular phenotype of A1ATD-related COPD, namely CB, and hence this may explain why it was not detected in GWAS which tend to consider COPD as one homogenous condition. In addition, SNPs causing A1ATD are not shown to be associated

with COPD at all when individuals of all ages are considered as opposed to a younger subset (123), proving the point that considering COPD as one single entity is not ideal.

Whilst A1ATD is a useful model of COPD (333) there is a recognised interaction between A1AT and the TNF-α pathway, meaning that TNF-α may be more pertinent to A1ATD-related COPD than usual COPD. A1AT has been shown to block the action of TACE which is responsible for cleaving mTNF-α to sTNF-α (76), and therefore in A1ATD patients enhanced TACE activity may occur leading to greater TNF-α and TNFR1 secretion by multiple cell types (75, 78). A1AT can also act as a competitor for TNF-α receptors and interrupt TNF-α autocrine feedback loops and hence its relative absence leads to increased TNF-α output from neutrophils (75) and monocytes (77). Given these findings it is probable that TNF-α plays a greater role in the pathogenesis of A1ATD-related COPD than in usual COPD and as such the rs361525 polymorphism, even if truely functional, may be of less relevance in a usual COPD population. Therefore, if the study of this particular polymorphism were to be continued it would be sensible to do this initially in usual COPD which is far more common than A1ATD (333) and thereby establish its relevance, if any, in the airway secretions of patients with the most prevalent form of the disease. It would be of benefit therefore to establish a large regional cohort of usual COPD patients who could be clinically phenotyped, genotyped for presence of the rs361525 polymorphism and take part in clinical and laboratory studies. Such a database is currently being established in the West Midlands to conduct a variety of COPD studies. This would address the logistical difficulties and hence make it more feasible to conduct repeated studies. However, it must also be considered that if the prevalence of the A allele is estimated at approximately 7% (124) (although if functional it may be higher in a COPD population) then it may still be too great a challenge to establish a regional cohort of

usual COPD patients and closely matched controls containing enough subjects with the polymorphism to power the suggested studies.

6.2.2 The differential roles of TNFR1 and TNFR2 in monocytes

A number of the findings from this aspect of the thesis merit further investigation. Firstly, it would be important to replicate and extend the current findings in monocytes or macrophages retrieved from patients with TNF-α associated disease, for example, rheumatoid arthritis or acute lung injury. Secondly, further delineation of the TNFR1 and TNFR2 intracellular signalling pathways in monocytes is also needed. That TNFR2 ligation may be able to induce downstream pathways that initiate IL-10 up-regulation in the absence of any significant up-regulation of pro-inflammatory cytokines, whilst TNFR1 ligation may be able to do both is of great interest. Determining the steps in these pathways might make it possible to interrupt pro-inflammatory downstream cascades whilst leaving IL-10 production switched on. To investigate this, TNFR1 and TNFR2 could be sequentially blocked with a mAb or knocked-down using a small interfering RNA (334) in order to allow TNF-α signalling via one receptor only. To then dissect the intracellular signalling pathways specific to each receptor one could employ increasing concentrations of commercially available inhibitors to a variety of known intra-cellular signalling messengers such as those shown in figures 1.6 and 1.7 and measure the effects on IL-10 and pro-inflammatory cytokine output at the mRNA and protein level using RT-qPCR and ELISA. To support these findings the Western blot technique could be used to demonstrate the presence of specific secondary messengers in their phosphorylated, i.e. activated state, when either TNFR1 or TNFR2 is stimulated. This involves separation of proteins from lysed cells by size using electrophoresis, followed by transfer to a membrane and application of mAbs specific to the proteins of interest (335). In addition, nuclear localisation of specific transcription factors could be determined using immunocytochemistry

whereby a primary mAb binds to the transcription factor of interest and is visualised by microscopy following addition of a secondary mAb conjugated to a fluorophore (329).

Thirdly, further work is needed to clarify the role of TNFR2 on monocytes as the current studies suggest it may play a dual anti- and pro-inflammatory role. Confirmation of the hypothesis that the majority of sTNF-α is being cleared from the pericellular environment via TNFR2 binding should be sought and its clinical relevance explored. Does this same phenomenon occur when monocytes are co-cultured with other cell types, for example epithelial cells or T-lymphocytes? These questions could be addressed by using fluorescence microscopy and fluorescently labelled exogenous sTNF-α with monocytes alone or in co-culture. Furthermore monocytes could be subdivided prior to fluorescence microscopy experiments by TNFR1/TNFR2 expression pattern and/or apoptotic markers, to determine if a particular monocyte group is responsible for sTNF-α clearance.

It would also be important to confirm if the bound sTNF-α is simply being removed or is able to activate TNFR2, which would contradict previously held wisdom that it is only mTNF-α which can stimulate downstream signalling pathways via this receptor (7). This could be determined by comparing IL-10 output from monocytes (with TNFR1 blocked) stimulated with exogenous sTNF-α. Membrane TNF-α signalling could be prevented in one arm of the experiment by addition of a blocking mAb prior to washing and then subsequent addition of exogenous sTNF-α.

Fourthly, changes to the expression of TNFR1 and TNFR2 on the monocyte surface over time, should be further investigated, initially by repeating experiments with greater subject numbers and more monocytes per sample. Dreschers *et al* have shown in monocytes that TNFR1 is down-regulated on monocytes by four hours post infection with *Escherichia coli*

and that this is due to internalisation of the receptor (289). It is possible therefore that the decrease in TNFR1 at the cell surface in LPS stimulated monocytes (as shown in figure 5.14) is also due to internalisation of the receptor complex rather than a down-regulation of the gene encoding the receptor or the translation of its mRNA sequence. However this could be confirmed by performing a time course profile of *TNFR1* mRNA expression and comparing this with time course profiles of cell surface and internal TNFR1 MFI values using flow cytometry on intact and permeabilised monocytes respectively (289). A small interfering RNA molecule could also be used to knock out TNFR2 to clarify if signalling via this receptor up-regulates TNFR1 production and expression.

Finally, it would be important to study the reasons why some isolated monocytes express only one of the TNF-α receptors, both or neither. Could this be related to the presence of both classical and possibly intermediate monocytes, or due to cell maturity or activation state? Of particular interest is whether monocytes which expressed both TNFR1 and TNFR2 differ substantially in function from the monocytes expressing only TNFR1 or only TNFR2 and whether an individual monocyte can change its expression pattern in response to a stimulus. These questions could be addressed by sorting monocytes on the basis of TNFR1 and TNFR2 expression. The presence of other monocyte markers, such as CD14, CD16 and others as outlined in table 1.4 could then be studied to characterise these subsets further, as could changes to TNFR1 and TNFR2 expression before and after stimulation. Monocyte functions such as cytokine secretion, ROS production and phagocytotic capability could also be studied by subtype if wished. However, as discussed in chapter 5 this would require a lot more cells in order to accurately study rare events such as monocytes only expressing TNFR1.

6.3 **Conclusions**

TNF-α is an important cytokine in the immune response of many chronic inflammatory disorders, particularly in A1ATD-related COPD. In COPD there is a need to identify markers of disease that could help to more accurately phenotype patients, to aid development of focussed disease modifying treatments and allow prognostic stratification. Identifying patients with functionally relevant SNPs is one way of phenotyping. Whilst the experiments presented here were negative, examining the effects of the rs361525 TNF-A polymorphism in monocytes, this data in conjuction with that showing a positive association of the SNP with TNF-α output in airway secretions from the same patient cohort (17) highlight the inherent complexity of investigating SNPs, beyond simply demonstrating an association with a disease. In this respect this thesis offers an important contribution to the field as it suggests that the effects of a SNP may be compartment, stimulus or cell type specific, and that negative findings in one setting may not negate a genuine effect of the SNP in an alternative setting.

This thesis also presents data that suggests that in monocytes from healthy subjects TNFR1 ligation leads to pro and anti-inflammatory (IL-10) cytokine production whereas TNFR2 ligation up-regulates only IL-10, possibly clears sTNF-α from the peri-cellular environment but also up-regulates TNFR1 on the monocyte surface. In susceptible individuals disordered or excessive TNF-α signalling leads to chronic inflammatory disease. As TNFR1 is ubiquitous and TNFR2 expression is limited mainly to leukocytes these findings may support the strategy of selective TNFR1 blockade for TNF-α associated chronic inflammatory disease. Given the current interest in these therapies in a clinical setting (293, 294) it would be important to use the data presented here to power future studies further examining the differential effects of TNFR1 and TNFR2 in human monocytes, the principal TNF-α secreting cell.

APPENDICES

7 Appendices

7.1 Published articles

Gane J, Stockley R, Sapey E. The rs361525 polymorphism does not increase production of tumor necrosis factor alpha by monocytes from alpha-1 antitrypsin deficient subjects with chronic obstructive pulmonary disease - a pilot study. J Negat Results Biomed. 2015; 14: 20. Published online 2015 Dec 1st. doi: 10.1186/s12952-015-0039-3

7.2 Published review articles

Gane J, Stockley R. Mechanisms of neutrophil transmigration across the vascular endothelium in COPD. Thorax. 2012 Jun; 67(6):553-61.

7.3 Published abstracts

Gane J, Sapey E, Stockley R. Does tumour necrosis factor alpha induced by lipopolysaccharide have a positive feedback effect on the up-regulation of interleukin-8 messenger RNA by monocytes from COPD patients? ERJ. 2013 Sep; 42(suppl 57):P3874

Gane J, Stockley R, Sapey, E. The differential roles of TNF-α receptors 1 and 2 in influencing the balance of pro- and anti-inflammatory cytokine output from monocytes: towards a new therapeutic approach in TNF-α associated chronic inflammatory diseases. Immunology. 2013 Nov; 140 (suppl s1):175

7.4 Prizes

Stephen Whittaker Prize (best scientific paper by a trainee physician)- awarded by the West Midlands Physicians Association for a spoken presentation at the 2013 Autumn meeting, entitled: The differential roles of TNF-α receptors 1 and 2 in influencing the balance of pro- and anti-inflammatory cytokine output from monocytes: towards a new therapeutic approach in TNF-α associated chronic inflammatory diseases.

REFERENCES

8 References

1. Hehlgans T, Pfeffer K. The intriguing biology of the tumour necrosis factor/tumour necrosis factor receptor superfamily: players, rules and the games. Immunology 2005; 115 (1): 1-20.
2. Carswell EA, Old LJ, Kassel RL, Green S, Fiore N, Williamson B. An endotoxin-induced serum factor that causes necrosis of tumors. Proc Natl Acad Sci U S A 1975; 72 (9): 3666-3670.
3. Parameswaran N, Patial S. Tumor necrosis factor-alpha signaling in macrophages. Crit Rev Eukaryot Gene Expr 2010; 20 (2): 87-103.
4. Aggarwal BB. Signalling pathways of the TNF superfamily: a double-edged sword. Nat Rev Immunol 2003; 3 (9): 745-756.
5. Wajant H, Pfizenmaier K, Scheurich P. Tumor necrosis factor signaling. Cell Death Differ 2003; 10 (1): 45-65.
6. Black RA, Rauch CT, Kozlosky CJ, Peschon JJ, Slack JL, Wolfson MF, et al. A metalloproteinase disintegrin that releases tumour-necrosis factor-alpha from cells. Nature 1997; 385 (6618): 729-733.
7. Horiuchi T, Mitoma H, Harashima S, Tsukamoto H, Shimoda T. Transmembrane TNF-alpha: structure, function and interaction with anti-TNF agents. Rheumatology (Oxford) 2010; 49 (7): 1215-1228.
8. Van Hauwermeiren F, Vandenbroucke RE, Libert C. Treatment of TNF mediated diseases by selective inhibition of soluble TNF or TNFR1. Cytokine Growth Factor Rev 2011; 22 (5-6): 311-319.
9. Blüml S, Scheinecker C, Smolen JS, Redlich K. Targeting TNF receptors in rheumatoid arthritis. Int Immunol 2012; 24 (5): 275-281.
10. Hoffmann E, Dittrich-Breiholz O, Holtmann H, Kracht M. Multiple control of interleukin-8 gene expression. J Leukoc Biol 2002; 72 (5): 847-855.
11. Peschon JJ, Torrance DS, Stocking KL, Glaccum MB, Otten C, Willis CR, et al. TNF receptor-deficient mice reveal divergent roles for p55 and p75 in several models of inflammation. J Immunol 1998; 160 (2): 943-952.
12. Sheehan KC, Pinckard JK, Arthur CD, Dehner LP, Goeddel DV, Schreiber RD. Monoclonal antibodies specific for murine p55 and p75 tumor necrosis factor receptors: identification of a novel in vivo role for p75. J Exp Med 1995; 181 (2): 607-617.
13. Zhang HG, Zhou T, Yang P, Edwards CK, Curiel DT, Mountz JD. Inhibition of tumor necrosis factor alpha decreases inflammation and prolongs adenovirus gene expression in lung and liver. Hum Gene Ther 1998; 9 (13): 1875-1884.
14. Gane J, Stockley R. Mechanisms of neutrophil transmigration across the vascular endothelium in COPD. Thorax 2012; 67 (6): 553-561.
15. Berkow RL, Wang D, Larrick JW, Dodson RW, Howard TH. Enhancement of neutrophil superoxide production by preincubation with recombinant human tumor necrosis factor. J Immunol 1987; 139 (11): 3783-3791.
16. Pay S, Musabak U, Erdem H, Simsek I, Pekel A, Sengul A, et al. Chimerical anti-TNF-alpha, infliximab, inhibits neutrophil chemotaxis and production of reactive oxygen species by blocking the priming effect of mononuclear cells on neutrophils. Immunopharmacol Immunotoxicol 2005; 27 (2): 187-198.
17. Sapey E, Wood AM, Ahmad A, Stockley RA. Tumor necrosis factor-alpha rs361525 polymorphism is associated with increased local production and downstream inflammation in chronic obstructive pulmonary disease. Am J Respir Crit Care Med 2010; 182 (2): 192-199.

18. Flynn JL, Goldstein MM, Chan J, Triebold KJ, Pfeffer K, Lowenstein CJ, et al. Tumor necrosis factor-alpha is required in the protective immune response against Mycobacterium tuberculosis in mice. Immunity 1995; 2 (6): 561-572.
19. Micheau O, Tschopp J. Induction of TNF receptor I-mediated apoptosis via two sequential signaling complexes. Cell 2003; 114 (2): 181-190.
20. Harper N, Hughes M, MacFarlane M, Cohen GM. Fas-associated death domain protein and caspase-8 are not recruited to the tumor necrosis factor receptor 1 signaling complex during tumor necrosis factor-induced apoptosis. J Biol Chem 2003; 278 (28): 25534-25541.
21. Yost J, Gudjonsson JE. The role of TNF inhibitors in psoriasis therapy: new implications for associated comorbidities. F1000 Med Rep 2009; 1.
22. Sieper J. Developments in therapies for spondyloarthritis. Nat Rev Rheumatol 2012; 8 (5): 280-287.
23. Feldmann M. Development of anti-TNF therapy for rheumatoid arthritis. Nat Rev Immunol 2002; 2 (5): 364-371.
24. Danese S, Fiocchi C. Ulcerative colitis. N Engl J Med 2011; 365 (18): 1713-1725.
25. Behm BW, Bickston SJ. Cochrane Database Syst Rev. Tumor necrosis factor-alpha antibody for maintenance of remission in Crohn's disease [internet]. 2008 [cited 2014 March 15]. Available from: http://www.ncbi.nlm.nih.gov/pubmed/18254120.
26. Lawson, M, Thomas, AG, Akobeng, AK. Cochrane Database Syst Rev. Tumour necrosis factor alpha blocking agents for induction of remission in ulcerative colitis [internet]. 2006 [cited 2014 March 14]. Available from: http://www.ncbi.nlm.nih.gov/pubmed/16856078.
27. Akobeng, AK, Zachos, M. Cochrane Database Syst Rev. Tumor necrosis factor-alpha antibody for induction of remission in Crohn's disease [internet]. 2004 [cited 2014 January 14]. Available from: http://www.ncbi.nlm.nih.gov/pubmed/14974022.
28. Arnason B, Jacobs G, Hanlon M, Harding Clay B, Noronha A, Auty A, et al. TNF neutralization in MS: results of a randomized, placebo-controlled multicenter study. The Lenercept Multiple Sclerosis Study Group and The University of British Columbia MS/MRI Analysis Group. Neurology 1999; 53 (3): 457-465.
29. Ramos-Casals M, Brito-Zeron P, Soto MJ, Cuadrado MJ, Khamashta MA. Autoimmune diseases induced by TNF-targeted therapies. Best Pract Res Clin Rheumatol 2008; 22 (5): 847-861.
30. National Clinical Guideline Centre. Chronic obstructive pulmonary disease: management of chronic obstructive pulmonary disease in adults in primary and secondary care [internet]. 2010 [cited 2014 Oct 13]. Available from: http://guidance.nice.org.uk/CG101/Guidance/pdf/English.
31. Lancet. Global, regional, and national age-sex specific all-cause and cause-specific mortality for 240 causes of death, 1990-2013: a systematic analysis for the Global Burden of Disease Study 2013 [internet]. 2014 [cited 2014 December]. Available from: http://www.ncbi.nlm.nih.gov/pubmed/25530442.
32. Wedzicha JA. Role of Viruses in Exacerbations of Chronic Obstructive Pulmonary Disease. Proc Am Thorac Soc 2004; 1 (2): 115-120.
33. Sethi S, Muscarella K, Evans N, Klingman KL, Grant BJ, Murphy TF. Airway inflammation and etiology of acute exacerbations of chronic bronchitis. Chest 2000; 118 (6): 1557-1565.

34. Peacock JL, Anderson HR, Bremner SA, Marston L, Seemungal TA, Strachan DP, et al. Outdoor air pollution and respiratory health in patients with COPD. Thorax 2011; 66 (7): 591-596.
35. Chung KF, Adcock IM. Multifaceted mechanisms in COPD: inflammation, immunity, and tissue repair and destruction. Eur Respir J 2008; 31 (6): 1334-1356.
36. Medical Research Council. Definition and classification of chronic bronchitis for clinical and epidemiological purposes. Lancet 1965; 1 (7389): 775-779.
37. Evans DJ, Green M. Small airways: a time to revisit? Thorax 1998; 53 (8): 629-630.
38. Pasteur MC, Bilton D, Hill AT. British Thoracic Society guideline for non-CF bronchiectasis. Thorax 2010; 65 Suppl 1: i1-58.
39. Sinden NJ, Stockley RA. Systemic inflammation and comorbidity in COPD: a result of 'overspill' of inflammatory mediators from the lungs? Review of the evidence. Thorax 2010; 65 (10): 930-936.
40. Lokke A, Lange P, Scharling H, Fabricius P, Vestbo J. Developing COPD: a 25 year follow up study of the general population. Thorax 2006; 61 (11): 935-939.
41. Hu G, Zhou Y, Tian J, Yao W, Li J, Li B, et al. Risk of COPD from exposure to biomass smoke: a metaanalysis. Chest 2010; 138 (1): 20-31.
42. Stockley RA. Alpha1-antitrypsin review. Clin Chest Med 2014; 35 (1): 39-50.
43. Foreman MG, Campos M, Celedon JC. Genes and chronic obstructive pulmonary disease. Med Clin North Am 2012; 96 (4): 699-711.
44. Amitani R, Wilson R, Rutman A, Read R, Ward C, Burnett D, et al. Effects of human neutrophil elastase and Pseudomonas aeruginosa proteinases on human respiratory epithelium. Am J Respir Cell Mol Biol 1991; 4 (1): 26-32.
45. Sullivan AL, Dafforn T, Hiemstra PS, Stockley RA. Neutrophil elastase reduces secretion of secretory leukoproteinase inhibitor (SLPI) by lung epithelial cells: role of charge of the proteinase-inhibitor complex. Respir Res 2008; 9: 60.
46. Wright JL, Farmer SG, Churg A. Synthetic serine elastase inhibitor reduces cigarette smoke-induced emphysema in guinea pigs. Am J Respir Crit Care Med 2002; 166 (7): 954-960.
47. Sinden NJ, Sapey, E., Walton G.M, Stockley, R.A. Neutrophil Cell Membrane Expression of Proteinase 3 and Its Relationship to Alpha-1-Antitrypsin Deficiency (A1ATD). Thorax 2012; 67 (Suppl 2): A41-A42.
48. Gabelloni ML, Sabbione F, Jancic C, Bass JF, Keitelman I, Iula L, et al. NADPH oxidase derived reactive oxygen species are involved in human neutrophil IL-1beta secretion but not in inflammasome activation. Eur J Immunol 2013; 43 (12): 3324-3335.
49. MacNee W. Pulmonary and systemic oxidant/antioxidant imbalance in chronic obstructive pulmonary disease. Proc Am Thorac Soc 2005; 2 (1): 50-60.
50. Culpitt SV, Rogers DF, Shah P, De Matos C, Russell RE, Donnelly LE, et al. Impaired inhibition by dexamethasone of cytokine release by alveolar macrophages from patients with chronic obstructive pulmonary disease. Am J Respir Crit Care Med 2003; 167 (1): 24-31.
51. Lim S, Roche N, Oliver BG, Mattos W, Barnes PJ, Chung KF. Balance of matrix metalloprotease-9 and tissue inhibitor of metalloprotease-1 from alveolar macrophages in cigarette smokers. Regulation by interleukin-10. Am J Respir Crit Care Med 2000; 162 (4 Pt 1): 1355-1360.
52. Barnes PJ. Alveolar macrophages as orchestrators of COPD. Copd 2004; 1 (1): 59-70.
53. Noda N, Matsumoto K, Fukuyama S, Asai Y, Kitajima H, Seki N, et al. Cigarette smoke impairs phagocytosis of apoptotic neutrophils by alveolar macrophages via inhibition of the histone deacetylase/Rac/CD9 pathways. Int Immunol 2013; 25 (11): 643-650.

54. Donnelly LE, Barnes PJ. Defective phagocytosis in airways disease. Chest 2012; 141 (4): 1055-1062.
55. Vandivier RW, Henson PM, Douglas IS. Burying the dead: the impact of failed apoptotic cell removal (efferocytosis) on chronic inflammatory lung disease. Chest 2006; 129 (6): 1673-1682.
56. Stockley JA, Walton GM, Lord JM, Sapey E. Aberrant neutrophil functions in stable chronic obstructive pulmonary disease: The neutrophil as an immunotherapeutic target. Int Immunopharmacol 2013; 17 (4): 1211-1217.
57. van der Strate BW, Postma DS, Brandsma CA, Melgert BN, Luinge MA, Geerlings M, et al. Cigarette smoke-induced emphysema: A role for the B cell? Am J Respir Crit Care Med 2006; 173 (7): 751-758.
58. Chrysofakis G, Tzanakis N, Kyriakoy D, Tsoumakidou M, Tsiligianni I, Klimathianaki M, et al. Perforin expression and cytotoxic activity of sputum CD8+ lymphocytes in patients with COPD. Chest 2004; 125 (1): 71-76.
59. Saha S, Brightling CE. Eosinophilic airway inflammation in COPD. Int J Chron Obstruct Pulmon Dis 2006; 1 (1): 39-47.
60. Araya J, Cambier S, Markovics JA, Wolters P, Jablons D, Hill A, et al. Squamous metaplasia amplifies pathologic epithelial-mesenchymal interactions in COPD patients. J Clin Invest 2007; 117 (11): 3551-3562.
61. Innes AL, Woodruff PG, Ferrando RE, Donnelly S, Dolganov GM, Lazarus SC, et al. Epithelial mucin stores are increased in the large airways of smokers with airflow obstruction. Chest 2006; 130 (4): 1102-1108.
62. Bosken CH, Wiggs BR, Pare PD, Hogg JC. Small airway dimensions in smokers with obstruction to airflow. Am Rev Respir Dis 1990; 142 (3): 563-570.
63. Howarth PH, Knox AJ, Amrani Y, Tliba O, Panettieri RA, Jr., Johnson M. Synthetic responses in airway smooth muscle. J Allergy Clin Immunol 2004; 114 (2 Suppl): S32-50.
64. Zhang J, Wu L, Qu JM, Bai CX, Merrilees MJ, Black PN. Pro-inflammatory phenotype of COPD fibroblasts not compatible with repair in COPD lung. J Cell Mol Med 2012; 16 (7): 1522-1532.
65. de Godoy I, Donahoe M, Calhoun WJ, Mancino J, Rogers RM. Elevated TNF-alpha production by peripheral blood monocytes of weight-losing COPD patients. Am J Respir Crit Care Med 1996; 153 (2): 633-637.
66. Day A, Barnes P, Donnelly L. COPD monocytes differentiate into pro-inflammatory macrophages regardless of environment. Eur Respir J 2013; 42 (Suppl 57).
67. Holme J, Stockley JA, Stockley RA. Age related development of respiratory abnormalities in non-index alpha-1 antitrypsin deficient studies. Respir Med 2013; 107 (3): 387-393.
68. Owen CA. Roles for proteinases in the pathogenesis of chronic obstructive pulmonary disease. Int J Chron Obstruct Pulmon Dis 2008; 3 (2): 253-268.
69. Duranton J, Bieth JG. Inhibition of proteinase 3 by [alpha]1-antitrypsin in vitro predicts very fast inhibition in vivo. Am J Respir Cell Mol Biol 2003; 29 (1): 57-61.
70. Korkmaz B, Attucci S, Jourdan ML, Juliano L, Gauthier F. Inhibition of neutrophil elastase by alpha1-protease inhibitor at the surface of human polymorphonuclear neutrophils. J Immunol 2005; 175 (5): 3329-3338.
71. Campbell EJ, Campbell MA, Boukedes SS, Owen CA. Quantum proteolysis by neutrophils: implications for pulmonary emphysema in alpha 1-antitrypsin deficiency. J Clin Invest 1999; 104 (3): 337-344.

72. Lomas DA, Evans DL, Finch JT, Carrell RW. The mechanism of Z alpha 1-antitrypsin accumulation in the liver. Nature 1992; 357 (6379): 605-607.
73. Patel IS, Roberts NJ, Lloyd-Owen SJ, Sapsford RJ, Wedzicha JA. Airway epithelial inflammatory responses and clinical parameters in COPD. Eur Respir J 2003; 22 (1): 94-99.
74. Parmar JS, Mahadeva R, Reed BJ, Farahi N, Cadwallader KA, Keogan MT, et al. Polymers of α1-Antitrypsin Are Chemotactic for Human Neutrophils. Am J Respir Cell Mol Biol 2002; 26 (6): 723-730.
75. Bergin DA, Reeves EP, Hurley K, Wolfe R, Jameel R, Fitzgerald S, et al. The circulating proteinase inhibitor alpha-1 antitrypsin regulates neutrophil degranulation and autoimmunity. Sci Transl Med [internet] 2014 [cited 2016 March 13]; 6 (217): 217ra211. Available from: http://www.ncbi.nlm.nih.gov/pubmed/24382893.
76. Bergin DA, Reeves EP, Meleady P, Henry M, McElvaney OJ, Carroll TP, et al. alpha-1 Antitrypsin regulates human neutrophil chemotaxis induced by soluble immune complexes and IL-8. J Clin Invest 2010; 120 (12): 4236-4250.
77. Janciauskiene SM, Nita IM, Stevens T. Alpha1-antitrypsin, old dog, new tricks. Alpha1-antitrypsin exerts in vitro anti-inflammatory activity in human monocytes by elevating cAMP. J Biol Chem 2007; 282 (12): 8573-8582.
78. Lockett AD, Kimani S, Ddungu G, Wrenger S, Tuder RM, Janciauskiene SM, et al. alpha(1)-Antitrypsin modulates lung endothelial cell inflammatory responses to TNF-alpha. Am J Respir Cell Mol Biol 2013; 49 (1): 143-150.
79. Barnes PJ. The Cytokine Network in Chronic Obstructive Pulmonary Disease. Am J Respir Cell Mol Biol 2009; 41 (6): 631-638.
80. Aaron SD, Angel JB, Lunau M, Wright K, Fex C, Le Saux N, et al. Granulocyte inflammatory markers and airway infection during acute exacerbation of chronic obstructive pulmonary disease. Am J Respir Crit Care Med 2001; 163 (2): 349-355.
81. Bathoorn E, Liesker JJ, Postma DS, Koeter GH, van der Toorn M, van der Heide S, et al. Change in inflammation in out-patient COPD patients from stable phase to a subsequent exacerbation. Int J Chron Obstruct Pulmon Dis 2009; 4: 101-109.
82. Anzueto A. Impact of exacerbations on COPD. Eur Respir Rev 2010; 19 (116): 113-118.
83. Churg A, Zhou S, Wang X, Wang R, Wright JL. The role of interleukin-1beta in murine cigarette smoke-induced emphysema and small airway remodeling. Am J Respir Cell Mol Biol 2009; 40 (4): 482-490.
84. Churg A, Sin DD, Wright JL. Everything prevents emphysema: are animal models of cigarette smoke-induced chronic obstructive pulmonary disease any use? Am J Respir Cell Mol Biol 2011; 45 (6): 1111-1115.
85. Churg A, Dai J, Tai H, Xie C, Wright JL. Tumor necrosis factor-alpha is central to acute cigarette smoke-induced inflammation and connective tissue breakdown. Am J Respir Crit Care Med 2002; 166 (6): 849-854.
86. Churg A, Wang RD, Tai H, Wang X, Xie C, Wright JL. Tumor necrosis factor-alpha drives 70% of cigarette smoke-induced emphysema in the mouse. Am J Respir Crit Care Med 2004; 170 (5): 492-498.
87. Wright JL, Tai H, Wang R, Wang X, Churg A. Cigarette smoke upregulates pulmonary vascular matrix metalloproteinases via TNF-alpha signaling. Am J Physiol Lung Cell Mol Physiol 2007; 292 (1): L125-133.
88. Hacievliyagil SS, Mutlu LC, Temel I. Airway inflammatory markers in chronic obstructive pulmonary disease patients and healthy smokers. Niger J Clin Pract 2013; 16 (1): 76-81.

89. Keatings VM, Collins PD, Scott DM, Barnes PJ. Differences in interleukin-8 and tumor necrosis factor-alpha in induced sputum from patients with chronic obstructive pulmonary disease or asthma. Am J Respir Crit Care Med 1996; 153 (2): 530-534.
90. Vernooy JH, Kucukaycan M, Jacobs JA, Chavannes NH, Buurman WA, Dentener MA, et al. Local and systemic inflammation in patients with chronic obstructive pulmonary disease: soluble tumor necrosis factor receptors are increased in sputum. Am J Respir Crit Care Med 2002; 166 (9): 1218-1224.
91. Tumkaya M, Atis S, Ozge C, Delialioglu N, Polat G, Kanik A. Relationship between airway colonization, inflammation and exacerbation frequency in COPD. Respir Med 2007; 101 (4): 729-737.
92. Hackett TL, Holloway R, Holgate ST, Warner JA. Dynamics of pro-inflammatory and anti-inflammatory cytokine release during acute inflammation in chronic obstructive pulmonary disease: an ex vivo study. Respir Res 2008; 9: 47.
93. Hodge G, Reynolds PN, Holmes M, Hodge S. Differential expression of pro-inflammatory cytokines in intra-epithelial T cells between trachea and bronchi distinguishes severity of COPD. Cytokine 2012; 60 (3): 843-848.
94. Hacievliyagil SS, Gunen H, Mutlu LC, Karabulut AB, Temel I. Association between cytokines in induced sputum and severity of chronic obstructive pulmonary disease. Respir Med 2006; 100 (5): 846-854.
95. Karadag F, Karul AB, Cildag O, Yilmaz M, Ozcan H. Biomarkers of systemic inflammation in stable and exacerbation phases of COPD. Lung 2008; 186 (6): 403-409.
96. Takabatake N, Nakamura H, Abe S, Inoue S, Hino T, Saito H, et al. The relationship between chronic hypoxemia and activation of the tumor necrosis factor-alpha system in patients with chronic obstructive pulmonary disease. Am J Respir Crit Care Med 2000; 161 (4 Pt 1): 1179-1184.
97. Sapey E, Ahmad A, Bayley D, Newbold P, Snell N, Rugman P, et al. Imbalances between interleukin-1 and tumor necrosis factor agonists and antagonists in stable COPD. J Clin Immunol 2009; 29 (4): 508-516.
98. Gaki E, Kontogianni K, Papaioannou AI, Bakakos P, Gourgoulianis KI, Kostikas K, et al. Associations between BODE index and systemic inflammatory biomarkers in COPD. COPD 2011; 8 (6): 408-413.
99. Liang B, Feng Y. The association of low bone mineral density with systemic inflammation in clinically stable COPD. Endocrine 2012; 42 (1): 190-195.
100. von Haehling S, Hopkinson NS, Polkey MI, Niethammer M, Anker SD, Genth-Zotz S. Elevated TNFalpha production in whole blood in patients with severe COPD: the potential link to disease severity. Wien Klin Wochenschr 2009; 121 (9-10): 303-308.
101. Paats MS, Bergen IM, Hoogsteden HC, van der Eerden MM, Hendriks RW. Systemic CD4+ and CD8+ T-cell cytokine profiles correlate with GOLD stage in stable COPD. Eur Respir J 2012; 40 (2): 330-337.
102. Foschino Barbaro MP, Carpagnano GE, Spanevello A, Cagnazzo MG, Barnes PJ. Inflammation, oxidative stress and systemic effects in mild chronic obstructive pulmonary disease. Int J Immunopathol Pharmacol 2007; 20 (4): 753-763.
103. Rabinovich RA, Figueras M, Ardite E, Carbo N, Troosters T, Filella X, et al. Increased tumour necrosis factor-alpha plasma levels during moderate-intensity exercise in COPD patients. Eur Respir J 2003; 21 (5): 789-794.
104. Casadevall C, Coronell C, Ramirez-Sarmiento AL, Martinez-Llorens J, Barreiro E, Orozco-Levi M, et al. Upregulation of pro-inflammatory cytokines in the intercostal muscles of COPD patients. Eur Respir J 2007; 30 (4): 701-707.

105. Skyba P, Ukropec J, Pobeha P, Ukropcova B, Joppa P, Kurdiova T, et al. Metabolic phenotype and adipose tissue inflammation in patients with chronic obstructive pulmonary disease. Mediators inflamm [internet] 2010 [cited 2016 March 12]. 173498. Available from: http://www.ncbi.nlm.nih.gov/pubmed/21197447.
106. Remels AH, Gosker HR, Schrauwen P, Hommelberg PP, Sliwinski P, Polkey M, et al. TNF-alpha impairs regulation of muscle oxidative phenotype: implications for cachexia? FASEB J 2010; 24 (12): 5052-5062.
107. Agusti A, Edwards LD, Rennard SI, MacNee W, Tal-Singer R, Miller BE, et al. Persistent systemic inflammation is associated with poor clinical outcomes in COPD: a novel phenotype. PLoS One [internet] 2012 [cited 2014 June 23]; 7 (5): e37483. Available from: http://www.ncbi.nlm.nih.gov/pubmed/22624038.
108. Eagan TM, Gabazza EC, D'Alessandro-Gabazza C, Gil-Bernabe P, Aoki S, Hardie JA, et al. TNF-alpha is associated with loss of lean body mass only in already cachectic COPD patients. Respir Res 2012; 13: 48.
109. Pinto-Plata V, Casanova C, Mullerova H, de Torres JP, Corado H, Varo N, et al. Inflammatory and repair serum biomarker pattern: association to clinical outcomes in COPD. Respir Res 2012; 13: 71.
110. Krommidas G, Kostikas K, Papatheodorou G, Koutsokera A, Gourgoulianis KI, Roussos C, et al. Plasma leptin and adiponectin in COPD exacerbations: associations with inflammatory biomarkers. Respir Med 2010; 104 (1): 40-46.
111. Markoulaki D, Kostikas K, Papatheodorou G, Koutsokera A, Alchanatis M, Bakakos P, et al. Hemoglobin, erythropoietin and systemic inflammation in exacerbations of chronic obstructive pulmonary disease. Eur J Intern Med 2011; 22 (1): 103-107.
112. Tracey D, Klareskog L, Sasso EH, Salfeld JG, Tak PP. Tumor necrosis factor antagonist mechanisms of action: a comprehensive review. Pharmacol Ther 2008; 117 (2): 244-279.
113. van der Vaart H, Koeter GH, Postma DS, Kauffman HF, ten Hacken NH. First study of infliximab treatment in patients with chronic obstructive pulmonary disease. Am J Respir Crit Care Med 2005; 172 (4): 465-469.
114. Rennard SI, Fogarty C, Kelsen S, Long W, Ramsdell J, Allison J, et al. The safety and efficacy of infliximab in moderate to severe chronic obstructive pulmonary disease. Am J Respir Crit Care Med 2007; 175 (9): 926-934.
115. Hajeer AH, Hutchinson IV. TNF-alpha gene polymorphism: clinical and biological implications. Microsc Res Tech 2000; 50 (3): 216-228.
116. Posch PE, Cruz I, Bradshaw D, Medhekar BA. Novel polymorphisms and the definition of promoter 'alleles' of the tumor necrosis factor and lymphotoxin alpha loci: inclusion in HLA haplotypes. Genes Immun 2003; 4 (8): 547-558.
117. Han MK, Agusti A, Calverley PM, Celli BR, Criner G, Curtis JL, et al. Chronic obstructive pulmonary disease phenotypes: the future of COPD. Am J Respir Crit Care Med 2010; 182 (5): 598-604.
118. Castaldi PJ, Cho MH, Cohn M, Langerman F, Moran S, Tarragona N, et al. The COPD genetic association compendium: a comprehensive online database of COPD genetic associations. Hum Mol Genet 2010; 19 (3): 526-534.
119. Gingo MR, Silveira LJ, Miller YE, Friedlander AL, Cosgrove GP, Chan ED, et al. Tumour necrosis factor gene polymorphisms are associated with COPD. Eur Respir J 2008; 31 (5): 1005-1012.

120. Hersh CP, Demeo DL, Lange C, Litonjua AA, Reilly JJ, Kwiatkowski D, et al. Attempted replication of reported chronic obstructive pulmonary disease candidate gene associations. Am J Respir Cell Mol Biol 2005; 33 (1): 71-78.
121. Smolonska J, Wijmenga C, Postma DS, Boezen HM. Meta-analyses on suspected chronic obstructive pulmonary disease genes: a summary of 20 years' research. Am J Respir Crit Care Med 2009; 180 (7): 618-631.
122. Zhou DC, Zhou CF, Toloo S, Shen T, Tong SL, Zhu QX. Association of a disintegrin and metalloprotease 33 (ADAM33) gene polymorphisms with the risk of COPD: an updated meta-analysis of 2,644 cases and 4,804 controls. Mol Biol Rep [internet] 2015 [cited 2016 February 22]; 42 (2): 409-422. Available from: http://www.ncbi.nlm.nih.gov/pubmed/25280544.
123. Turner AM. Fifty Years On: GWAS Confirms the Role of a Rare Variant in Lung Disease. PLoS Genet 2013; 9 (8): e1003768.
124. Simmonds MJ, Heward JM, Howson JMM, Foxall H, Nithiyananthan R, Franklyn JA, et al. A systematic approach to the assessment of known TNF-alpha polymorphisms in Graves' disease. Genes Immun 2004; 5 (4): 267-273.
125. Wood AM, Simmonds MJ, Bayley DL, Newby PR, Gough SC, Stockley RA. The TNFalpha gene relates to clinical phenotype in alpha-1-antitrypsin deficiency. Respir Res 2008; 9: 52.
126. Zhu J, Qu H, Chen X, Wang H, Li J. Single nucleotide polymorphisms in the tumor necrosis factor-alpha gene promoter region alter the risk of psoriasis vulgaris and psoriatic arthritis: a meta-analysis. PLoS One [internet] 2013 [cited 2014 March 23]; 8 (5): e64376. Available from: http://www.ncbi.nlm.nih.gov/pubmed/23717605.
127. Fong CL, Siddiqui AH, Mark DF. Identification and characterization of a novel repressor site in the human tumor necrosis factor alpha gene. Nucleic Acids Res 1994; 22 (6): 1108-1114.
128. Kiss-Toth E, Harlock E, Lath D, Quertermous T, Wilkinson JM. A TNF variant that associates with susceptibility to musculoskeletal disease modulates thyroid hormone receptor binding to control promoter activation. PLoS One [internet] 2013 [cited 2014 December 15]; 8 (9): e76034. Available from: http://www.ncbi.nlm.nih.gov/pubmed/24069456.
129. Knight JC, Keating BJ, Rockett KA, Kwiatkowski DP. In vivo characterization of regulatory polymorphisms by allele-specific quantification of RNA polymerase loading. Nat Genet 2003; 33 (4): 469-475.
130. Kaijzel EL, van Krugten MV, Brinkman BM, Huizinga TW, van der Straaten T, Hazes JM, et al. Functional analysis of a human tumor necrosis factor alpha (TNF-alpha) promoter polymorphism related to joint damage in rheumatoid arthritis. Mol Med 1998; 4 (11): 724-733.
131. Mekinian A, Tamouza R, Pavy S, Gestermann N, Ittah M, Mariette X, et al. Functional study of TNF-alpha promoter polymorphisms: literature review and meta-analysis. Eur Cytokine Netw 2011; 22 (2): 88-102.
132. Pissetti CW, Correia D, de Oliveira RF, Llaguno MM, Balarin MA, Silva-Grecco RL, et al. Genetic and functional role of TNF-alpha in the development Trypanosoma cruzi infection. PloS Neglect Trop Dis [internet] 2011 [cited 2014 June 23]; 5 (3): e976. Available from: http://www.ncbi.nlm.nih.gov/pubmed/21408088.
133. Westendorp RG, Langermans JA, Huizinga TW, Verweij CL, Sturk A. Genetic influence on cytokine production in meningococcal disease. Lancet 1997; 349 (9069): 1912-1913.

134. Haddy N, Sass C, Maumus S, Marie B, Droesch S, Siest G, et al. Biological variations, genetic polymorphisms and familial resemblance of TNF-alpha and IL-6 concentrations: STANISLAS cohort. Eur J Hum Genet 2005; 13 (1): 109-117.
135. Oregon-Romero E, Vazquez-Del Mercado M, Ruiz-Quezada SL, Navarro-Hernandez RE, Rangel-Villalobos H, Martinez-Bonilla G, et al. Tumor necrosis factor alpha-308 and -238 polymorphisms in rheumatoid arthritis. Association with messenger RNA expression and sTNF-alpha. J Investig Med 2008; 56 (7): 937-943.
136. Pociot F, D'Alfonso S, Compasso S, Scorza R, Richiardi PM. Functional analysis of a new polymorphism in the human TNF alpha gene promoter. Scand J Immunol 1995; 42 (4): 501-504.
137. Lu MC, Yang KL, Tung CH, Huang KY, Yu HC, Liu SQ, et al. Higher LPS-stimulated TNF-alpha mRNA levels in peripheral blood mononuclear cells from Chinese ankylosing spondylitis patients with -308G/A polymorphism in promoter region of tumor necrosis factor: association with distinct A33/B58/Cw10 haplotypes. Rheumatol Int 2008; 29 (2): 189-195.
138. O'Dwyer MJ, Mankan AK, Ryan AW, Lawless MW, Stordeur P, Kelleher D, et al. Characterization of tumour necrosis factor-alpha genetic variants and mRNA expression in patients with severe sepsis. Int J Immunogenet 2008; 35 (4-5): 279-285.
139. Sharma S, Ghosh B, Sharma SK. Association of TNF polymorphisms with sarcoidosis, its prognosis and tumour necrosis factor (TNF)-alpha levels in Asian Indians. Clin Exp Immunol 2008; 151 (2): 251-259.
140. Kaluza W, Reuss E, Grossmann S, Hug R, Schopf RE, Galle PR, et al. Different transcriptional activity and in vitro TNF-alpha production in psoriasis patients carrying the TNF-alpha 238A promoter polymorphism. J Invest Dermatol 2000; 114 (6): 1180-1183.
141. Uglialoro AM, Turbay D, Pesavento PA, Delgado JC, McKenzie FE, Gribben JG, et al. Identification of three new single nucleotide polymorphisms in the human tumor necrosis factor-alpha gene promoter. Tissue Antigens 1998; 52 (4): 359-367.
142. Huizinga TW, Westendorp RG, Bollen EL, Keijsers V, Brinkman BM, Langermans JA, et al. TNF-alpha promoter polymorphisms, production and susceptibility to multiple sclerosis in different groups of patients. J Neuroimmunol 1997; 72 (2): 149-153.
143. Falvo JV, Uglialoro AM, Brinkman BM, Merika M, Parekh BS, Tsai EY, et al. Stimulus-specific assembly of enhancer complexes on the tumor necrosis factor alpha gene promoter. Mol Cell Biol 2000; 20 (6): 2239-2247.
144. Falvo JV, Tsytsykova AV, Goldfeld AE. Transcriptional control of the TNF gene. Curr Dir Autoimmun 2010; 11: 27-60.
145. Falvo JV, Jasenosky LD, Kruidenier L, Goldfeld AE. Epigenetic control of cytokine gene expression: regulation of the TNF/LT locus and T helper cell differentiation. Adv Immunol 2013; 118: 37-128.
146. Sullivan KE, Reddy AB, Dietzmann K, Suriano AR, Kocieda VP, Stewart M, et al. Epigenetic regulation of tumor necrosis factor alpha. Mol Cell Biol 2007; 27 (14): 5147-5160.
147. Lee JY, Kim NA, Sanford A, Sullivan KE. Histone acetylation and chromatin conformation are regulated separately at the TNF-alpha promoter in monocytes and macrophages. J Leukoc Biol 2003; 73 (6): 862-871.
148. Kouzarides T. Acetylation: a regulatory modification to rival phosphorylation? EMBO J 2000; 19 (6): 1176-1179.
149. Garrett S, Dietzmann-Maurer K, Song L, Sullivan KE. Polarization of primary human monocytes by IFN-gamma induces chromatin changes and recruits RNA Pol II to the TNF-alpha promoter. J Immunol 2008; 180 (8): 5257-5266.

150. Mahlknecht U, Will J, Varin A, Hoelzer D, Herbein G. Histone deacetylase 3, a class I histone deacetylase, suppresses MAPK11-mediated activating transcription factor-2 activation and represses TNF gene expression. J Immunol 2004; 173 (6): 3979-3990.
151. El Gazzar M, Yoza BK, Hu JY, Cousart SL, McCall CE. Epigenetic silencing of tumor necrosis factor alpha during endotoxin tolerance. J Biol Chem 2007; 282 (37): 26857-26864.
152. Suriano AR, Sanford AN, Kim N, Oh M, Kennedy S, Henderson MJ, et al. GCF2/LRRFIP1 represses tumor necrosis factor alpha expression. Mol Cell Biol 2005; 25 (20): 9073-9081.
153. Taggart CC, Cryan SA, Weldon S, Gibbons A, Greene CM, Kelly E, et al. Secretory leucoprotease inhibitor binds to NF-kappaB binding sites in monocytes and inhibits p65 binding. J Exp Med 2005; 202 (12): 1659-1668.
154. Osman F, Jarrous N, Ben-Asouli Y, Kaempfer R. A cis-acting element in the 3'-untranslated region of human TNF-alpha mRNA renders splicing dependent on the activation of protein kinase PKR. Genes Dev 1999; 13 (24): 3280-3293.
155. Mijatovic T, Houzet L, Defrance P, Droogmans L, Huez G, Kruys V. Tumor necrosis factor-a mRNA remains unstable and hypoadenylated upon stimulation of macrophages by lipopolysaccharides. Eur J Biochem 2000; 267: 6004-6012.
156. Giambelluca M, Rollet-Labelle E, Bertheau-Mailhot G, Laflamme C, Pouliot M. Post-transcriptional regulation of tumour necrosis factor alpha biosynthesis: Relevance to the pathophysiology of rheumatoid arthritis. OA Inflammation 2013; 1 (1): 1-6.
157. Armstrong L, Godinho SI, Uppington KM, Whittington HA, Millar AB. Contribution of TNF-alpha converting enzyme and proteinase-3 to TNF-alpha processing in human alveolar macrophages. Am J Respir Cell Mol Biol 2006; 34 (2): 219-225.
158. Milatovich A, Song K, Heller RA, Francke U. Tumor necrosis factor receptor genes, TNFR1 and TNFR2, on human chromosomes 12 and 1. Somat Cell Mol Genet 1991; 17 (5): 519-523.
159. Dembic Z, Loetscher H, Gubler U, Pan YC, Lahm HW, Gentz R, et al. Two human TNF receptors have similar extracellular, but distinct intracellular, domain sequences. Cytokine 1990; 2 (4): 231-237.
160. Banner DW, D'Arcy A, Janes W, Gentz R, Schoenfeld HJ, Broger C, et al. Crystal structure of the soluble human 55 kd TNF receptor-human TNF beta complex: implications for TNF receptor activation. Cell 1993; 73 (3): 431-445.
161. MacEwan DJ. TNF receptor subtype signalling: differences and cellular consequences. Cell Signal 2002; 14 (6): 477-492.
162. Upadhyay V, Fu YX. Lymphotoxin signalling in immune homeostasis and the control of microorganisms. Nat Rev Immunol 2013; 13 (4): 270-279.
163. Medvedev AE, Espevik T, Ranges G, Sundan A. Distinct roles of the two tumor necrosis factor (TNF) receptors in modulating TNF and lymphotoxin alpha effects. J Biol Chem 1996; 271 (16): 9778-9784.
164. Grell M, Wajant H, Zimmermann G, Scheurich P. The type 1 receptor (CD120a) is the high-affinity receptor for soluble tumor necrosis factor. Proc Natl Acad Sci U S A 1998; 95 (2): 570-575.
165. Grell M, Douni E, Wajant H, Lohden M, Clauss M, Maxeiner B, et al. The transmembrane form of tumor necrosis factor is the prime activating ligand of the 80 kDa tumor necrosis factor receptor. Cell 1995; 83 (5): 793-802.
166. Haas E, Grell M, Wajant H, Scheurich P. Continuous autotropic signaling by membrane-expressed tumor necrosis factor. J Biol Chem 1999; 274 (25): 18107-18112.

167. Rauert H, Wicovsky A, Muller N, Siegmund D, Spindler V, Waschke J, et al. Membrane tumor necrosis factor (TNF) induces p100 processing via TNF receptor-2 (TNFR2). J Biol Chem 2010; 285 (10): 7394-7404.
168. Tartaglia LA, Pennica D, Goeddel DV. Ligand passing: the 75-kDa tumor necrosis factor (TNF) receptor recruits TNF for signaling by the 55-kDa TNF receptor. J Biol Chem 1993; 268 (25): 18542-18528.
169. Weiss T, Grell M, Hessabi B, Bourteele S, Muller G, Scheurich P, et al. Enhancement of TNF receptor p60-mediated cytotoxicity by TNF receptor p80: requirement of the TNF receptor-associated factor-2 binding site. J Immunol 1997; 158 (5): 2398-2404.
170. Chen X, Oppenheim JJ. The phenotypic and functional consequences of tumour necrosis factor receptor type 2 expression on CD4(+) FoxP3(+) regulatory T cells. Immunology 2011; 133 (4): 426-433.
171. Matsumoto M, Fu YX, Molina H, Chaplin DD. Lymphotoxin-alpha-deficient and TNF receptor-I-deficient mice define developmental and functional characteristics of germinal centers. Immunol Rev 1997; 156: 137-144.
172. Ebach DR, Riehl TE, Stenson WF. Opposing effects of tumor necrosis factor receptor 1 and 2 in sepsis due to cecal ligation and puncture. Shock 2005; 23 (4): 311-318.
173. Tartaglia LA, Goeddel DV, Reynolds C, Figari IS, Weber RF, Fendly BM, et al. Stimulation of human T-cell proliferation by specific activation of the 75-kDa tumor necrosis factor receptor. J Immunol 1993; 151 (9): 4637-4641.
174. Kim EY, Priatel JJ, Teh SJ, Teh HS. TNF receptor type 2 (p75) functions as a costimulator for antigen-driven T cell responses in vivo. J Immunol 2006; 176 (2): 1026-1035.
175. Chen X, Baumel M, Mannel DN, Howard OM, Oppenheim JJ. Interaction of TNF with TNF receptor type 2 promotes expansion and function of mouse CD4+CD25+ T regulatory cells. J Immunol 2007; 179 (1): 154-161.
176. Zheng L, Fisher G, Miller RE, Peschon J, Lynch DH, Lenardo MJ. Induction of apoptosis in mature T cells by tumour necrosis factor. Nature 1995; 377 (6547): 348-351.
177. Xu J, Chakrabarti AK, Tan JL, Ge L, Gambotto A, Vujanovic NL. Essential role of the TNF-TNFR2 cognate interaction in mouse dendritic cell-natural killer cell crosstalk. Blood 2007; 109 (8): 3333-3341.
178. Kafrouni MI, Brown GR, Thiele DL. The role of TNF-TNFR2 interactions in generation of CTL responses and clearance of hepatic adenovirus infection. J Leukoc Biol 2003; 74 (4): 564-571.
179. Shibata H, Yoshioka Y, Abe Y, Ohkawa A, Nomura T, Minowa K, et al. The treatment of established murine collagen-induced arthritis with a TNFR1-selective antagonistic mutant TNF. Biomaterials 2009; 30 (34): 6638-6647.
180. D'Hulst AI, Bracke KR, Maes T, De Bleecker JL, Pauwels RA, Joos GF, et al. Role of tumour necrosis factor-alpha receptor p75 in cigarette smoke-induced pulmonary inflammation and emphysema. Eur Respir J 2006; 28 (1): 102-112.
181. Kontoyiannis D, Pasparakis M, Pizarro TT, Cominelli F, Kollias G. Impaired on/off regulation of TNF biosynthesis in mice lacking TNF AU-rich elements: implications for joint and gut-associated immunopathologies. Immunity 1999; 10 (3): 387-398.
182. Abu-Amer Y, Erdmann J, Alexopoulou L, Kollias G, Ross FP, Teitelbaum SL. Tumor necrosis factor receptors types 1 and 2 differentially regulate osteoclastogenesis. J Biol Chem 2000; 275 (35): 27307-27310.

183. Dayer Schneider J, Seibold I, Saxer-Sekulic N, Paredes BE, Saurer L, Mueller C. Lack of TNFR2 expression by CD4(+) T cells exacerbates experimental colitis. Eur J Immunol 2009; 39 (7): 1743-1753.
184. Shibata H, Yoshioka Y, Ohkawa A, Abe Y, Nomura T, Mukai Y, et al. The therapeutic effect of TNFR1-selective antagonistic mutant TNF-alpha in murine hepatitis models. Cytokine 2008; 44 (2): 229-233.
185. Sudo K, Yamada Y, Moriwaki H, Saito K, Seishima M. Lack of tumor necrosis factor receptor type 1 inhibits liver fibrosis induced by carbon tetrachloride in mice. Cytokine 2005; 29 (5): 236-244.
186. Yamada Y, Webber EM, Kirillova I, Peschon JJ, Fausto N. Analysis of liver regeneration in mice lacking type 1 or type 2 tumor necrosis factor receptor: requirement for type 1 but not type 2 receptor. Hepatology 1998; 28 (4): 959-970.
187. Suvannavejh GC, Lee HO, Padilla J, Dal Canto MC, Barrett TA, Miller SD. Divergent roles for p55 and p75 tumor necrosis factor receptors in the pathogenesis of MOG(35-55)-induced experimental autoimmune encephalomyelitis. Cell Immunol 2000; 205 (1): 24-33.
188. Nomura T, Abe Y, Kamada H, Shibata H, Kayamuro H, Inoue M, et al. Therapeutic effect of PEGylated TNFR1-selective antagonistic mutant TNF in experimental autoimmune encephalomyelitis mice. J Control Release 2011; 149 (1): 8-14.
189. Arnett HA, Mason J, Marino M, Suzuki K, Matsushima GK, Ting JP. TNF alpha promotes proliferation of oligodendrocyte progenitors and remyelination. Nat Neurosci 2001; 4 (11): 1116-1122.
190. Monden Y, Kubota T, Inoue T, Tsutsumi T, Kawano S, Ide T, et al. Tumor necrosis factor-alpha is toxic via receptor 1 and protective via receptor 2 in a murine model of myocardial infarction. Am J Physiol Heart Circ Physiol 2007; 293 (1): H743-753.
191. Hamid T, Gu Y, Ortines RV, Bhattacharya C, Wang G, Xuan YT, et al. Divergent tumor necrosis factor receptor-related remodeling responses in heart failure: role of nuclear factor-kappaB and inflammatory activation. Circulation 2009; 119 (10): 1386-1397.
192. Chandrasekharan UM, Siemionow M, Unsal M, Yang L, Poptic E, Bohn J, et al. Tumor necrosis factor alpha (TNF-alpha) receptor-II is required for TNF-alpha-induced leukocyte-endothelial interaction in vivo. Blood 2007; 109 (5): 1938-1944.
193. Winzen R, Kracht M, Ritter B, Wilhelm A, Chen CY, Shyu AB, et al. The p38 MAP kinase pathway signals for cytokine-induced mRNA stabilization via MAP kinase-activated protein kinase 2 and an AU-rich region-targeted mechanism. EMBO J 1999; 18 (18): 4969-4980.
194. Naudé PJ, den Boer JA, Luiten PG, Eisel UL. Tumor necrosis factor receptor cross-talk. FEBS J 2011; 278 (6): 888-898.
195. Fotin-Mleczek M, Henkler F, Samel D, Reichwein M, Hausser A, Parmryd I, et al. Apoptotic crosstalk of TNF receptors: TNF-R2-induces depletion of TRAF2 and IAP proteins and accelerates TNF-R1-dependent activation of caspase-8. J Cell Sci 2002; 115 (Pt 13): 2757-2770.
196. Gordon S, Taylor PR. Monocyte and macrophage heterogeneity. Nat Rev Immunol 2005; 5 (12): 953-964.
197. Barreda DR, Hanington PC, Belosevic M. Regulation of myeloid development and function by colony stimulating factors. Dev Comp Immunol 2004; 28 (5): 509-554.
198. Capsoni F, Minonzio F, Ongari AM, Carbonelli V, Galli A, Zanussi C. IL-10 up-regulates human monocyte phagocytosis in the presence of IL-4 and IFN-gamma. J Leukoc Biol 1995; 58 (3): 351-358.

199. Cathcart MK. Regulation of Superoxide Anion Production by NADPH Oxidase in Monocytes/Macrophages: Contributions to Atherosclerosis. Arterioscler Thromb Vasc Biol 2004; 24 (1): 23-28.
200. O'Dea KP, Young AJ, Yamamoto H, Robotham JL, Brennan FM, Takata M. Lung-marginated monocytes modulate pulmonary microvascular injury during early endotoxemia. Am J Respir Crit Care Med 2005; 172 (9): 1119-1127.
201. Auffray C, Fogg D, Garfa M, Elain G, Join-Lambert O, Kayal S, et al. Monitoring of blood vessels and tissues by a population of monocytes with patrolling behavior. Science 2007; 317 (5838): 666-670.
202. Murray PJ, Wynn TA. Protective and pathogenic functions of macrophage subsets. Nat Rev Immunol 2011; 11 (11): 723-737.
203. Yang J, Zhang L, Yu C, Yang XF, Wang H. Monocyte and macrophage differentiation: circulation inflammatory monocyte as biomarker for inflammatory diseases. Biomark Res 2014; 2 (1): 1.
204. Wong KL, Tai JJ, Wong WC, Han H, Sem X, Yeap WH, et al. Gene expression profiling reveals the defining features of the classical, intermediate, and nonclassical human monocyte subsets. Blood [internet] 2011 [cited 2014 February 18]; 118 (5): e16-31. Available from: http://www.bloodjournal.org/content/bloodjournal/118/115/e116.full.pdf.
205. Bazan JF, Bacon KB, Hardiman G, Wang W, Soo K, Rossi D, et al. A new class of membrane-bound chemokine with a CX3C motif. Nature 1997; 385 (6617): 640-644.
206. Cros J, Cagnard N, Woollard K, Patey N, Zhang SY, Senechal B, et al. Human CD14dim monocytes patrol and sense nucleic acids and viruses via TLR7 and TLR8 receptors. Immunity 2010; 33 (3): 375-386.
207. Belge KU, Dayyani F, Horelt A, Siedlar M, Frankenberger M, Frankenberger B, et al. The proinflammatory CD14+CD16+DR++ monocytes are a major source of TNF. J Immunol 2002; 168 (7): 3536-3542.
208. Ginhoux F, Jung S. Monocytes and macrophages: developmental pathways and tissue homeostasis. Nat Rev Immunol 2014; 14 (6): 392-404.
209. Byrne AJ, Mathie SA, Gregory LG, Lloyd CM. Pulmonary macrophages: key players in the innate defence of the airways. Thorax 2015; 70 (12): 1189-1196.
210. Mosser DM, Edwards JP. Exploring the full spectrum of macrophage activation. Nat Rev Immunol 2008; 8 (12): 958-969.
211. Arnold L, Henry A, Poron F, Baba-Amer Y, van Rooijen N, Plonquet A, et al. Inflammatory monocytes recruited after skeletal muscle injury switch into antiinflammatory macrophages to support myogenesis. J Exp Med 2007; 204 (5): 1057-1069.
212. Italiani P, Boraschi D. From Monocytes to M1/M2 Macrophages: Phenotypical vs. Functional Differentiation. Front Immunol 2014; 5: 514.
213. Guilliams M, De Kleer I, Henri S, Post S, Vanhoutte L, De Prijck S, et al. Alveolar macrophages develop from fetal monocytes that differentiate into long-lived cells in the first week of life via GM-CSF. J Exp Med 2013; 210 (10): 1977-1992.
214. Yona S, Kim KW, Wolf Y, Mildner A, Varol D, Breker M, et al. Fate mapping reveals origins and dynamics of monocytes and tissue macrophages under homeostasis. Immunity 2013; 38 (1): 79-91.
215. Hashimoto D, Chow A, Noizat C, Teo P, Beasley MB, Leboeuf M, et al. Tissue-resident macrophages self-maintain locally throughout adult life with minimal contribution from circulating monocytes. Immunity 2013; 38 (4): 792-804.

216. Desch AN, Gibbings SL, Goyal R, Kolde R, Bednarek J, Bruno T, et al. Flow Cytometric Analysis of Mononuclear Phagocytes in Nondiseased Human Lung and Lung-Draining Lymph Nodes. Am J Respir Crit Care Med 2015; 193 (6): 614-626.
217. Yarilina A, Park-Min K, Antoniv T, Hu X, Ivashkiv LB. TNF activates an IRF1-dependent autocrine loop leading to sustained expression of chemokines and STAT1-dependent type I interferon-response genes. Nat Immunol 2008; 9 (4): 378-387.
218. Lombardo E, Alvarez-Barrientos A, Maroto B, Bosca L, Knaus UG. TLR4-mediated survival of macrophages is MyD88 dependent and requires TNF-alpha autocrine signalling. J Immunol 2007; 178 (6): 3731-3739.
219. Witsell AL, Schook LB. Tumor necrosis factor alpha is an autocrine growth regulator during macrophage differentiation. Proc Natl Acad Sci U S A 1993; 90 (10): 4763.
220. Arenzana-Seisdedos F, Mogensen SC, Vuillier F, Fiers W, Virelizier JL. Autocrine secretion of tumor necrosis factor under the influence of interferon-gamma amplifies HLA-DR gene induction in human monocytes. Proc Natl Acad Sci U S A 1988; 85 (16): 6087-6091.
221. Rushworth SA, Shah S, MacEwan DJ. TNF mediates the sustained activation of Nrf2 in human monocytes. J immunol 2011; 187 (2): 702-707.
222. Wanidworanun C, Strober W. Predominant role of tumor necrosis factor-alpha in human monocyte IL-10 synthesis. J Immunol 1993; 151 (12): 6853-6861.
223. Sheng WS, Hu S, Kravitz FH, Peterson PK, Chao CC. Tumor necrosis factor alpha upregulates human microglial cell production of interleukin-10 in vitro. Clin Diagn Lab Immunol 1995; 2 (5): 604-608.
224. Foey AD, Parry SL, Williams LM, Feldmann M, Foxwell BM, Brennan FM. Regulation of monocyte IL-10 synthesis by endogenous IL-1 and TNF-alpha: role of the p38 and p42/44 mitogen-activated protein kinases. J Immunol 1998; 160 (2): 920-928.
225. Vestbo J, Hurd SS, Agustí AG, Jones PW, Vogelmeier C, Anzueto A, et al. Global Strategy for the Diagnosis, Management, and Prevention of Chronic Obstructive Pulmonary Disease. Am J Respir Crit Care Med 2013; 187 (4): 347-365.
226. Guidelines for the measurement of respiratory function. Recommendations of the British Thoracic Society and the Association of Respiratory Technicians and Physiologists. Respir Med 1994; 88 (3): 165-194.
227. Armbruster DA, Pry T. Limit of blank, limit of detection and limit of quantitation. Clin Biochem Rev 2008; 29 Suppl 1: S49-52.
228. Life Technologies. Real-time PCR handbook [internet]. 2014 [cited 2014 March 16]. Available from URL: http://www.lifetechnologies.com/uk/en/home/life-science/pcr/real-time-pcr/qpcr-education/real-time-pcr-handbook.html.
229. Guhaniyogi J, Brewer G. Regulation of mRNA stability in mammalian cells. Gene 2001; 265 (1-2): 11-23.
230. Life Technologies. Basic principles of RT-qPCR. [internet]. 2014 [cited 2014 May 15]. Available from: http://www.lifetechnologies.com/uk/en/home/brands/thermo-scientific/molecular-biology/molecular-biology-learning-center/molecular-biology-resource-library/basic-principles-rt-qpcr.html
231. Wong ML, Medrano JF. Real-time PCR for mRNA quantitation. Biotechniques 2005; 39 (1): 75-85.
232. Sigma-Aldrich. Accutase® solution [internet]. 2014 [cited 2014 September 9]. Available from: http://www.sigmaaldrich.com/catalog/product/sigma/a6964?lang=en&region=GB.

233. Hoffman R.A. Pulse width for particle sizing [internet]. Curr Protoc Cytom. 2009 [cited 2016 February 23]. Chapter 1. Available from: doi: 10.1002/0471142956.cy0123s50.
234. Koopman G, Reutelingsperger CP, Kuijten GA, Keehnen RM, Pals ST, van Oers MH. Annexin V for flow cytometric detection of phosphatidylserine expression on B cells undergoing apoptosis. Blood 1994; 84 (5): 1415-1420.
235. Zembruski NC, Stache V, Haefeli WE, Weiss J. 7-Aminoactinomycin D for apoptosis staining in flow cytometry. Anal Biochem 2012; 429 (1): 79-81.
236. BD Biosciences. Annexin V Staining of Adherent Cells for Flow Cytometry [internet]. 2013 [cited 2016 March 3]. Available from: http://www.bdbiosciences.com/documents/BD_Protocol_AnnexinV_Staining.pdf.
237. Stephenson DA, Toltl LJ, Beaudin S, Liaw PC. Modulation of monocyte function by activated protein C, a natural anticoagulant. J Immunol 2006; 177 (4): 2115-2122.
238. Tu W. Basic Principles of Statistical Inference. In: Ambrosius W, editor. Topics in Biostatistics. Springer; 2007 [cited 2016 March 3]. Available from: http://link.springer.com/protocol/10.1007/978-1-59745-530-5_4.
239. Huggett J, Dheda K, Bustin S, Zumla A. Real-time RT-PCR normalisation; strategies and considerations. Genes Immun 2005; 6 (4): 279-284.
240. Dheda K, Huggett JF, Bustin SA, Johnson MA, Rook G, Zumla A. Validation of housekeeping genes for normalizing RNA expression in real-time PCR. Biotechniques 2004; 37 (1): 112-119.
241. Rylander R. Endotoxin in the environment-exposure and effects. J Endotoxin Res 2002; 8 (4): 241-252.
242. Life Technologies. Dynabeads® Untouched™ Human Monocytes Kit [internet]. [cited 2014 May 15]. Available from URL: http://www.lifetechnologies.com/order/catalog/product/11350D.
243. Skrzeczynska-Moncznik J, Bzowska M, Loseke S, Grage-Griebenow E, Zembala M, Pryjma J. Peripheral blood CD14high CD16+ monocytes are main producers of IL-10. Scand J Immunol 2008; 67 (2): 152-159.
244. Skinner NA, MacIsaac CM, Hamilton JA, Visvanathan K. Regulation of Toll-like receptor (TLR)2 and TLR4 on CD14dimCD16+ monocytes in response to sepsis-related antigens. Clin Exp Immunol 2005; 141 (2): 270-278.
245. Hulspas R, O'Gorman MR, Wood BL, Gratama JW, Sutherland DR. Considerations for the control of background fluorescence in clinical flow cytometry. Cytometry B Clin Cytom 2009; 76 (6): 355-364.
246. Baumgarth N, Roederer M. A practical approach to multicolor flow cytometry for immunophenotyping. J Immunol Methods 2000; 243 (1-2): 77-97.
247. Maecker HT, McCoy JP, Nussenblatt R. Standardizing immunophenotyping for the Human Immunology Project. Nat Rev Immunol 2012; 12 (3): 191-200.
248. R and D Systems. R and D Systems ELISAs: Quality Manufacturing and Evaluation of Performance [internet]. [cited 2014 Apr 14]. Available from URL: http://www.rndsystems.com/product_detail_objectname_elisa_quality.aspx.
249. Life Technologies. Human Tumor Necrosis Factor Receptor I (soluble) (sTNF-RI) ELISA kit protocol [internet]. [cited 2014 May 15]. Available from URL: https://tools.lifetechnologies.com/content/sfs/manuals/KAC1761_Rev1.pdf.
250. Life Technologies. Human Tumor Necrosis Factor Receptor II (soluble) (sTNF-RII) ELISA kit protocol [internet]. [cited 2014 May 15]. Available from URL: https://tools.lifetechnologies.com/content/sfs/manuals/KAC1771_Rev1.pdf.

251. Davis D. Principles of Curve Fitting for Multiplex Sandwich Immunoassays- tech note 2861 [internet]. 2015 [cited 2015 March 23]. Available from: http://www.dartmouth.edu/dartlab/uploads/Bio-RadTechNote2861_principles_of_curve_fitting.pdf.
252. Thermo Scientific. T042-Technical Bulletin. NanoDrop Spectrophotometers-Assessment of Nucleic Acid Purity [internet]. 2016 [cited 2016 February 18]. Available from: http://www.nanodrop.com/Library/T042-NanoDrop-Spectrophotometers-Nucleic-Acid-Purity-Ratios.pdf.
253. Bustin SA, Benes V, Garson JA, Hellemans J, Huggett J, Kubista M, et al. The MIQE guidelines: minimum information for publication of quantitative real-time PCR experiments. Clin Chem 2009; 55 (4): 611-622.
254. Schumann RR, Leong SR, Flaggs GW, Gray PW, Wright SD, Mathison JC, et al. Structure and function of lipopolysaccharide binding protein. Science 1990; 249 (4975): 1429-1431.
255. Wright SD, Ramos RA, Tobias PS, Ulevitch RJ, Mathison JC. CD14, a receptor for complexes of lipopolysaccharide (LPS) and LPS binding protein. Science 1990; 249 (4975): 1431-1433.
256. Li Q, Verma IM. NF-kappaB regulation in the immune system. Nat Rev 2002; Immunology. 2 (10): 725-734.
257. Gallay P, Jongeneel CV, Barras C, Burnier M, Baumgartner JD, Glauser MP, et al. Short time exposure to lipopolysaccharide is sufficient to activate human monocytes. J Immunol 1993; 150 (11): 5086-5093.
258. Miao F, Gonzalo IG, Lanting L, Natarajan R. In vivo chromatin remodeling events leading to inflammatory gene transcription under diabetic conditions. J Biol Chem 2004; 279 (17): 18091-18097.
259. Hasday JD, Bascom R, Costa JJ, Fitzgerald T, Dubin W. Bacterial endotoxin is an active component of cigarette smoke. Chest 1999; 115 (3): 829-835.
260. Korsgren M, Linden M, Entwistle N, Cook J, Wollmer P, Andersson M, et al. Inhalation of LPS induces inflammatory airway responses mimicking characteristics of chronic obstructive pulmonary disease. Clin Physiol Funct Imaging 2012; 32 (1): 71-79.
261. Zykova SN, Svartberg J, Seljelid R, Iversen H, Lund A, Svistounov DN, et al. Release of TNF-alpha from in vitro-stimulated monocytes is negatively associated with serum levels of apolipoprotein B in patients with type 2 diabetes. Scand J Immunol 2004; 60 (5): 535-542.
262. Danis VA, Millington M, Hyland VJ, Grennan D. Cytokine production by normal human monocytes: inter-subject variation and relationship to an IL-1 receptor antagonist (IL-1Ra) gene polymorphism. Clin Exp Immunol 1995; 99 (2): 303-310.
263. Singh J, Schwartz DA. Endotoxin and the lung: Insight into the host-environment interaction. J Allergy Clin Immunol 2005; 115 (2): 330-333.
264. Opal SM, Scannon PJ, Vincent JL, White M, Carroll SF, Palardy JE, et al. Relationship between plasma levels of lipopolysaccharide (LPS) and LPS-binding protein in patients with severe sepsis and septic shock. J Infect Dis 1999; 180 (5): 1584-1589.
265. Owen CA, Campbell EJ, Stockley RA. Monocyte adherence to fibronectin: role of CD11/CD18 integrins and relationship to other monocyte functions. J Leukoc Biol 1992; 51 (4): 400-408.
266. Murphey ED, Traber DL. Protective effect of tumor necrosis factor-alpha against subsequent endotoxemia in mice is mediated, in part, by interleukin-10. Crit Care Med 2001; 29 (9): 1761-1766.

267. Gantner F, Kupferschmidt R, Schudt C, Wendel A, Hatzelmann A. In vitro differentiation of human monocytes to macrophages: change of PDE profile and its relationship to suppression of tumour necrosis factor-alpha release by PDE inhibitors. Br J Pharmacol 1997; 121 (2): 221-231.
268. Tsai CS, Chen DL, Lin SJ, Tsai JC, Lin TC, Lin CY, et al. TNF-alpha inhibits toll-like receptor 4 expression on monocytic cells via tristetraprolin during cardiopulmonary bypass. Shock 2009; 32 (1): 40-48.
269. Perera LP, Waldmann TA. Activation of human monocytes induces differential resistance to apoptosis with rapid down regulation of caspase-8/FLICE. Proc Natl Acad Sci U S A 1998; 95 (24): 14308-14313.
270. Mangan DF, Welch GR, Wahl SM. Lipopolysaccharide, tumor necrosis factor-alpha, and IL-1 beta prevent programmed cell death (apoptosis) in human peripheral blood monocytes. J Immunol 1991; 146 (5): 1541-1546.
271. Kiener PA, Davis PM, Starling GC, Mehlin C, Klebanoff SJ, Ledbetter JA, et al. Differential induction of apoptosis by Fas-Fas ligand interactions in human monocytes and macrophages. J Exp Med 1997; 185 (8): 1511-1516.
272. Appelt U, Sheriff A, Gaipl US, Kalden JR, Voll RE, Herrmann M. Viable, apoptotic and necrotic monocytes expose phosphatidylserine: cooperative binding of the ligand Annexin V to dying but not viable cells and implications for PS-dependent clearance. Cell Death Differ 2005; 12 (2): 194-196.
273. Ottonello L, Bertolotto M, Montecucco F, Bianchi G, Dallegri F. Delayed apoptosis of human monocytes exposed to immune complexes is reversed by oxaprozin: role of the Akt/IkappaB kinase/nuclear factor kappaB pathway. Br J Pharmacol 2009; 157 (2): 294-306.
274. Ryan JG, Aksentijevich I. Tumor necrosis factor receptor-associated periodic syndrome: toward a molecular understanding of the systemic autoinflammatory diseases. Arthritis Rheum 2009; 60 (1): 8-11.
275. Wang W, Alpert E. Downregulation of phorbol 12-myristate 13-acetate-induced tumor necrosis factor-alpha and interleukin-1 beta production and gene expression in human monocytic cells by human alpha-fetoprotein. Hepatology 1995; 22 (3): 921-928.
276. Krabbe KS, Pedersen M, Bruunsgaard H. Inflammatory mediators in the elderly. Exp Gerontol 2004; 39 (5): 687-699.
277. Lapperre TS, Postma DS, Gosman MME, Snoeck-Stroband JB, ten Hacken NHT, Hiemstra PS, et al. Relation between duration of smoking cessation and bronchial inflammation in COPD. Thorax 2006; 61 (2): 115-121.
278. Newton AC. Protein kinase C: poised to signal. Am J Physiol Endocrinol Metab [internet] 2010 [cited 2016 February 18]; 298 (3): E395-402. Available from: http://www.ncbi.nlm.nih.gov/pubmed/19934406.
279. Dufresne M, Seva C, Fourmy D. Cholecystokinin and gastrin receptors. Physiol Rev 2006; 86 (3): 805-847.
280. Mendoza MC, Er EE, Blenis J. The Ras-ERK and PI3K-mTOR pathways: cross-talk and compensation. Trends Biochem Sci 2011; 36 (6): 320-328.
281. Liese AM, Siddiqi MQ, Siegel JH, Denny T, Spolarics Z. Augmented TNF-alpha and IL-10 production by primed human monocytes following interaction with oxidatively modified autologous erythrocytes. J Leukoc Biol 2001; 70 (2): 289-296.
282. Lu YC, Yeh WC, Ohashi PS. LPS/TLR4 signal transduction pathway. Cytokine 2008; 42 (2): 145-151.

283. Shames BD, Selzman CH, Pulido EJ, Meng X, Meldrum DR, McIntyre RC, Jr., et al. LPS-Induced NF-kappaB activation and TNF-alpha release in human monocytes are protein tyrosine kinase dependent and protein kinase C independent. J Surg Res 1999; 83 (1): 69-74.
284. Barnes PJ. Immunology of asthma and chronic obstructive pulmonary disease. Nat Rev Immunol 2008; 8 (3): 183-192.
285. Kim YS, Choi EJ, Lee WH, Choi SJ, Roh TY, Park J, et al. Extracellular vesicles, especially derived from Gram-negative bacteria, in indoor dust induce neutrophilic pulmonary inflammation associated with both Th1 and Th17 cell responses. Clin Exp Allergy 2013; 43 (4): 443-454.
286. Xu P, Liu J, Sakaki-Yumoto M, Derynck R. TACE activation by MAPK-mediated regulation of cell surface dimerization and TIMP3 association. Sci Signal [internet] 2012 [cited 2016 March 3]; 5 (222): ra34. Available from: http://www.ncbi.nlm.nih.gov/pubmed/22550340.
287. Poon IK, Lucas CD, Rossi AG, Ravichandran KS. Apoptotic cell clearance: basic biology and therapeutic potential. Nat Rev Immunol 2014; 14 (3): 166-180.
288. McGarry N, Greene CM, McElvaney NG, Weldon S, Taggart CC. The Ability of Secretory Leukocyte Protease Inhibitor to Inhibit Apoptosis in Monocytes Is Independent of Its Antiprotease Activity. J Immunol Res [internet] 2015 [cited 2016 March 3]: 507315. Available from: http://www.ncbi.nlm.nih.gov/pubmed/26247039.
289. Dreschers S, Gille C, Haas M, Grosse-Ophoff J, Schneider M, Leiber A, et al. Infection-induced bystander-apoptosis of monocytes is TNF-alpha-mediated. PLoS One [internet] 2013 [cited 2016 February 18]; 8 (1): e53589. Available from: http://www.ncbi.nlm.nih.gov/pubmed/23349721.
290. Segundo C, Medina F, Rodriguez C, Martinez-Palencia R, Leyva-Cobian F, Brieva JA. Surface molecule loss and bleb formation by human germinal center B cells undergoing apoptosis: role of apoptotic blebs in monocyte chemotaxis. Blood 1999; 94 (3): 1012-1020.
291. Elliott MR, Chekeni FB, Trampont PC, Lazarowski ER, Kadl A, Walk SF, et al. Nucleotides released by apoptotic cells act as a find-me signal to promote phagocytic clearance. Nature 2009; 461 (7261): 282-286.
292. Riss TL, Moravec RA, Niles AL, Benink HA, Worzella TJ, Minor L. Cell Viability Assays. In: Sittampalam GS, Coussens NP, Nelson H, Arkin M, Auld D, Austin C, et al., editors. Assay Guidance Manual [internet]. Bethesda 2004 [cited 2016 February 18]. Available from: http://www.ncbi.nlm.nih.gov/pubmed/23805433.
293. Baliopharm. Product Pipeline /ATROSAB. [internet]. 2016 [cited 2016 January 2]. Available from: http://www.baliopharm.com/de/product-pipeline/atrosab.html.
294. Proudfoot A, O'Kane C, Bayliffe A, Serone A, Bareille P, Smith S, et al. A Novel TNFR1-Targeting Domain Antibody Attenuates Pulmonary Inflammation In A Human Model Of Lung Injury, Via Actions On The Lung Micro-Vascular Endothelium. 2014: A6589.
295. Rossol M, Heine H, Meusch U, Quandt D, Klein C, Sweet MJ, et al. LPS-induced cytokine production in human monocytes and macrophages. Crit Rev Immunol 2011; 31 (5): 379-446.
296. Raetz CR, Whitfield C. Lipopolysaccharide endotoxins. Annu Rev Biochem 2002; 71: 635-700.
297. Bettini M, Vignali DA. Regulatory T cells and inhibitory cytokines in autoimmunity. Curr Opin Immunol 2009; 21 (6): 612-618.
298. R and D Systems. Product datasheet. [internet]. 2015 [cited 2015 January 2]. Available from: http://www.rndsystems.com/pdf/MAB726.pdf.

299. R and D Systems. Product datasheet [internet]. 2015 [cited 2015 Jan 02]. Available from: http://www.rndsystems.com/pdf/MAB625.pdf.
300. Sullivan DE, Ferris M, Pociask D, Brody AR. Tumor necrosis factor-alpha induces transforming growth factor-beta1 expression in lung fibroblasts through the extracellular signal-regulated kinase pathway. Am J Respir Cell Mol Biol 2005; 32 (4): 342-349.
301. Li X, Mai J, Virtue A, Yin Y, Gong R, Sha X, et al. IL-35 is a novel responsive anti-inflammatory cytokine-a new system of categorizing anti-inflammatory cytokines. PLoS One [internet] 2012 [cited 2015 March 4]; 7 (3): e33628. Available from: http://www.ncbi.nlm.nih.gov/pubmed/22438968.
302. Parry SL, Sebbag M, Feldmann M, Brennan FM. Contact with T cells modulates monocyte IL-10 production: role of T cell membrane TNF-alpha. J Immunol 1997; 158 (8): 3673-3681.
303. Saraiva M, O'Garra A. The regulation of IL-10 production by immune cells. Nat Rev Immunol 2010; 10 (3): 170-181.
304. van der Poll T, Jansen J, Levi M, ten Cate H, ten Cate JW, van Deventer SJ. Regulation of interleukin 10 release by tumor necrosis factor in humans and chimpanzees. J Exp Med 1994; 180 (5): 1985-1988.
305. Dickensheets HL, Freeman SL, Smith MF, Donnelly RP. Interleukin-10 upregulates tumor necrosis factor receptor type-II (p75) gene expression in endotoxin-stimulated human monocytes. Blood 1997; 90 (10): 4162-4171.
306. Hofmann SR, Rosen-Wolff A, Tsokos GC, Hedrich CM. Biological properties and regulation of IL-10 related cytokines and their contribution to autoimmune disease and tissue injury. Clin Immunol 2012; 143 (2): 116-127.
307. Asadullah K, Sterry W, Volk HD. Interleukin-10 therapy-review of a new approach. Pharmacol Rev 2003; 55 (2): 241-269.
308. Wang H, Peters T, Kess D, Sindrilaru A, Oreshkova T, Van Rooijen N, et al. Activated macrophages are essential in a murine model for T cell-mediated chronic psoriasiform skin inflammation. J Clin Invest 2006; 116 (8): 2105-2114.
309. Stratis A, Pasparakis M, Rupec RA, Markur D, Hartmann K, Scharffetter-Kochanek K, et al. Pathogenic role for skin macrophages in a mouse model of keratinocyte-induced psoriasis-like skin inflammation. J Clin Invest 2006; 116 (8): 2094-2104.
310. Mahida YR. The key role of macrophages in the immunopathogenesis of inflammatory bowel disease. Inflamm Bowel Dis 2000; 6 (1): 21-33.
311. Kigerl KA, Gensel JC, Ankeny DP, Alexander JK, Donnelly DJ, Popovich PG. Identification of two distinct macrophage subsets with divergent effects causing either neurotoxicity or regeneration in the injured mouse spinal cord. J Neurosci 2009; 29 (43): 13435-13444.
312. Filion LG, Graziani-Bowering G, Matusevicius D, Freedman MS. Monocyte-derived cytokines in multiple sclerosis. Clin Exp Immunol 2003; 131 (2): 324-334.
313. Imamura K, Spriggs D, Kufe D. Expression of tumor necrosis factor receptors on human monocytes and internalization of receptor bound ligand. J Immunol 1987; 139 (9): 2989-2992.
314. Perneger TV. What's wrong with Bonferroni adjustments. BMJ 1998; 316 (7139): 1236-1238.
315. Hoy T. Guide to Flow Cytometry: Rare-event detection [internet]. 2005 [cited 2015 February 18]. Available from: www.dako.com/08065_15dec05_guide_to_flow_cytometry_rare-event.

316. Barbara JA, Smith WB, Gamble JR, Van Ostade X, Vandenabeele P, Tavernier J, et al. Dissociation of TNF-alpha cytotoxic and proinflammatory activities by p55 receptor- and p75 receptor-selective TNF-alpha mutants. EMBO J 1994; 13 (4): 843-850.
317. Bryde S, Grunwald I, Hammer A, Krippner-Heidenreich A, Schiestel T, Brunner H, et al. Tumor necrosis factor (TNF)-functionalized nanostructured particles for the stimulation of membrane TNF-specific cell responses. Bioconjug Chem 2005; 16 (6): 1459-1467.
318. Youn JH, Oh YJ, Kim ES, Choi JE, Shin J-S. High mobility group box 1 protein binding to lipopolysaccharide facilitates transfer of lipopolysaccharide to CD14 and enhances lipopolysaccharide-mediated TNF-alpha production in human monocytes. J Immunol 2008; 180 (7): 5067-5074.
319. Li T, Hu J, Thomas JA, Li L. Differential induction of apoptosis by LPS and taxol in monocytic cells. Mol Immunol 2005; 42 (9): 1049-1055.
320. Heidenreich S, Schmidt M, August C, Cullen P, Rademaekers A, Pauels HG. Regulation of human monocyte apoptosis by the CD14 molecule. J Immunol 1997; 159 (7): 3178-3188.
321. Rossol M, Meusch U, Pierer M, Kaltenhauser S, Hantzschel H, Hauschildt S, et al. Interaction between transmembrane TNF and TNFR1/2 mediates the activation of monocytes by contact with T cells. J Immunol 2007; 179 (6): 4239-4248.
322. Rossato M, Curtale G, Tamassia N, Castellucci M, Mori L, Gasperini S, et al. IL-10-induced microRNA-187 negatively regulates TNF-alpha, IL-6, and IL-12p40 production in TLR4-stimulated monocytes. Proc Natl Acad Sci U S A [internet] 2012 [cited 2016 January 3]; 109 (45): E3101-3110. Available from: http://www.ncbi.nlm.nih.gov/pubmed/23071313.
323. Huang HC, Yu HR, Huang LT, Huang HC, Chen RF, Lin IC, et al. miRNA-125b regulates TNF-alpha production in CD14+ neonatal monocytes via post-transcriptional regulation. J Leukoc Biol 2012; 92 (1): 171-182.
324. Laurent Frenzel NS, Ghada Alsaleh, Dominique Wachsmann, Jacques-Eric Gottenberg and Jean Sibilia. A new mode of TNF-[alpha] inhibition by microRNA. J Immunol 2009; 181: 99.26.
325. Shi L, Song L, Fitzgerald M, Maurer K, Bagashev A, Sullivan KE. Noncoding RNAs and LRRFIP1 regulate TNF expression. J Immunol 2014; 192 (7): 3057-3067.
326. NE II, Heward JA, Roux B, Tsitsiou E, Fenwick PS, Lenzi L, et al. Long non-coding RNAs and enhancer RNAs regulate the lipopolysaccharide-induced inflammatory response in human monocytes. Nat Commun 2014; 5: 3979.
327. Li Z, Chao TC, Chang KY, Lin N, Patil VS, Shimizu C, et al. The long noncoding RNA THRIL regulates TNFalpha expression through its interaction with hnRNPL. Proc Natl Acad Sci U S A 2014; 111 (3): 1002-1007.
328. Zheng L, Teschler H, Guzman J, Hubner K, Striz I, Costabel U. Alveolar macrophage TNF-alpha release and BAL cell phenotypes in sarcoidosis. Am J Respir Crit Care Med 1995; 152 (3): 1061-1066.
329. Hellermann GR, Nagy SB, Kong X, Lockey RF, Mohapatra SS. Mechanism of cigarette smoke condensate-induced acute inflammatory response in human bronchial epithelial cells. Respir Res 2002; 3: 22.
330. Jahan-Tigh RR, Ryan C, Obermoser G, Schwarzenberger K. Flow cytometry. J Invest Dermatol [internet] 2012 [cited 2016 February 18]; 132 (10): e1. Available from: http://www.ncbi.nlm.nih.gov/pubmed/22971922.
331. Case, L. Power and Sample Size. In: Ambrosius W, editor. Topics in Biostatistics. Springer; 2007 [cited 2016 March 3]. Available from: http://link.springer.com/protocol/10.1007/978-1-59745-530-5_4.

332. Cho MH, McDonald ML, Zhou X, Mattheisen M, Castaldi PJ, Hersh CP, et al. Risk loci for chronic obstructive pulmonary disease: a genome-wide association study and meta-analysis. Lancet Respir Med 2014; 2 (3): 214-225.
333. Wood AM, Stockley RA. Alpha one antitrypsin deficiency: from gene to treatment. Respiration 2007; 74 (5): 481-492.
334. Troegeler A, Lastrucci C, Duval C, Tanne A, Cougoule C, Maridonneau-Parini I, et al. An efficient siRNA-mediated gene silencing in primary human monocytes, dendritic cells and macrophages. Immunol Cell Biol 2014; 92 (8): 699-708.
335. Mahmood T, Yang PC. Western blot: technique, theory, and trouble shooting. N Am J Med Sci 2012; 4 (9): 429-434.